



January 2012

The Urotsa Bladder Cell Model For Heavy Metal Carcinogenesis: Characterization With Respect To The Role Of Beclin-1 And Sparc Expression

Jennifer Larson

Follow this and additional works at: <https://commons.und.edu/theses>

Recommended Citation

Larson, Jennifer, "The Urotsa Bladder Cell Model For Heavy Metal Carcinogenesis: Characterization With Respect To The Role Of Beclin-1 And Sparc Expression" (2012). *Theses and Dissertations*. 1298.
<https://commons.und.edu/theses/1298>

This Dissertation is brought to you for free and open access by the Theses, Dissertations, and Senior Projects at UND Scholarly Commons. It has been accepted for inclusion in Theses and Dissertations by an authorized administrator of UND Scholarly Commons. For more information, please contact zeinebyousif@library.und.edu.

THE UROTSIA BLADDER CELL MODEL FOR HEAVY METAL
CARCINOGENESIS: CHARACTERIZATION WITH RESPECT TO THE ROLE OF
BECLIN-1 AND SPARC EXPRESSION

by

Jennifer L. Larson
Bachelor of Science, the University of Akron, 2007

A Dissertation
Submitted to the Graduate Faculty

of the

University of North Dakota

In partial fulfillment of the requirements

for the degree of

Doctor of Philosophy


Grand Forks, North Dakota

August
2012

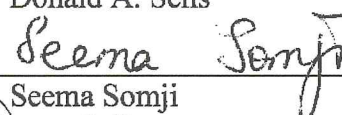
This dissertation, submitted by Jennifer L. Larson in partial fulfillment of the requirements for the Degree of Doctor of Philosophy from the University of North Dakota, has been read by the Faculty Advisory Committee under whom the work has been done and is hereby approved.



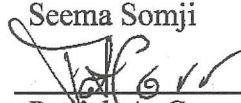
Jane R. Dunleavy, Chairperson



Donald A. Sens



Seema Somji

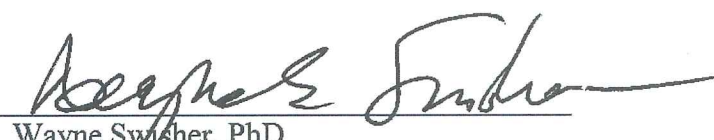


Patrick A. Carr



Diane Darland

This dissertation meets the standards for appearance, conforms to the style and format requirements of the Graduate School of the University of North Dakota, and is hereby approved.



Wayne Swisher, PhD
Dean of the Graduate School

July 16, 2012 

Date

PERMISSION

Title: The UROtsa Bladder Cell Model for Heavy Metal Carcinogenesis:
Characterization with Respect to the Role of Beclin-1 and SPARC
Expression

Department: Anatomy and Cell Biology

Degree: Doctor of Philosophy

In presenting this dissertation in partial fulfillment of the requirements for a graduate degree from the University of North Dakota, I agree that the library of this University shall make it freely available for inspection. I further agree that permission for extensive copying for scholarly purposes may be granted by the professor who supervised my dissertation work, or in her absence, by the chairperson of the department or the dean of the Graduate School. It is understood that any copying or publication or other use of this dissertation or part thereof for financial gain shall not be allowed without my written permission. It is also understood that due recognition shall be given to me and to the University of North Dakota in any scholarly use which may be made of any material in my dissertation.

Jennifer L. Larson
July 16, 2012

TABLE OF CONTENTS

LIST OF TABLES	x
LIST OF FIGURES	xi
ACKNOWLEDGEMENTS	xvi
ABSTRACT.....	xviii
CHAPTER	
I. INTRODUCTION	1
Characterization of Bladder Carcinomas	1
Toxicology of Arsenic and Cadmium.....	5
Cell Death: Apoptosis, Necrosis, and Autophagy	13
Matricellular Proteins of the Extracellular Matrix	21
SPARC	22
Characterization of the UROtsa Cell Lines	32
Rationales, Purposes, and Hypotheses.....	45
II. BECLIN-1 EXPRESSION IN NORMAL BLADDER AND IN CD ⁺² AND AS ⁺³ EXPOSED AND TRANSFORMED HUMAN UROTHELIAL CELLS (UROtsA)	48
Abstract	50
Introduction.....	50
Materials and Methods.....	53
Human Bladder Specimen for Immunohistochemical and Molecular Analysis	53

	Immunohistochemistry	53
	RNA and Protein Isolation from Human Bladder.....	54
	Cell Culture.....	54
	Visualization of DAPI-Stained Cells	55
	Real Time Analysis of Beclin-1 mRNA Expression	55
	Western Analysis of Beclin-1, Atg-5, Atg-7, Atg-12 and LC3B Expression	56
	Results.....	57
	Expression of Beclin-1 in Normal Urothelium.....	57
	Basal Expression of Beclin-1 in Parental UROtsa Cells and UROtsa Cells Transformed by As ⁺³ and Cd ⁺²	58
	Beclin-1 Expression in Parental UROtsa Cells Exposed to Cd ⁺² and As ⁺³	59
	Beclin-1 Expression in Cultures of Cd ⁺² and As ⁺³ Transformed UROtsa Cells Exposed to Cd ⁺² and As ⁺³	60
	Expression of Atg-5, Atg-7, Atg-12 and LC3B Proteins in Parental UROtsa Cells and UROtsa Cells Transformed by Cd ⁺² and As ⁺³	60
	Discussion	62
	References.....	66
III.	SPARC GENE EXPRESSION IS REPRESSED IN HUMAN UROTHELIAL CELLS (UROtsa) EXPOSED TO OR MALIGNANTLY TRANSFORMED BY CADMIUM OR ARSENITE.....	103
	Abstract.....	105
	Introduction.....	106
	Materials and Methods.....	108

Cell Culture.....	108
Basal Expression of SPARC in UROtsa Cells and Tumor Heterotransplants	109
Immunolocalization of SPARC in Parental UROtsa Cells	110
Immunohistochemical Localization of SPARC in Tumor Heterotransplants and Archival Specimens of Human Bladder Cancer	111
Expression of SPARC in UROtsa Cells Exposed to Cd^{+2} and As^{+3}	112
Treatment of Cd^{+2} and As^{+3} Transformed UROtsa Cells with 5-Aza-2'-deoxycytidine (5-AZC) and Histone Deacetylase Inhibitor.....	112
Statistics	112
Results.....	113
SPARC mRNA and Protein Expression in Parental UROtsa Cells and Cd^{+2} and As^{+3} Transformed Cell Lines.....	113
SPARC mRNA and Protein Expression in Tumor Heterotransplants Produced From Cd^{+2} and As^{+3} Transformed UROtsa Cell Lines	113
SPARC mRNA Expression in Parental and As^{+3} and Cd^{+2} Transformed UROtsa Cells Following Treatment with Inhibitors of DNA Methylation and Acetylation	114
SPARC Expression in Parental UROtsa Cells Exposed to Cd^{+2} and As^{+3}	115
Immunohistochemical Staining of SPARC in Normal Human Bladder, Cystitis, Noninvasive, and Invasive Urothelial Carcinoma.....	116
Discussion.....	118
References.....	122

IV.	THE FORCED EXPRESSION OF SPARC IN TRANSFORMED HUMAN UROTHELIAL CELLS (UROtsa): CHARACTERIZATION OF MIGRATION PROPERTIES AND TUMORGENICITY	139
	Abstract	140
	Introduction.....	141
	Materials and Methods.....	144
	Cell Culture.....	144
	Stable Transfection of Select Transformed UROtsa Cell Lines	144
	mRNA and Protein Expression in Parental, As ⁺³ -and Cd ⁺² -Transformed, SPARC-Transfected UROtsa Cell Lines, and Mouse Heterotransplants	146
	Immunolocalization of SPARC in Parental, As ⁺³ -and Cd ⁺² -Transformed, and SPARC-Transfected UROtsa Cell Lines	147
	Cellular Migration and Invasion Assays.....	148
	Mouse Heterotransplants: Tumorigenicity in Soft Agar and Nude Mice	149
	Immunohistochemical Localization of SPARC Expression in Mouse Heterotransplants and Archival Specimens of Human Bladder Cancer	150
	Results.....	151
	SPARC mRNA and Protein Expression in SPARC- Transfected and Blank Vector UROtsa Cell Lines	151
	Morphology and Growth Rates of SPARC-Transfected and Blank Vector Cell Lines.....	153
	Migration Properties of SPARC-Transfected, Blank Vector, and Non-Transfected Cell Lines	154

Tumorigenicity and SPARC Protein Analysis of Mouse Heterotransplants Generated from the SPARC-Transfected, Blank Vector, and Non-Transfected Cell Lines	158
SPARC and BSD mRNA Expression in Cell Lines and Mouse Heterotransplants Generated from the SPARC-Transfected, Blank Vector, and Non-Transfected Cell Lines	161
Discussion	162
References	168
V. DISCUSSION	205
REFERENCES	218
APPENDIX.....	235

LIST OF TABLES

Table		Page
IV-1.	Doubling times for SPARC-transfected and DEST-transfected UROtsa cells	172

LIST OF FIGURES

Figure		Page
I-1.	An illustration depicting the extent of tumor invasion of primary bladder cancer	3
I-2.	Intracellular metabolism of inorganic arsenic.....	7
I-3.	The sequential ultrastructural changes seen in necrosis (left) and apoptosis (right).....	15
I-4.	Schematic diagram of beclin-1 and the Atg proteins within the autophagic pathway	19
I-5.	The structure of human SPARC protein	24
II-1.	Expression of beclin-1 in human bladder tissue	68
II-2.	Expression of beclin-1 in human bladder tissue and the UROtsa cell lines...	69
II-3.	Baseline mRNA expression of beclin-1 in UROtsa cell lines.....	70
II-4.	Baseline protein expression of beclin-1 in UROtsa cell lines.....	71
II-5.	Protein expression of beclin-1 in UROtsa parent cell line treated with cadmium.....	72
II-6.	Protein expression of beclin-1 in UROtsa parent cell line treated with arsenic	73
II-7.	Growth effect on beclin-1 expression in UROtsa parent cells.....	74
II-8.	Protein expression of beclin-1 in UROtsa Cd ^{#1} cells	75
II-9.	Protein expression of beclin-1 in UROtsa Cd ^{#7} cells	76
II-10.	Protein expression of beclin-1 in UROtsa As ^{#1} cells	77
II-11.	Protein expression of beclin-1 in UROtsa As ^{#6} cells	78

II-12.	Expression of autophagy proteins, Atg-5 and -7, in UROtsa parent and UROtsa Cd ⁺² transformed cell lines.....	79
II-13.	Expression of autophagy proteins, Atg-12 and LC3B, in UROtsa parent and UROtsa Cd ⁺² transformed cell lines.....	80
II-14.	Expression of autophagy proteins, Atg-5 and -7, in UROtsa parent and UROtsa As ⁺³ transformed cell lines.....	81
II-15.	Expression of autophagy proteins, Atg-12 and LC3B, in UROtsa parent and UROtsa As ⁺³ transformed cell lines.....	82
II-16.	Real time RT-PCR analysis of autophagy genes, Atg-5 and -7, in UROtsa parent and UROtsa Cd ⁺² transformed cell lines.....	83
II-17.	Real time RT-PCR analysis of autophagy genes, Atg-12 and LC3B, in UROtsa parent and UROtsa Cd ⁺² transformed cell lines.....	84
II-18.	Real time RT-PCR analysis of autophagy genes, Atg-5 and -7, in UROtsa parent and UROtsa As ⁺³ transformed cell lines.....	85
II-19.	Real time RT-PCR analysis of autophagy genes, Atg-12 and LC3B, in UROtsa parent and UROtsa As ⁺³ transformed cell lines.....	86
II-20.	Protein expression of Atg-5 in UROtsa Cd ^{#1} cells.....	87
II-21.	Protein expression of Atg-7 in UROtsa Cd ^{#1} cells.....	88
II-22.	Protein expression of Atg-12 in UROtsa Cd ^{#1} cells.....	89
II-23.	Protein expression of LC3B in UROtsa Cd ^{#1} cells.....	90
II-24.	Protein expression of Atg-5 in UROtsa Cd ^{#7} cells.....	91
II-25.	Protein expression of Atg-7 in UROtsa Cd ^{#7} cells.....	92
II-26.	Protein expression of Atg-12 in UROtsa Cd ^{#7} cells.....	93
II-27.	Protein expression of LC3B in UROtsa Cd ^{#7} cells.....	94
II-28.	Protein expression of Atg-5 in UROtsa As ^{#1} cells.....	95
II-29.	Protein expression of Atg-7 in UROtsa As ^{#1} cells.....	96
II-30.	Protein expression of Atg-12 in UROtsa As ^{#1} cells.....	97

II-31.	Protein expression of LC3B in UROtsa As ^{#1} cells	98
II-32.	Protein expression of Atg-5 in UROtsa As ^{#6} cells	99
II-33.	Protein expression of Atg-7 in UROtsa As ^{#6} cells	100
II-34.	Protein expression of Atg-12 in UROtsa As ^{#6} cells	101
II-35.	Protein expression of LC3B in UROtsa As ^{#6} cells	102
III-1.	Expression of SPARC mRNA and protein	125
III-2.	Localization of SPARC protein expression	126
III-3.	Expression of SPARC mRNA and protein in tumor heterotransplants	127
III-4.	Expression of SPARC protein in tumor heterotransplants.....	128
III-5.	Real-time RT-PCR analysis of SPARC mRNA levels in parental UROtsa cells, and UROtsa cells transformed by Cd ⁺² and As ⁺³ treated with the epigenetic regulator, MS-275.....	129
III-6.	Real-time RT-PCR analysis of SPARC mRNA levels in parental UROtsa cells, and UROtsa cells transformed by Cd ⁺² and As ⁺³ treated with the epigenetic regulator, 5-AZC.....	131
III-7.	Real-time RT-PCR analysis of SPARC mRNA levels in parental UROtsa cells, and UROtsa cells transformed by Cd ⁺² and As ⁺³ treated with a combination of epigenetic regulators	133
III-8.	Expression of SPARC mRNA and protein in parental UROtsa cells exposed to Cd ⁺²	134
III-9.	Expression of SPARC mRNA and protein in parental UROtsa cells exposed to As ⁺³	135
III-10.	Expression of SPARC mRNA and protein during the transformation process in UROtsa cells exposed to 1 μ M As ⁺³	136
III-11.	Immunohistochemical staining of SPARC in normal human bladder, cystitis, invasive, and noninvasive urothelial carcinoma.....	137
IV-1.	Expression of SPARC mRNA and protein in parental UROtsa cells, SPARC-transfected cells, and non-transfected and blank vector (DEST) control cells lines.....	173
IV-2.	Expression of secreted SPARC protein	174

IV-3.	Intracellular localization of SPARC protein by immunofluorescent staining	175
IV-4.	Phase contrast light microscopy of the SPARC-transfected and DEST-transfected UROtsa cell lines demonstrating epithelial morphology in all lines	176
IV-5.	Migratory ability of UROtsa parent, and malignantly transformed As ⁺³ cell lines, with the MDA-MB-231 malignant breast cancer cells used a positive control.....	177
IV-6.	Migratory ability of UROtsa parent, and malignantly transformed Cd ⁺² cell lines, with the MDA-MB-231 malignant breast cancer cells used a positive control.....	178
IV-7.	Relative cell chemotaxis migration of MDA-MB-231 and UROtsa cells transformed by As ⁺³ or Cd ⁺² compared to the parent UROtsa cells	179
IV-8.	Migratory ability of UROtsa parent, non-transfected, SPARC-transfected, and blank vector (DEST) cell lines with MDA-MB-231 malignant breast cells used as a positive control	180
IV-9.	Relative cell migration of MDA-MB-231, non-transfected UROtsa, SPARC-transfected, and blank vector (DEST) cells lines compared to the parent UROtsa cells.....	182
IV-10.	MTT assessing cell viability of UROtsa parent, breast cancer, and As ⁺³ -transformed UROtsa cell lines	183
IV-11.	MTT analysis assessing cell viability of UROtsa cells transformed by Cd ⁺³ and the cells transfected with SPARC (S) and DEST (D) vectors	184
IV-12.	Wound healing assay of the UROtsa parent cells, breast cancer cell lines, MDA-MB231 and HS578T, and UROtsa cells transformed by As ⁺³	186
IV-13.	Wound healing assay of UROtsa cells transformed by Cd ⁺²	188
IV-14.	Wound healing assay of UROtsa As ⁺³ cells transfected with SPARC or blank vector (DEST) and their non-transfected counterparts	189
IV-15.	Wound healing assay of UROtsa Cd ⁺² cells transfected with SPARC or blank vector (DEST) and their non-transfected counterparts	190
IV-16.	Invasion capability of UROtsa parent, and malignantly transformed As ⁺³ cell lines, with the Hs578T malignant breast cancer cell line as a positive control.....	191

IV-17.	Invasion capability of UROtsa parent, and malignantly transformed Cd ⁺² cell lines, with the Hs578T malignant breast cancer cell line as a positive control.....	192
IV-18.	Relative cell invasion of Hs578T and UROtsa cells transformed by As ⁺³ or Cd ⁺² compared to the parent UROtsa cells.....	193
IV-19.	Invasion capability of UROtsa parent, non-transfected, SPARC-transfected, and blank vector (DEST) cell lines, with the Hs578T malignant breast cancer cell line as a positive control	194
IV-20.	Relative cell invasion of Hs578T, non-transfected UROtsa, SPARC-transfected, and blank vector (DEST) cells lines compared to the parent UROtsa cells	196
IV-21.	Soft agar morphology of SPARC-transfected and DEST-transfected UROtsa cell lines.....	197
IV-22.	Expression of SPARC in mouse heterotransplants using different SPARC specific antibodies	198
IV-23.	Expression of SPARC in archival human bladder cancer and mouse heterotransplants using 2 different SPARC specific antibodies	200
IV-24.	Expression of human SPARC protein in mouse heterotransplants and corresponding cell lines.....	202
IV-25.	Expression of BSD and human SPARC mRNA in mouse heterotransplants and corresponding cell lines.....	203
IV-26.	Expression of mouse SPARC mRNA in mouse heterotransplants and corresponding cell lines.....	204

ACKNOWLEDGEMENTS

I would like to take this opportunity to express my most sincere gratitude to my principle advisor, Dr. Jane R. Dunlevy, for her enthusiasm, encouragement, and absolute dedication to my training. She truly has a great passion for research and I feel lucky and honored to be a part of her lab. Her steadfast belief in my abilities, especially when I doubted myself, has propelled me into a research based career. I have thoroughly enjoyed the time I have spent in the Dunlevy lab and cannot believe the end is nearing. My research has also been enhanced by the joint effort of our collaborating lab group, including Dr. Donald Sens, Dr. Seema Somji, Dr. Scott Garrett, Dr. Mary Ann Sens, and Dr. Xu Dong Zhou who have provided not only monetary support but also technical, procedural, and troubleshooting guidance. This collaborative group works so smoothly, with each professor having an “expertise;” I always had someone to go to that could troubleshoot my problems. This collaboration has greatly broadened my knowledge and truly enriched my graduate career. I would also like to thank all the members of our lab, including graduate students, for their friendship, support, and advice.

I would also like to express my sincerest gratefulness to Dr. Donald Sens for his generosity to me and to the others around him. Dr. Sens not only provided the financial means to support my project, but took the time to listen to my results, give feedback, as well as advice for my career and the future. For this, I am very appreciative.

Additionally I would like to recognize Dr. Xu Dong Zhou and Yan Wang for their assistance with immunohistochemical analysis and their willingness to allow me to shadow them in the animal facilities. I am also thankful for my committee members, Dr. Dunlevy, Dr. Sens, Dr. Somji, Dr. Patrick Carr, and Dr. Diane Darland. Without their advice I would not have been able to complete my dissertation.

Finally, I would like to thank my loving and caring family and friends; most especially my fiancé, Joseph Casey, who has had infinite patience, understanding, and has supported me from the moment we met. My parents, Rebecca and the late Calvin Larson, have instilled the power of dedication, hard work, and perseverance into me. My brothers, Michael and Gregory Larson, have provided a wonderful companionship that has been an amazing gift and one that I am very fortunate to have. For these reasons, I thank my family for their continuous advice and support throughout the many years that I have spent pursuing my education.

To My Family

ABSTRACT

The development of bladder cancer is known to have a strong association with environmental toxins. This laboratory employs the human UROtsa cell line model to explore the relationship between As^{+3} and Cd^{+2} exposure and the development of urothelial cancer.

The parental UROtsa cells and their As^{+3} and Cd^{+2} transformed counterparts have been used to define the mechanism of cell death (apoptosis and/or necrosis). A third mechanism of cell death, autophagy, has not yet been investigated. The hypothesis for the current study is that the autophagy pathway involving beclin-1 plays a role in UROtsa cell death mechanisms. A combination of real time RT-PCR, western analysis, and immunohistochemistry showed that beclin-1 is expressed in the urothelium of normal human bladder, but large alterations in beclin-1 and its associated autophagy genes are not found in heavy metal induced bladder cancer cells.

SPARC, a glycoprotein with counter adhesive properties, has the ability to modulate cell-cell and cell-matrix interactions. Microarray analysis indicated that SPARC gene expression was greatly decreased between parental and all transformed UROtsa cell lines. The hypothesis for this study is that a reduction in SPARC expression is necessary for a malignant phenotype to develop. SPARC expression was determined in human parental UROtsa cells, their Cd^{+2} and As^{+3} transformed counterparts, and in archival specimens of human bladder cancer using a combination of RT-PCR, western

analysis, immunofluorescence localization, and immunohistochemical staining. This study showed that exposure to As^{+3} or Cd^{+2} greatly reduced SPARC expression in UROtsa cells.

To further analyze SPARC expression, SPARC was stably transfected into select transformed UROtsa cell lines which were characterized based on growth rates, morphology, wound closure, migration, invasion, and tumorigenicity. Tumors generated by injection of the SPARC-transfected cell lines into nude mice, showed an absence of SPARC expression within the epithelial tumor component, but were positive for the transfected vector. This study suggests post-transcriptional down-regulation of SPARC expression in urothelial carcinoma cells within the mouse tumor environment. Overall, results from this study show that autophagy does not play a large cell death role within the UROtsa system however, down-regulation of SPARC expression does strongly correlate with the malignant phenotype.

CHAPTER I

INTRODUCTION

Characterization of Bladder Carcinomas

Normal human bladder is histologically characterized by the transitional urothelium that protects the urogenital tract, starting at the renal pelvis and continuing to the urethra. The mucosa of the urinary bladder consists of a stratified epithelium that is comprised of three to seven layers of cells in which three differing cell types have been identified, namely the basal cells, intermediate cells, and the superficial cells or “umbrella cells” (Castillo-Martin et al., 2010). The basal cells form a layer of one cell in thickness with a cuboidal shape that rests on the basal membrane. The intermediate cells constitute the majority of cells in the urothelium, with these cells being more columnar in nature. The most superficial cells or umbrella cells protrude into the lumen of the bladder and have the unique ability to preserve the impermeability of the epithelium to urine, even when it is fully distended. Deep to the urothelium, the lamina propria consists of connective tissue rich in capillary plexus. Below the lamina propria, the muscularis propria contains three layers of smooth muscle which are organized into an inner longitudinal, outer circular, and outermost longitudinal orientation. Surrounding the muscular wall is perivesical soft tissue containing blood vessels and lymphatic vessels.

Carcinoma of the bladder is the fourth most common cancer for men and the ninth most common cancer for women in the United States (Fajkovic et al., 2011), with occurrences found more frequently in men than women, at a ratio of 3:1 respectively

(Jacobs et al., 2010; Jemal et al., 2010; Tanaka and Sonpavde, 2011). Cancer of the urinary bladder was responsible for approximately 14,680 deaths related to the disease in 2010 with approximately 70,530 new cases also diagnosed (Jemal et al., 2010). Usually recognized by microscopic or gross hematuria (~80% of cases), bladder cancer is relatively common in the elderly with an average diagnosis age of 70 years. More than 90% of bladder cancers in the United States are urothelial carcinomas that arise from the urothelium lining of the bladder. In many developing countries, however, urothelial carcinomas show squamous cell differentiation, which is another type of histological presentation of the cancer. Squamous cell carcinoma (SCC) of the bladder is thought to arise from a parasite known as *Schistosoma haematobium*, as seen in 75% of these cases. SCC does occur in Western countries, but accounts for only five percent of all bladder cancers and is usually associated with prolonged catheterization (Jacobs et al., 2010; Tanaka and Sonpavde, 2011). In addition to urothelial carcinoma and SCC, several other histological forms of bladder cancer exist; however these forms are rare, but can include adenocarcinomas, sarcomas, and small cell carcinomas (Volanis et al., 2010).

The majority of malignant tumors arising in the urinary bladder are of epithelial origin. A staging system for bladder cancer has been developed to uniformly describe the extent the cancer has spread. The TNM (tumor, node, metastasis) staging system classifies cancers based on three differing pieces of information. The “T” category followed by a letter and/or number describes the extent of tumor growth through the bladder wall, with a higher T number indicating more extensive growth. The “N” category followed by a number from 0 to 3 indicates if the cancer has spread to lymph nodes near the bladder and the “M” category followed by a 0 or 1 indicates if the cancer

has metastasized to a distant site (Jacobs et al., 2010). Tumors of the bladder are classified into two different groups, non-muscle invasive and muscle invasive. Non-muscle invasive tumors account for nearly 80% of bladder tumors while the remaining 20% are muscle-invasive bladder cancer and are usually associated with poor prognosis (Volanis et al., 2010). Ta, carcinoma in situ (CIS or Tis), and T1 categories of tumors are grouped under non-muscle invasive, while T2, T3, and T4 are classified as muscle invasive tumors. Non-muscle invasive tumors are either confined to the mucosa, as seen in Ta and CIS/Tis tumors, or invade into the lamina propria (T1), but do not invade into the muscularis propria (Figure I-1). Stage Ta tumors typically have a low risk of progression over time; however, CIS or Tis is flat, high-grade bladder cancer that is difficult to detect, has a very high rate of reoccurrence, and has been shown to progress to

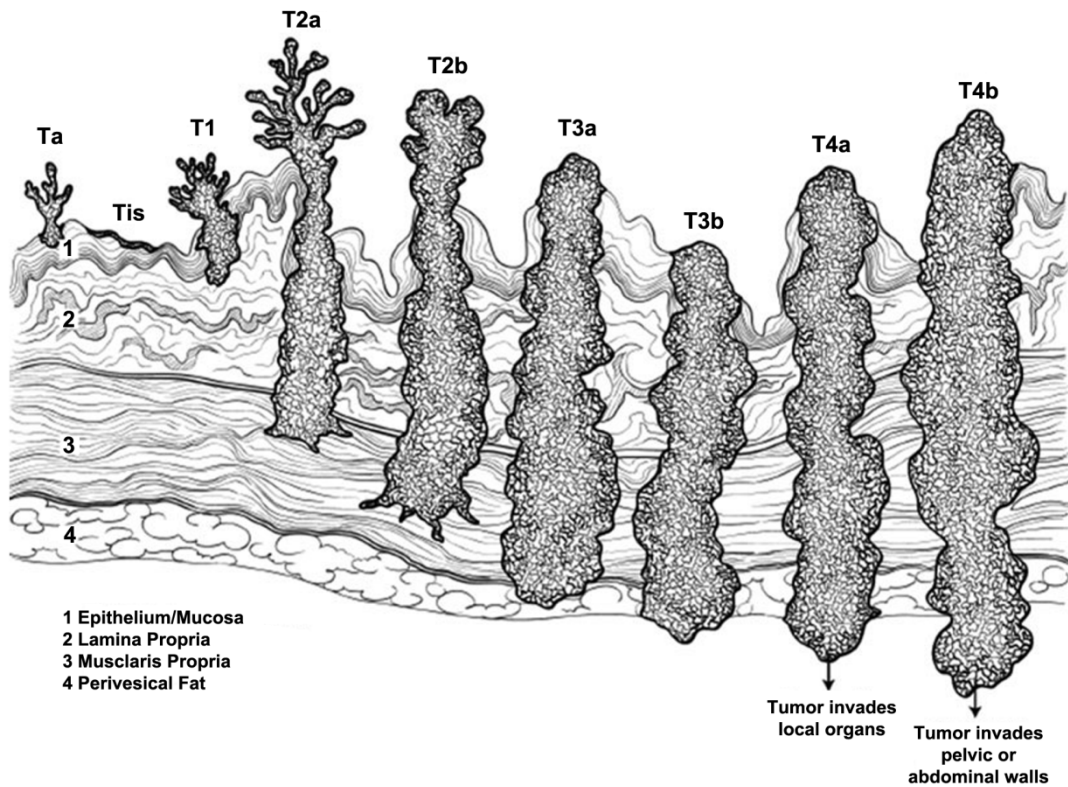


Figure I-1. An illustration depicting the extent of tumor invasion of primary bladder cancer. Adapted from Jacobs et al. (2010).

invasive bladder cancer in 60-80% of cases (Castillo-Martin et al., 2010). Stage T1 tumors have progressed through the transitional epithelium and have invaded into the lamina propria and frequently progress to the muscularly invasive T2 stage tumors. The prognosis is improved when the tumor is confined to the organ (T2a and T2b), as opposed to when metastasis through the bladder wall and into the perivesical fat (T3) occurs. Urothelial carcinomas can spread beyond the fatty tissue of the bladder and into nearby organs (T4) and usually seed on the stroma of the prostate, seminal vesicles, uterus, vagina, and pelvic or abdominal wall (Jacobs et al., 2010).

Despite current treatment and improved technology, bladder cancer still has an extremely high recurrence rate, usually reappearing within five years with higher grade tumors having an even greater risk for progression of the cancer (Goodison et al., 2009). Non-muscle invasive bladder tumors have been shown to recur 50-70% of the time and between 10-30% of those tumors will progress to muscle-invasive tumors (Soloway et al., 2002). With medical costs ranging between \$99,000-120,000 per patient from time of diagnosis to the time of death, bladder cancer is the most expensive cancer per patient. Due to the high rate of recurrence, patients are usually kept under strict routine surveillance (Lokeshwar and Selzer, 2006). Cystoscopy allows for visual examination of the bladder and resection of biopsies for histopathological analysis. Biopsies are routinely performed every three months for the first two years after removal of the tumor, then every six months for the following two years, and yearly thereafter (Goodison et al., 2009). High recurrence rates, escalating medical costs, increased diagnoses, and often poor prognosis makes identifying risk factors that directly cause or lead to the progression of bladder cancer an area of intense research.

Many environmental factors have been clearly associated with bladder cancer, with the strongest risk factor being cigarette smoking (Zeegers et al., 2000). Cigarette smokers are estimated to have a two to four times increased risk for bladder cancer than those who do not smoke and the risk is enhanced with increased number of cigarettes and longer duration of smoking (Negri and La Vecchia, 2001). Interestingly, cessation of smoking has been attributed to a 40% reduction of bladder cancer within one year, but the risk remains appreciable for up to 25 years (Volanis et al., 2010). After smoking, occupational exposure is the second greatest risk factor that can lead to bladder cancer (Kogevinas et al., 2003). The link between occupational exposure and the development of bladder cancer was first noted by a German surgeon, Dr. Ludwig Rehn in the late 19th century (Rehn, 1895). Dr. Rehn noted that factory workers exposed to aromatic amines had a greater propensity for this cancer. Dr. Rehn's keen observations paved the way for further investigation of other chemicals attributed to the development of bladder cancer. Autoworkers, truck drivers, metalworkers, paper and rubber manufacturers, dry cleaners, dental technicians, hairdressers, marine engineers, and individuals who are continuously exposed to paint and leather industrial byproducts have an increased probability of developing bladder cancer (Jacobs et al., 2010). Bladder cancer due to occupational exposures often does not appear until 30 to 50 years following exposure to the aforementioned environmental conditions.

Toxicology of Arsenic and Cadmium

Arsenic and cadmium have been classified by the International Agency for Research on Cancer as known human carcinogens (IARC (International Agency for Research on Cancer), 1980; IARC (International Agency for Research on Cancer), 1993)

and these heavy metals have also been associated with the formation of bladder cancer. Observations over time have determined that exposure to arsenic can cause extremely serious health effects such as neurological problems, cardiovascular diseases, skin lesions, and cancers, including skin, liver, lung, kidney, and bladder cancer (Rahman et al., 2009; Smith et al., 1992). There are many exogenous risk factors associated with the development of bladder cancer and individuals may be exposed to arsenic from many sources, such as ingested food, air, and drinking water. One source of environmental exposure to arsenic is through contaminated drinking water, which has been documented in at least 30 different countries (Chakraborti et al., 2002). Epidemiologic research has provided substantial evidence linking the ingestion of arsenic contaminated drinking water with the development of bladder cancer (Steinmaus et al., 2000); specifically, evidence from incidences in Taiwan (Chiou et al., 1995), Argentina (Hopenhayn-Rich et al., 1996), Chile (Smith et al., 1998), and Japan (Tsuda et al., 1995).

Arsenic is a ubiquitously expressed metalloid in the environment that can exist as a pure element or in combination with other metals (Guha Mazumder, 2008). Arsenic is capable of forming both organic and inorganic compounds in the environment and in the human body (Orloff et al., 2009). Inorganic arsenic, the most abundant form in nature, is formed by the combination of arsenic with other compounds, such as oxygen, iron, sulfur, and chlorine; which is toxic. When arsenic binds with hydrogen or carbon, it is referred to as organic arsenic; which is not considered toxic. Arsenic is capable of being metabolized, but the process of its metabolism is highly complex and gives rise to several species of arsenic. The differing forms of arsenic each have varying toxicities, some that are extremely toxic to those that have a low order of toxicity (Carter et al., 2003). When

arsenic enters the body (Figure I-2), it is usually in the form of trivalent inorganic As(III) or arsenite, while only a small amount of pentavalent inorganic form As(V), or arsenate, can enter and is then rapidly reduced to the trivalent arsenic (Cohen et al., 2006). After ingestion, inorganic arsenic is absorbed into the blood stream and then taken up by cells in tissues, primarily the liver. In the liver, arsenic undergoes a series of reductions and oxidative methylations to form pentavalent monomethylarsonic acid [MMA(V)] and dimethylarsinic acid [DMA(V)] (Le et al., 2000). During the metabolism of inorganic arsenic, trivalent intermediates, monomethylarsonous acid [MMA(III)] and dimethylarsinous acid [DMA(III)] are generated. The methylation reactions appear to facilitate the excretion of arsenic, thereby decreasing its toxic effects (Carter et al., 2003).

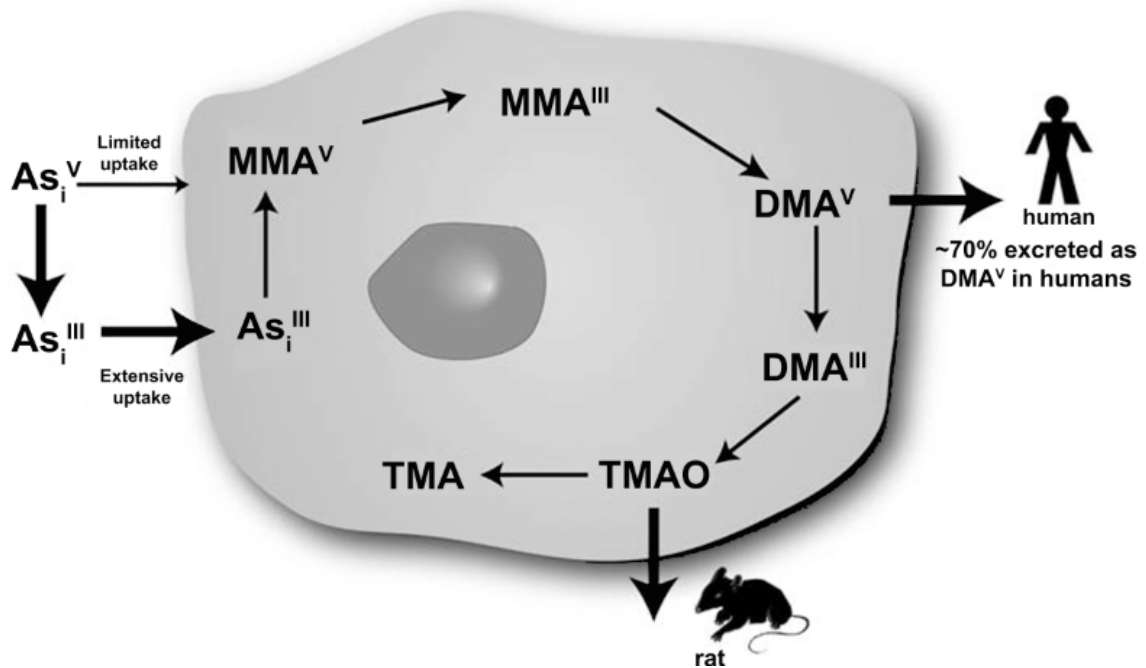


Figure I-2. Intracellular metabolism of inorganic arsenic. Adapted from Cohen et al. (2006). Abbreviations: As_i^{III} , inorganic arsenite; As_i^V , inorganic arsenate; DMA^{III} , trivalent dimethylarsinous acid; DMA^V , pentavalent dimethylarsinic acid; MMA^{III} , trivalent monomethylarsonous acid; MMA^V , pentavalent monomethylarsonic acid; TMA , trimethylarsine; $TMAO$, trimethylarsine oxide.

However, the MMA(III) and DMA(III) intermediates are structurally distinct compounds from the pentavalent MMA(V) and DMA(V) compounds and these trivalent methylated arsenicals formed during the metabolism of inorganic arsenic are highly reactive and believed to be the most carcinogenic forms of arsenic (Cohen et al., 2006). Therefore, methylated trivalent arsenic is more toxic than As_i(III), whereas methylated pentavalent arsenic is less toxic than As_i(III) in humans. However, in general the trivalent arsenicals [arsenite, MMA(III), and DMA(III)] are more potent toxicants than the pentavalent arsenicals [arsenate, MMA(V), and DMA(V)]. While, MMA(III) was shown to be more toxic than DMA(III) (Carter et al., 2003). It remains unknown which exact form of these arsenicals is responsible for arsenic-induced cancers in humans.

Interestingly, up to 70% of arsenic absorbed or taken in is excreted from the body via urine (Cohen et al., 2006). In most animal species, including humans, the intracellular metabolism of inorganic arsenic involves extensive metabolism to DMA(V). Humans also excrete significant amounts of MMA(V). However, the *Rattus norvegicus* (rat) however behaves differently than other mammals regarding the metabolism of arsenic and excretes a trimethylated form, trimethylarsine oxide (TMAO), which in turn alters its sensitivity to arsenic as a toxicant (Vahter, 1994). To further complicate matters, some animals (marmoset monkey, tamarin, squirrel monkey, and chimpanzee) do not methylate inorganic arsenic at all. Within animals that cannot methylate arsenic, the most toxic arsenic species is As_i(III), while in animals that can methylate arsenic it is MMA(III) (Carter et al., 2003). The efficiency of arsenic methylation to DMA(V) in most experimental animals may attribute as to why arsenic is less toxic in these animals and has proven difficult to study. Animal studies have been used to show

that high doses of inorganic arsenic administered as sodium arsenite or sodium arsenate in the diet or in drinking water of mice lead to increased proliferation of the bladder urothelium and tumor development (Suzuki et al., 2008). Cytotoxicity with extensive necrosis and exfoliation was also observed in the bladder epithelium of female mice treated with 50 or 100 $\mu\text{g/g}$ As_i (III) with dietary supplication (Suzuki et al., 2008). Advances in generating knockout animals with greater sensitivity to arsenic carcinogenesis, led to the generation of an As3mt knockout mouse model. Arsenic methyltransferase (As3mt) catalyzes reactions that convert inorganic arsenic to methylated metabolites. The inhibition of arsenic methylation has been shown to result in the concentration of inorganic arsenic in the urinary bladder of As3mt knockout mice. After treatment with arsenate, a five-fold increase in the sum of all arsenicals was seen in the bladder of the As3mt knockout mice compared to wild-type mice (Yokohira et al., 2010). This study also indicated that inorganic arsenic, in the absence of metabolism to methylated trivalent species, is capable of causing cytotoxic damage and regenerative hyperplasia in the bladder (Yokohira et al., 2010). If sustained, this increase in urothelial proliferation ultimately can result in bladder tumors (Waalkes et al., 2006). Consequently, the differences in metabolic characteristics, toxicity, and excretion of arsenic in humans and animal models have set limitations on determining arsenic carcinogenesis.

Cadmium is a ubiquitously expressed metal in the environment with no known health benefits or beneficial physiologic function in humans (Nzengue et al., 2011). Unlike arsenic, cadmium is not metabolized and is toxic at very low concentrations (Nzengue et al., 2011). Cadmium also has a high rate of soil-to-plant transfer leading to

contamination of most foodstuffs, rendering the diet as one source of exposure (Satarug et al., 2011). Cadmium is present in nearly all foods, but concentrations vary widely depending on food type and the level found naturally within the soil. Bivalve mollusks and crustaceans have high levels of cadmium due to their filter feeding behavior that allows them to accumulate metals from their aquatic environment (Whyte et al., 2009). High cadmium levels are also found in offal products, such as the liver and kidney; this is especially seen in older animals. Other sources of cadmium are in oilseeds, cocoa beans, and in certain wild mushrooms (Prankel et al., 2005; Prugarova and Kovac, 1987; Reeves and Vanderpool, 1997; Zhu et al., 2011). Food from plants generally contains higher concentrations of cadmium than animal products (meat, milk, eggs, and dairy products). Wheat, rice, green leafy vegetables, potatoes, and carrots contain higher concentrations than other sources and accounts for more than 80% of cadmium consumption (Olsson et al., 2002).

In addition to dietary exposure, cadmium has been found to be generated in occupational environments, such as in battery manufacturing, metal soldering, and welding facilities (Siemiatycki et al., 1994). At these facilities, cadmium exposure can occur by breathing in contaminated air. Another avenue of cadmium exposure, like that of arsenic is through consumption of tobacco products (Waalkes, 2000). Due to the ability of tobacco leaves to accumulate cadmium, each cigarette contains between 1-2 μg of cadmium and about 50% of cadmium inhaled from cigarette smoke can enter the systemic circulation (Matovic et al., 2011). The elimination of cadmium from the body is very slow and therefore leads to its accumulation with age, predominantly within the kidney.

Although the epidemiologic data on cadmium is less extensive than that of arsenic, environmental cadmium exposure has been linked to the development of cancers in the breast, kidney, pancreas, and urinary bladder (Huff et al., 2007). The toxic effects of cadmium were first noted in 1950 with the outbreak of “Itai-itai” disease, or “ouch-ouch” disease in Toyama Prefecture, Japan. The naming of this ailment was due to the tortuous screams of patients that were suffering excruciating pain in their joints and spine; this condition was caused by the ingestion of cadmium contaminated runoff water, released from mining companies, that was used to irrigate crops, especially rice paddies. Itai-itai is characterized by multiple fractures and distortion of the long bones in the skeleton. There was also decalcification and fractures of other bones including compression fractures of the spine (Jarup and Akesson, 2009). The disease exhibits a mixed pattern of mainly osteomalacia but also osteoporosis in combination with kidney damage (Kagawa, 1994).

Cadmium has been shown to accumulate in the liver, kidney, and other tissues (primarily muscle, bone, and skin) and is usually found bound to metallothionein, a metal binding protein, which may serve to temporarily detoxify the metal (Waalkes, 2003). However, cadmium cannot be metabolized into a less toxic species and is poorly excreted; therefore, the body has a limited capacity to respond to cadmium exposure. With no specific entry into the cell, cadmium utilizes the routes that physiological metals use to pass through the cell membranes. In particular, cadmium has been shown to interfere with many essential metals and metalloids including but not limited to, calcium, magnesium, sodium, potassium, zinc, copper, iron, and manganese (Moullis, 2010). With a similar structure to zinc, cadmium is known to replace zinc in tissues and in enzyme

binding sites. A recent study determined that cadmium could also enter cells through the ZIP8 family of zinc-dependent transporters and an increase in these proteins at the cell surface increases the influx of cadmium (He et al., 2006). Additional analysis of ZIP8 expression showed human bladder cells and normal human bladder tissue had a paranuclear localization of ZIP8 protein. The association of ZIP8 with the nucleus could indicate a possible involvement in providing zinc to zinc-requiring transcription factors and potentially a route for cadmium to gain entry into the nucleus and induce DNA damage (Ajjimaporn et al., 2012). Also, this study demonstrated that ZIP8 protein expression was variable in the normal human bladder cell line and in human bladder cells malignantly transformed by cadmium or arsenite depending on the time following feeding the cells with fresh growth media. This indicates that ZIP8 expression can vary depending on nutritional status (Ajjimaporn et al., 2012). Intestinal absorption of cadmium was also shown to be increased when the nutritional status of calcium, iron, or zinc was low. This is caused by the up-regulation of the duodenal iron transporter during iron deficiency, leading to an increased cadmium absorption into the intestine (Menke et al., 2009). This is primarily seen in women, whose prevalence of iron depletion is generally higher than that of men (Vahter et al., 2007).

Only a few studies have focused on the relationship between cadmium exposure and the development of bladder cancer. A population-based study of the associations between various cancers and occupational exposures in Canada found some evidence, albeit weak, that cadmium compounds are a risk factor for bladder cancer (Siemiatycki et al., 1994). Also it was determined from a patient set that included 10 individuals with bladder cancer, 60% had increased urinary cadmium content compared to the urinary

cadmium content in healthy individuals (Darewicz et al., 1998). Kellen et al. (2007) conducted a case-control study in Belgium to assess the association between blood cadmium levels and the risk of urinary bladder cancer. The risk for bladder cancer was enhanced with increasing levels of blood cadmium and the risk was eight times higher in the group of individuals with the highest blood cadmium concentrations, after taking sex, age, and occupational exposure into account (Kellen et al., 2007). The results remained significant even after adjusting for smoking habits, indicating that other routes of cadmium exposure were significant and this study was not just an indicator of smoking behavior. Taken together, these studies indicate an involvement of cadmium in promoting bladder carcinogenesis.

Although cadmium and arsenic have obvious differences in physical properties, transport, and metabolism, both metals have been implicated as environmental agents leading to bladder cancer. Epidemiologically, bladder cancer represents one of the first cancers in which industrial carcinogens were shown to be a major factor in the causation of the disease (Zhou et al., 2006). A majority of bladder cancers are believed to be a result of cigarette smoking, while the remaining cases are induced by industrial or agricultural exposure to carcinogens.

Cell Death: Apoptosis, Necrosis, and Autophagy

Cell death occurs under a variety of physiological and pathological conditions and has been shown to be a critical process during development, homeostasis, and immune regulation of multicellular organisms. The cell has several routes by which it can die, including apoptosis, necrosis, and autophagy. Each of the cell death types is characterized by distinct morphological features and is regulated by differing signaling

pathways that eventually lead to irreversible physiological events. Although these forms of cell death operate through differing mechanisms, their pathways are not mutually exclusive or even independent. In fact, some of the pivotal regulatory factors originally characterized for apoptosis and autophagy appear to guide the induction of necrotic mechanisms of cell death.

Apoptosis is a highly conserved pathway that is found naturally in virtually all tissues and constitutes a default state that must be actively inhibited in most cell types. Apoptosis eliminates cells that have been intrinsically signaled that the cell is no longer useful or that it has become dangerous to the organism, by activating enzymes that degrade the cells' own nuclear DNA and proteins. Apoptosis is morphologically associated with cell shrinkage, membrane blebbing, and chromatin condensation (Figure I-3). Within an apoptotic cell, the chromatin aggregates into highly condensed masses and the nucleus may also break up into fragments. Apoptosis is characterized by plasma membrane integrity that persists until late in the process. The plasma membrane of apoptotic cells acquires an altered structure, especially within the orientation of lipids (Kumar et al., 2010). The membrane blebbing that occurs leads to the fragmentation of membrane-bound apoptotic bodies that contain cytoplasm and tightly packaged organelles. Apoptotic bodies are generated by the controlled breakdown of cellular contents which are then targeted and engulfed by surrounding cells and phagocytes before the cell ruptures. Since the cell is rapidly cleared before its contents leaks out, there is no inflammatory reaction in the host.

Apoptotic cells exhibit specific biochemical modifications that underlie the structural changes. The breakdown of proteins involves the activation of several

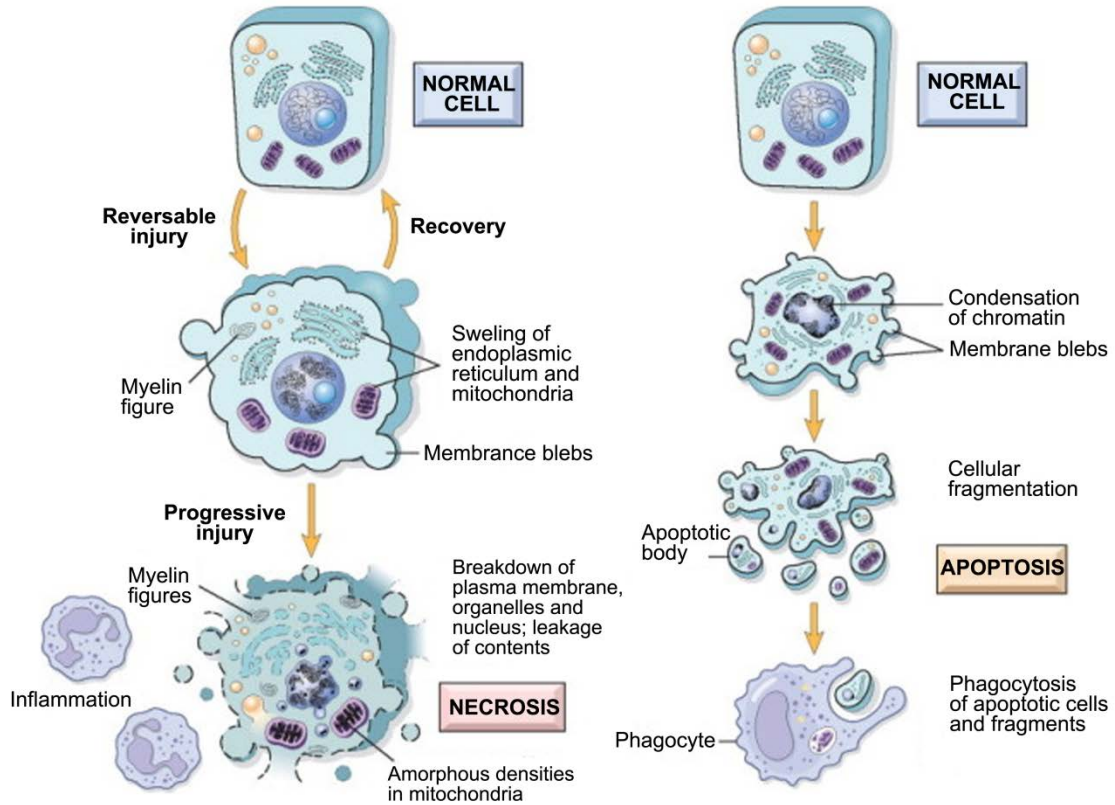


Figure I-3. The sequential ultrastructural changes seen in necrosis (left) and apoptosis (right). Adapted from Kumar et al. (2010).

members of a family of cysteine proteases or caspases (Fuentes-Prior and Salvesen, 2004). Caspases are present in cells as an inactive pro-enzyme that need to be proteolytically cleaved in order to be activated. Activated caspases cleave several vital cellular proteins, break down the cytoskeleton and nuclear scaffold, and can activate DNAses, leading to the degradation of nuclear DNA (Kumar et al., 2010). Apoptotic cells also express phosphatidylserine on the outermost layers of the plasma membrane. This phospholipid is usually found on the inner membrane, or cytosolic side of the cell, but when a cell undergoes apoptosis phosphatidylserine is no longer restricted to the cytosolic part of the membrane and becomes exposed on the surface of the cell. This

alteration allows for detection of an apoptotic cell by macrophages, leading to phagocytosis of the cell before the cell ruptures (Majno and Joris, 1995).

During embryological development, apoptotic cell death plays an important role in organogenesis and tissue remodeling; such as in the development of the eye, in shaping of the inner ear, in cardiac morphogenesis, in muscle development, and in removal of interdigital webs (Penaloza et al., 2006). In adult organisms, apoptosis is critical in maintaining cellular homeostasis, as in post-lactational mammary gland regression, ovarian follicular atresia, and elimination of activated immune cells to terminate an immune response (Elmore, 2007). Dysregulation or dysfunction of the apoptotic program is implicated in a variety of pathological conditions. Defects in apoptosis can result in cancer, autoimmune diseases, and spreading of viral infections, while neurodegenerative disorders, AIDS, and ischemic diseases are caused or enhanced by excessive apoptosis (Fadeel et al., 1999).

Another form of cell death is necrosis. Necrosis is mainly caused by physical or chemical trauma to the cell and begins with an impairment of the cell's ability to maintain homeostasis, leading to an influx of water and extracellular ions (Vanlangenakker et al., 2008). Morphologically, necrosis is associated with cellular swelling, membrane disruption, and profound nuclear changes (Figure I-3). Necrotic cells do not fragment into discrete bodies as apoptotic cells do, rather the whole cell as well as intracellular organelles, most notably the mitochondria, swell rapidly and rupture. Due to organelle swelling, ribosomes disassociate from the endoplasmic reticulum, small amorphous densities appear within the mitochondria, and lysosomes rupture. Nuclear changes within a necrotic cell may show several varying patterns caused by the

nonspecific breakdown of DNA, including, nuclear condensation, fragmentation, or dissolution of the nucleus (Kumar et al., 2010). Laminated structures or myelin figures are usually present in a necrotic cell. These structures are derived from damaged membranes of organelles and the plasma membrane. They appear as large, whorled phospholipid masses. Due to the ultimate breakdown of the plasma membrane, the cytoplasmic contents including lysosomal enzymes are released into the extracellular environment. This type of cell death causes a potentially damaging inflammatory response and is often associated with extensive tissue damage. Necrosis has traditionally been defined as an unregulated cell death process that lacks an energy (ATP) requirement that is related to the loss of regulation of ion homeostasis and later random digestion of DNA (Majno and Joris, 1995; Vanlangenakker et al., 2008).

Necrosis is also involved in physiologically relevant processes, such as ovulation, the death of chondrocytes associated with the longitudinal growth of bones, and cellular turnover in the small and large intestines (Festjens et al., 2006). Reducing the number of T lymphocytes after an immune response is an important mechanism that involves necrotic cell death (Holler et al., 2000). Pathological conditions have been associated with necrosis during ischemia/reperfusion, which can lead to the injury of organs, including the heart, brain, liver, kidney, and intestine (Neumar, 2000). Necrotic cell death has also been shown to contribute to excitotoxicity, which may be involved in stroke, traumatic brain injury, and several neurodegenerative diseases (Ankarcrona et al., 1995).

Autophagy, the process by which cells recycle cytoplasm and dispose of defective organelles (Shintani and Klionsky, 2004), plays a central role in maintaining homeostasis

within a cell. Due to its pro-survival function, autophagy can be also induced by a change of environmental conditions or during stress, such as nutrient depletion. Within autophagy, cells are protected from dying by the elimination of harmful organelles and aged cytoplasmic components. In most cases, autophagy constitutes a protective response activated by dying cells in an attempt to cope with stress (Galluzzi et al., 2012). In most tissues, autophagy occurs at a basal level and allows for routine cytoplasmic and protein turnover. The morphological hallmark of autophagy is the formation of the double or multi-membrane bound structures, called autophagosome or autophagic vacuole, in the cytoplasm of cells. The autophagosome is formed *de novo* and sequesters the desired material to be removed, the vacuole then fuses with a lysosome or late endosome where the cellular contents are broken down and reutilized under conditions of resource deprivation (Bursch, 2001). A distinguishing feature of autophagy that separates it from apoptosis is the source of lysosomal enzymes used for the dying cell's degradation. Apoptotic cells rely on being phagocytosed and then use the phagocytic cell's lysosomes for degradation, but autophagic cells use their own lysosomal machinery (Shintani and Klionsky, 2004).

Autophagic signaling acts through the mTOR (mammalian target of rapamycin) signaling pathway, which is a protein kinase important in controlling cell-cycle progression, translation, and is an inhibitor of autophagy. When mTOR is inhibited by starvation or with treatment of rapamycin, autophagy is induced and leads to activation of downstream effectors including the autophagy-related (Atg) genes which participate in the elongation and closure of the membrane associated with the autophagosome (Jung et al., 2009). At least 30 Atg genes have been identified and have been suggested to

participate in autophagy at different steps throughout the process (He and Klionsky, 2009). The synthesis of autophagic vacuoles requires vesicular nucleation, which is initiated by another complex, the PI3KC3 (class 3 phosphatidylinositol 3-kinase) complex. This complex includes beclin-1/Atg-6 and leads to the generation of PI3P which controls the membrane dynamics that are associated with autophagosome formation. To mediate vesicle membrane elongation, other Atg proteins are recruited. Implicated in this process is the activation of two ubiquitin-like conjugation systems (Figure I-4), the Atg-5/Atg-12 and the light chain-3 (LC3) complexes (He and Klionsky, 2009). Briefly, activation of Atg-12 requires Atg-7 which catalyzes the covalent binding of Atg-5 with Atg-12. Subsequent interactions between Atg-5/Atg-12 and Atg-16 recruit these molecules and attach them to the autophagophore (He and Klionsky, 2009). At the same time, LC3 is lipidated by binding to phosphatidylethanolamine (PE). In contrast to

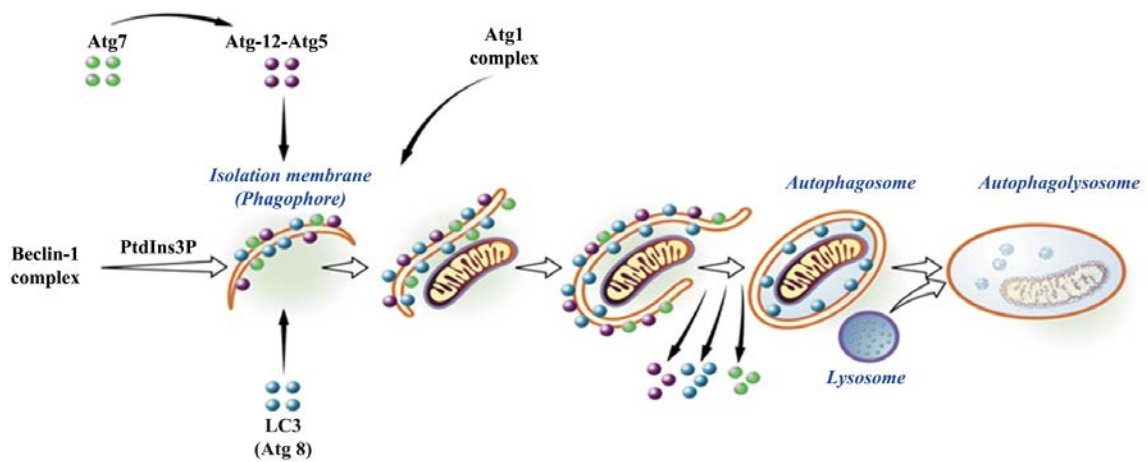


Figure I-4. Schematic diagram of beclin-1 and the Atg proteins within the autophagic pathway. Activation of autophagy proteins leads to the generation of the autophagic vacuole in which cellular organelles are sequestered and then degraded following fusion of the vesicles with lysosomes. The digested materials are recycled to provide nutrients for the cell. Adapted from Pattingre et al. (2008).

the cytoplasmic localization of LC3, LC3-PE or more commonly known as LC3-II, is localized to the autophagosome membrane and is generally used as an autophagic marker. Finally, the autophagosome fuses with a lysosome, and releases its autophagic content into the lysosomal lumen for degradation by hydrolases (He and Klionsky, 2009)

Beclin-1 plays a central role in autophagy and appears to be an essential gene for this type of cell death. Beclin-1 was first identified as a Bcl-2 interacting protein from a mouse brain library (Pattingre et al., 2008). Interestingly, Bcl-2 as well as several other anti-apoptotic Bcl-2 family members down-regulate autophagy by binding to beclin-1 and blocking its function. However, during starvation or other environmental stresses, Bcl-2 becomes phosphorylated and therefore releases beclin-1 and promotes autophagy (Pattingre et al., 2008). From studies done in yeast, beclin-1 was shown to be involved in the early steps of autophagosome formation (Figure I-4) and beclin-1 is responsible for the recruitment of the Atg proteins to the autophagosome leading to membrane elongation and closure of the of the autophagosome, therefore stimulating autophagy (Pattingre et al., 2008). The beclin-1 gene has been shown to be deleted in up to 75% of ovarian, 50% of breast, and 40% of prostate cancers (Aita et al., 1999). Other cancers have been shown to have decreased expression of beclin-1 including human brain tumors and cervical cell carcinoma (Aita et al., 1999). Inhibition of beclin-1 expression is associated with protection against autophagic cell death and actually induces apoptosis (Boya et al., 2005).

Autophagic cell death has been primarily described in developmental processes that require extensive cell destruction and removal. The development of the salivary gland cells has been associated with the induction of autophagy in *Drosophila* and mice

(Berry and Baehrecke, 2007). Studies have shown that beclin-1 knockout mice die early in embryogenesis, while atg-5 and atg-7 knockout mice are born normally, but die soon after birth (Sinha and Levine, 2008; Yue et al., 2003). The role of autophagy in cancer is highly debated as it can function to prevent accumulation of toxic cellular substances, some of which may be carcinogenic and allow for autophagy to act as a tumor suppressor, and it may also function to support cell survival in conditions of hypoxia aiding in the survival of tumors leading autophagy to be a tumor promoter.

Matricellular Proteins of the Extracellular Matrix

The extracellular matrix (ECM) is an intricate arrangement of proteoglycans, collagens, glycoproteins, and growth factors that not only act as a physical scaffold for the attachment and organization of cellular structures, but also as a mediator of intracellular signaling through cell surface receptors that recognize these ECM molecules. Most of the glycoproteins in the ECM promote cell adhesion and cause reorganization of the cytoskeleton that lead to signals directing differentiation and promotion of cell survival. Examples of these structural glycoproteins include fibronectin, vitronectin, collagen, and laminin. However, the ECM contains another group of proteins which can function as both soluble and insoluble proteins in the extracellular environment or matrix called “matricellular proteins.” The term “matricellular protein” was first introduced by Bornstein in 1995 to classify a nonhomologous group of regulatory macromolecules which are not structural components of the ECM, but rather mediate interactions between cells and the ECM (Bornstein, 1995). Matricellular proteins function to modulate cell-matrix interactions by binding to the structural matrix proteins, activating cell-surface receptors, and modulating

the activity of growth factors and cytokines. This group of proteins includes thrombospondins (TSP) -1 and -2, tenascins (TN) -C and -X, CCN family (including connective tissue growth factor), and SPARC (secreted protein, acidic and rich in cysteine), naming a few. Even though these proteins are structurally distinct, they appear to perform similar functions. They have counter-adhesive effects that can lead to the rounding of cells and can disrupt cell-matrix interactions. Expression of these proteins is often required for embryonic development, but their expression is generally low in steady-state conditions of adult tissue. However, the expression of matricellular proteins is up-regulated in wound healing and tissue remodeling, and they contribute to several cellular processes such as cell adhesion, migration, cell survival, and proliferation. The unusual expression pattern of these proteins is often associated with tumor development and progression. The expression of several matricellular proteins has been found and characterized in many types of cancer (Podhajcer et al., 2008). Within the tumor microenvironment, tumor epithelial cells and the surrounding stromal cells both secrete matricellular proteins. The ability of matricellular proteins to have a close interaction with the ECM allows for their influence on each step of cancer progression.

SPARC

SPARC, secreted protein rich in cysteine, also known as BM-40 or osteonectin, is an extracellular matrix associated glycoprotein. First founded as the most abundant non-collagenous component of bone by Termine et al. (1981), SPARC was found to bind to collagen fibrils, and specifically hydroxyapatite at distinct sites. Later it was found to be secreted by endothelial cells *in vitro* (Sage et al., 1984), a product of fibroblasts in culture (Otsuka et al., 1984), and a protein secreted from mouse embryonic endoderm (Mason et

al., 1986). The SPARC gene is located on chromosome 5q31.3-32 (Swaroop et al., 1988) and is highly conserved among different species, with the human gene having 92% homology with the mouse gene. Containing ten exons separated by nine introns, the human gene spans 25.9 kb with the first non-coding exon followed by a large 10.6 kb intron. The last exon contains the entire 3' non-translated region (Villarreal et al., 1989). The 300 bp CpG island, spanning from exon 1, to the first intron has been shown to be methylated in several cancers (Sato et al., 2003). The SPARC promoter lies between nucleotides -51 to -120 in the human gene and lacks a TATA or CAAT box, but is composed almost entirely of purines with a repetitive GGA motif, called a GGA box (Hafner et al., 1995).

The vertebrate SPARC gene encodes a 303 amino acid protein that contains an initial 17 hydrophobic amino acids signaling peptide and can be post-translationally modified by N-linked glycosylation. The SPARC protein has a predicted molecular mass of 32,511 daltons, but the secreted form of the protein migrates at 43 kDa on sodium dodecyl sulfate polyacrylamide gel electrophoresis (SDS-PAGE) most likely due to the addition of carbohydrates (Sage et al., 1984). All members of the SPARC family of proteins, including testican-1, -2, and -3, SPARC-like 1 (hevin), and SPARC-related modular calcium binding (SMOC)-1 and -2 have three similar domains (Figure I-5): the N-terminus (NT), the follistatin-like (FS), and the extracellular calcium binding C-terminus (EC) (Brekken and Sage, 2001). The first of three modular domains in SPARC contains amino acids 1-52 and is encoded on exons 3 and 4. This highly acidic NH₂-terminal domain is rich in glutamic acid, binds hydroxyapatite (Lane and Sage, 1994), and up to eight calcium ions with low affinity (Engel et al., 1987). The N-terminal

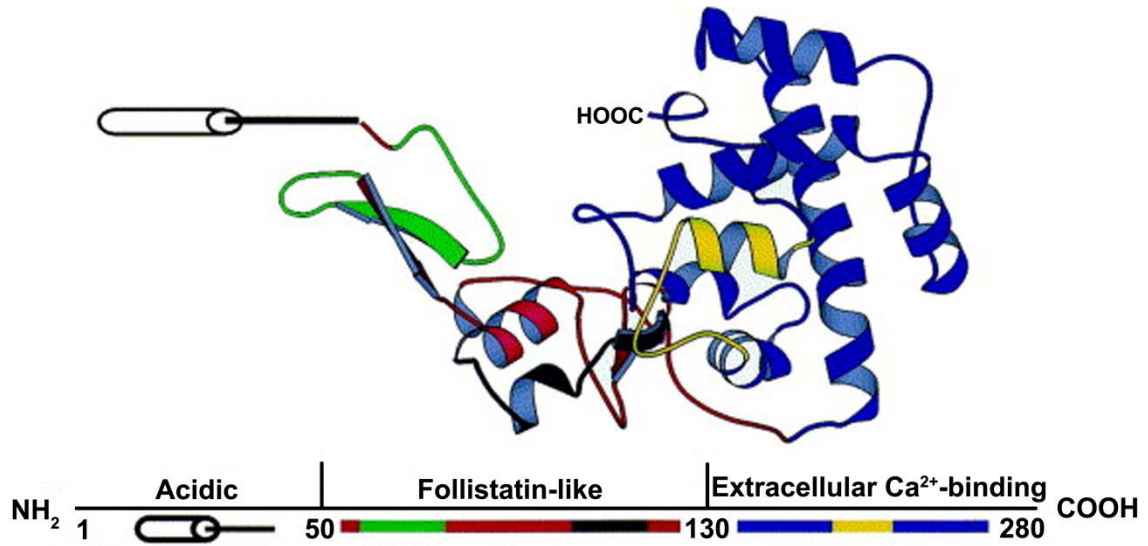


Figure I-5. The structure of human SPARC protein. A ribbon diagram was derived from the crystallographic data and indicates the three domains within the SPARC protein. The acidic domain (domain one) is shown in black and contains amino acids 1-52. The follistatin-like domain (domain two), amino acids 53-137, is shown in red, except for peptide 2.1, amino acids 55-74, and peptide 2.3, amino acids 114-130, which are shown in green and black respectively. The extracellular Ca²⁺-binding domain (domain three), amino acids 138-286, is shown in blue except for peptide 4.2, amino acids 255-274, which is shown in yellow. Adapted from Brekken and Sage (2001).

domain contains a sequence designated peptide 1.1, containing amino acids 4-23, is an efficient inhibitor of endothelial cell spreading (Lane and Sage, 1990) and increase matrix metalloproteinase (MMP)-2 activation (Gilles et al., 1998). Also, this structural region of the SPARC protein is the most distinct when compared to the other members of the SPARC family.

The second domain (amino acids 53-137), also known as the follistatin-like domain, is encoded within exons 5 and 6 and is homologous to a repeated domain in follistatin (Clark and Sage, 2008). This domain is stabilized and ridged due to its cysteine-rich region in which all the cysteine residues are disulfide-bonded. The

follistatin domain in SPARC also contains bioactive peptides that exert differing effects on endothelial cells. Peptide 2.1 (amino acids 55-74) stimulates proliferation of fibroblasts, but inhibits endothelial cell proliferation (Funk and Sage, 1993), and plays a role in the disassembly of focal adhesions on endothelial cells (Murphy-Ullrich et al., 1995). Peptide 2.3 (amino acids 113-130) which contains two copper binding sites and the copper binding sequence (K)GHK, has been determined to stimulate endothelial cellular proliferation (Funk and Sage, 1991; Funk and Sage, 1993) and angiogenesis (Lane and Sage, 1994).

The third domain encompasses amino acids 138-286, which is encoded within exons 7-9, and is the most conserved region of SPARC. This domain has a calcium-binding region that is folded into an α -helical globular structure (Sasaki et al., 1998) and contains two EF-hand motifs (Hohenester et al., 1997). It is within this third domain that SPARC is capable of binding to fibrillar and basement membrane collagens (Sasaki et al., 1998). Peptide 4.2 (amino acids 254-273), which is within the second EF-hand domain, contains a sequence that has been shown to bind to endothelial cells and inhibit their proliferation and migration (Hasselaar and Sage, 1992; Kupprion et al., 1998; Motamed and Sage, 1998). This peptide has also been shown to block the effects of VEGF (vascular endothelial growth factor) (Kupprion et al., 1998), bFGF (basic fibroblast growth factor) (Hasselaar and Sage, 1992; Motamed et al., 2003; Sage et al., 1995), and PDGF (platelet derived growth factor) (Motamed et al., 2003) in multiple cell types and participates in the disassembly of focal adhesions (Murphy-Ullrich et al., 1995).

With diverse functional domains, SPARC also plays a role in many physiological processes. SPARC has three distinct functions, including de-adhesion, anti-proliferation,

and regulation of the extracellular matrix and several growth factors. The de-adhesive properties of SPARC have shown it to impair cell attachment to the ECM by causing a restructuring in the focal adhesions and stress fibers (Murphy-Ullrich, 2001). The exogenous addition of SPARC to cells in culture has been shown to induce rounding on confluent monolayers of endothelial cells, fibroblasts, and smooth muscle cells, and maintain the rounded morphology of newly plated fibroblast by inhibiting their spreading (Sage et al., 1989). However, the established cell lines F9 embryonic carcinoma cells, PYS-2 parietal endoderm cells, and 3T3 fibroblast cells had normal cell morphology with the addition of exogenous SPARC (Sage et al., 1989). The ability to disassemble focal adhesions and reorganize actin stress fibers to the periphery of cultured endothelial cells has been localized to peptide 2.1 of FS module and part of the EC module when SPARC is added exogenously (Murphy-Ullrich et al., 1995). Exogenous addition of SPARC has also been shown to increase endothelial cell permeability leading to barrier dysfunction in pulmonary vascular endothelial cells. These changes in cell shape were F-actin dependent and coincident with the appearance of intercellular gaps, that provided a paracellular pathway for extravasation of macromolecules (Goldblum et al., 1994). The counter-adhesive properties may indicate SPARC plays a role in migration, a necessary process for the progression of metastatic tumors.

The anti-proliferative function of SPARC has been directly linked to the inhibition of bovine aortic endothelial cells into the S-phase of the cell cycle after exogenous addition of the protein (Funk and Sage, 1991). Human umbilical vein endothelial cells, fetal bovine endothelial cells, and bovine capillary endothelial cells were also arrested from progressing from the G₁ to S-phase in response to SPARC (Funk

and Sage, 1993). In contrast to the growth inhibition, SPARC differentially influences the growth of fibroblasts. Peptide 2.1 in the FS module of SPARC was shown to stimulate proliferation of fibroblast at concentrations of 0.1-0.4 mM; however, at higher concentrations of the peptide this effect was reversed. While peptide 1.1 was shown to inhibit endothelial cell spreading, but did not affect cell-cycle progression in these cells (Funk and Sage, 1991). Also of interest, fibroblasts, smooth muscle cells, and mesangial cells extracted from SPARC-null mice have a higher proliferation rate than cells from wild-type mice (Bradshaw et al., 1999). Within injured tissue, SPARC is strongly expressed in endothelial cells, epithelial cells, macrophages, and fibroblasts (Framson and Sage, 2004). Increased SPARC expression was also associated with an increased capacity for invasion *in vitro* in prostate cancer, gastric cancer, breast cancer, glioblastoma, and malignant melanoma (Tai and Tang, 2008). SPARC was also significantly increased in the necrotic region of myocardial infarction in mice and promoted the migration of fibroblasts (Wu et al., 2006). From this study, it was assumed that the enhanced SPARC expression modulate the interactions between cells and their surrounding matrix leading to the migration of fibroblasts into the injured area. (Wu et al., 2006). The ability of SPARC to stop cell cycle progression and regulate proliferation of specific cells may also lead to the migratory characteristics found in tumor cells.

SPARC has been shown to bind to several ECM proteins and may regulate the structural integrity of the ECM. SPARC has been shown to bind to several types of collagen, including, Types I, II, III, IV, V, and VIII , and influence collagen fibril assembly and morphology (Yan and Sage, 1999). Since SPARC has the capacity to bind to both fibrillar and nonfibrillar collagens, SPARC can function to regulate the ECM

assembly in connective tissue and in the basal lamina. However, SPARC's interactions with collagen are dependent on the presence of glycosylation, calcium, and protease activation. Therefore, tissue-specific alterations in the structure of SPARC can greatly affect its binding affinity to the ECM (Kaufmann et al., 2004).

The generation of SPARC-null mice has further provided a means to examine the role of SPARC in the ECM. SPARC-deficient mice exhibit a wide range of phenotypes, including early cataract formation, accelerated dermal wound-closure, osteopenia, lax skin, and a kinked tail (Bradshaw et al., 2003b). The development of premature cataracts is caused by disorganization of laminin and collagen IV in the lens epithelial basement membrane (Yan et al., 2003). Deficiencies were also found in the connective tissues of the SPARC-null mice, including decreased collagen I levels in skin, adipose, heart, and bone (Bradshaw et al., 2003a; Bradshaw et al., 2003b). Also collagen fibrils of the skin in SPARC knockout mice were uniformly smaller in diameter, showed a reduction in the collagen content to about half of the collagen content seen in wild type mice, and was reduced in terms of maturation and tensile strength (Bradshaw et al., 2003b). The accelerated wound-healing in the dermis of SPARC-null mice was determined to be a result of the increase contractility of the skin (Bradshaw et al., 2003b). Even though the deletion of SPARC led to a wide range of affected tissues in mouse tissue, the resulting aberrations in each tissue were due to altered production or assembly of the ECM (Framson and Sage, 2004). Since SPARC is a primary mediator of collagen assembly and stability in several tissues, these studies show SPARC is required for proper collagen maturation and function within the ECM.

SPARC has also been shown to modulate the formation of the ECM by increasing the activity (Gilles et al., 1998) and production of matrix metalloproteinases (MMP), specifically MMP-1, MMP-2, and MMP-3 (Tremble et al., 1993). SPARC can also contribute to the reformation of the ECM by the induction of a type 1 plasminogen activator inhibitor (PAI-1), an protease inhibitor (Lane et al., 1992). After the exogenous addition of SPARC to subconfluent endothelial cells, PAI-1 secretion was detected. However, PAI-1 was not secreted from contact-inhibited endothelial monolayers after exogenous treatment with SPARC, suggesting that SPARC may lead to the active remodeling of the ECM (Lane et al., 1992). SPARC is also a known regulator of several growth factors and cytokines. SPARC can sequester growth factors like VEGF or PDGF and has been shown to activate cytokines such as transforming growth factor (TGF)- β 1 as well as insulin-like growth factor 1 (Bornstein and Sage, 2002; Chandrasekhar et al., 1994).

While SPARC has an important role in the adhesion and proliferation of normal cells, much data suggests that SPARC affects the progression of several cancers. The role of SPARC in cancer appears to depend on its diverse functions within specific tissues. In some types of cancer, SPARC is expressed at high levels in tumor cells and correlates with disease progression and poor prognosis, while in others SPARC functions as a tumor suppressor. Aberrant expression of SPARC has been proposed to contribute to malignancies such as breast cancer (Bellahcene and Castronovo, 1995; Gilles et al., 1998), glioblastoma (Rempel et al., 1998), melanoma (Ledda et al., 1997a), ovarian cancer (Porter et al., 1995), and pancreatic cancer (Sato et al., 2003) to name just a few. Although low SPARC expression may be associated with some malignant tumors,

stromal tissue surrounding the tumor may be SPARC positive. The expression and secretion of SPARC in ovarian cancer cells is reduced compared to normal ovarian epithelial cells, which express and secrete SPARC at high levels. Also, forced expression or exogenous addition of SPARC inhibits *in vitro* and *in vivo* tumor growth in ovarian cancer cells (Socha et al., 2009). Within breast cancer, over expression of SPARC inhibited tumor growth and reduced invasion of MDA-MB231 cells through Matrigel (Koblinski et al., 2005). However, others have shown that SPARC increases invasion of breast cancer and prostate cancer cells (Jacob et al., 1999). Increased expression of SPARC has been correlated with increased malignancy in other cancers as well. In malignant melanoma, decreased SPARC expression by transfection using an antisense expression vector resulted in the loss of the ability for these cells to adhere and invade *in vitro* (Ledda et al., 1997b). Knockdown of SPARC with siRNA also decreased glioma cell invasion (Shi et al., 2007). Fibroblasts and/or inflammatory cells in the tumor microenvironment often express SPARC, which may contribute to metastasis in some cancers (Sangaletti and Colombo, 2008), or may be a type of wound healing response to the presence of the tumor. These observations suggest that regulation and function of SPARC are dependent on cellular type. An interesting study done by Haber et al. (2008), demonstrated that SPARC alters the proliferation of stromal cells but not melanoma cells. This raises the idea that the differential expression of SPARC may exist within a tumor and may also affect the progression of the tumor.

Studies on the growth of tumors in SPARC-null mice reveal alterations in the production and organization of the ECM components within and surrounding implanted tumors. The tumor was poorly encapsulated, contained less collagen, collagen fibers

were smaller, and also exhibited a lack of macrophage recruitment (Brekken et al., 2003). These changes in the tumors of SPARC-deficient mice were believed to be due to the changes in the organization of the ECM that created a less restrictive microenvironment for tumor progression. The formation of tumors by the injection of malignant cells into SPARC-null mice has led to controversial results. Subcutaneous injection of lung cancer cells and T cell lymphoma cells showed larger tumor formation in SPARC-null mice compared to wild-type mice (Brekken et al., 2003), while breast cancer cells exhibited a reduced tumor growth in SPARC-null mice compared to wild-type mice (Sangaletti et al., 2003). The mixed results from tumorigenic studies in SPARC-null mice, furthers the evidence that SPARC's role in tumorigenesis is context and cell-type dependent (Arnold et al., 2008; Brekken et al., 2003).

The importance of SPARC expression in human urothelial cancers has been the focus of a limited number of studies. Hudson et al. (2005) was the first group to localize SPARC protein expression to the apical region of suprabasal cells in normal human bladder tissue. Hudson et al. also showed primary urothelial cells to have inhibited cell spreading after addition of recombinant SPARC protein. This inhibition was transient, as cultures were nearly comparable to controls at 6 h and fully recovered by 24 h. The authors suggested urothelial cells may quickly secrete adhesive factors in response to SPARC activity or the recombinant SPARC was quickly degraded or rendered inactive by extracellular processes, as possible explanations to the recovery (Hudson et al., 2005). The anti-spreading ability of SPARC in human urothelial cells was attributed to the C-terminal portion of the third domain in the SPARC protein (Delostrinos et al., 2006).

Another group showed strong SPARC expression in tumor-associated myofibroblasts surrounding invasive urothelial carcinoma human tumors (Nimphius et al., 2007).

Since tumors are a heterogeneous mixture of several cell types, cross-talk is important between the tumor cells and the surrounding stroma to create an environment that is capable of tumor growth and invasion. The tumor cells, their stromal components, and the extracellular matrix are important factors that influence the complex effects of SPARC. Moreover, the location and concentration of SPARC and interactions between SPARC and other molecules, also contribute to the impact of SPARC on target cells. The ability of several cell types to actively produce and secrete SPARC within a tumor can lead to SPARC exerting its effect through a paracrine and autocrine fashion. The expression of SPARC in cancer appears to be dependent on cell type and location, since SPARC has been shown to act as both a tumor suppressor and a tumor promoter; further adding to the complexity of SPARC's influence during tumorigenesis. The therapeutic approach to SPARC, either as a therapy or as a therapeutic target, will depend on the specific role for SPARC in each cell type (Bos et al., 2004).

Characterization of the UROtsa Cell Lines

Although several urothelial bladder cell lines exist, many are not ideal for long-term carcinogenesis studies. The UROtsa cell line was derived from the urothelium lining the ureter of a twelve-year-old female and was immortalized with the simian virus 40 (SV40) large T-antigen (Petzoldt et al., 1995). After immortalization, these cells were non-tumorigenic, as characterized by the inability to form colonies in soft agar and grow tumors in nude mice. The UROtsa cells, when grown in serum containing growth medium, formed a monolayer of cells that was not stratified and has features of basal

epithelial cells (Rossi et al., 2001). However, when the UROtsa cells are adapted to grow in media that does not contain serum, these cells had an altered morphology. Once the serum free cultures gain confluency, they continue to proliferate and form raised three-dimensional structures that were determined by ultrastructural examination to be a stratified layer of cells that strongly resemble the intermediate layer of *in situ* bladder uroepithelium. Numerous desmosomal connections between cells are present as well as abundant cytoplasmic intermediate filaments (Rossi et al., 2001). These cells also retained the properties of immortality and non-tumorigenicity. In order to determine if the process of immortalization altered the expression level of some stress response genes, several metallothioneins (MT) and heat-shock proteins were examined. The expression patterns of MT-1E, MT-1X, and MT-2A genes and MT-1 and 2 proteins as well as Hsp 27, Hsp 60, Hsp 70, and Hsc 70 genes and protein in the UROtsa cells were in agreement with what was observed in the *in situ* human urothelium (Rossi et al., 2001).

Several studies have examined the ability of arsenic to cause toxicity in the UROtsa cells. Rossi et al. (2002) showed that 100 μM of As^{+3} had no effect on the viability of UROtsa cells with an exposure of 4 h and a recovery of 48 h. With a 16 day time-course, up to 4 μM As^{+3} had no effect on cell viability, while 8 μM of As^{+3} caused significant cell death after 8 days (Rossi et al., 2002). Styblo et al. (2000) studied the effect of several different species of arsenic. Exposure of the UROtsa cells to pentavalent arsenicals, arsenate (As^{+5}); monomethylarsonic acid [MMA(V)]; and dimethylarsinic acid [DMA(V)], up to 20 μM for 24 h did not affect cell viability. However, exposure to the trivalent arsenicals, arsenite (As^{+3}), monomethylarsonous acid [MMA(III)], and dimethylarsinous acid [DMA(III)], caused an increase in toxicity in a time- and

concentration- dependent manner. It was determined that trivalent, methylated species of arsenic were the most cytotoxic to UROtsa cells grown in 10% fetal calf serum, and also revealed that MMA(III) caused the greatest toxicity and was the most cytotoxic species of the trivalent arsenicals (Styblo et al., 2000). Bredfeldt et al. (2006) determined that MMA(III) was 20 times more toxic than As^{+3} in UROtsa cells. UROtsa cells had a very low tolerance to the exposure of MMA(III) since concentrations greater than 2 μM were cytotoxic; however, concentrations less than 2 μM induced cell proliferation (Bredfeldt et al., 2006).

Since the methylated arsenicals were determined to cause greater toxicity to UROtsa cells, Styblo and colleagues (2000) analyzed the ability of UROtsa cells to metabolize or methylate arsenic. With culturing in growth media containing fetal calf serum, the UROtsa cells were unable to alter the methylation or metabolism of arsenicals in the cells (Styblo et al., 2000). However, Bredfeldt et al. (2004) found that under serum free culturing conditions, UROtsa cells could methylate As^{+3} to MMA(III) at a low capacity. The differences in methylation when compared to Styblo and colleagues (2000) may be due to culturing the UROtsa cells in serum free growth media, as Rossi et al. (2001) found when UROtsa cells were grown in serum free conditions the cell layer became more stratified. Additional experiments by Drobna et al. (2005) used cloned UROtsa cells expressing the rat arsenic (+3 oxidation state)-methyltransferase (rAS₃MT), termed UROtsa/F₃₅. This cell line has the ability to methylate As^{+3} to MMA(V), MMA(III), DMA(V), and DMA(III), while the normal UROtsa cells cannot methylate As^{+3} when cultured in serum free growth media. After acute treatment with As^{+3} , UROtsa/F₃₅ cells had a greater level of toxicity than the non-expressing parent UROtsa

cells. Further analysis showed the UROtsa/F₃₅ cells had actually retained less arsenic than the UROtsa cells, but a significant portion of the arsenic retained by the UROtsa/F₃₅ cells were methylated metabolites of As⁺³ and these metabolites were found to be absent from the parent UROtsa cells (Drobna et al., 2005). Thus, the increased susceptibility of UROtsa/F₃₅ cells to As⁺³ was associated with the production and cellular retention of methylated arsenicals (Hester et al., 2009). Recently, Ren et al. (2011) translated their findings from yeast mutants to the UROtsa cells. Over-expressing N-6 adenine-specific-DNA methyltransferase 1 (N6AMT1), a methyltransferase, in UROtsa cells led to an increased resistance to the toxic effects of As⁺³ or MMA(III). These cells were capable of converting MMA(III) to the less toxic forms MMA(V) and DMA(V) through methylation (Ren et al., 2011).

The stress induced response of the UROtsa cells to arsenic was analyzed by Bredfeldt et al. (2004), who described an increase in ubiquitin-conjugated proteins was a result from an acute, low-level As⁺³ exposure. The increase in ubiquitin-conjugated proteins was also seen following exposure of UROtsa cells to buthionine sulfoximine, a compound that decreases the glutathione concentration, implying stressors may deplete the cells of antioxidants making them more susceptible to As⁺³ induced toxicity (Bredfeldt et al., 2004). Since antioxidants play a role in protecting UROtsa cells from As⁺³ toxicity, the notion that As⁺³ may induce the formation of reactive oxygen species (ROS) was explored. Eblin et al. (2006) reported that both As⁺³ and MMA(III) increased ROS in UROtsa cells and this induction was inhibited when cells were pretreated with antioxidants. Wang and colleagues (2007a) established that Nrf2, a transcription factor which regulates cellular antioxidant response, provided protection of the UROtsa cells

from the toxicity of As^{+3} or MMA(III). The cells were also more resistant to the toxicity of As^{+3} at concentrations ranging from 0-80 μM and MMA(III) concentrations ranging from 0-12 μM when Nrf2 was activated by known pathway inducers (Wang et al., 2007a). Similarly, UROtsa cells with Nrf2 knockdown were more sensitive to the toxic effects of As^{+3} and MMA(III) and had higher levels of ROS (Wang et al., 2007a).

Although the epidemiological evidence for the support of arsenic induced carcinogenesis is substantial, the ability of arsenic to malignantly transform urothelial cells had not yet been determined. Bredfeldt et al. (2006) determined that the parental UROtsa cells were capable of transformation by the toxic, trivalent methylated species of arsenic, MMA(III). It was demonstrated that parental UROtsa cells chronically exposed to 50 nM MMA(III) for a period of 52 weeks underwent phenotypic changes consistent with malignant transformation, i.e., increased rate of proliferation, anchorage independent growth, and formation of tumors in immune-compromised mice (Bredfeldt et al., 2006). The morphology of the MMA(III) transformed cells were similar in size to the non-treated parents, but the transformed cells had a cell membrane that was less defined and an increase in the appearance of multinucleated cells that contained an abundance of cytoplasm. The histology of the tumors that were generated by the heterotransplants of UROtsa cells transformed by MMA(III) into immune-compromised mice were characteristic of squamous cell carcinoma with moderate differentiation and contained numerous deposits of keratin (Bredfeldt et al., 2006).

Although Bredfeldt et al. (2006) determined the transformation of UROtsa cells with 50 nM MMA(III) took 52 weeks (URO-MS52), Wnek et al. (2010) was able to observe the malignant changes Bredfeldt et al. (2006) saw, in as early as 12 weeks of

exposure using the same concentration of MMA(III). Interestingly, the UROtsa cells exposed for 12 weeks, were then also cultured for additional 12 or 24 weeks in the absence of MMA(III). After 12 weeks of MMA(III) exposure (URO-MS12), there was a 30% decrease in cell doubling time to 26 h as compared to the non-treated parent at 38 h. The doubling times were also decreased upon removal of MMA(III) as demonstrated in URO-MS12+12(-) and URO-MS12+24(-), cells cultured for 12 or 24 weeks after the removal of the MMA(III), compared to parental UROtsa cells. The morphology by confocal microscopy of the URO-MS12 cells as well as the URO-MS12+12(-) and URO-MS12+24(-) were similar to that of the URO-MS52 cells (Wnek et al., 2010). The only morphological difference was the URO-MS12 cells had an increase in cell diameter compared to non-treated UROtsa and URO-MS52 cells and the increased cell diameter held true for the cells cultured for additional 12 or 24 weeks without the MMA(III). The assessment of these cells for tumorigenicity by growth in soft agar was first seen at 12 weeks of MMA(III) exposure. When these cells were cultured after the removal of MMA(III) for an additional 12 or 24 weeks, there was an increase in colony formation in soft agar as compared to UROtsa controls or URO-MS12 cells. An increase of tumorigenicity was also seen in the ability of these cells to form larger tumors in immunodeficient mice, with the largest tumors formed by the URO-MS12+24(-) cells.

Several proinflammatory cytokines (IL-1 β , IL-6 and IL-8) were significantly over-expressed in UROtsa cells acutely exposed (12 h) to MMA(III) and the cellular production of these cytokines was sustained in cells transformed by MMA(III) for 12 weeks (Escudero-Lourdes et al., 2010). IL-8 mRNA expression levels had a threefold

induction in URO-MSC12 cells compared to unexposed cells and IL-8 was also found to be secreted into the growth media at five times greater than was seen in controls (Escudero-Lourdes et al., 2012). The receptor of IL-8, CXCR1, had a significantly enhanced internalization rate in URO-MSC12 cells. Similarly, the production of IL-8 was also found to be increased in the tumors derived from these cells compared to non-exposed UROtsa heterotransplants. Additionally the expression of MMP-9, cyclin D1, bcl-2, and VEGF were significantly up-regulated in the same cells that up-regulated IL-8 expression; however, with IL-8 gene silencing these mitogen-activated kinases were significantly decreased. Also affected with IL-8 gene silencing, was a decrease in cellular proliferation rate and a reduced ability to form colonies in soft agar. These results suggest a relevant role of IL-8 in MMA(III) induced UROtsa cell transformation.

Since the human bladder is exposed to several different environmental carcinogens, Sens et al. (2004) determined if As^{+3} and/or Cd^{+2} could directly cause the malignant transformation of human urothelium cells. This group was the first laboratory to develop transformed bladder cell lines using these metals. A long-term *in vitro* exposure to a low dose of Cd^{+2} or As^{+3} on the non-tumorigenic UROtsa cell line was used to generate transformed UROtsa cell lines. Using confluent cultures of serum free or serum containing UROtsa cells, 1 μM of either Cd^{+2} or As^{+3} was added to the growth media and thereafter cells were fed every three days with fresh growth media containing 1 μM of Cd^{+2} or As^{+3} . During the first 30 days of exposure, no cell death was detected with only a slight increase in granular appearance. However, between 30 and 48 days of exposure, over 95% of the cells in all four experimental groups died. These cells were continually fed on the three day cycle with 1 μM of either Cd^{+2} or As^{+3} and within 15 to

30 days all four groups had multiple clones of proliferating cells, which were allowed to attain confluency and passaged at a 1:4 ratio. With routine culturing of feeding and passaging, the four groups again experienced a round of over 95% cell death. Again, clones developed and proliferated quickly overtime. Once confluent cultures were attained and subcultured, the growth rates of all four experimental groups were determined to be much faster than the parental UROtsa cells. The serum free cells were thereafter subcultured at a 1:10 ratio and the serum containing cultures at 1:20. These cultures were subcultured an additional eight passages in the presence of 1 μM of Cd^{+2} or As^{+3} to guarantee no additional cell death occurred.

The morphology, as examined by phase microscopy, determined that all the cultures retained an epithelial morphology regardless of growth media or exposure to Cd^{+2} or As^{+3} . However, the previous differences that existed in the morphology of cells grown in serum free media were no longer apparent. After exposure to Cd^{+2} or As^{+3} , the cells lost their ability to stratify upon attaining confluence. All four experimental groups were capable of forming colonies in soft agar and generated tumors when heterotransplanted into nude mice. The Cd^{+2} or As^{+3} treated cells in serum containing growth media formed tumors in 9 of 10 mice. As^{+3} exposed cells in serum free growth media formed tumors in 5 of 8 nude mice (with 2 dying of unknown causes) and the Cd^{+2} exposed cell in serum free media formed tumors in 7 of 10 mice. The tumors that resulted from the injection of UROtsa cells transformed by Cd^{+2} were epithelial in nature and had features consistent with those found in urothelial carcinoma, with only modest evidence of squamous differentiation. The As^{+3} -transformed cells formed tumors that displayed dominant features of squamous differentiation, including concentrically laminated

deposits resembling keratin “pearls,” granules resembling the keratohyaline seen in the granular layer of the epidermis, and cells with prominent intercellular connections similar to the granulosa or spinous cells within the epidermis (Sens et al., 2004). Within the general patient population, the majority of bladder cancers are urothelial carcinoma with little to no evidence of squamous differentiation. However the presence of squamous differentiation within bladder tumors is usually associated with a more aggressive cancer and a poorer prognosis.

Next, an additional round of UROtsa cell line transformation with Cd^{+2} (Somji et al., 2010) or As^{+3} (Cao et al., 2010) was performed to determine if independent exposures of the UROtsa cells to the heavy metals would result in cell lines with similar phenotypic properties. In total, seven Cd^{+2} and six As^{+3} isolates were established. For the Cd^{+2} cell lines, each isolate had varying doubling times ranging from 16.4 ± 1.8 h to 27.8 ± 0.6 h while the UROtsa parent had a doubling time of 33.2 ± 0.8 h. All seven Cd^{+2} transformed cell lines had a similar epithelial morphology, formed colonies in soft agar, and formed tumors in nude mice with an urothelial carcinoma histological presentation with modest differences in the degree of squamous differentiation. However, only one isolate, $\text{Cd}^{\#1}$, was effective at forming tumors when injected within the peritoneal cavity of immune-compromised mice (Somji et al., 2010). The additional five isolates of As^{+3} -transformed urothelial cells had varying doubling times ranging from 14.1 ± 0.9 h to 33.3 ± 1.4 h, had similar epithelial morphology, formed colonies in soft agar, and formed tumors in nude mice with each displaying prominent areas of squamous differentiation. Thus the additional As^{+3} isolates had similar phenotypic properties to the initial As^{+3} -transformed isolate (Cao et al., 2010). Following intraperitoneal injection of each of the

six As⁺³-transformed isolates, As^{#1} and As^{#3} were able to form hundreds of tumor nodules within the peritoneal cavity of nude mice. As^{#4} and As^{#6} isolates were only able to form a few tumor nodules, while As^{#2} and As^{#5} did not form any nodules after intraperitoneal infection. It should be noted that the parental UROtsa cells do not form tumors when injected either subcutaneously or into the peritoneal cavity of nude mice. Since bladder cancer has been shown to spread locally within the human body after penetrating through the bladder wall, tumor cells are capable of colonizing multiple peritoneal organs. Aggressive tumors extend into the bladder wall; while more advanced stages may invade the adjacent prostate and seminal vesicles in males, and the ureters and retroperitoneum in both males and females (Cao et al., 2010). The ability of the Cd⁺² and As⁺³-transformed UROtsa cell lines to likewise form intraperitoneal tumors further enhances the translational capacity of this cell line.

Since the expression of keratin 7 has been shown to be expressed in normal human urothelium and its expression can be altered after malignant transformation, Somji et al. (2010 and 2011a) characterized its expression in the UROtsa cell lines. It was determined that keratin 7 was expressed in 6 of the 7 Cd⁺²-transformed UROtsa cell lines and in 4 of the 6 As⁺³-transformed cell lines (Somji et al. 2010 and 2011a). Interestingly, the cell lines that did not express keratin 7 were the only cell lines that were capable of forming tumors when injected into the intraperitoneal cavity of immune-compromised mice. The transformed cell lines that lacked keratin 7 expression, also lacked keratin 7 expression in the subcutaneous tumors generated from these cell lines. (Somji et al., 2010; Somji et al., 2011a). Therefore, it was determined that urothelial tumors produced through arsenite exposure can repress and gain keratin 7 expression depending on

transplantation site. Further analysis determined that although keratin 7 expression levels varied within the Cd⁺² and As⁺³-transformed cell lines, the expression of its keratin 19 binding partner remained relatively constant (Somji et al., 2011a). The expression of keratin 6, 16, and 17 was also examined for the localization of these proteins to areas of squamous differentiation within urothelial tumors, as areas of squamous differentiation in patients with bladder cancer have been associated with a more aggressive cancer and a poor prognosis. Results showed the expression of keratin 6, 16, and 17 were very similar within the Cd⁺² and As⁺³-transformed cell lines (Cao et al., 2010; Somji et al., 2008; Somji et al., 2011a). A special emphasis was placed on keratin 6 expression, with keratin 6 having the potential to be a sensitive marker for squamous differentiation in Cd⁺² and As⁺³ induced urothelial cancers. The expression of keratin 6 was shown to be localized to areas of squamous differentiation within the subcutaneous tumors generated by the Cd⁺² and As⁺³-transformed cell lines. When the intraperitoneal tumors were analyzed for histological expression of keratin 6, areas of squamous differentiation were also positive for its expression (Cao et al., 2010; Somji et al., 2011a). The expression patterns and localization of several keratin proteins within the UROtsa cell lines show the marked differences in keratin expression that exist between regions with and without squamous differentiation in urothelial carcinoma.

Since substantial evidence exists to support the ability of arsenic and cadmium to exert their carcinogenetic effect through the induction of epigenetic changes leading to aberrant gene expression, the UROtsa cell lines were analyzed for histone modifications after treatment with Cd⁺², As⁺³, or MMA(III) or after malignant transformation by those heavy metals. Chu et al. (2001) analyzed the UROtsa cells for histone modifications that

resulted after treatment with two forms of arsenic, As⁺³ or MMA(III). Using the metabolic labeling technique called SILAC or Stable Isotope Labeling of Amino acid in Cell culture, it was determined there was a reduction in the acetylation levels on several histones (Chu et al., 2011). Specifically, histones H3 and H4 lysine residues had decreased acetylation levels in UROtsa cells exposed to arsenic when compared to non-treated UROtsa controls (Chu et al., 2011). Jo and colleagues (2009) similarly treated UROtsa cells with both As⁺³ or MMA(III), and determined a reduction of acetylation at histone H4 lysine 16 (H4K16) using mass spectrometry. When the expression of MYST1, an H4K16 acetyltransferase, was knocked down in the UROtsa cells, a reduction in the acetylation of H4K16 was seen that also correlated with an increased sensitivity to the toxic effects of As⁺³ or MMA(III) (Jo et al., 2009).

Epigenetic changes were also seen in the UROtsa cells transformed by 50 nM MMA(III). In studies by Wnek et al. (2010), the DNA methylation patterns between the non-transformed and MMA(III) transformed UROtsa cells were analyzed. An interesting finding was that the observed phenotypic changes that occurred during the transformation of the UROtsa cells by MMA(III), i.e. hyperproliferation, colony formation in soft agar, and tumor formation in immune-compromised mice, coincided with changes in the DNA methylation of gene promoter regions that are associated with malignant transformation. These changes include the expression of genes involved in an oxidative stress response, decreases in specific DNA repair genes, up-regulation of genes involved in proliferation, and the suppression of inflammatory components (Medeiros et al., 2012). The UROtsa cells transformed by MMA(III) for 12 weeks showed no difference in the methylation of these promoter regions compared to the normal UROtsa parent cells. However, an

increase in DNA methylation was seen in the 12 week MMA(III) transformed cells that were continually cultured after the MMA(III) was removed, with the highest frequency of DNA methylation seen in the URO-MS12+24(-) cells (Wnek et al., 2010).

Another study by Somji et al. (2011b) examined the differences in epigenetic regulation of metallothionein 3 (MT-3) gene expression between the parental UROtsa cells and the Cd⁺² and As⁺³-transformed UROtsa cell lines. Since MT-3 is not expressed in normal urothelium or in the UROtsa cell lines, but MT-3 is expressed in urothelial cancer and in tumors generated from the UROtsa cells that have been transformed by Cd⁺² or As⁺³; the role of the epigenetic regulation was analyzed (Somji et al., 2011b). Histone H4 acetylation was found to be increased in the MT-3 promoter of both the parental and transformed cell lines after treatment with the epigenetic regulator MS-275, indicating a state of transcriptional readiness. The H4 antibody was not able to distinguish between the four potentially acetylated lysines 5, 8, 12, and 16. Also, an increase in histone methylation was determined in histone H3 lysine 9 and 27 of the transformed cells, leading to a transcriptionally repressed state (Somji et al., 2011b). It was therefore concluded that the MT-3 promoter in the Cd⁺² and As⁺³-transformed UROtsa cell lines had gained bivalent chromatin structure, that is having elements of “transcriptionally repressed” and “transcriptionally ready,” when compared to the parental UROtsa cells (Somji et al., 2011b). Taken together, these studies revealed posttranslational modifications on chromatin proteins, especially histones, modulate alterations in the accessibility of DNA in response to environmental exposures and heavy metals.

The UROtsa cell lines were further characterized in terms of their mechanisms of cell death when exposed to Cd^{+2} or As^{+3} . The UROtsa parent cells when treated with Cd^{+2} or As^{+3} primarily had a route of cell death that was through apoptosis, however there was also a significant contribution of necrotic cell death (Somji et al., 2006). The determination that both processes were responsible for cell death was made by both qualitative and quantitative measurements. Approximately 30% of the parental UROtsa cells died by necrosis and it appeared that the remaining 70% died through apoptosis when exposed to either metal. Interestingly, the Cd^{+2} or As^{+3} malignantly transformed UROtsa cells showed a differing route of cell death than the parental UROtsa cells. The transformed UROtsa cells were more resistant to the effects of each metal and shifted away from apoptosis and more toward a mechanism of cell death by necrosis. The transformed cells did show some signs of apoptosis by DAPI staining, DNA laddering, and caspase activation, but at reduced levels relative to the parental cells. In contrast, lactate dehydrogenase (LDH) release into the growth media was significantly up-regulated in the transformed cells as compared to the parental cells. Therefore, the UROtsa parental cells mainly die through the controlled cell death via apoptosis while the Cd^{+2} and As^{+3} -transformed cells were found to predominately die by necrosis when exposed to toxic levels of the metals.

Rationales, Purposes, and Hypotheses

A previous paper by Chai et al. (2007) showed that normal human urothelial cells treated with arsenic had an increase in the expression of beclin-1 protein and also the appearance of double membrane-bound vacuoles in the cytoplasm of these cells. The increase in autophagy markers was seen with increasing concentrations of arsenic

treatment. Since the UROtsa cell lines have been previously characterized for the role of cell death by necrosis and apoptosis, the purpose of the first study outlined in chapter two is to determine the role autophagy plays within the UROtsa cell model for bladder carcinogenesis by extending the characterization of cell death mechanisms to include autophagy. The hypothesis of this study is that autophagy will play a role within the cell death mechanisms of the UROtsa cell model and that the expression of beclin-1 as well as several autophagy associated gene products will increase after treatment of the UROtsa cells with Cd^{+2} or As^{+3} .

The second study, outlined in chapter three, was motivated by the results of a microarray analysis that revealed SPARC to be the most repressed gene across all the cadmium and arsenic transformed UROtsa cell lines. These results were surprising since no other gene has been shown to be down-regulated within all 13 of the transformed UROtsa cell lines. The purpose of this study is to determine the gene expression of SPARC in the UROtsa cell model as well as in bladder cancer through the hypothesis that a reduction in SPARC expression is associated with a malignant phenotype.

The third study, outlined in chapter four, is an extension of the second study. It was previously determined that SPARC expression was at the limit of detection in the Cd^{+2} or As^{+3} transformed cell lines, the malignant epithelial component of tumor heterotransplants derived from the transformed cell lines, and the tumor cells of archival specimens of human bladder cancer. The purpose of this study is to determine if SPARC can be transfected into select transformed UROtsa cell lines and if the forced expression of SPARC alters the ability of these cells to be tumorigenic. The hypothesis of the third study is that the SPARC transfected UROtsa cell lines will have a decrease in malignant

properties and that these cells are likely to have altered migration, invasion, and wound closing capabilities compared to low SPARC-expressing controls.

CHAPTER II

BECLIN-1 EXPRESSION IN NORMAL BLADDER AND IN CD⁺² AND AS⁺³ EXPOSED AND TRANSFORMED HUMAN UROTHELIAL CELLS (URO TSA)

Jennifer L. Larson¹, Seema Somji², Xu Dong Zhou², Mary Ann Sens²,
Scott H. Garrett², Donald A. Sens², and Jane R. Dunlevy¹

Department of Anatomy and Cell Biology¹

Department of Pathology²

School of Medicine and Health Sciences

University of North Dakota

Grand Forks, ND

Toxicology Letters 195 (2010) 15-22

Copyright
2010
by
Elsevier Limited
The Boulevard
Langford Lane
Kidlington, Oxford OX5 1GB UK

Used by permission
49

Abstract

The expression of beclin-1 in normal human bladder and in Cd⁺² and As⁺³ exposed and transformed urothelial cells (UROtsa) was examined in this study. It was shown using a combination of real-time PCR, western analysis and immunohistochemistry that beclin-1 was expressed in the urothelial cells of the normal bladder. It was also demonstrated that the parental UROtsa cell line expressed beclin-1 mRNA and protein at levels similar to that of the *in situ* urothelium. The level of beclin-1 expression underwent only modest alterations when the UROtsa cells were malignantly transformed by Cd⁺² or As⁺³ or when the parental cells were exposed acutely to Cd⁺² or As⁺³. While there were instances of significant alterations at individual time points and within cell line-to-cell line comparisons there was no evidence of a dose-response relationship or correlations to the phenotypic properties of the cell lines. Similar results were obtained for the expression of the Atg-5, Atg-7, Atg-12 and LC3B autophagy-related proteins. The findings provide initial evidence for beclin-1 expression in normal bladder and that large alterations in the expression of beclin-1 and associated proteins do not occur when human urothelial cells are malignantly transformed with, or exposed to, either Cd⁺² or As⁺³.

Introduction

The UROtsa cells are an immortalized cell culture model of human urothelium that was developed through immortalization of a primary culture of human urothelial cells with the SV40 large T-antigen (Petzoldt et al., 1994; Petzoldt et al., 1995). The UROtsa cells grow as a contact inhibited monolayer and are not tumorigenic as judged by the inability to form colonies in soft agar and tumors in nude mice. When adapted for

growth in a serum free medium, they show enhanced differentiation with a stratified morphology consistent with the structural features associated with the intermediate layers of the urothelium (Rossi et al., 2001). This laboratory has shown that exposure of the UROtsa cells to either Cd^{+2} or As^{+3} can directly cause malignant transformation of the cells (Sens et al., 2004). The tumor heterotransplants produced by the Cd^{+2} and As^{+3} transformed cells had histologic features consistent with human urothelial cell carcinoma of the bladder. The parental UROtsa cells and their Cd^{+2} and As^{+3} transformed counterparts have been used to define the mechanism of cell death following exposure of the cells to cytotoxic levels of Cd^{+2} and As^{+3} (Somji et al., 2006). In this study it was demonstrated that the parental UROtsa cells died by both apoptosis and necrosis when exposed to either metal. It was also shown that apoptosis was the more prominent mechanism of cell death in the parental cells, accounting for over 50% of cell death. For the transformed UROtsa cells, it was shown that they were more resistant to the toxic effects of both metals and that the apoptotic mechanism of cell death was decreased and necrosis increased compared to the parental UROtsa cells. Subsequently, a third mechanism of cell death, called autophagic cell death, has been proposed in the literature that can operate separately or in concert with necrosis or apoptosis (Kroemer and Levine, 2008; Maiuri et al., 2009; Sinha and Levine, 2008; Todde et al., 2009). It has been suggested that arsenic salts can induce autophagic cell death in SV40 immortalized human urothelial cells (Chai et al., 2007).

Autophagic cell death has been characterized by the large scale sequestration of portions of the cellular cytoplasm in autophagosomes, which gives the cell a vacuolated appearance characteristic of autophagy (Kroemer and Levine, 2008). Transmission

electron microscopy is used to identify autophagosomes as double-membrane vesicles that contain cytosol or morphologically identifiable cytoplasmic organelles.

Autolysosomes arise from the fusion of autophagosomes and lysosomes which are characterized by a single membrane that contains degenerating organelles undergoing the process of digestion by lysosomal enzymes. The autophagy pathway is conserved among all eukaryotes, is active under homeostatic conditions to remove aged organelles, and many autophagy effectors (Atg proteins) as well as other protein regulators have been identified in the last decade (Sinha and Levine, 2008). Among these effectors, beclin-1, has been shown to be an essential effector of autophagy (Sinha and Levine, 2008). Mice with a biallelic loss of beclin-1 are early embryonically lethal (Qu et al., 2003; Yue et al., 2003). Mice with monoallelic loss of beclin-1 have an increased incidence of spontaneous tumor formation (Qu et al., 2003; Yue et al., 2003), have abnormal proliferation of mammary epithelial cells (Qu et al., 2003), increased susceptibility to neurodegeneration (Pickford et al., 2008) and cardiomyopathy (Tannous et al., 2008). In humans, monoallelic deletions of beclin-1 are observed frequently in sporadic breast, ovarian and prostate cancer (Aita et al., 1999). Due to the essential role of beclin-1 in effecting the autophagic process in cells, the present study examines its expression in normal urothelium and in urothelial cells exposed to, and transformed by, Cd^{+2} and As^{+3} . The first goal was to determine if beclin-1 is expressed in normal bladder urothelium. The second goal was to determine if beclin-1 expression is altered by malignant transformation of urothelial cells by Cd^{+2} or As^{+3} . Lastly, to determine if beclin-1 expression was altered by acute exposure of urothelial cells to Cd^{+2} or As^{+3} .

Materials and Methods

Human Bladder Specimen for Immunohistochemical and Molecular Analysis

Specimens of normal human bladder were obtained from five patients undergoing a cystectomy for bladder cancer. For molecular analysis, the samples were immediately snap-frozen in liquid nitrogen. For immunohistochemical analysis, paraffin blocks were routinely fixed in neutral buffered formalin for 16-18 h. All tissues were transferred to 70% ethanol and dehydrated in 100% ethanol. Dehydrated tissues were cleared in xylene, infiltrated, and embedded in paraffin. All tissue acquisition was approved by the institutional review board (IRB) for human research.

Immunohistochemistry

Serial sections were cut at 3-5 μm for use in immunohistochemical protocols. After deparaffinization, sections were immersed in preheated Target Retrieval Solution (Dako, Carpinteria, CA) and heated in a steamer for 20 min. The sections were allowed to cool for 30 min at room temperature and immersed into Tris Buffered Saline with Tween 20 (Dako) for 5-10 min. Beclin-1 was detected using the Dako EnvisionTM+ kit (Dako) with an anti-beclin-1 rabbit polyclonal antibody (1:100) purchased from Cell Signaling (Cell Signaling Technology, Beverly, MA). After antigen retrieval, the sections were treated with Peroxidase Blocking Reagent for 10 min at room temperature. The slides were incubated overnight with the primary antibody at 4°C after which they were rinsed with the wash buffer (Dako). The slides were then incubated with the Peroxidase Labeled Polymer for 30 min at room temperature, rinsed and developed using liquid diaminobenzidine for visualization of the reaction product. The slides were rinsed in distilled water, counterstained with hematoxylin, dehydrated in graded ethanol, cleared

in xylene and cover slipped. Normal human breast and prostate tissues were used as positive controls, and a negative control consisted of omission of the primary antibody from the immunohistochemical sequence.

RNA and Protein Isolation from Human Bladder

Frozen tissue was ground to a powder under liquid nitrogen. Total cellular RNA was isolated from the frozen, powdered tissue using protocols supplied with TRI REAGENT™ (MRC, Cincinnati, OH) as previously described by this laboratory (Garrett et al., 1998). Purity and concentration of each sample were determined by spectrophotometric assay. All RNA samples utilized demonstrated no evidence of degradation as determined by intact bands of 18S and 28S ribosomal RNA following electrophoresis on 1.2% agarose gels. Proteins were extracted from the powdered tissue by dissolving it in 2% SDS containing 50 mM Tris-HCl, pH 6.8, followed by boiling for 10 min. DNA was sheared by passing the tissue extract through a 23-gauge needle. Protein concentration was determined by the bicinchoninic acid (BCA) protein assay (Pierce Chemical Co., Rockford, IL) before 100 mM dithiothreitol (DTT) was added to each sample.

Cell Culture

Stock cultures of the parental UROtsa cell line and UROtsa cell lines malignantly transformed by Cd⁺² and As⁺³ were maintained in 75 cm² tissue culture flasks using Dulbecco's modified Eagles' medium (DMEM) containing 5% v/v fetal calf serum in a 37°C, 5% CO₂: 95% air atmosphere (Rossi et al., 2001). Confluent flasks were sub-cultured at a 1:4 ratio using trypsin-EDTA (0.05%, 0.02%) and the cells were fed fresh growth medium every 3 days.

Visualization of DAPI-Stained Cells

Toxic effects of Cd⁺² and As⁺³ on the UROtsa cells was determined by visualization of 4',6-diamidino-2-phenylindole (DAPI)-stained nuclei as described previously by this laboratory (Somji et al., 2004). At the indicated time points, cell monolayers were washed twice with phosphate buffered saline (PBS), fixed for 10 min in 70% ethanol, rehydrated in 1 mL PBS, and stained with 10 µL DAPI (10 µg/ml in distilled water). For analysis, each well was examined under epifluorescent illumination at 40 x magnification on a Zeiss Axiovert 35 inverted microscope with SPOT RT Slider digital camera using Adobe Photoshop.

Real Time Analysis of Beclin-1 mRNA Expression

The expression of beclin-1 mRNA was determined by real-time reverse transcription polymerase chain reaction (RT-PCR) using commercially available primers from Qiagen (Valencia, CA). Total RNA was purified from the cell lines as well as the tissue sample and 1 µg was subjected to cDNA synthesis using the iScript cDNA synthesis kit (Bio-Rad Laboratories, Hercules, CA) in a total volume of 20 µL. Amplification of the cDNA was performed using the SYBR Green kit (Bio-Rad Laboratories) with 2 µL cDNA and 0.2 µM primers in a total volume of 20 µL in an iCycler iQ real-time detection system (Bio-Rad Laboratories). Amplification was monitored by SYBR Green fluorescence. Cycling parameters consisted of denaturation at 95°C for 15 sec, annealing at 55°C for 30 sec, and extension at 72°C for 30 sec, which gave optimal amplification efficiency. The expression levels for the autophagy genes in the normal and transformed cell lines and human bladder tissue were determined relative to the UROtsa parental cells using serial dilutions of this sample for the standard curve.

The resulting relative levels were then normalized to the change in β -actin expression evaluated by the same assay using the primers, sense: CGACAACGGCTCCGGCATGT, and antisense: TGCCGTGCTCGATGGGGTACT, with cycling parameters of annealing/extension at 62°C for 45 sec and denaturing at 95°C for 15 sec.

Western Analysis of Beclin-1, Atg-5, Atg-7, Atg-12 and LC3B Expression

Confluent cultures were harvested in 2% SDS and 50 mM Tris-HCl, pH 6.8, followed by boiling for 10 min and DNA shearing through a 23-gauge needle. Protein concentration was determined by the BCA protein assay before 100 mM DTT was added to each sample. Ten micrograms of total cellular protein was separated on a 12.5 % SDS-PAGE gel and transferred to a hybond-P polyvinylidene difluoride (PVDF) membrane (Amersham Biosciences, Piscataway, NJ). Membranes were blocked in Tris buffered saline (TBS) containing 0.1% Tween-20 (TBS-T) and 5% (w/v) non-fat dry milk for 1 h at room temperature. After blocking, the membranes were probed with the appropriate primary antibody diluted in blocking buffer overnight. The primary antibodies used were beclin-1 (1:2000), Atg-5 (1:2000), Atg-7 (1:1000), Atg-12 (1:1000) and LC3B (1:1000). All primary antibodies were purchased from Cell Signaling Technology. After washing three times in TBS-T, membranes were incubated with the anti-mouse or anti-rabbit secondary antibody (1:10,000) in antibody dilution buffer for one hour. The blots were visualized using the Phototope-HRP Western blot detection system (Cell Signaling). To determine equal loading of samples, membranes were stripped of bound proteins by incubating in 100mM 2-Mercaptoethanol, 2% SDS, 62.5 mM Tris HCl pH 6.7 at 50°C for 30 min. Membranes were washed twice with PBS in 0.5% Tween-20 at room temperature and blocked following the previously mentioned protocol. Membranes were

reprobed using 0.2 µg/ml of the anti β-actin antibody (Abcam, Cambridge, MA) followed by incubation with a 1:10,000 dilution of the anti-mouse secondary antibody. The western blots were quantified using NIH Image J Software by determining the Integrated Optical Density (IOD) for each band and graphed relative to the UROtsa parent or control. Statistical analysis consisted of ANOVA with Tukey posthoc testing using GraphPad PRISM 4 software with a level of significance of $p < 0.001$.

Results

Expression of Beclin-1 in Normal Urothelium

Five samples of human bladder obtained from a surgical procedure after completion of diagnostic needs were used to determine the expression and localization of beclin-1 protein (Figure II-1). The results demonstrated that the urothelium was moderately immunoreactive for beclin-1, with the suggestion of a gradient of increasing expression from the basal cell layer to the apical urothelial cells. The bladder stroma had limited expression of beclin-1, but there were scattered inflammatory and stromal cells throughout that were clearly immunoreactive for beclin-1. The illustration presented is from a specimen where normal urothelium was well-removed geographically from tumor tissue, but all five samples gave similar staining patterns for beclin-1 in areas of normal urothelium. Total RNA prepared from the sample used above to illustrate beclin-1 staining was shown to contain beclin-1 specific mRNA using real time PCR and beclin-1 specific primers (Figure II-2A). A protein extract prepared from the same sample was shown to contain beclin-1 protein using western analysis and a beclin-1 specific antibody (Figure II-2B). Lower molecular weight bands were noted on the western blot using beclin-1 and β-actin antibodies, respectively. These bands presumably are degradation

products due to the length of time between surgical removal and preparation of the sample for research. The other four samples also showed beclin-1 mRNA and protein expression, but due to the extent of tumor involvement they might contain some contamination from urothelial cancer cells.

Basal Expression of Beclin-1 in Parental UROtsa Cells and UROtsa Cells Transformed by As⁺³ and Cd⁺²

The laboratory has described the direct malignant transformation of the parental UROtsa cells by both As⁺³ and Cd⁺² (Sens et al., 2004). Recent studies have isolated additional independent isolates of As⁺³ and Cd⁺² transformed UROtsa cells (Cao et al., 2010; Somji et al., 2010). The parental UROtsa cells, the 6 independent isolates of the As⁺³ transformed cells, and the 7 independent isolates of the Cd⁺² transformed cells were all assessed for their basal expression of beclin-1 mRNA (Figure II-3) and protein (Figure II-4). The expression of beclin-1 mRNA was similar between the parental UROtsa cells and 4 of the 6 isolates of the As⁺³, and 3 of the 7 isolates of Cd⁺², transformed UROtsa cells (Figure II-3). Two isolates of the As⁺³ transformed cells and 4 isolates of the Cd⁺² transformed cells had elevated expression of beclin-1 mRNA (Figure II-3). The corresponding analysis of beclin-1 protein demonstrated that 4 of the 6 As⁺³ transformed isolates had a reduced expression of beclin-1 compared to parental UROtsa cells (Figure II-4). Beclin-1 expression in the other 2 isolates showed one to be identical to parental control and the other elevated compared to parent cells. Beclin-1 protein expression when compared to parent was elevated in 5 of the 7 isolates of Cd⁺² transformed cells and reduced in two isolates (Figure II-4). A comparison of beclin-1 mRNA and protein expression among the isolates demonstrates that there is only a very weak correlation between the level of mRNA and the corresponding expression of

beclin -1 protein. For the As^{+3} transformed UROtsa cells, only isolate #6 shows an increase in both beclin-1 mRNA and protein. For the Cd^{+2} transformed UROtsa cells, 4 of 7 isolates show an agreement between an elevated level of mRNA and increased protein expression, but the magnitude of the increase in protein does not follow the pattern of mRNA expression. The differences in the level of beclin-1 protein among all the isolates were modest, varying between a decrease of 50% and a 2-fold increase over control.

Beclin-1 Expression in Parental UROtsa Cells Exposed to Cd^{+2} and As^{+3}

The parental UROtsa cells were exposed to 1.0, 2.0 and 4.0 μM Cd^{+2} with extracts prepared at 8, 16, 24, 36 and 48 h of exposure for the analysis of beclin-1 protein. Similarly, to determine the effect of As^{+3} , the cells were exposed to 2.5, 4.5 and 6.0 μM As^{+3} with extracts prepared at 4, 8, 16, 24, and 36 h of exposure for the analysis of beclin-1 protein. The concentrations and times of exposure were chosen such that no loss of cell viability would occur at the lowest 2 concentrations over the time course, while the highest concentration would cause at least a 50% loss of cell viability at the final point in the respective time course. The concentrations and times of exposure were based on data from previous studies from the laboratory (Somji et al., 2006) and cell viabilities were confirmed in the present study (data not shown). The results of this analysis demonstrated that there was only a minimal alteration in the level of beclin-1 protein when UROtsa cells were exposed to concentrations of Cd^{+2} (Figure II-5) and As^{+3} (Figure II-6) that elicited no loss of cell viability. An interesting finding was that there did appear to be an effect on basal beclin-1 expression following addition of fresh growth medium to the cells. When the parental UROtsa cells were fed fresh growth medium to

initiate the experiment, the beclin-1 protein levels in control cells increased for 24 h following the addition of fresh growth medium (Figure II-7).

Beclin-1 Expression in Cultures of Cd⁺² and As⁺³ Transformed UROtsa Cells Exposed to Cd⁺² and As⁺³

Two isolates of the Cd⁺² and As⁺³ transformed UROtsa cells were assessed for beclin-1 protein expression when re-exposed to Cd⁺² and As⁺³. The concentrations and times of exposure were chosen from past studies which showed transformation altered subsequent exposure to Cd⁺² and As⁺³ (Somji et al., 2006). The concentrations and times of exposure were chosen such that no loss of cell viability would occur at the lowest 2 concentrations over the time course while the highest concentration would cause at least a 50% loss of cell viability at the final point in the respective time course. The isolates for testing were chosen based on the phenotypic property of the cells being able to colonize the organs of the peritoneal cavity, with one isolate able to colonize and the other unable to colonize the peritoneal cavity (Cao et al., 2010; Somji et al., 2010). Specifically, UROtsa Cd^{#1} (Figure II-8), Cd^{#7} (Figure II-9), As^{#1} (Figure II-10), and As^{#6} (Figure II-11) were analyzed. The results showed that although there were modest alterations in beclin-1 expression at selected time points, there were no significant alterations that corresponded to a dose response at any given concentration (Figures II-8-11).

Expression of Atg-5, Atg-7, Atg-12 and LC3B Proteins in Parental UROtsa Cells and UROtsa Cells Transformed by Cd⁺² and As⁺³

Employing the protein extracts described above, the expression of the Atg-5, Atg-7, Atg-12 and LC3B proteins were determined in the parental UROtsa cells and their Cd⁺² and As⁺³ transformed counterparts. The Atg-5 protein expression was reduced between 10 and 85% in the Cd⁺² transformed cells compared to control (Figure II-12A).

There was a marked reduction of the Atg-7 protein in all the Cd⁺² transformed cell lines (Figure II-12B). The Atg-12 protein was also reduced in 5 of the 7 Cd⁺² transformed cell lines, with 2 being close to control levels (Figure II-13A). The expression of the LC3B protein was similar to control in 4 of the 7 Cd⁺² transformed cell lines, elevated in one isolate, and reduced in the other 2 isolates (Figure II-13B). An examination of each protein among all the isolates failed to disclose any consistent relationship between the pattern of expression of any protein among the isolates. There was also no consistent pattern of expression of the proteins among the isolates when the expression was judged examining the entire group of proteins. For the As⁺³ transformed cell lines, the Atg-5 protein was increased in 5 of the 6 isolates and was at control levels in the remaining isolate (Figure II-14A). The Atg-7 protein was elevated in 2 isolates, reduced in 3 isolates and unchanged from parental cells in the remaining isolate (Figure II-14B). The Atg-12 protein was elevated in 2 isolates, reduced in an isolate and was unchanged in 3 isolates (Figure II-15A). The LC3B protein was elevated in all but one of the As⁺³ transformed cell lines (Figure II-15B). There was no consistent pattern of expression of the proteins within and among the isolates. The mRNA expression of Atg-5, Atg-7, Atg-12 and LC3B were also analyzed, but the expression patterns within the Cd⁺² and As⁺³ transformed UROtsa cell lines did not match that of the protein expression patterns (Figures II-16, 17, 18, 19).

The extracts from the two isolates of Cd⁺² and As⁺³ transformed UROtsa cells that were re-exposed to Cd⁺² and As⁺³ and analyzed for beclin-1 expression as described above, were also assessed for the expression of the Atg-5, Atg-7, Atg-12 and LC3B proteins (Figures II-20-35). The results showed that although there were modest

alterations in the expression of each protein at selected time points, there were no significant alterations that corresponded to a dose response at any given concentration for any isolate.

Discussion

The initial goal of the present study was to determine if beclin-1 was expressed in the normal human bladder. A combination of real time PCR, western analysis and immunohistochemistry was used to show that beclin-1 is expressed in the urothelium of the bladder. The profile of immunoreactivity suggested that staining increased from the basal cells to the umbrella cells of the stratified urothelium. The staining with the beclin-1 antibody also showed that a few scattered stromal and inflammatory cells stained intensely for beclin-1 within the beclin-1 negative underlying muscular layer of the bladder. It is not possible to quantify the absolute level of beclin-1 expression in the bladder, but the level was similar to that present in the UROtsa parental cell line as judged by western analysis. The levels of beclin-1 are close between the tissue and cell line when one considers that the stromal layer of the tissue had minimal expression of beclin-1 as judged by immunostaining using the beclin-1 antibody. To the author's knowledge this is the first documentation of beclin-1 expression in human urothelium.

The two additional goals of the current study were motivated by the report which showed that beclin-1 expression was elevated in As⁺³ exposed human urothelial cells and that an increase in autophagy correlated with the increased expression of beclin-1 (Chai et al., 2007). This observation was extended in the present report using the immortalized, but not tumorigenic, UROtsa cell line to examine the relationship between beclin-1 expression and As⁺³ exposure. The UROtsa cell line was chosen for analysis since it has

been directly malignantly transformed by exposure to both Cd^{+2} and As^{+3} and the resultant cell lines shown to form tumor heterotransplants with preservation of a histology consistent with human urothelial cancer (Sens et al., 2004). In addition, multiple independently generated cell lines of both Cd^{+2} and As^{+3} transformed cells have been generated and characterized for some basic phenotypic properties (Cao et al., 2010; Somji et al., 2010). An important feature of these additional cell lines was that all produced subcutaneous tumor heterotransplants, but only 2 of the 6 isolates of the As^{+3} transformed cell lines and 1 of the 7 isolates of Cd^{+2} transformed cell lines were able to colonize organs of the peritoneal cavity following injection of tumor cells into the peritoneal cavity. Thus, the employment of this cell system allowed the examination of beclin-1 expression: in parental UROtsa cells; in UROtsa cells transformed by Cd^{+2} or As^{+3} ; in Cd^{+2} and As^{+3} transformed cells having different potentials to colonize peritoneal organ sites; and in UROtsa cells exposed to Cd^{+2} or As^{+3} . The results did show some alterations in the expression of the beclin-1 protein that reached significance; however, these were very modest alterations in the level of the beclin-1 protein between parental UROtsa cells and their malignantly transformed counterparts and between and among the transformed cell lines themselves. The small magnitude of these alterations would render it likely that they would lose significance if several identical experiments were performed at independent times of experiment initiation. The study was also extended to include the expression of the Atg-5, Atg-7, Atg-12 and LC3B proteins associated with later stages of the autophagic process. Similar to that found for beclin-1, there were only modest alterations in expression between parental UROtsa cells and their malignantly transformed counterparts, and between and among the transformed cell lines themselves.

This finding provides initial evidence that large alterations in the expression of beclin-1 and associated proteins do not occur when human urothelial cells are malignantly transformed with either Cd^{+2} or As^{+3} .

The acute exposure of the parental UROtsa cells to either Cd^{+2} or As^{+3} also resulted in only modest changes in beclin-1 protein expression and no alterations that could be viewed as a strong dose response relationship. This was also true for the other proteins associated with the autophagic process. However, these experiments did reveal what appeared to be an increase of beclin-1 protein expression in the parental UROtsa cells as a function of the cultures being fed fresh growth medium. This observation could be important since many cultured cells are on a 3 day feeding cycle and it is likely that they may be deprived of nutrients on the day prior to receiving fresh growth medium. The present finding suggests that cultured cells, especially when confluent, could be activating and de-activating the pathway of autophagy as a function of the feeding schedule of the cells. If true, this would complicate data interpretation in studies using cultured cells to explore the role of autophagy in cell death and survival. This might be especially true for malignant cells that have elevated growth rates and therefore high rates of nutrient utilization. The major reason for including Cd^{+2} in the proposed study was that it is a known carcinogen and its relationship with autophagy in the human bladder has not been examined previously. The potential role cadmium may play in bladder cancer is related to the increased incidence of bladder cancer in smokers and the high level of cadmium accumulation in humans that is known to occur through tobacco smoke (Satarug et al., 2010).

The present study does not rule out a role for beclin-1 in Cd⁺² and As⁺³ exposed and transformed urothelial cells since it focuses solely on the level of expression. The interaction of beclin-1 with its binding partners could still be altered by exposure to Cd⁺² and As⁺³ and this could have significant effects of cell survival and cell death.

References

- Aita, V.M., Liang, X.H., Murty, V.V., Pincus, D.L., Yu, W., Cayanis, E., Kalachikov, S., Gilliam, T.C., Levine, B., 1999. Cloning and genomic organization of beclin 1, a candidate tumor suppressor gene on chromosome 17q21, *Genomics* 59, 59-65.
- Cao, L., Zhou, X.D., Sens, M.A., Garrett, S.H., Zheng, Y., Dunlevy, J.R., Sens, D.A., Somji, S., 2010. Keratin 6 expression correlates to areas of squamous differentiation in multiple independent isolates of As(+3)-induced bladder cancer, *J. Appl. Toxicol.* 30, 416-430.
- Chai, C.Y., Huang, Y.C., Hung, W.C., Kang, W.Y., Chen, W.T., 2007. Arsenic salts induced autophagic cell death and hypermethylation of DAPK promoter in SV-40 immortalized human uroepithelial cells, *Toxicol. Lett.* 173, 48-56.
- Garrett, S.H., Somji, S., Todd, J.H., Sens, D.A., 1998. Exposure of human proximal tubule cells to cd^{2+} , zn^{2+} , and Cu^{2+} induces metallothionein protein accumulation but not metallothionein isoform 2 mRNA, *Environ. Health Perspect.* 106, 587-595.
- Kroemer, G., Levine, B., 2008. Autophagic cell death: the story of a misnomer, *Nat. Rev. Mol. Cell Biol.* 9, 1004-1010.
- Maiuri, M.C., Tasdemir, E., Criollo, A., Morselli, E., Vicencio, J.M., Carnuccio, R., Kroemer, G., 2009. Control of autophagy by oncogenes and tumor suppressor genes, *Cell Death Differ.* 16, 87-93.
- Petzoldt, J.L., Leigh, I.M., Duffy, P.G., Masters, J.R., 1994. Culture and characterisation of human urothelium in vivo and in vitro, *Urol. Res.* 22, 67-74.
- Petzoldt, J.L., Leigh, I.M., Duffy, P.G., Sexton, C., Masters, J.R., 1995. Immortalisation of human urothelial cells, *Urol. Res.* 23, 377-380.
- Pickford, F., Masliah, E., Britschgi, M., Lucin, K., Narasimhan, R., Jaeger, P.A., Small, S., Spencer, B., Rockenstein, E., Levine, B., Wyss-Coray, T., 2008. The autophagy-related protein beclin 1 shows reduced expression in early Alzheimer disease and regulates amyloid beta accumulation in mice, *J. Clin. Invest.* 118, 2190-2199.
- Qu, X., Yu, J., Bhagat, G., Furuya, N., Hibshoosh, H., Troxel, A., Rosen, J., Eskelinen, E.L., Mizushima, N., Ohsumi, Y., Cattoretti, G., Levine, B., 2003. Promotion of tumorigenesis by heterozygous disruption of the beclin 1 autophagy gene, *J. Clin. Invest.* 112, 1809-1820.

- Rossi, M.R., Masters, J.R., Park, S., Todd, J.H., Garrett, S.H., Sens, M.A., Somji, S., Nath, J., Sens, D.A., 2001. The immortalized UROtsa cell line as a potential cell culture model of human urothelium, *Environ. Health Perspect.* 109, 801-808.
- Satarug, S., Garrett, S.H., Sens, M.A., Sens, D.A., 2010. Cadmium, environmental exposure, and health outcomes, *Environ. Health Perspect.* 118, 182-190.
- Sens, D.A., Park, S., Gurel, V., Sens, M.A., Garrett, S.H., Somji, S., 2004. Inorganic cadmium- and arsenite-induced malignant transformation of human bladder urothelial cells, *Toxicol. Sci.* 79, 56-63.
- Sinha, S., Levine, B., 2008. The autophagy effector Beclin 1: a novel BH3-only protein, *Oncogene* 27 Suppl 1, S137-48.
- Somji, S., Garrett, S.H., Sens, M.A., Gurel, V., Sens, D.A., 2004. Expression of metallothionein isoform 3 (MT-3) determines the choice between apoptotic or necrotic cell death in Cd²⁺-exposed human proximal tubule cells, *Toxicol. Sci.* 80, 358-366.
- Somji, S., Zhou, X.D., Garrett, S.H., Sens, M.A., Sens, D.A., 2006. Urothelial cells malignantly transformed by exposure to cadmium (Cd²⁺) and arsenite (As³⁺) have increased resistance to Cd²⁺ and As³⁺-induced cell death, *Toxicol. Sci.* 94, 293-301.
- Somji, S., Zhou, X.D., Mehus, A., Sens, M.A., Garrett, S.H., Lutz, K.L., Dunlevy, J.R., Zheng, Y., Sens, D.A., 2010. Variation of keratin 7 expression and other phenotypic characteristics of independent isolates of cadmium transformed human urothelial cells (UROtsa), *Chem. Res. Toxicol.* 23, 348-356.
- Tannous, P., Zhu, H., Johnstone, J.L., Shelton, J.M., Rajasekaran, N.S., Benjamin, I.J., Nguyen, L., Gerard, R.D., Levine, B., Rothermel, B.A., Hill, J.A., 2008. Autophagy is an adaptive response in desmin-related cardiomyopathy, *Proc. Natl. Acad. Sci. U. S. A.* 105, 9745-9750.
- Todde, V., Veenhuis, M., van der Klei, I.J., 2009. Autophagy: principles and significance in health and disease, *Biochim. Biophys. Acta* 1792, 3-13.
- Yue, Z., Jin, S., Yang, C., Levine, A.J., Heintz, N., 2003. Beclin 1, an autophagy gene essential for early embryonic development, is a haploinsufficient tumor suppressor, *Proc. Natl. Acad. Sci. U. S. A.* 100, 15077-15082.

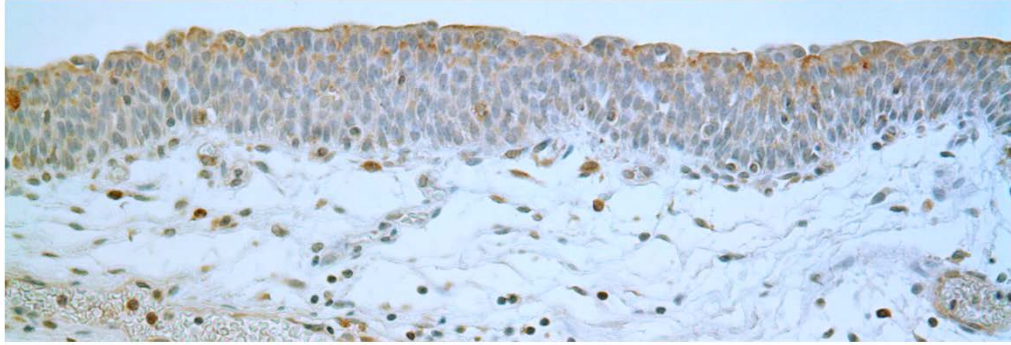


Figure II-1. Expression of beclin-1 in human bladder tissue. Immunohistochemical staining of beclin-1 in normal human urothelium. The urothelium was moderately immunoreactive for beclin-1, with the staining of superficial layers stronger than the basal layer. Some scattered inflammatory cells in the lamina propria were also positive for beclin-1(x 200).

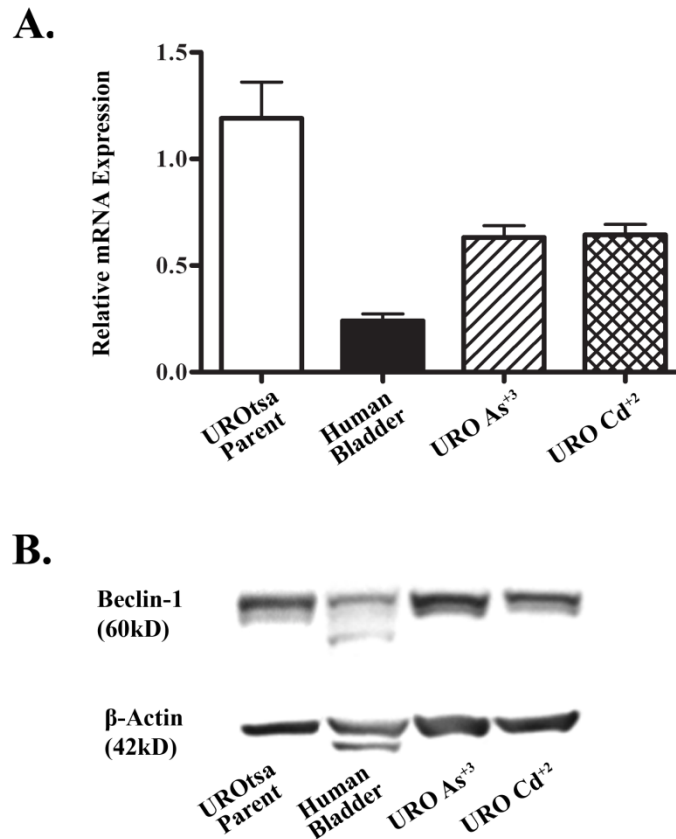


Figure II-2. Expression of beclin-1 in human bladder tissue and the UROtsa cell lines. (A) Real time RT-PCR analysis of beclin-1 mRNA levels. mRNA levels were normalized to β -actin and are shown as relative mRNA levels \pm SE for the UROtsa parent cell line, human bladder tissue, and UROtsa cell lines transformed with arsenic (URO As⁺³) and cadmium (URO Cd⁺²). (B) Western blot analysis of beclin-1 protein levels from the same cell lines and tissue shown in (A). Duplicate blots were stained for beclin-1 and β -actin as a control.

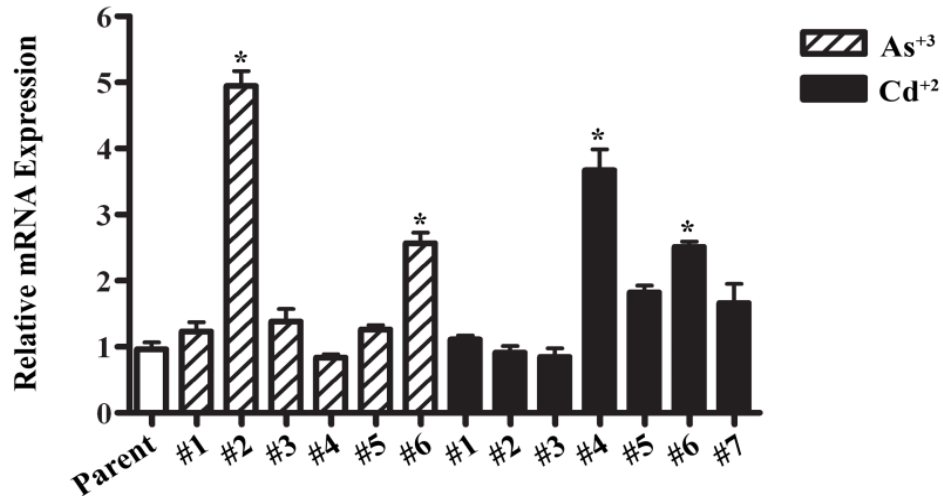


Figure II-3. Baseline mRNA expression of beclin-1 in UROtsa cell lines. Real time RT-PCR analysis of beclin-1 mRNA levels. mRNA levels were normalized to β -actin and are shown as relative mRNA levels \pm SE for the UROtsa parent cell line and UROtsa cell lines transformed with arsenic (As^{+3}) and cadmium (Cd^{+2}). The #'s identify the independent cell lines isolated by the exposure of UROtsa cells to As^{+3} and Cd^{+2} as described by (Cao et al., 2010; Somji et al., 2010), respectively. Statistically significant compared to UROtsa parent (*), $p < 0.001$.

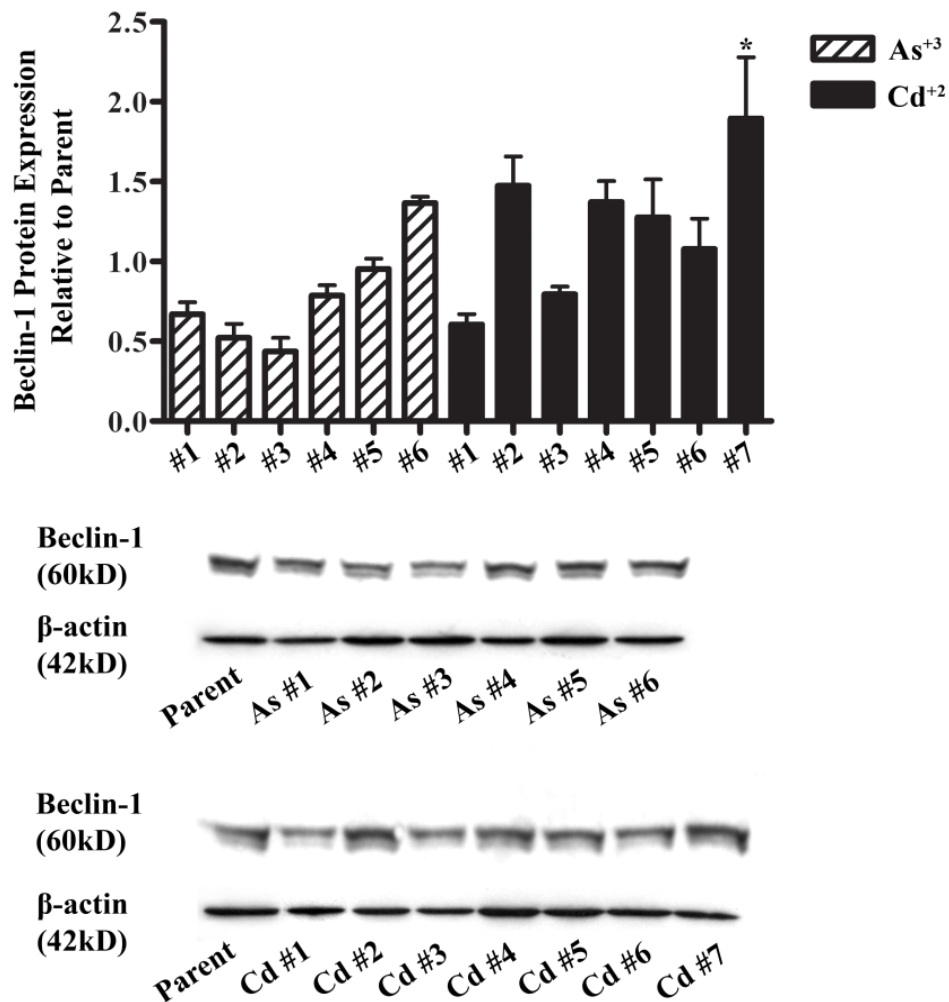


Figure II-4. Baseline protein expression of beclin-1 in UROtsa cell lines. Western blot analysis of beclin-1 protein levels relative to parent from the same cell lines shown in Figure II-3. Duplicate blots were stained for beclin-1 and β -actin as a control. Graph is representative of the integrated optical density (IOD) of the western blot below it. Protein levels are shown as the mean \pm SE. Statistically significant compared to UROtsa parent (*), $p < 0.001$.

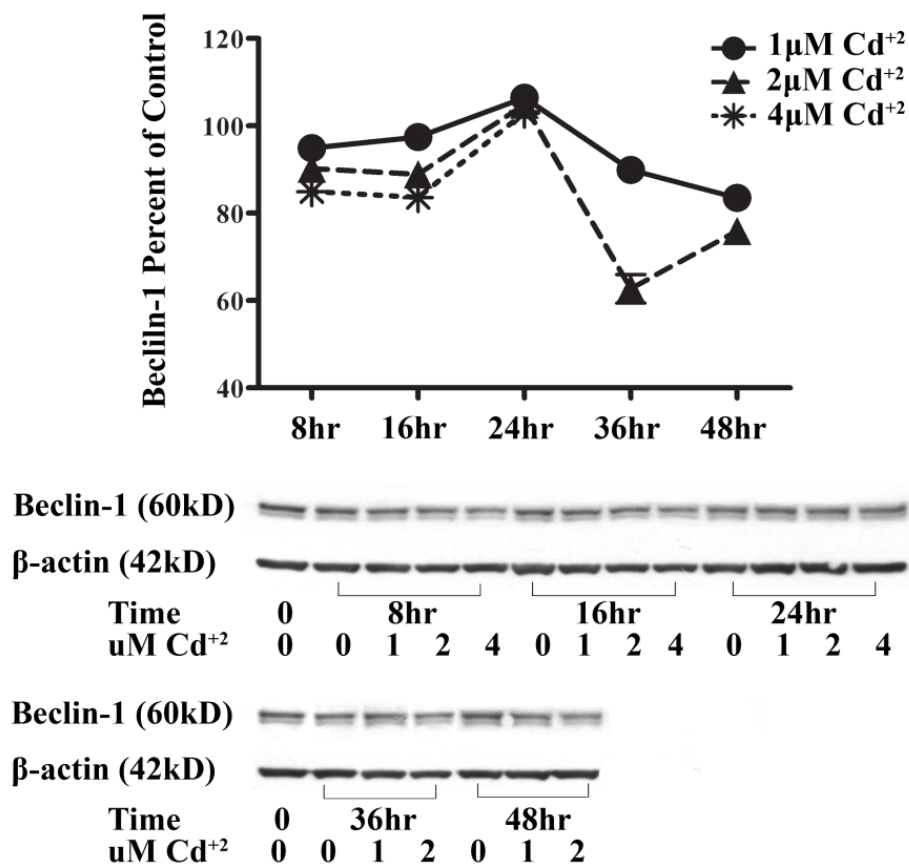


Figure II-5. Protein expression of beclin-1 in UROtsa parent cell line treated with cadmium. Western blot analysis of beclin-1 protein expression relative to control at various time points with treatment of Cd²⁺. Treatment with 1 μM Cd²⁺, 2 μM Cd²⁺, and 4 μM Cd²⁺ are represented by circle, triangle, and star symbols respectively. 36 h and 48 h treatments with 4 μM Cd²⁺ were omitted due to loss of cell viability. Duplicate blots were stained for beclin-1 and β-actin as a control. Graph is representative of the IOD of the western blot below it. Protein levels are shown as the mean ±SE.

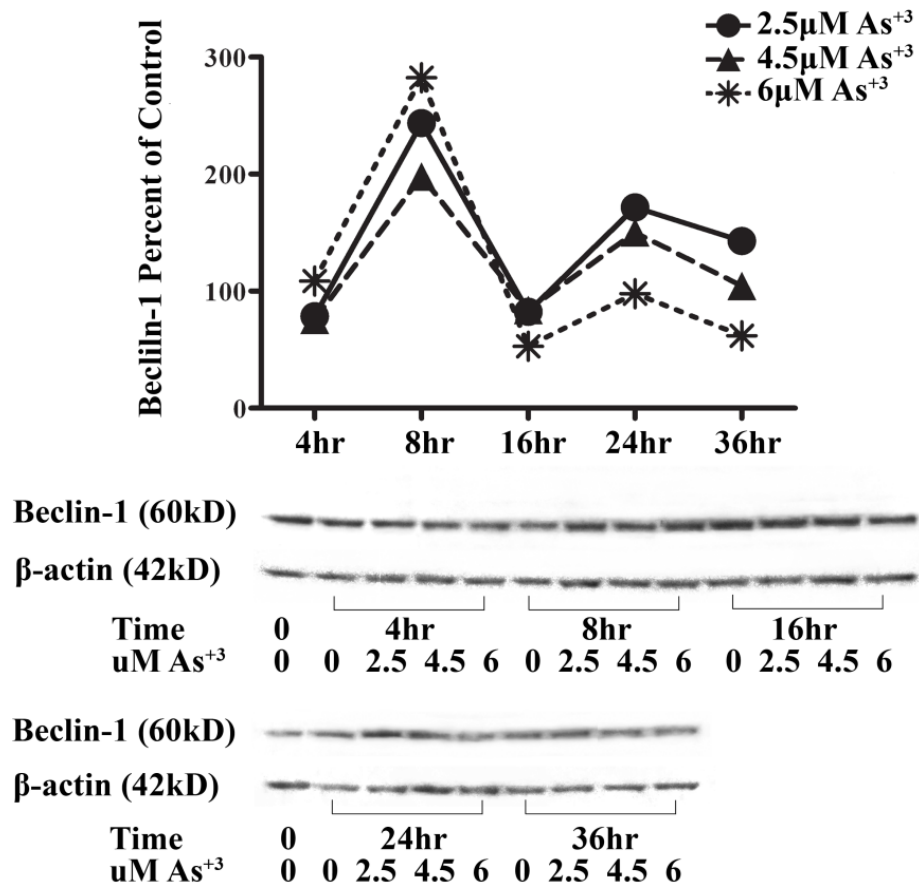


Figure II-6. Protein expression of beclin-1 in UROtsa parent cell line treated with arsenic. Western blot analysis of beclin-1 protein expression relative to control at various time points with treatment of As³⁺. Treatment with 2.5 μM As³⁺, 4.5 μM As³⁺, and 6 μM As³⁺ are represented by circle, triangle, and star symbols respectively. Duplicate blots were stained for beclin-1 and β-actin as a control. Graph is representative of the IOD of the western blot below it. Protein levels are shown as the mean ±SE.

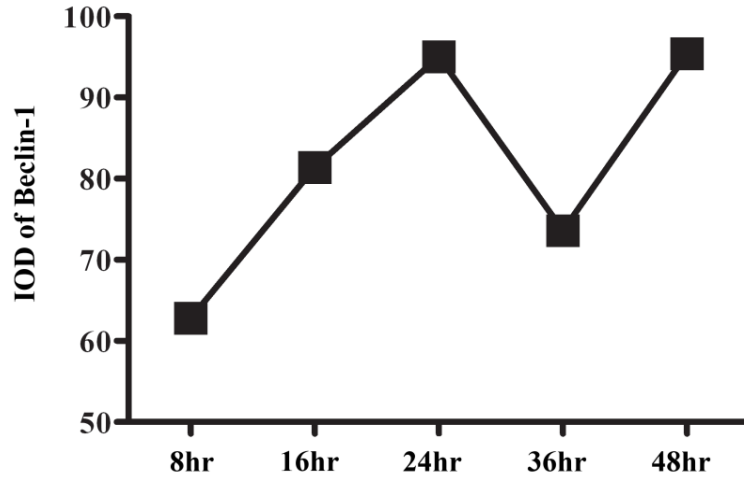


Figure II-7. Growth effect on beclin-1 expression in UROtsa parent cells. IOD of beclin-1 protein is shown at various time points. Protein levels are shown as the mean \pm SE.

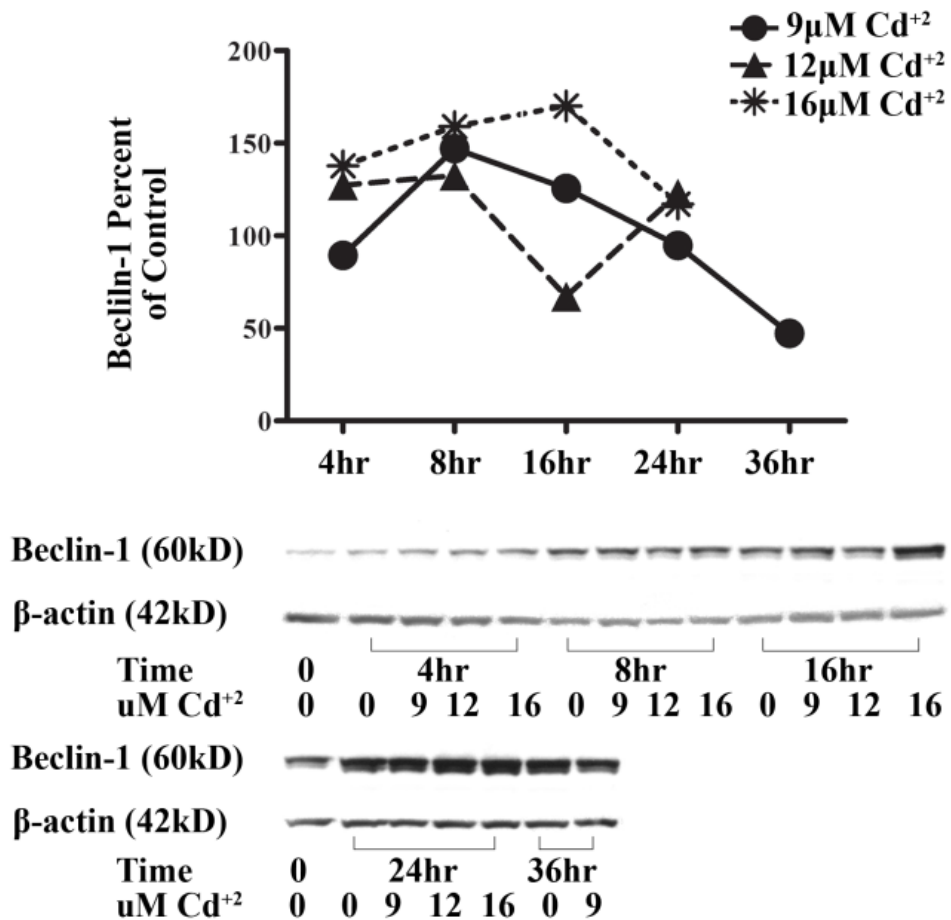


Figure II-8. Protein expression of beclin-1 in UROtsa Cd[#]1 cells. Western blot analysis of beclin-1 protein expression relative to percent of control in UROtsa Cd[#]1 cells treated with Cd²⁺. 36 h treatment with 12 µM Cd²⁺ and 16 µM Cd²⁺ were omitted due to loss of cell viability. Duplicate blots were stained for beclin-1 and β-actin as a control. Graph is representative of the IOD of the western blot below it. Protein levels are shown as the mean ±SE.

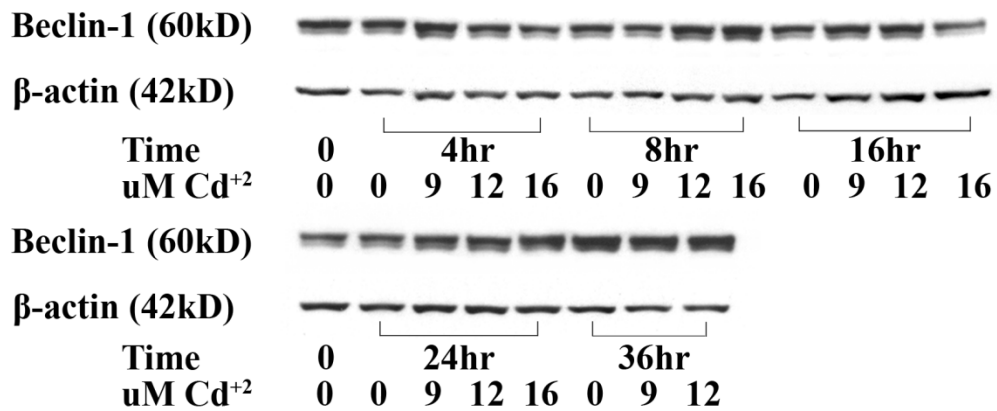
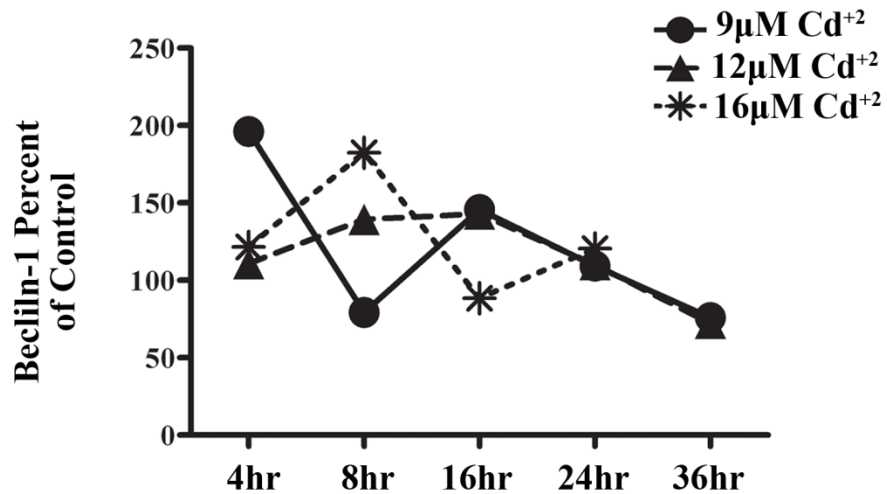


Figure II-9. Protein expression of beclin-1 in UROtsa Cd^{#7} cells. Western blot analysis of beclin-1 protein expression relative to percent of control in UROtsa Cd^{#7} cells treated with cadmium. 36 h treatment with 16 μM Cd²⁺ was omitted due to loss of cell viability. Duplicate blots were stained for beclin-1 and β-actin as a control. Graph is representative of the IOD of the western blot below it. Protein levels are shown as the mean ±SE.

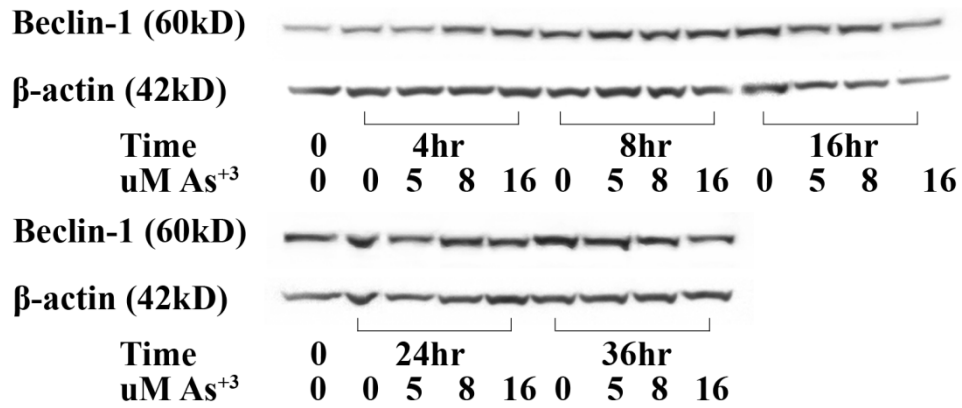
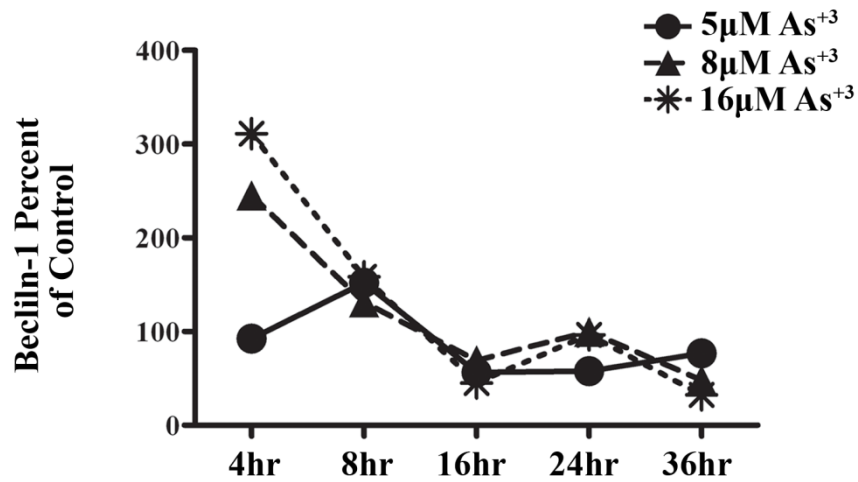


Figure II-10. Protein expression of beclin-1 in UROtsa As[#]1 cells. Western blot analysis of beclin-1 protein expression relative to percent of control in UROtsa As[#]1 cells treated with As³⁺. Duplicate blots were stained for beclin-1 and β-actin as a control. Graph is representative of the IOD of the western blot below it. Protein levels are shown as the mean ±SE.

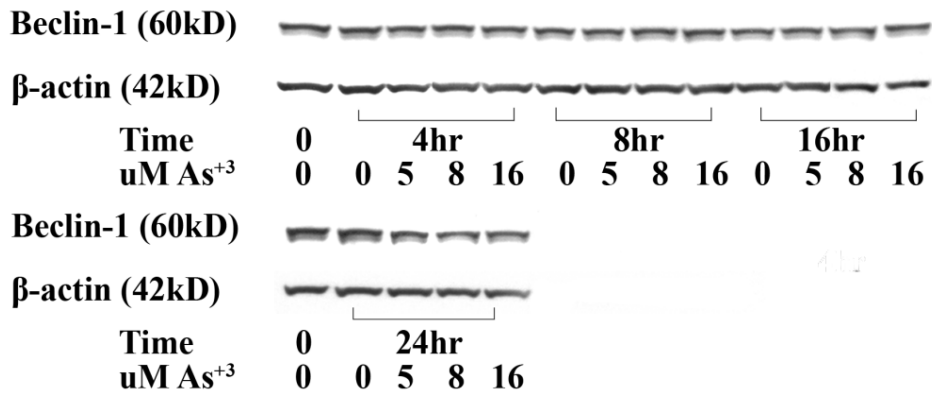
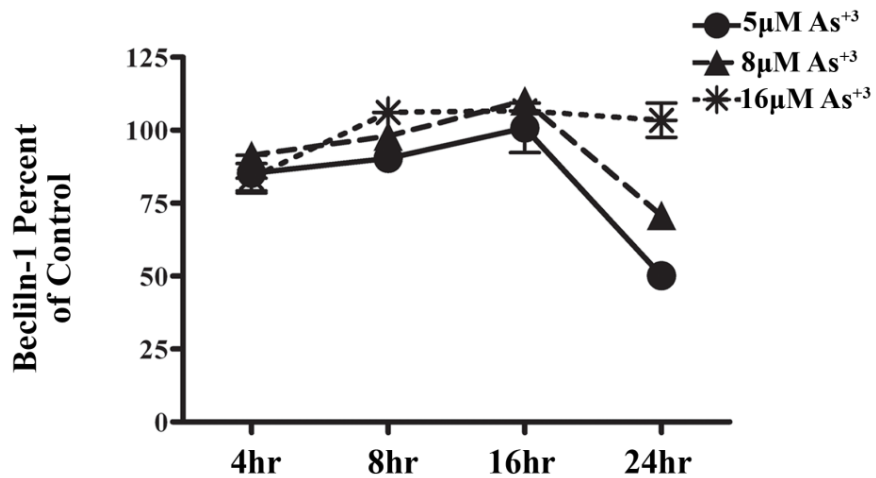


Figure II-11. Protein expression of beclin-1 in UROtsa As^{#6} cells. Western blot analysis of beclin-1 protein expression relative to percent of control in UROtsa As^{#6} cells treated with As³⁺. 36 h treatment of As^{#6} was omitted due to loss of cell viability. Duplicate blots were stained for beclin-1 and β-actin as a control. Graph is representative of the IOD of the western blot below it. Protein levels are shown as the mean ±SE.

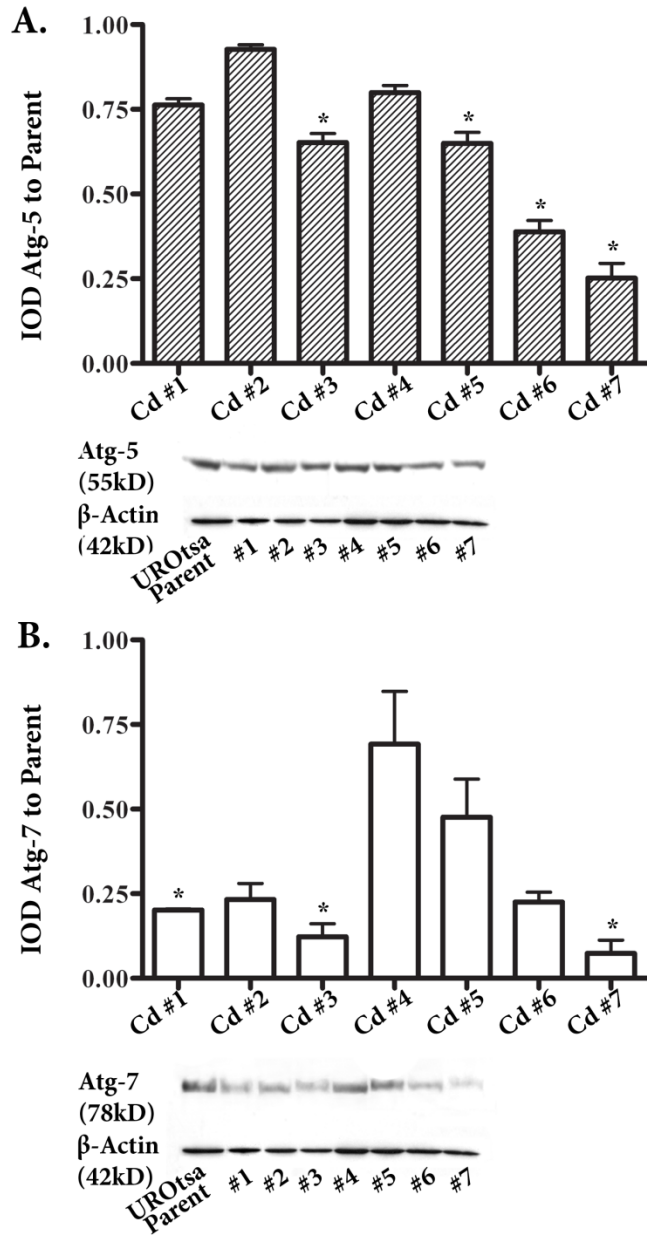


Figure II-12. Expression of autophagy proteins, Atg-5 and -7, in UROtsa parent and UROtsa Cd²⁺ transformed cell lines. Western blot analysis of (A) Atg-5 and (B) Atg-7 protein expression relative to the UROtsa parent cells. Duplicate blots were stained for each autophagy protein and β -actin as a control. Graph is representative of the IOD of the western blot below it. Protein levels are shown as the mean \pm SE. Statistically significant compared to UROtsa parent (*), $p < 0.001$.

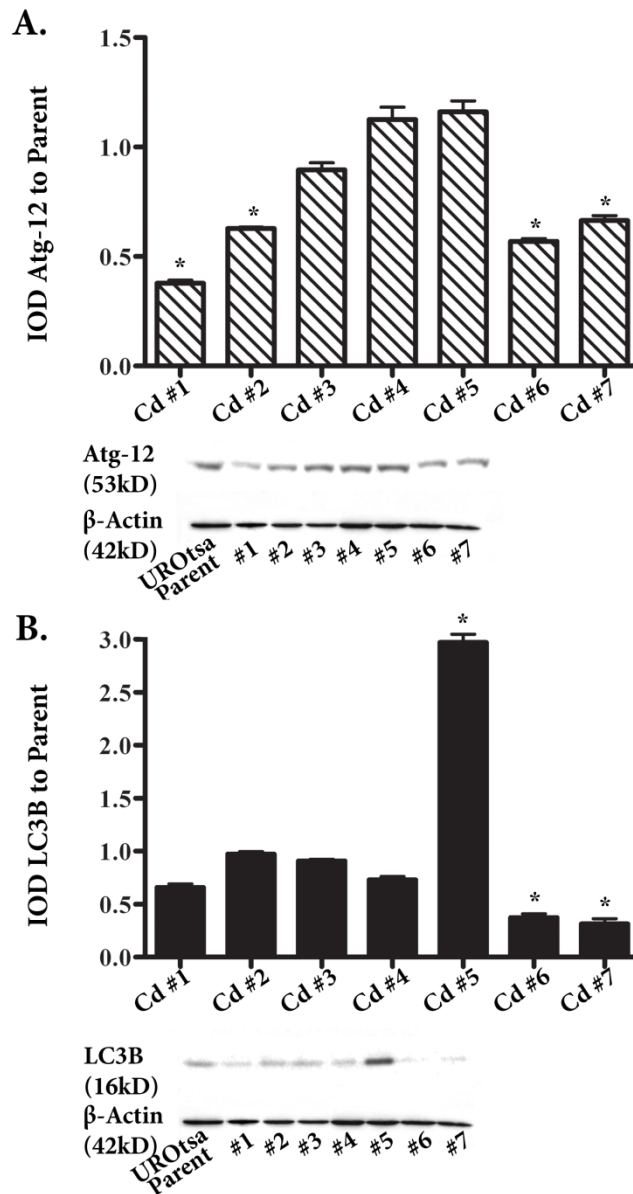


Figure II-13. Expression of autophagy proteins, Atg-12 and LC3B, in UROtsa parent and UROtsa Cd²⁺ transformed cell lines. Western blot analysis of (A) Atg-12 and (B) LC3B protein expression relative to the UROtsa parent cells. Duplicate blots were stained for each autophagy protein and β -actin as a control. Graph is representative of the IOD of the western blot below it. Protein levels are shown as the mean \pm SE. Statistically significant compared to UROtsa parent (*), $p < 0.001$.

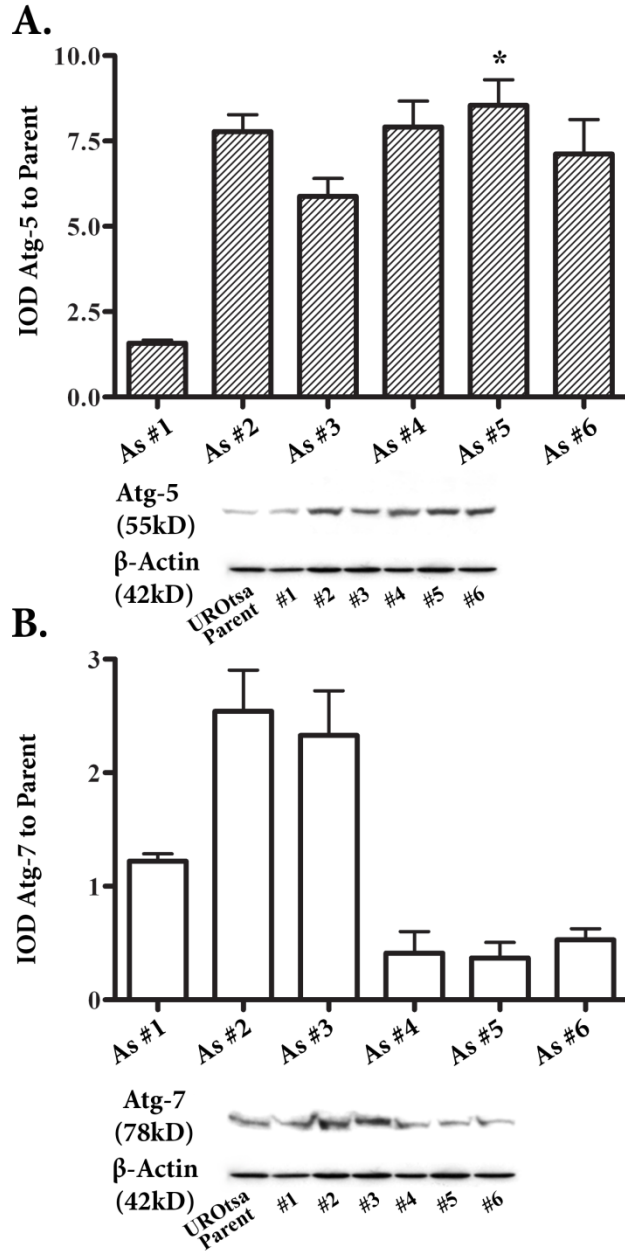


Figure II-14. Expression of autophagy proteins, Atg-5 and -7, in UROtsa parent and UROtsa As⁺³ transformed cell lines. Western blot analysis of (A) Atg-5 and (B) Atg-7 protein expression relative to the UROtsa parent cells. Duplicate blots were stained for each autophagy protein and β -actin as a control. Graph is representative of the IOD of the western blot below it. Protein levels are shown as the mean \pm SE. Statistically significant compared to UROtsa parent (*), $p < 0.001$.

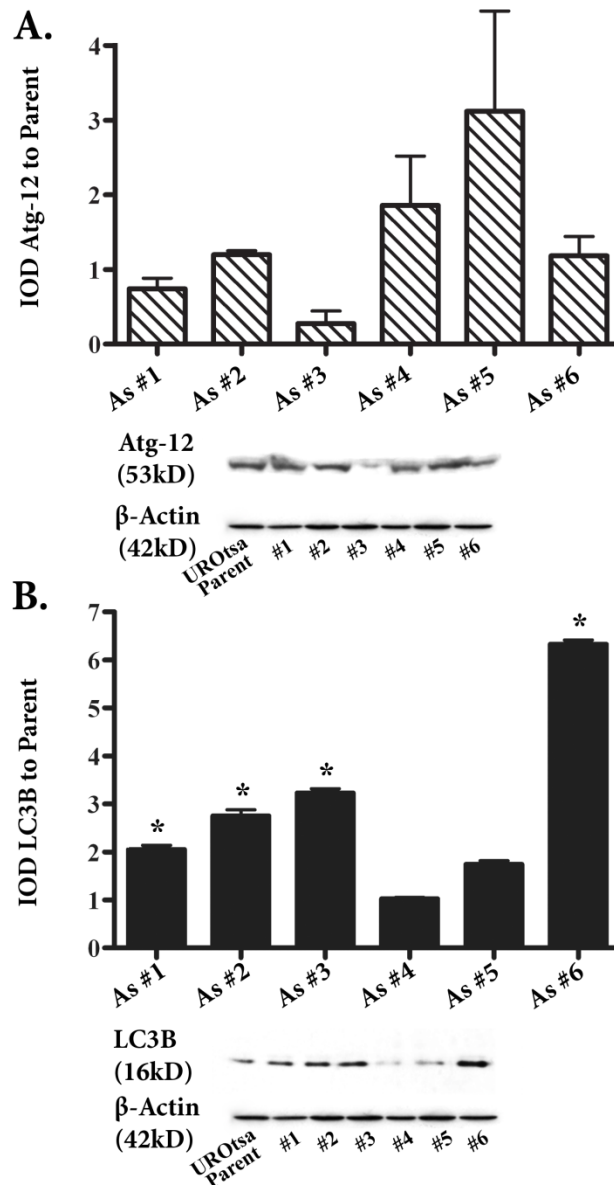


Figure II-15. Expression of autophagy proteins, Atg-12 and LC3B, in UROtsa parent and UROtsa As⁺³ transformed cell lines. Western blot analysis of (A) Atg-12 and (B) LC3B protein expression relative to the UROtsa parent cells. Duplicate blots were stained for each autophagy protein and β -actin as a control. Graph is representative of the IOD of the western blot below it. Protein levels are shown as the mean \pm SE. Statistically significant compared to UROtsa parent (*), $p < 0.001$.

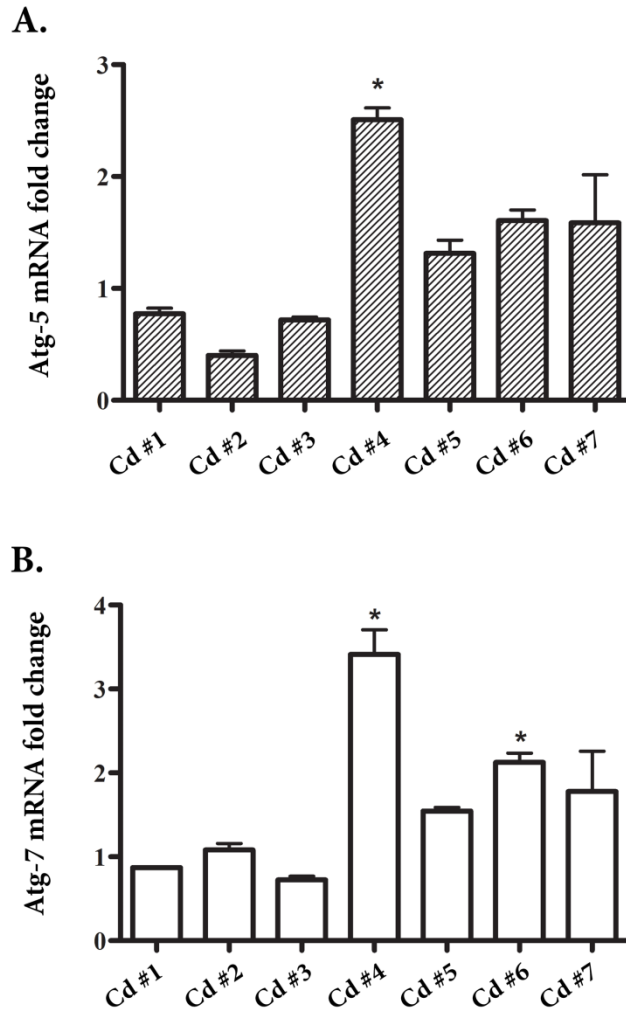


Figure II-16. Real time RT-PCR analysis of autophagy genes, Atg-5 and -7, in UROtsa parent and UROtsa Cd⁺² transformed cell lines. mRNA analysis of (A) Atg-5 and (B) Atg-7 gene expression relative to the UROtsa parent cells. mRNA levels were normalized to β -actin and are shown as relative mRNA levels \pm SE for the UROtsa parent cell line and UROtsa cell lines transformed with Cd⁺². Statistically significant compared to UROtsa parent (*), $p < 0.05$.

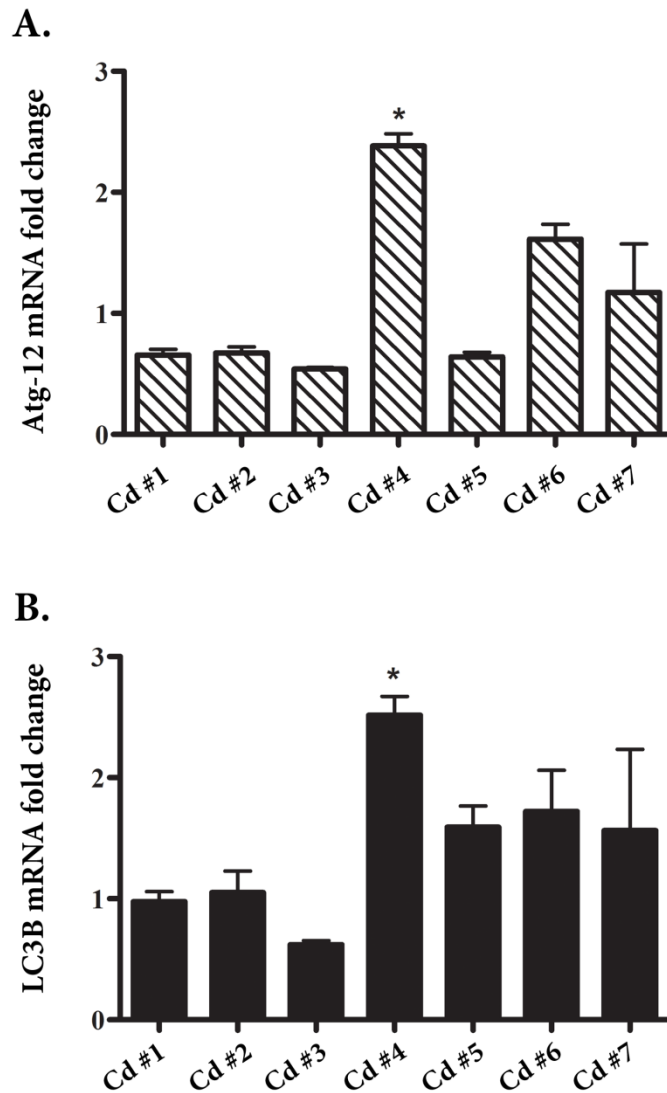


Figure II-17. Real time RT-PCR analysis of autophagy genes, Atg-12 and LC3B, in UROtsa parent and UROtsa Cd⁺² transformed cell lines. mRNA analysis of (A) Atg-12 and (B) LC3B gene expression relative to the UROtsa parent cells. mRNA levels were normalized to β -actin and are shown as relative mRNA levels \pm SE for the UROtsa parent cell line and UROtsa cell lines transformed with Cd⁺². Statistically significant compared to UROtsa parent (*), $p < 0.05$.

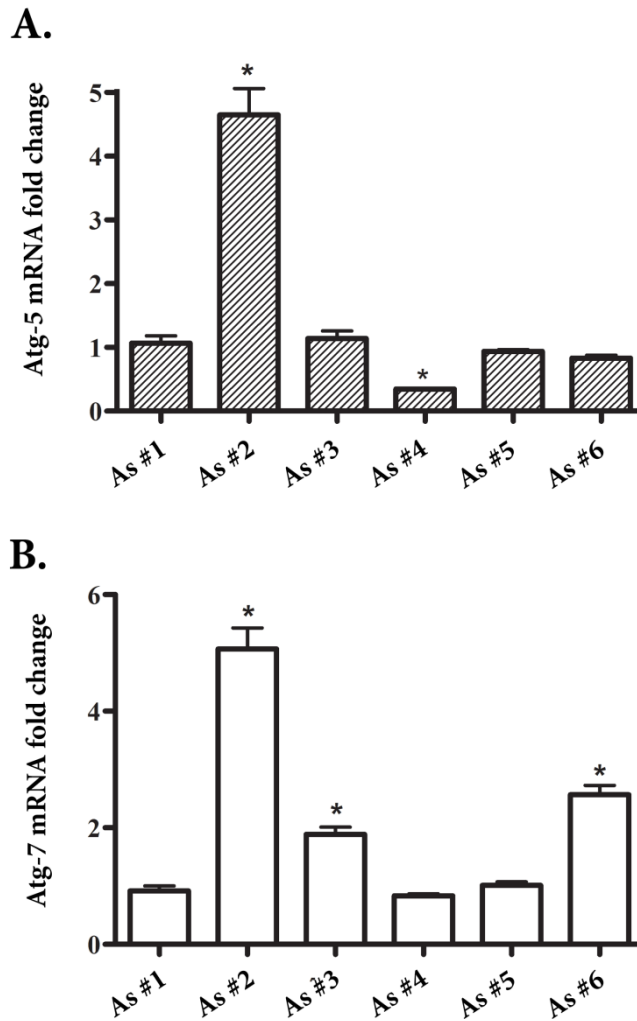


Figure II-18. Real time RT-PCR analysis of autophagy genes, Atg-5 and -7, in UROtsa parent and UROtsa As⁺³ transformed cell lines. mRNA analysis of (A) Atg-5 and (B) Atg-7 gene expression relative to the UROtsa parent cells. mRNA levels were normalized to β -actin and are shown as relative mRNA levels \pm SE for the UROtsa parent cell line and UROtsa cell lines transformed with As⁺³. Statistically significant compared to UROtsa parent (*), $p < 0.05$.

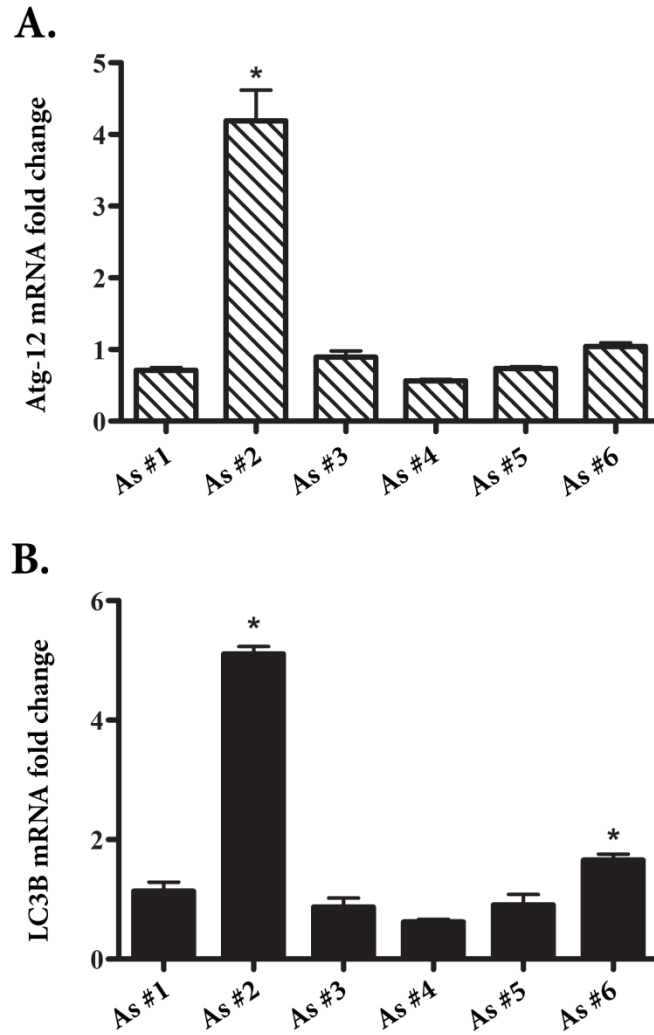


Figure II-19. Real time RT-PCR analysis of autophagy genes, Atg-12 and LC3B, in UROtsa parent and UROtsa As⁺³ transformed cell lines. mRNA analysis of (A) Atg-12 and (B) LC3B gene expression relative to the UROtsa parent cells. mRNA levels were normalized to β -actin and are shown as relative mRNA levels \pm SE for the UROtsa parent cell line and UROtsa cell lines transformed with As⁺³. Statistically significant compared to UROtsa parent (*), $p < 0.05$.

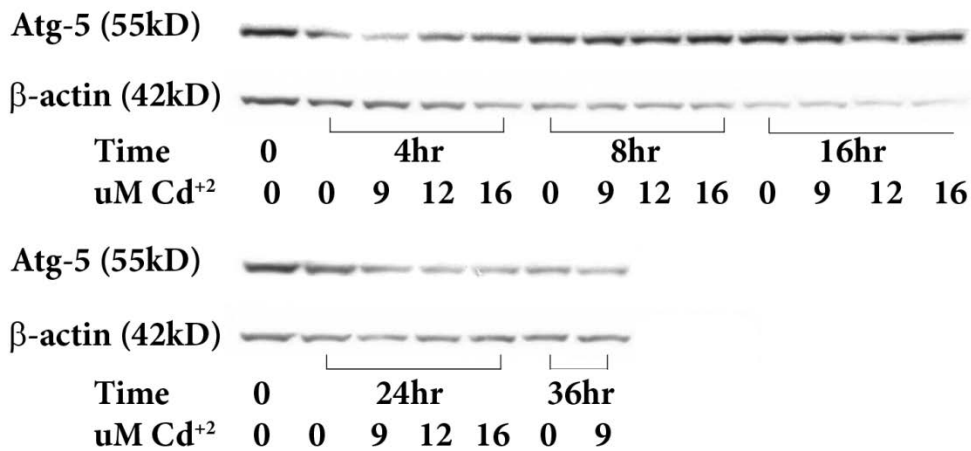
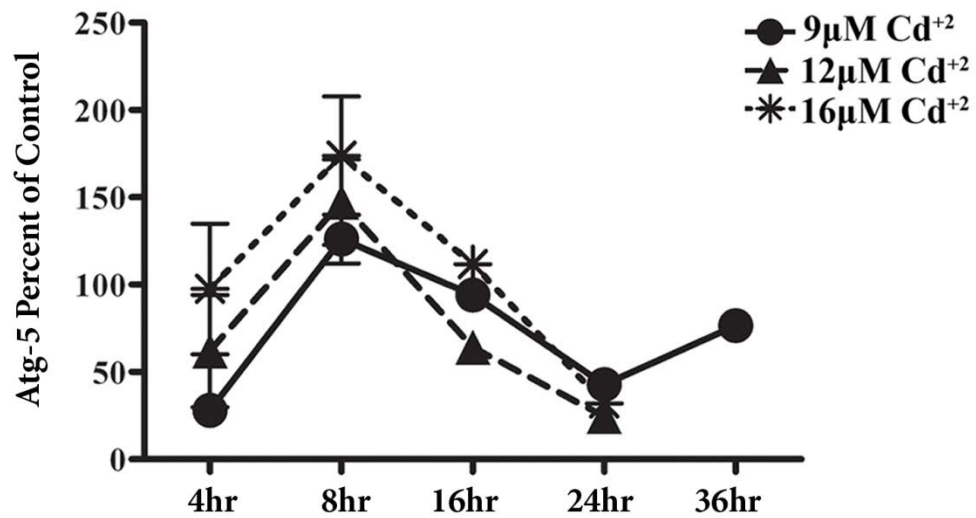


Figure II-20. Protein expression of Atg-5 in UROtsa Cd[#]1 cells. Western blot analysis of Atg-5 protein expression relative to percent of control in UROtsa Cd[#]1 cells treated with Cd²⁺. 36 h treatment with 12 μM Cd²⁺ and 16 μM Cd²⁺ were omitted due to loss of cell viability. Duplicate blots were stained for Atg-5 and β-actin as a control. Graph is representative of the IOD of the western blot below it. Protein levels are shown as the mean ±SE.

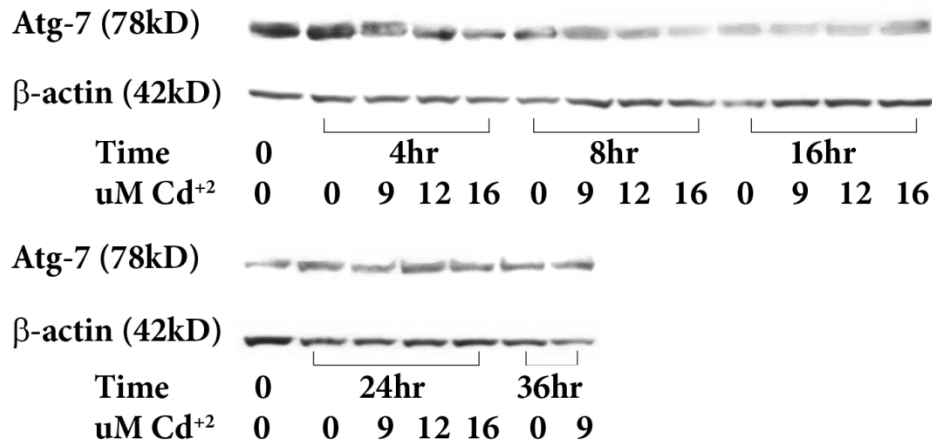
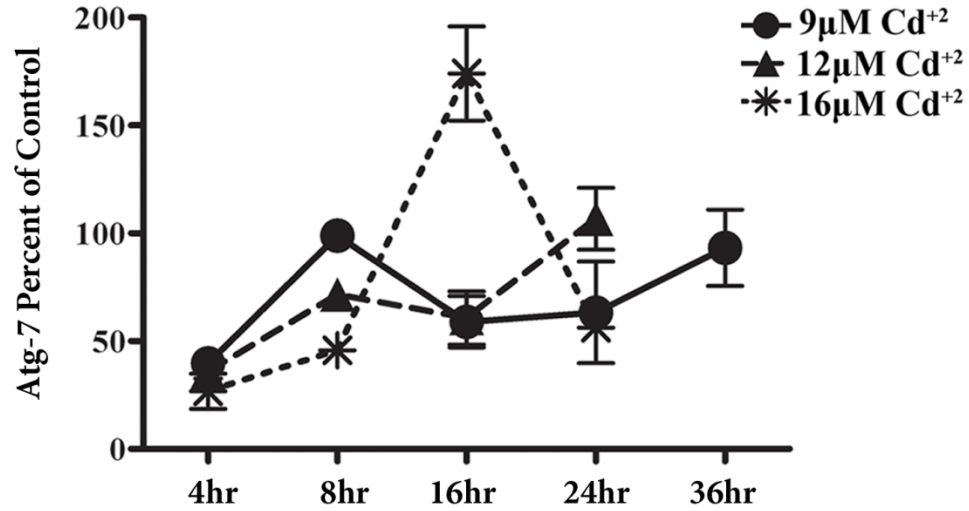


Figure II-21. Protein expression of Atg-7 in UROtsa Cd^{#1} cells. Western blot analysis of Atg-7 protein expression relative to percent of control in UROtsa Cd^{#1} cells treated with Cd²⁺. 36 h treatment with 12 μM Cd²⁺ and 16 μM Cd²⁺ were omitted due to loss of cell viability. Duplicate blots were stained for Atg-7 and β-actin as a control. Graph is representative of the IOD of the western blot below it. Protein levels are shown as the mean ±SE.

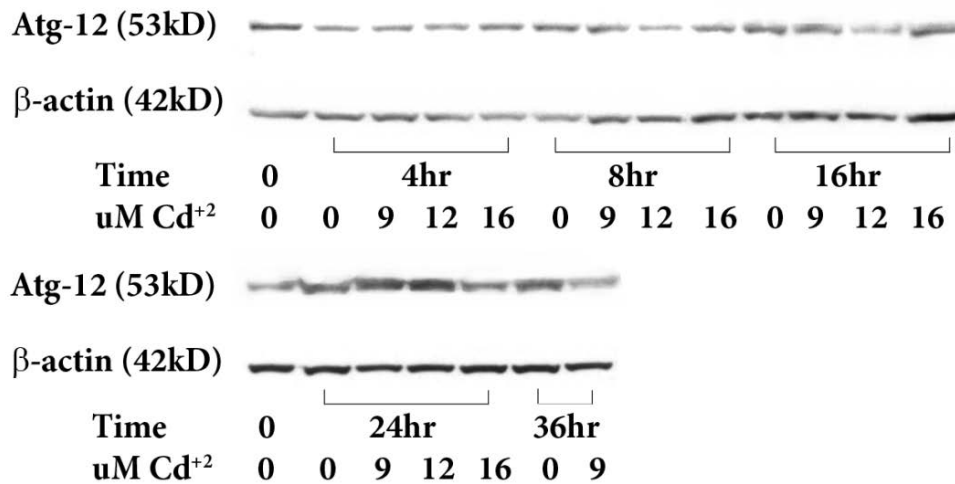
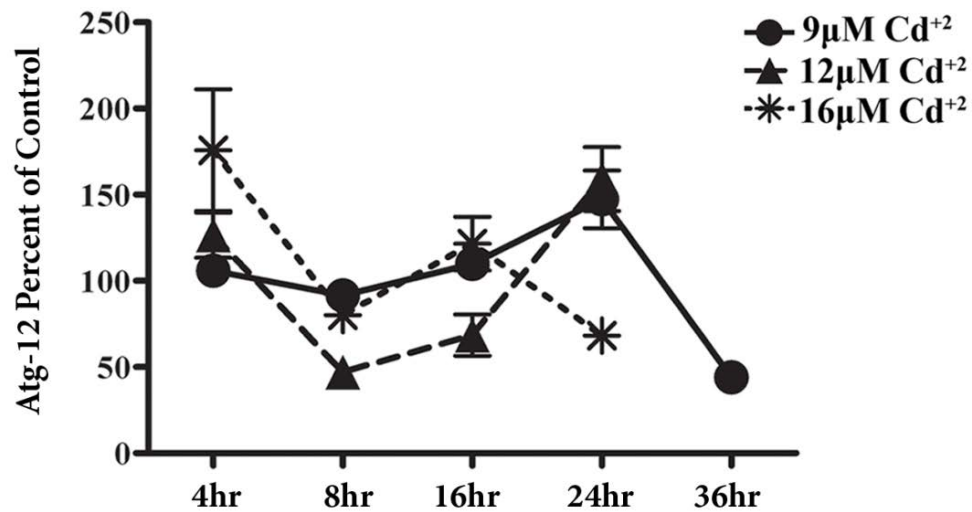


Figure II-22. Protein expression of Atg-12 in UROtsa Cd[#]1 cells. Western blot analysis of Atg-12 protein expression relative to percent of control in UROtsa Cd[#]1 cells treated with Cd²⁺. 36 h treatment with 12 μM Cd²⁺ and 16 μM Cd²⁺ were omitted due to loss of cell viability. Duplicate blots were stained for Atg-12 and β-actin as a control. Graph is representative of the IOD of the western blot below it. Protein levels are shown as the mean ±SE.

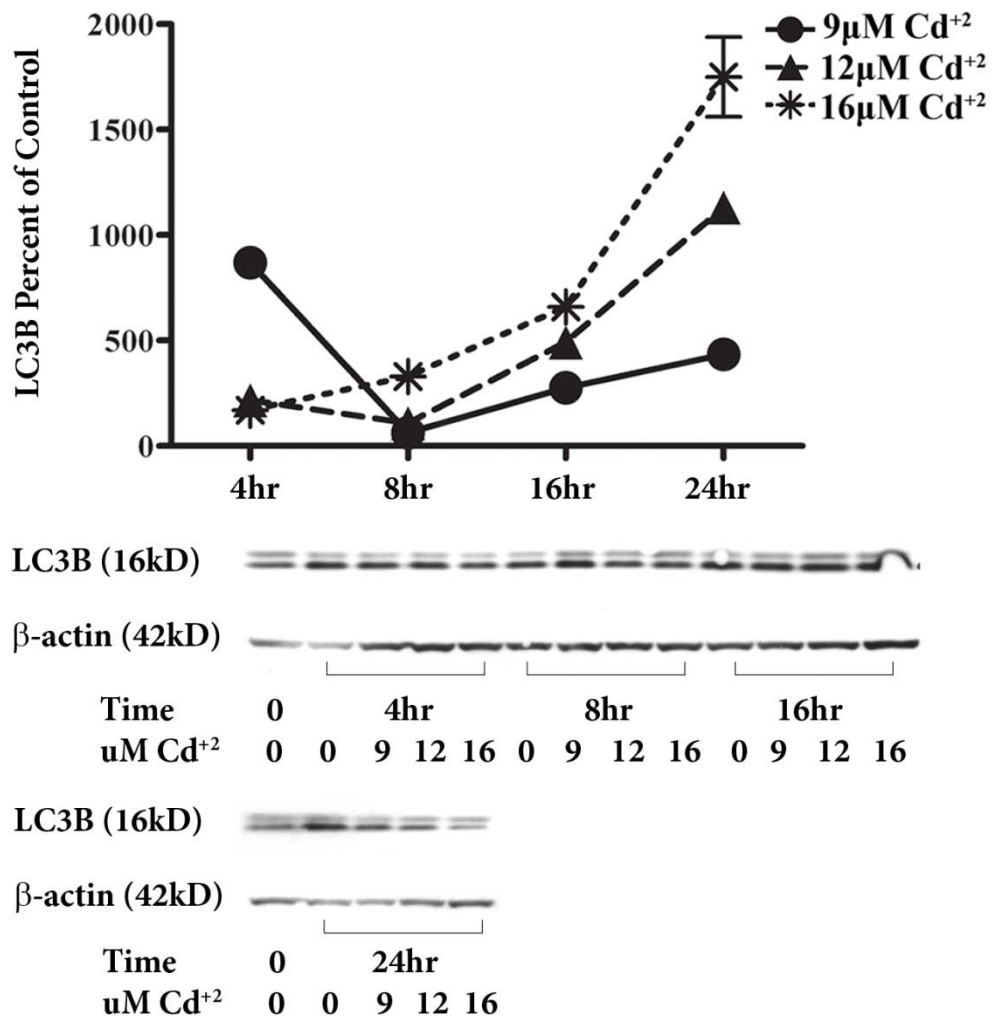


Figure II-23. Protein expression of LC3B in UROtsa Cd^{#1} cells. Western blot analysis of LC3B protein expression relative to percent of control in UROtsa Cd^{#1} cells treated with Cd²⁺. 36 h treatment with 12 µM Cd²⁺ and 16 µM Cd²⁺ were omitted due to loss of cell viability. Duplicate blots were stained for LC3B and β-actin as a control. Graph is representative of the IOD of the western blot below it. Protein levels are shown as the mean ±SE.

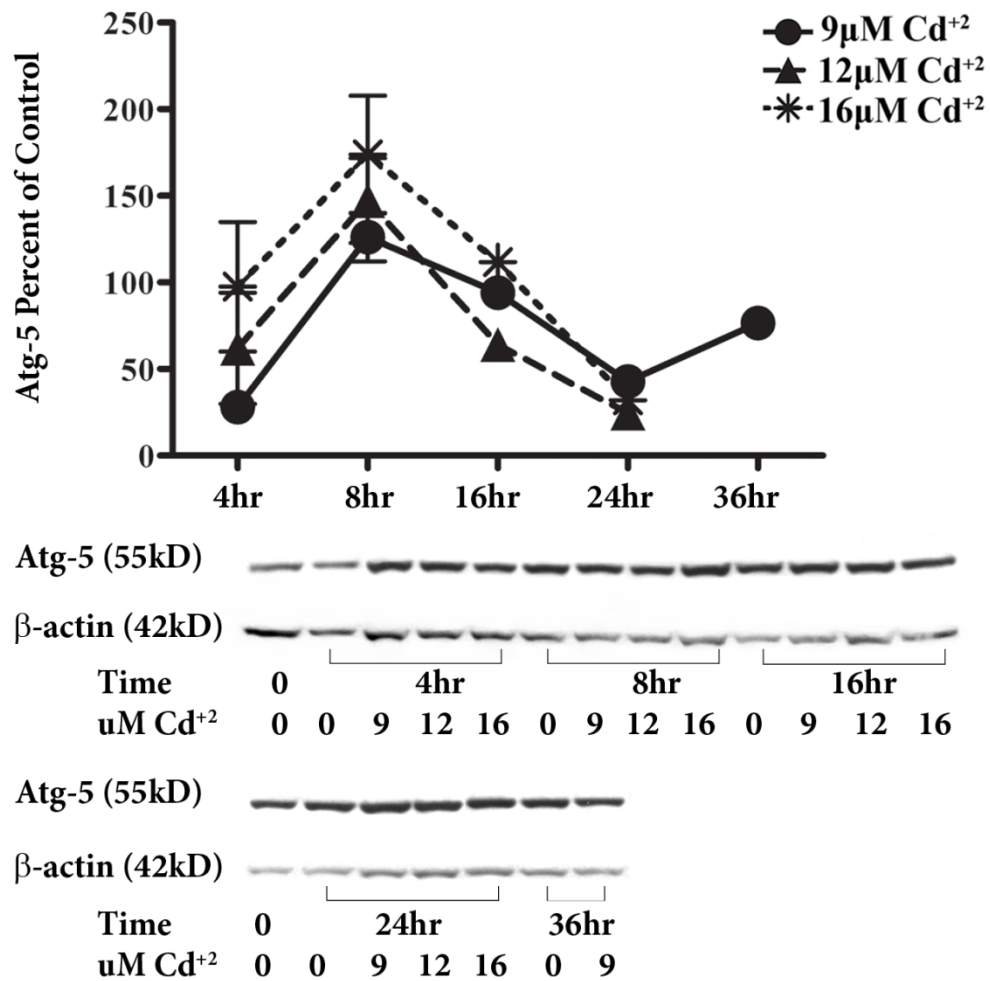


Figure II-24. Protein expression of Atg-5 in UROtsa Cd^{#7} cells. Western blot analysis of Atg-5 protein expression relative to percent of control in UROtsa Cd^{#7} cells treated with cadmium. 36 h treatment with 12 µM Cd²⁺ and 16 µM Cd²⁺ was omitted due to loss of cell viability. Duplicate blots were stained for Atg-5 and β-actin as a control. Graph is representative of the IOD of the western blot below it. Protein levels are shown as the mean ±SE.

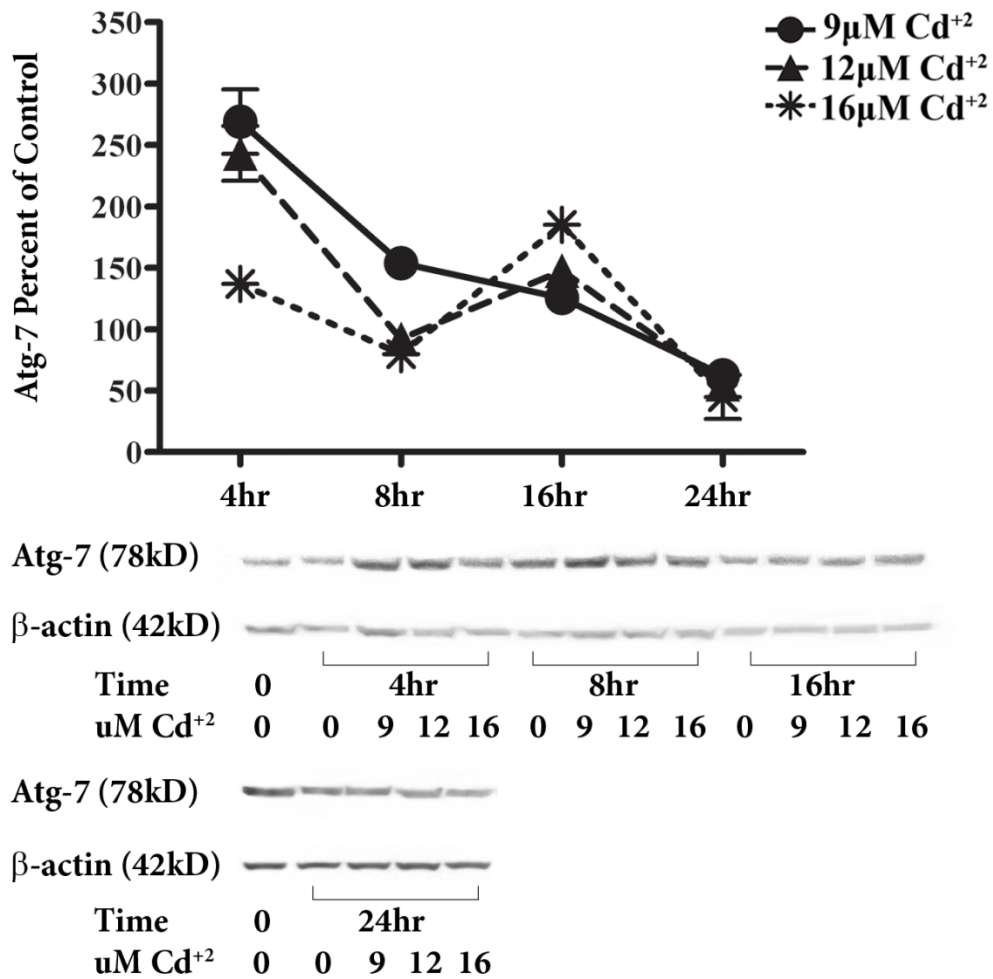


Figure II-25. Protein expression of Atg-7 in UROtsa Cd^{#7} cells. Western blot analysis of Atg-7 protein expression relative to percent of control in UROtsa Cd^{#7} cells treated with cadmium. 36 h treatment was omitted due to loss of cell viability. Duplicate blots were stained for Atg-7 and β-actin as a control. Graph is representative of the IOD of the western blot below it. Protein levels are shown as the mean ±SE.

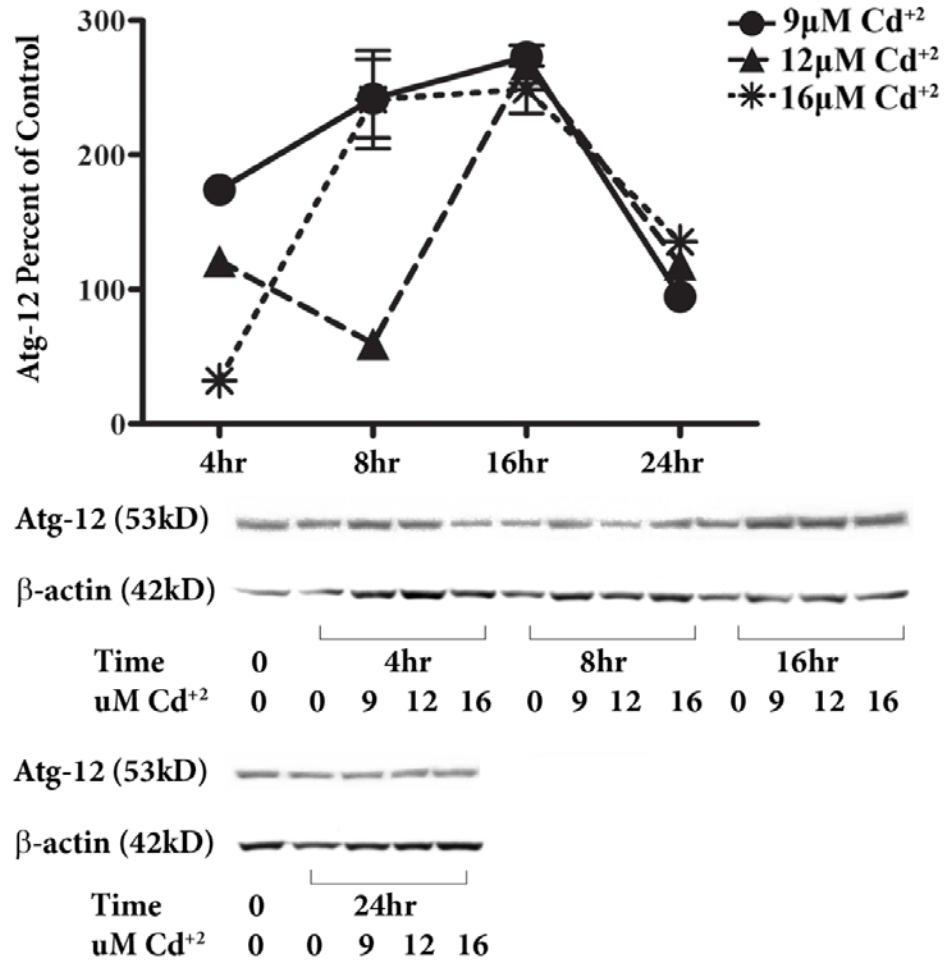


Figure II-26. Protein expression of Atg-12 in UROtsa Cd^{#7} cells. Western blot analysis of Atg-12 protein expression relative to percent of control in UROtsa Cd^{#7} cells treated with cadmium. 36 h treatment was omitted due to loss of cell viability. Duplicate blots were stained for Atg-12 and β-actin as a control. Graph is representative of the IOD of the western blot below it. Protein levels are shown as the mean ±SE.

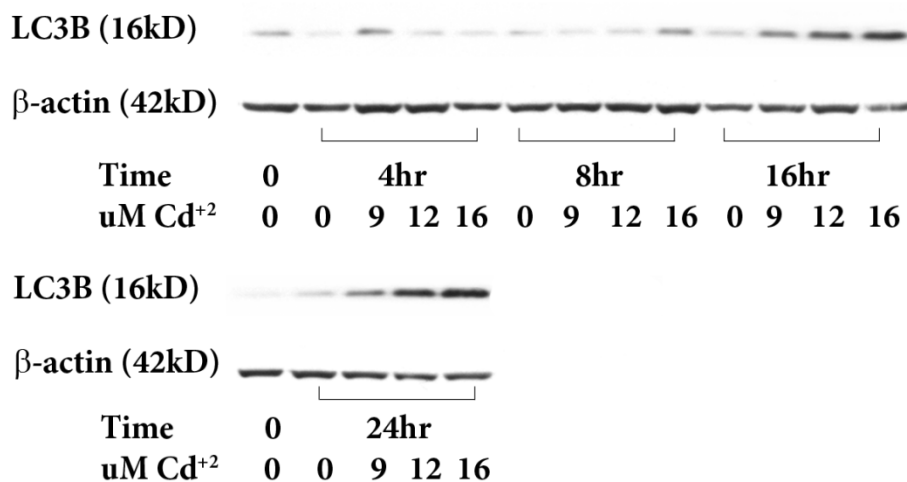
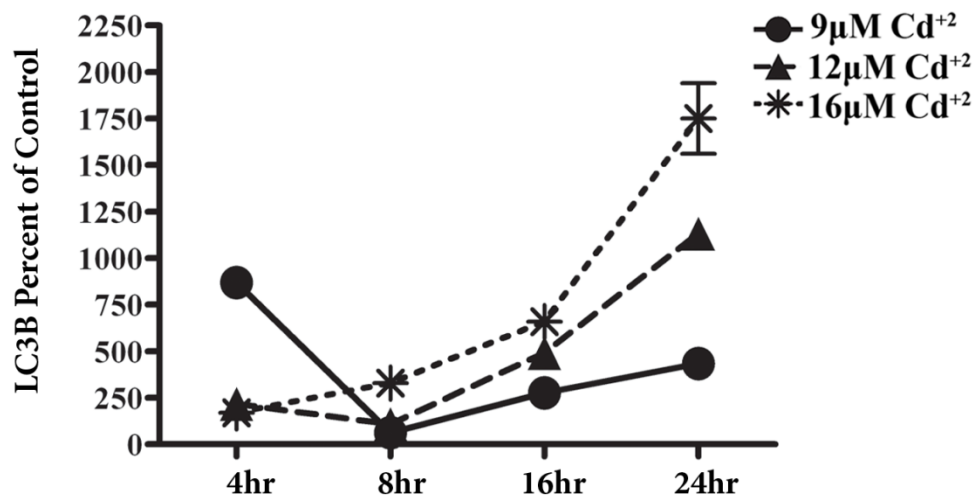


Figure II-27. Protein expression of LC3B in UROtsa Cd^{#7} cells. Western blot analysis of LC3B protein expression relative to percent of control in UROtsa Cd^{#7} cells treated with cadmium. 36 h treatment was omitted due to loss of cell viability. Duplicate blots were stained for LC3B and β -actin as a control. Graph is representative of the IOD of the western blot below it. Protein levels are shown as the mean \pm SE.

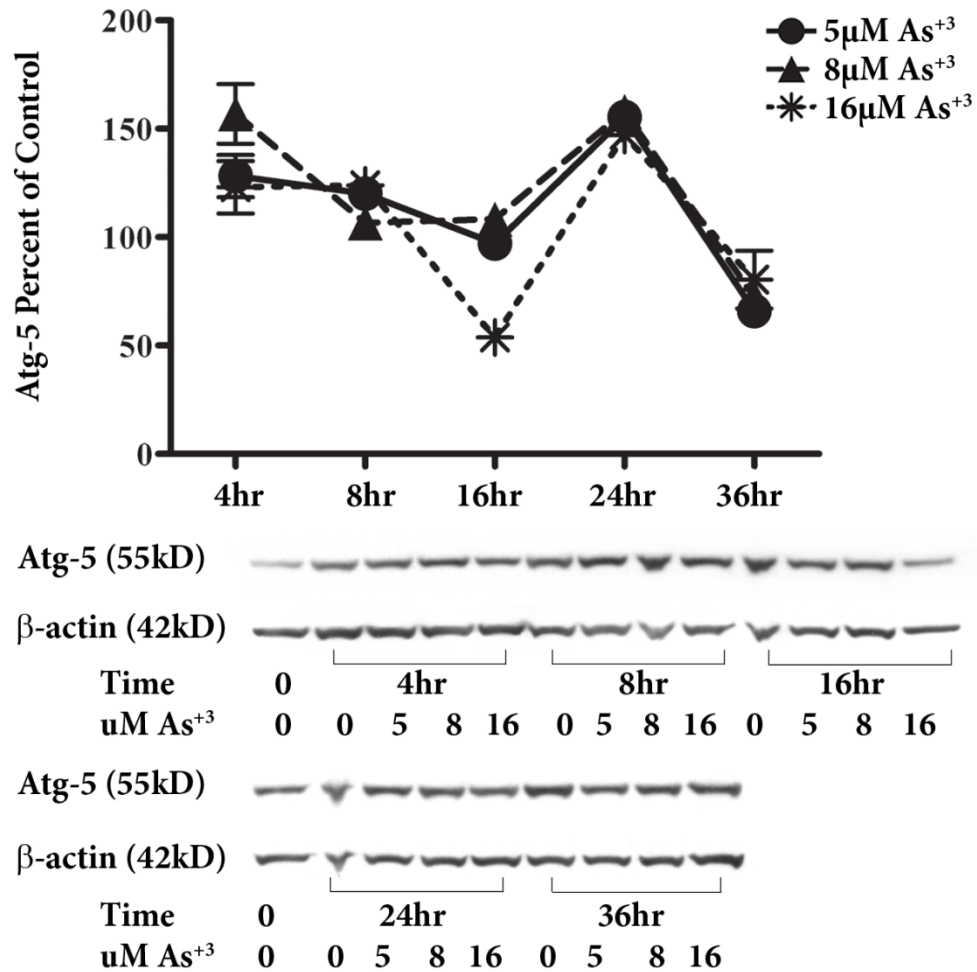


Figure II-28. Protein expression of Atg-5 in UROtsa As^{#1} cells. Western blot analysis of Atg-5 protein expression relative to percent of control in UROtsa As^{#1} cells treated with As⁺³. Duplicate blots were stained for Atg-5 and β-actin as a control. Graph is representative of the IOD of the western blot below it. Protein levels are shown as the mean ±SE.

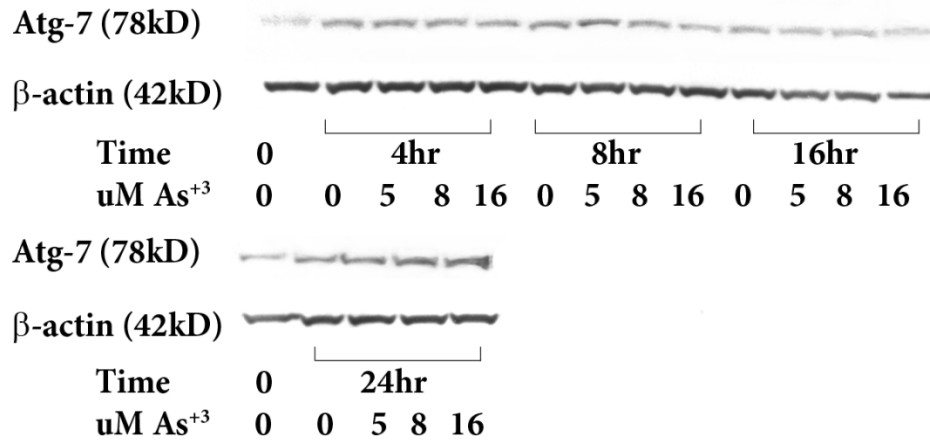
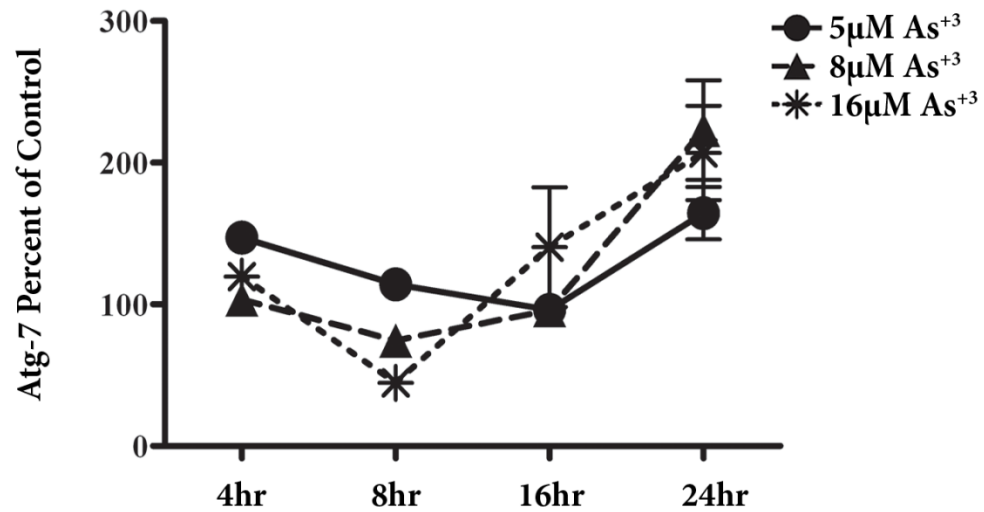


Figure II-29. Protein expression of Atg-7 in UROtsa As^{#1} cells. Western blot analysis of Atg-7 protein expression relative to percent of control in UROtsa As^{#1} cells treated with As⁺³. 36 h treatment was omitted due to loss of cell viability. Duplicate blots were stained for Atg-7 and β -actin as a control. Graph is representative of the IOD of the western blot below it. Protein levels are shown as the mean \pm SE.

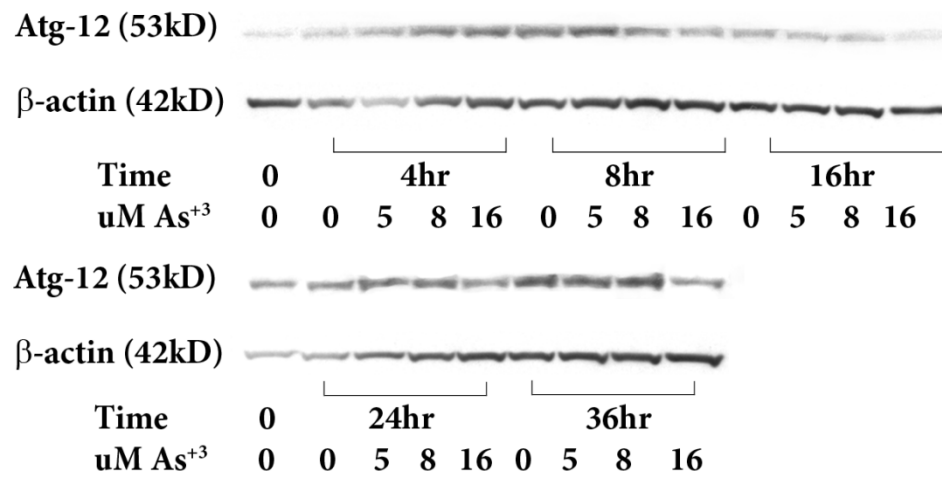
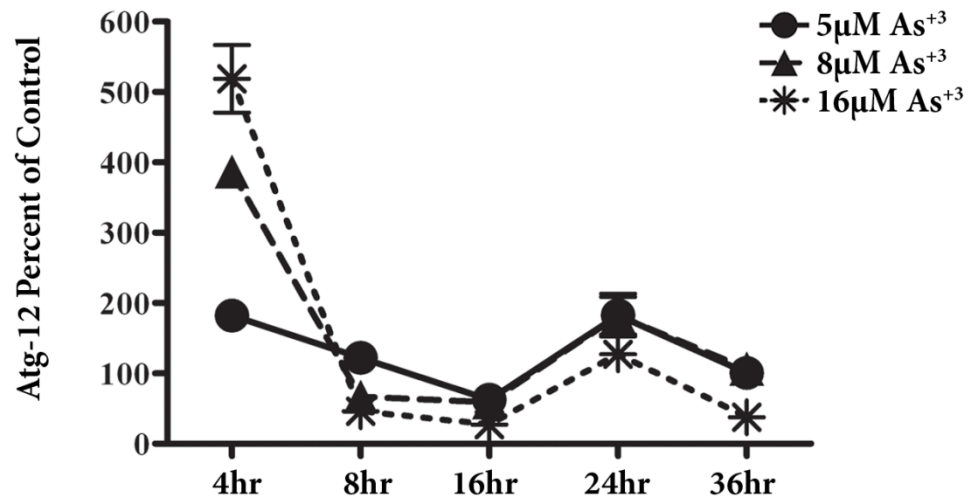


Figure II-30. Protein expression of Atg-12 in UROtsa As^{#1} cells. Western blot analysis of Atg-12 protein expression relative to percent of control in UROtsa As^{#1} cells treated with As⁺³. Duplicate blots were stained for Atg-12 and β-actin as a control. Graph is representative of the IOD of the western blot below it. Protein levels are shown as the mean ±SE.

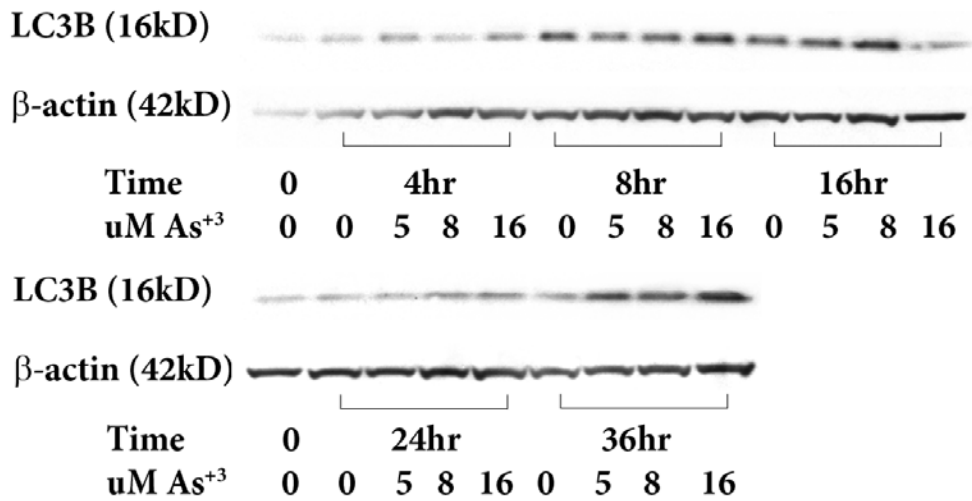
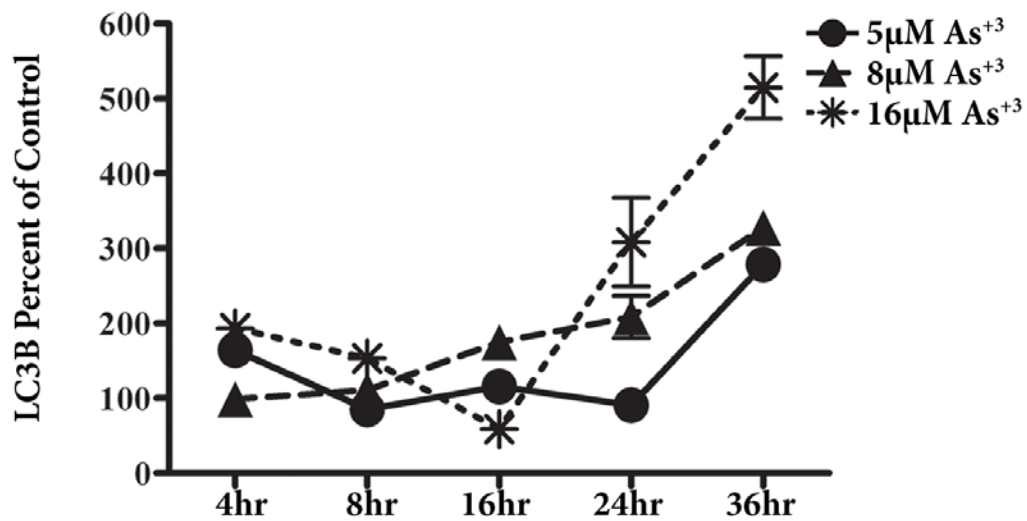


Figure II-31. Protein expression of LC3B in UROtsa As^{#1} cells. Western blot analysis of LC3B protein expression relative to percent of control in UROtsa As^{#1} cells treated with As³⁺. Duplicate blots were stained for LC3B and β-actin as a control. Graph is representative of the IOD of the western blot below it. Protein levels are shown as the mean ±SE.

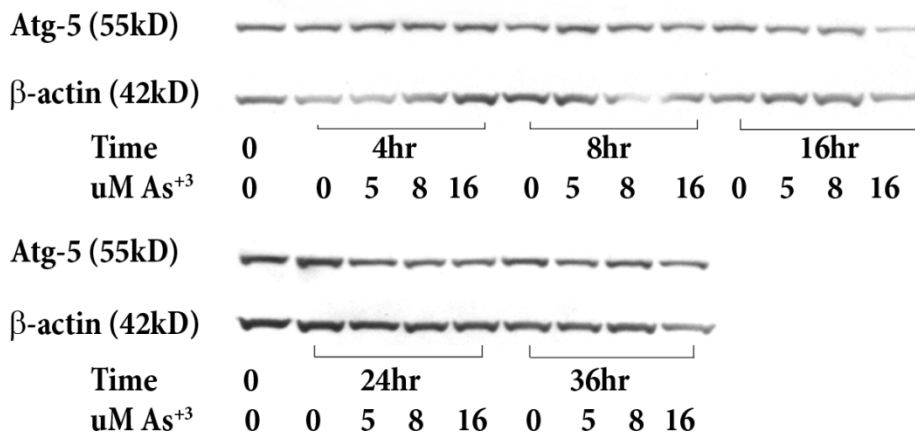
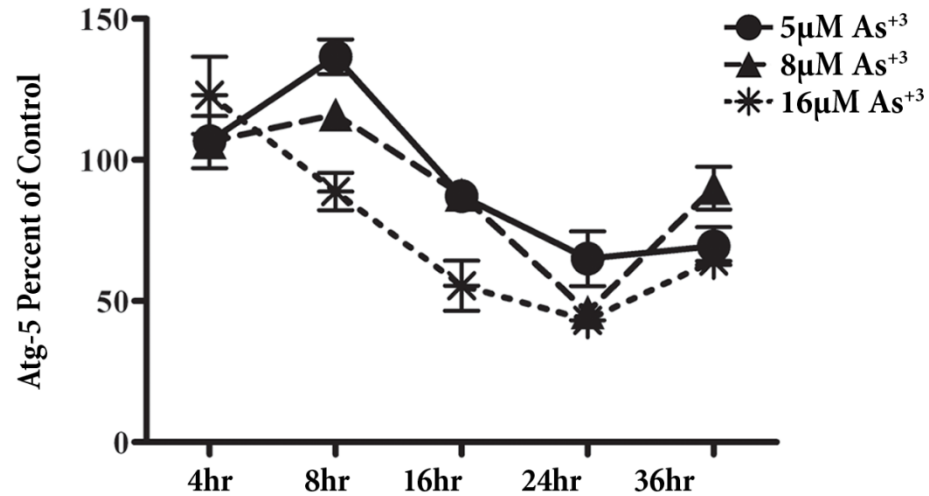


Figure II-32. Protein expression of Atg-5 in UROtsa As^{#6} cells. Western blot analysis of Atg-5 protein expression relative to percent of control in UROtsa As^{#6} cells treated with As³⁺. Duplicate blots were stained for Atg-5 and β-actin as a control. Graph is representative of the IOD of the western blot below it. Protein levels are shown as the mean ±SE.

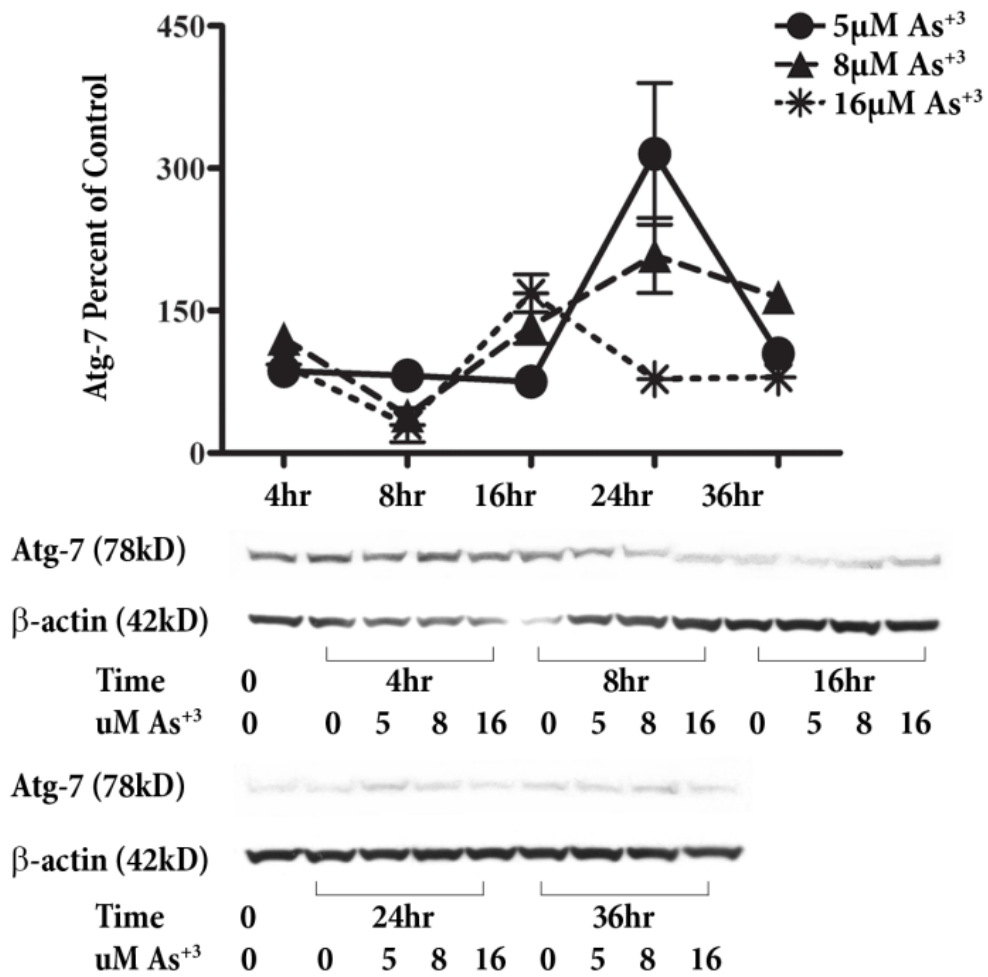


Figure II-33. Protein expression of Atg-7 in UROtsa As^{#6} cells. Western blot analysis of Atg-7 protein expression relative to percent of control in UROtsa As^{#6} cells treated with As⁺³. Duplicate blots were stained for Atg-7 and β-actin as a control. Graph is representative of the IOD of the western blot below it. Protein levels are shown as the mean ±SE.

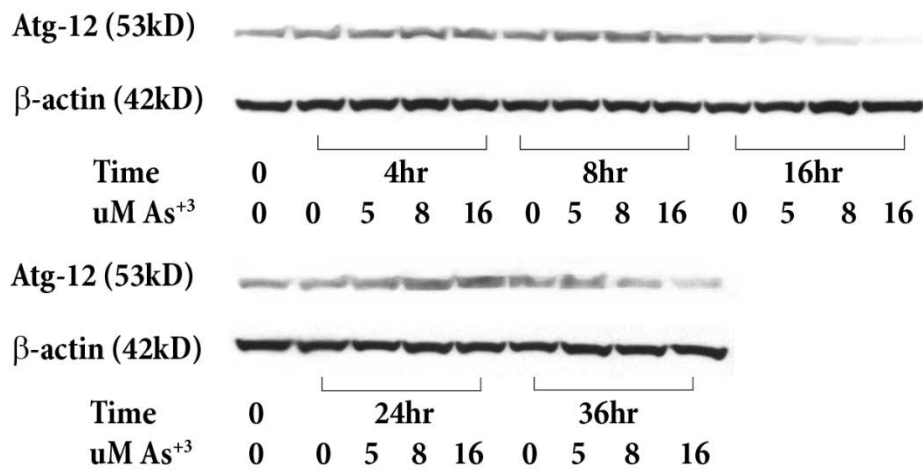
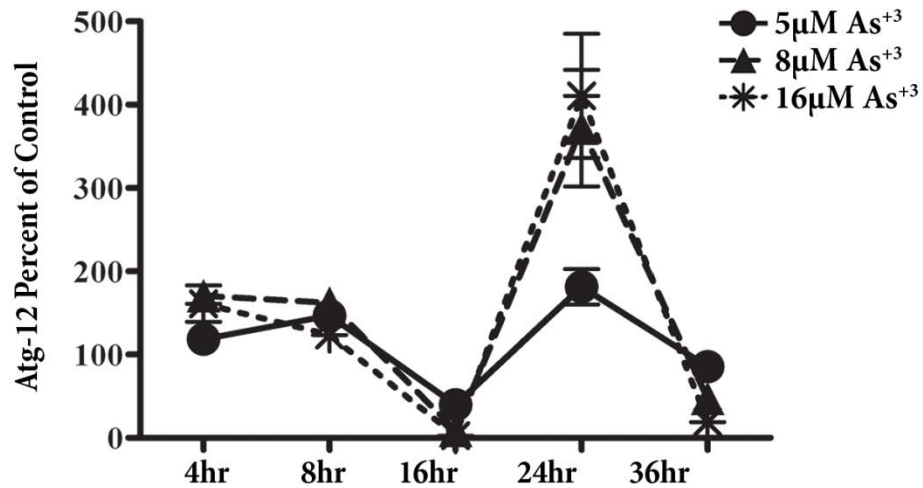


Figure II-34. Protein expression of Atg-12 in UROtsa As^{#6} cells. Western blot analysis of Atg-12 protein expression relative to percent of control in UROtsa As^{#6} cells treated with As⁺³. Duplicate blots were stained for Atg-12 and β-actin as a control. Graph is representative of the IOD of the western blot below it. Protein levels are shown as the mean ±SE.

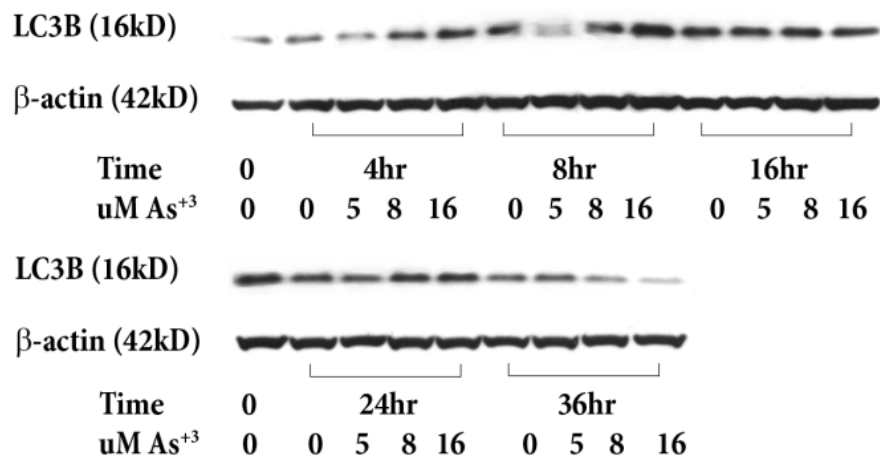
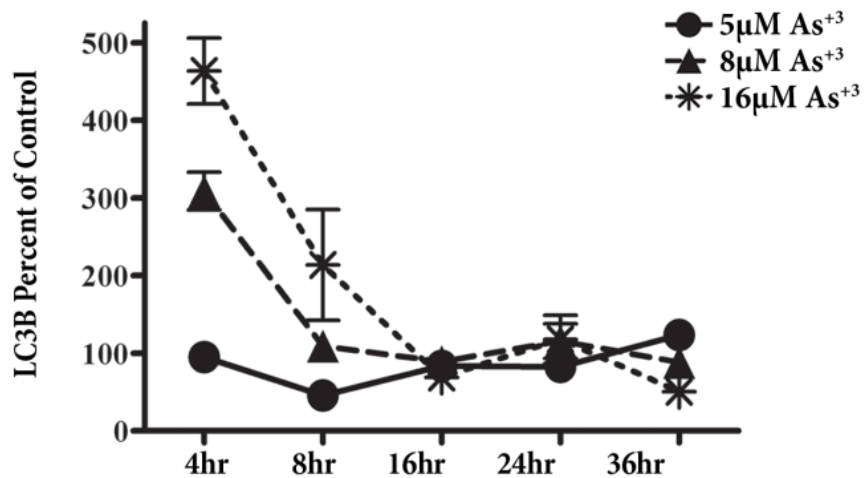


Figure II-35. Protein expression of LC3B in UROtsa As^{#6} cells. Western blot analysis of LC3B protein expression relative to percent of control in UROtsa As^{#6} cells treated with As³⁺. Duplicate blots were stained for LC3B and β-actin as a control. Graph is representative of the IOD of the western blot below it. Protein levels are shown as the mean ±SE.

CHAPTER III

SPARC GENE EXPRESSION IS REPRESSED IN HUMAN UROTHELIAL CELLS
(UROTSA) EXPOSED TO OR MALIGNANTLY TRANSFORMED BY CADMIUM
OR ARSENITE

Jennifer L. Larson², Tahmina Yasmin¹, Donald A. Sens¹, Xu Dong Zhou¹, Mary Ann
Sens¹, Scott H. Garrett¹, Jane R. Dunlevy², Ling Cao¹, and Seema Somji¹

Departments of Pathology¹

Anatomy and Cell Biology²

School of Medicine and Health Sciences

University of North Dakota

Grand Forks, ND 58202

Toxicology Letters 199 (2010) 166-172

Copyright
2010
by
Elsevier Limited
The Boulevard
Langford Lane
Kidlington, Oxford OX5 1GB UK

Used by permission
104

Abstract

SPARC belongs to a class of extracellular matrix-associated proteins that have counteradhesive properties. The ability of SPARC to modulate cell-cell and cell-matrix interactions provides a strong rationale for studies designed to determine its expression in cancer. The objective of this study was to determine if SPARC expression was altered in cadmium (Cd^{+2}) and arsenite (As^{+3}) induced bladder cancer and if these alterations were present in archival specimens of human bladder cancer. The expression of SPARC was determined in human parental UROtsa cells, their Cd^{+2} and As^{+3} transformed counterparts and derived tumors, and in archival specimens of human bladder cancer using a combination of real time reverse transcriptase-polymerase chain reaction, western blotting, immunofluorescence localization, and immunohistochemical staining. It was demonstrated that SPARC expression was down-regulated in Cd^{+2} and As^{+3} transformed UROtsa cells. In addition, the malignant epithelial component of tumors derived from these cell lines were also down-regulated for SPARC expression, but the stromal cells recruited to these tumors was highly reactive for SPARC. This finding was shown to translate to specimens of human bladder cancer where tumor cells were SPARC negative, but stromal cells were positive. Acute exposure of UROtsa cells to both cadmium and arsenite reduced the expression of SPARC through a mechanism that did not involve changes in DNA methylation or histone acetylation. These studies suggest that environmental exposure to As^{+3} or Cd^{+2} can alter cell-cell and cell-matrix interactions in normal urothelial cells through a reduction in the expression of SPARC. The SPARC associated loss of cell-cell and cell-matrix contacts may participate in the multi-step process of bladder carcinogenesis.

Introduction

SPARC (secreted protein acidic and rich in cysteine), also known as BM-40 and osteonectin, is a 43 kDa protein and a prototype for a class of extracellular matrix-associated proteins with counteradhesive properties (Hudson et al., 2005; Lane and Sage, 1994; Motamed et al., 1995; Sage and Bornstein, 1991). This property includes the ability to dismantle focal adhesions (Motamed et al., 1995; Murphy-Ullrich et al., 1995; Murphy-Ullrich, 2001). In association with thombospondin-1 and tenascin C, this class comprises a non-homologous functional group of secreted matricellular proteins that interact with cell surface receptors, growth factors, and the extracellular matrix (Bornstein, 1995; Chiquet-Ehrismann, 1993; Crossin, 1996; Erickson, 1993; Hudson et al., 2005). The mechanism(s) that control the expression of the SPARC gene in individual cells and tissues are not known. The ability of SPARC to modulate cell-cell and cell-matrix interactions and to have de-adhesive properties has led to many studies assessing its role in cancer (Tai and Tang, 2008). SPARC has been shown to be associated with highly aggressive tumors in some cancers, while in others it appears to function as a tumor suppressor. There have been limited studies of SPARC expression in human bladder cancer. The level of SPARC mRNA has been shown to correlate with increased histological grade, pathological stage, and poor prognosis (Yamanaka et al., 2001); however, the expression of SPARC protein has not been determined. In normal bladder, the SPARC protein has been localized to basal urothelial cells in mice as discrete 20-100 μm foci (Bassuk et al., 2000). In humans, SPARC has been shown to be expressed at the luminal surface of normal urothelium (Alpers et al., 2002). Primary cultures of human urothelial cells have been shown to express SPARC and secrete

SPARC into the conditioned growth medium (Delostrinos et al., 2006; Hudson et al., 2005).

The development of bladder cancer is known to have a strong association with environmental exposures (Bischoff and Clark, 2009). This laboratory employs the human UROtsa cell line as a model to explore the relationship between As^{+3} and Cd^{+2} exposure and the development of urothelial cancer. The UROtsa cell line is an immortalized, but not tumorigenic model that retains features of transitional urothelium when propagated on a serum free growth medium (Rossi et al., 2001). This cell line has been used to show that both Cd^{+2} and As^{+3} can cause the malignant transformation of human urothelial cells (Sens et al., 2004). The laboratory has subsequently isolated and characterized 6 additional Cd^{+2} transformed cell lines and 5 additional As^{+3} transformed cell lines (Cao et al., 2010; Somji et al., 2010b). These cell lines were all shown to retain a morphology consistent with human urothelial cancer and to display phenotypic differences characteristic of tumor heterogeneity. The histology of subcutaneous tumor heterotransplants produced by these transformed isolates displayed histologic features of human urothelial carcinoma with areas of squamous differentiation. This observation is important since urothelial carcinoma is the most prominent type of bladder cancer in western countries and accounts for over 95% of all cases and is 5th in overall occurrence (Bischoff and Clark, 2009). The association of bladder cancer with environmental exposure is particularly strong for arsenic and correlates to the same endemic areas of the world where populations were identified with arsenic-induced skin cancer (Cantor and Lubin, 2007; Chiou et al., 1995; Luster and Simeonova, 2004; Smith et al., 1998; Steinmaus et al., 2000; Tsuda et al., 1995). The association of Cd^{+2} with urothelial

cancer is not as strong, but several epidemiological studies have implicated Cd^{+2} in the development of bladder cancer (Kellen et al., 2007; Siemiatycki et al., 1994; Waalkes, 2000). The high level of Cd^{+2} accumulation in individuals who smoke cigarettes, along with the strong association of bladder cancer and smoking, is the major factor indirectly implicating Cd^{+2} in the development of urothelial cancer (Satarug and Moore, 2004; Satarug et al., 2010).

The first goal of the present study was to show that SPARC expression is altered when UROtsa cells are exposed to, or malignantly transformed, by As^{+3} or Cd^{+2} . The second was to characterize SPARC expression in subcutaneous tumors generated from the Cd^{+2} and As^{+3} transformed cell lines. The third goal was to implicate or eliminate DNA methylation and histone acetylation as potential regulatory mechanisms for control of SPARC gene expression and the final goal was to show translation of the findings to human bladder cancer by characterizing SPARC expression in archival samples of human urothelial cancer.

Materials and Methods

Cell Culture

The procedures for the culture of the parental UROtsa cell line and the Cd^{+2} and As^{+3} induced malignant transformants have been described previously (Cao et al., 2010; Sens et al., 2004; Somji et al., 2010b). Briefly, stock cultures of the parental UROtsa cell line were maintained in 75 cm^2 tissue culture flasks using Dulbecco's modified Eagle's medium (DMEM) containing 5% v/v fetal calf serum in a 37°C, 5% CO_2 : 95% air atmosphere (Rossi et al., 2001). The Cd^{+2} and As^{+3} transformed UROtsa cell lines were grown and maintained using identical conditions. Confluent flasks were subcultured at a

1:4 ratio using trypsin-EDTA (0.05%, 0.02%) and the cells were fed fresh growth medium every 3 days

Basal Expression of SPARC in UROtsa Cells and Tumor Heterotransplants

The preparation of total RNA and protein from the parental UROtsa cell line and from the Cd⁺² and As⁺³ transformed cell lines and their subcutaneous heterotransplants have been described previously (Cao et al., 2010; Sens et al., 2004; Somji et al., 2010b). Pre-existing samples from these studies were used to determine the basal expression of SPARC mRNA and protein in this study. The expression of SPARC mRNA was determined using real time RT-PCR and SPARC specific primers obtained from Qiagen (Valencia, CA). Briefly, 1 µg of purified RNA was subjected to complementary DNA (cDNA) synthesis using the iScript cDNA synthesis kit (Bio-Rad Laboratories, Hercules, CA) in a total volume of 20 µL. Real-time PCR was performed utilizing the SYBR Green kit (Bio-Rad Laboratories) with 2 µL of cDNA, 0.2 µM primers in a total volume of 20 µL in an iCycler iQ real-time detection system (Bio-Rad Laboratories). Amplification was monitored by SYBR Green fluorescence. The level of SPARC mRNA was determined relative to the UROtsa cells grown in serum containing medium using serial dilutions of this sample as the standard curve. The resulting relative levels were then normalized to the fold change in β-actin expression assessed by the same assay using the primers, sense: CGACAACGGCTCCGGCATGT and antisense: TGCCGTGCTCGATGGGGTACT, giving a product size of 194 bp and with the cycling parameters of annealing/extension at 62°C for 45 sec and denaturation at 95°C for 15 sec.

The expression of SPARC protein was determined by western blotting using 20 µg of total cellular protein. After blocking, the membranes were probed with mouse

anti-human osteonectin primary antibody (5 µg/mL; Haematologic Technologies Inc., Essex Junction, VT) in blocking buffer for 1 h at room temperature. After washing 3 times with Tris buffered saline (TBS) containing 0.1% Tween 20 (TBS-T), the membranes were incubated with the anti-mouse secondary antibody (1:2000) in antibody dilution buffer for 1 h. The blots were visualized using the Phototope-HP (horseradish peroxidase) western blot detection system (Cell Signaling Technology, Beverly, MA).

Immunolocalization of SPARC in Parental UROtsa Cells

The UROtsa cell lines were grown in 24 well plates containing 12 mm glass coverslips at 37° C, 5% carbon dioxide. Cells at a subconfluent density were then fixed and stained according to published protocols (Cao et al., 2010; Sens et al., 2004; Somji et al., 2010b). Briefly, cells were fixed in 3.7% buffered paraformaldehyde for 10 min at room temperature. Coverslips were then quenched of free aldehyde with 0.1 M ammonium chloride for 15 min, followed by permeabilization with 0.1% Igepal (NP-40) for 10 min. Cells were stained for SPARC by incubation for 45-60 min at 37° C with a 1:20 dilution of mouse anti-onectin antibody (Leica Microsystems Inc., Bannockburn, IL). Primary antibody was detected by incubating cells with 4.0 µg/mL of Alexa Fluor 594 goat anti-mouse IgG (Invitrogen, Carlsbad, CA) for 45-60 min at 37° C. Controls consisted of coverslips treated with the appropriate secondary antibody only. Coverslips were then mounted in ProLong Gold anti-fade reagent with 4',6-diamidino-2-phenylindole (DAPI) (Invitrogen) for nuclear counter staining. Cells were observed and images captured using a Zeiss LSM 510 Meta Confocal Microscope with LSM 510 software (Carl Zeiss MicroImaging Inc.). Images were composed by capturing z-slices at

a depth of 0.5 μm , stacking the z-slices together, and merging with the DAPI image of the same field so all cells in the field could be identified.

Immunohistochemical Localization of SPARC in Tumor Heterotransplants and Archival Specimens of Human Bladder Cancer

The production of subcutaneous nude mouse heterotransplants from the Cd^{+2} and As^{+3} transformed UROtsa cell lines has been previously described (Sens et al., 2004). Tumor tissues taken from these and related studies (Cao et al., 2010; Somji et al., 2010b) were utilized in the present study to determine the localization and expression of SPARC in tumor heterotransplants. Tissue sections for the immunohistochemical analysis of SPARC expression in human bladder were obtained from archival paraffin blocks that originated from previously completed patient diagnostic procedures. These archival specimens contained no patient identifiers and use was approved by the University of North Dakota Internal Review Board. Prior to immunostaining, after routine deparaffinization and rehydration, sections were immersed in preheated 10 mM sodium citrate buffer (pH 6.0) and heated in a steamer for 20 min. The sections were allowed to cool to room temperature for 30 min and then immersed into TSB-T (Dako, Carpinteria, CA) for 5 min. Endogenous peroxidase was extinguished by incubating the sections in Peroxidase Blocking Reagent (Dako) for 10 min. SPARC was localized by incubating the slides with mouse monoclonal anti-osteonectin antibody (Leica Microsystems Inc.) for 30 min at room temperature. For archival human bladder specimens, the signal was detected using Dako EnVision + Dual Link System-HP (Dako). For tumor heterotransplants, Dakocytomation ARK (Animal Research Kit) was used to visualize the signal, following manufacturer's instruction. For both human tissue and mouse tumor heterotransplants, liquid diaminobenzidine (Dako) was used as chromogen.

Expression of SPARC in UROtsa Cells Exposed to Cd⁺² and As⁺³

Preliminary experiments were performed to determine the conditions of exposure to Cd⁺² and As⁺³ that were near to, but below, a level that produced cell death in confluent cultures of the parental UROtsa cells over a 10 day period of exposure. From these preliminary determinations, 3 concentrations of cadmium chloride (1.0, 2.0, and 4.0 μ M) and sodium arsenite (1.0, 3.0 and 6.0 μ M) were then chosen for experimental use such that over the 10 day time course, one concentration would result in minimal cell death and another that would result in appreciable cell death early in the time course. Cell viability, as an indicator of cytotoxicity, was determined by measuring the capacity of the UROtsa cells to reduce MTT (3-(4, 5-dimethylthiazol-2-yl)-2, 5-diphenyltetrazolium bromide) to formazan (Sens et al., 2002). The determination of SPARC mRNA using real time RT-PCR and protein by western blotting was as described above.

Treatment of Cd⁺² and As⁺³ Transformed UROtsa Cells with 5-Aza-2'-deoxycytidine (5-AZC) and Histone Deacetylase Inhibitor

The parental and transformed UROtsa cell lines were seeded at a ratio of 1:10 and the next day they were exposed to 0.5, 1.0 and 3.0 μ M 5-AZC or the histone deacetylase inhibitor MS-275 at 0.5, 1.5, and 5.0 μ M until the cells reached confluency (48 h). Cells were then harvested to determine SPARC mRNA expression.

Statistics

Statistical analysis consisted of ANOVA with Tukey *post-hoc* testing performed by Graphpad PRISM 4. All statistical significance is denoted at $p < 0.05$.

Results

SPARC mRNA and Protein Expression in Parental UROtsa Cells and Cd⁺² and As⁺³ Transformed Cell Lines

The expression and localization of SPARC was determined for the parental UROtsa cells and the 7 Cd⁺² and 6 As⁺³ transformed cell lines. The parental UROtsa cells expressed a moderate amount of SPARC mRNA when compared to the common transcript, β -actin (Figure III-1A). In contrast, SPARC mRNA expression was at the limit of detection in the UROtsa cell lines malignantly transformed by either Cd⁺² or As⁺³ (Figure III-1A). A corresponding analysis of SPARC protein expression by western blotting showed that only the parental UROtsa cell line had expression of the SPARC protein (Figure III-1B). None of the 13 independent UROtsa cell lines transformed by either Cd⁺² or As⁺³ showed any evidence of expression of the SPARC protein (Figure III-1B). The localization of SPARC within the UROtsa cells was determined by immunofluorescence analysis. The analysis showed that the majority of the parental UROtsa cells showed intracellular expression of the SPARC protein, with only very infrequent cell profiles showing no SPARC immunoreactivity (Figure III-2A). In contrast, none of the 13 independent UROtsa cell lines transformed by either Cd⁺² or As⁺³ had cell profiles that were immunoreactive for the SPARC protein (Figure III-2B). When present, SPARC was localized to the cytoplasm (Figure III-2C) and appeared as distinct vesicles (Figure III-2D).

SPARC mRNA and Protein Expression in Tumor Heterotransplants Produced From Cd⁺² and As⁺³ Transformed UROtsa Cell Lines

The expression of SPARC mRNA and protein was determined on extracts prepared from the subcutaneous tumors generated from the 7 Cd⁺² and 6 As⁺³

transformed cell lines (Figure III-3). For all the isolates, the expression of SPARC mRNA was at the limit of detection (Figure III-3A) and western blotting failed to demonstrate any expression of the SPARC protein (Figure III-3B). The immunohistochemical analysis of SPARC expression in the heterotransplants showed no staining of SPARC in the urothelial cancer cells from any of the 7 Cd⁺² and 6 As⁺³ transformed cell lines (Figure III-4). In contrast, the stromal components of the urothelial tumors generated from the cell lines were positive for the expression of the SPARC protein. An example of this immunostaining pattern of SPARC is illustrated for one tumor generated from a Cd⁺² transformed cell line (Figure III-4A) and one from a As⁺³ transformed cell line (Figure III-4B) (Yasmin, 2009).

SPARC mRNA Expression in Parental and As⁺³ and Cd⁺² Transformed UROtsa Cells Following Treatment with Inhibitors of DNA Methylation and Acetylation

The parental cell line and single isolates of the As⁺³ and Cd⁺² transformed UROtsa cells were treated with the histone deacetylase inhibitor, MS-275, and the methylation inhibitor, 5-AZC, to determine the possible role of epigenetic modifications on SPARC mRNA expression. This analysis demonstrated that none of the cell lines, parental or transformed, treated with MS-275 (Figure III-5A) or 5-AZC (Figure III-6A) expressed increased levels of SPARC mRNA compared to the untreated controls. Additional experiments were performed where treatment of the cells with MS-275 or 5-AZC was increased to 48 h and 72 h with no change in the results (Figures III-5B, C and Figure III-6B, C). The treatment of the three cell lines with a combination of the two drugs also had no effect on SPARC mRNA expression (Figure III-7). An identical protocol has been used by the laboratory to show that treatment of MCF-10 human breast

cells with 5-AZC and MS-275 induces the expression of MT-3 mRNA (Somji et al., 2010a).

SPARC Expression in Parental UROtsa Cells Exposed to Cd⁺² and As⁺³

The expression of SPARC was determined in parental UROtsa cells following exposure to Cd⁺² and As⁺³. The results showed that the expression of SPARC mRNA was significantly reduced following a 24 h exposure to as little as 1 μM of Cd⁺² (Figure III-8A). The expression of SPARC mRNA showed further reductions when either the level of Cd⁺² was increased during a 24 h period of exposure or when the period of exposure to 1 μM Cd⁺² was extended to 5 days. The expression of SPARC protein was also reduced significantly following Cd⁺² exposure and in general followed the pattern of SPARC mRNA, when an expected slower rate of SPARC protein degradation is taken into account (Figure III-8B). The expression of SPARC was also shown to be reduced in parental UROtsa cells following exposure to As⁺³ (Figure III-9A, B). The level of SPARC mRNA and protein was not reduced following a 24 h exposure of the cells to 1, 3 or 6 μM As⁺³. In contrast, a reduction in SPARC mRNA and protein occurred when the parental UROtsa cells were exposed to 1, 3 or 6 μM As⁺³ for 3, 5 and 7 days of exposure.

During the process of transforming the UROtsa cells with Cd⁺² or As⁺³, cells were harvested and frozen down during the time course needed to fully transform these cells. The expression of SPARC was therefore determined in the UROtsa As^{#3} cell line at an early passage (P6) within the transformation process and also at a later passage (P26) within the transformation process. The resulting mRNA and protein levels of SPARC were compared to the UROtsa parental cell line and the fully transformed As^{#3} cell line.

The mRNA and protein expression of SPARC decreased roughly by half in the As^{#3} P6 cell line compared to the UROtsa parent and SPARC expression was further reduced in the As^{#3} P26. The expression of SPARC mRNA and protein detected within the fully transformed As^{#3} cell line was very similar to that seen in the As^{#3} P26 cell line.

Immunohistochemical Staining of SPARC in Normal Human Bladder, Cystitis, Noninvasive, and Invasive Urothelial Carcinoma

The immunohistochemical staining of SPARC was determined on 4 samples of non-cancerous “normal” urothelium, 5 cases of low grade urothelial cancer and 6 cases of high grade urothelial cancer. Two cases of normal urothelium had no evidence of cystitis or inflammation. In these two cases, SPARC was moderately expressed in the upper superficial cells of the urothelium (Figure III-10A). In addition, SPARC was also expressed in a few small stromal cells located in the superficial lamina propria just beneath the urothelium. There was no SPARC staining of the blood vessels in the normal lamina propria. One case of archived normal urothelium was accompanied by frozen tissue and total RNA and protein were prepared and shown to contain SPARC mRNA and protein (Figure III-10A, B). The other 2 cases of normal urothelium were non-cancerous, but did have prominent inflammation (cystitis). The expression of SPARC in the urothelium of these two samples was identical to that of the above samples, with SPARC expression localized to the superficial layer of the urothelium. However, in these samples with inflammation, there were more frequent profiles of SPARC expression localized to stromal cells and also for the endothelium of the blood vessels located in the lamina propria (Figure III-10B). The stromal cells that express SPARC were usually spindle-shaped and could be located anywhere in the bladder where inflammation was present; not being limited in expression to the superficial lamina propria as that found in

normal bladder specimens with no inflammation. In an area with granulation formation, the newly formed blood vessels with plump endothelial cells were strongly positive for SPARC, while the flat endothelial cells in mature blood vessels located deep in the lamina propria were only weakly positive or negative for SPARC (Figure III-10C).

In contrast to normal urothelium, all 5 cases of low grade bladder cancer were found to have no expression of SPARC in the tumor urothelium (Figure III-10D). In cases where there was no tumor-associated inflammation or necrosis, only a few SPARC positive stromal cells were present in the papillary core, while more stromal cells expressing SPARC could be found in the basal area of the tumor, where the tumor connects to the wall of the bladder (data not shown). The endothelial cells of the blood vessels in the papillary cores of the tumors were usually strongly stained for SPARC (Figure III-10D). In some of the cases of low grade carcinoma, a band of inflammatory reaction could be identified in the interface between tumor and bladder wall; and in these instances there was an increase in the number of SPARC reactive stromal cells (data not shown). In areas of necrosis, whether in the tumor or in a tumor free area, there was a large number of SPARC-positive stromal cells that surrounded the area of necrosis (Figure III-10E).

Identical to that found in low grade urothelial cancer, the tumor cells of high grade, invasive urothelial cancer were found to have no expression of SPARC protein (Figure III-10F). The high grade urothelial cancers did have a prominent desmoplastic stromal reaction that was present in and around the invasive carcinoma. These desmoplastic stromal cells were prominently stained for SPARC as were the endothelial cells of the blood vessels in or adjacent to the invasive carcinoma (Figure III-10F). The

stromal cells that stained for SPARC were more prominent in areas surrounding the invasive carcinoma than the stromal cells located within the invasive carcinoma itself. In areas of the invasive carcinomas that did not exhibit a prominent stromal reaction there were fewer SPARC reactive stromal cells, but the associated blood vessels, when present, had endothelium that was strongly positive for SPARC (data not shown). The expression of SPARC in the stromal cells of the tumor free areas from the cases of invasive carcinoma was similar to that noted above for normal bladder, depending on the degree of inflammation (data not shown).

Discussion

The present study is the first to show that the heavy metals, Cd^{+2} and As^{+3} , may down-regulate the expression of SPARC during the development and progression of bladder cancer. It is known from previous studies that SPARC is expressed in normal urothelium and urothelial cell cultures (Alpers et al., 2002; Bassuk et al., 2000; Delostrinos et al., 2006; Hudson et al., 2005). The present study shows that SPARC is also expressed in the parental UROtsa cells and that SPARC expression is reduced to the limit of detection when the cells are malignantly transformed by both Cd^{+2} and As^{+3} . Immunohistochemical analysis showed that the expression of SPARC was also down-regulated to background levels in the epithelial component of the tumors produced from cells injected subcutaneously into nude mice. In contrast, the stromal component of these tumors showed strong immunoreactivity for the SPARC protein. The stromal component originates from the murine host and is likely recruited to the tumor site by secretions from the tumor cells. The murine origin of the stromal component caused some minor difficulty in the interpretation of SPARC expression since the real time PCR primers and

antibody used to assess human SPARC expression were chosen to perform optimally on human cells and tissue. While the human SPARC antibody was effective in the immunohistochemical localization of SPARC in murine stroma, it performed very poorly when used for western blotting. The sequence of the primers used for real time analysis of SPARC mRNA in humans is not preserved in the murine sequence. Despite these technical limitations, the results clearly show that SPARC expression is down-regulated when UROtsa cells are transformed by Cd⁺² or As⁺³ and that the stroma recruited to tumors produced by the SPARC negative epithelial cells are strongly immunoreactive for SPARC.

Another significant finding is that the above alterations in SPARC expression found in tumors from Cd⁺² and As⁺³ transformed UROtsa cells translates to human urothelial cancer. The present study confirmed that SPARC is expressed in normal urothelium. A new finding in this study using archival specimens of human bladder cancer was that SPARC expression is absent in the malignant urothelial cells comprising human urothelial cancer, but is highly expressed in the stromal component of these tumors. The expression of SPARC was also noted in endothelial cells in areas of inflammation and in inflammatory cells at these sites. These findings impact on the previous report that SPARC expression is increased in human urothelial cancer (Yamanaka et al., 2001). In this study, SPARC expression was determined only at the level of mRNA expression with no determination of the SPARC protein by immunohistochemical localization. It is highly likely that this study noted increased expression of SPARC in urothelial cancer due to SPARC expression in the tumor recruited stroma and not in the malignant urothelial cells themselves. Using this

interpretation, the previous study would have actually correlated to increased expression of SPARC in the stromal component of urothelial cancer, and not to the cancer cells themselves, with increased histological grade, pathological stage, and poor prognosis. A future retrospective study will need to be performed to determine if it is the amount of stroma that expresses SPARC or the level of SPARC expression in the stroma, or both, that correlated to these important clinical parameters.

It was also determined that acute exposure of the parental UROtsa cells to both Cd^{+2} and As^{+3} resulted in a reduction in the expression of SPARC mRNA and protein. The reduction was especially pronounced for Cd^{+2} , but reductions by both agents occurred at concentrations routinely used to mimic the effects of environmental exposure to these pollutants. To our knowledge, this is the first indication that exposure to Cd^{+2} or As^{+3} might cause a reduction in the expression of SPARC in human cells. The study also showed that SPARC expression was not changed in the normal or transformed cells by treatment of the cells with either a histone deacetylase inhibitor or a demethylating agent. The possibility that SPARC expression might be influenced by histone modification or DNA methylation was suggested by studies showing aberrant methylation of the SPARC gene in human lung and ovarian cancers (Socha et al., 2009; Suzuki et al., 2005). The finding that both Cd^{+2} and As^{+3} had similar effects on SPARC expression before and following malignant transformation suggests a similar mechanism of action once the agents are fully elaborated inside the cell. The laboratory employs both agents in environmental bladder cancer research since each has distinctly different modes of cellular uptake and processing once inside the cell. This is especially pronounced for cellular processing since Cd^{+2} remains chemically unaltered inside the cell and As^{+3}

requires methylation to become active. The present study implicates both Cd^{+2} and As^{+3} as agents affecting SPARC expression in bladder cancer.

References

- Alpers, C.E., Hudkins, K.L., Segerer, S., Sage, E.H., Pichler, R., Couser, W.G., Johnson, R.J., Bassuk, J.A., 2002. Localization of SPARC in developing, mature, and chronically injured human allograft kidneys, *Kidney Int.* 62, 2073-2086.
- Bassuk, J.A., Grady, R., Mitchell, M., 2000. Review article: The molecular era of bladder research. Transgenic mice as experimental tools in the study of outlet obstruction, *J. Urol.* 164, 170-179.
- Bischoff, C.J., Clark, P.E., 2009. Bladder cancer, *Curr. Opin. Oncol.* 21, 272-277.
- Bornstein, P., 1995. Diversity of function is inherent in matricellular proteins: an appraisal of thrombospondin 1, *J. Cell Biol.* 130, 503-506.
- Cantor, K.P., Lubin, J.H., 2007. Arsenic, internal cancers, and issues in inference from studies of low-level exposures in human populations, *Toxicol. Appl. Pharmacol.* 222, 252-257.
- Cao, L., Zhou, X.D., Sens, M.A., Garrett, S.H., Zheng, Y., Dunlevy, J.R., Sens, D.A., Somji, S., 2010. Keratin 6 expression correlates to areas of squamous differentiation in multiple independent isolates of As(+3)-induced bladder cancer, *J. Appl. Toxicol.* 30, 416-430.
- Chiou, H.Y., Hsueh, Y.M., Liaw, K.F., Horng, S.F., Chiang, M.H., Pu, Y.S., Lin, J.S., Huang, C.H., Chen, C.J., 1995. Incidence of internal cancers and ingested inorganic arsenic: a seven-year follow-up study in Taiwan, *Cancer Res.* 55, 1296-1300.
- Chiquet-Ehrismann, R., 1993. Tenascin and other adhesion-modulating proteins in cancer, *Semin. Cancer Biol.* 4, 301-310.
- Crossin, K.L., 1996. Tenascin: a multifunctional extracellular matrix protein with a restricted distribution in development and disease, *J. Cell. Biochem.* 61, 592-598.
- Delostrinos, C.F., Hudson, A.E., Feng, W.C., Kosman, J., Bassuk, J.A., 2006. The C-terminal Ca²⁺-binding domain of SPARC confers anti-spreading activity to human urothelial cells, *J. Cell. Physiol.* 206, 211-220.
- Erickson, H.P., 1993. Tenascin-C, tenascin-R and tenascin-X: a family of talented proteins in search of functions, *Curr. Opin. Cell Biol.* 5, 869-876.
- Hudson, A.E., Feng, W.C., Delostrinos, C.F., Carmean, N., Bassuk, J.A., 2005. Spreading of embryologically distinct urothelial cells is inhibited by SPARC, *J. Cell. Physiol.* 202, 453-463.

- Kellen, E., Zeegers, M.P., Hond, E.D., Buntinx, F., 2007. Blood cadmium may be associated with bladder carcinogenesis: the Belgian case-control study on bladder cancer, *Cancer Detect. Prev.* 31, 77-82.
- Lane, T.F., Sage, E.H., 1994. The biology of SPARC, a protein that modulates cell-matrix interactions, *FASEB J.* 8, 163-173.
- Luster, M.I., Simeonova, P.P., 2004. Arsenic and urinary bladder cell proliferation, *Toxicol. Appl. Pharmacol.* 198, 419-423.
- Motamed, K., Bassuk, J.A., Sage, E.H., 1995. Anti-adhesive properties of SPARC: Structural and functional correlates. In: Crossin, K.L. (Ed.), *Tenascin and Other Counteradhesive Molecules of the Extracellular Matrix*. Harwood Academic Press, Amsterdam, pp. 111-131.
- Murphy-Ullrich, J.E., 2001. The de-adhesive activity of matricellular proteins: is intermediate cell adhesion an adaptive state? *J. Clin. Invest.* 107, 785-790.
- Murphy-Ullrich, J.E., Lane, T.F., Pallero, M.A., Sage, E.H., 1995. SPARC mediates focal adhesion disassembly in endothelial cells through a follistatin-like region and the Ca(2+)-binding EF-hand, *J. Cell. Biochem.* 57, 341-350.
- Rossi, M.R., Masters, J.R., Park, S., Todd, J.H., Garrett, S.H., Sens, M.A., Somji, S., Nath, J., Sens, D.A., 2001. The immortalized UROtsa cell line as a potential cell culture model of human urothelium, *Environ. Health Perspect.* 109, 801-808.
- Sage, E.H., Bornstein, P., 1991. Extracellular proteins that modulate cell-matrix interactions. SPARC, tenascin, and thrombospondin, *J. Biol. Chem.* 266, 14831-14834.
- Satarug, S., Garrett, S.H., Sens, M.A., Sens, D.A., 2010. Cadmium, environmental exposure, and health outcomes, *Environ. Health Perspect.* 118, 182-190.
- Satarug, S., Moore, M.R., 2004. Adverse health effects of chronic exposure to low-level cadmium in foodstuffs and cigarette smoke, *Environ. Health Perspect.* 112, 1099-1103.
- Sens, D.A., Park, S., Gurel, V., Sens, M.A., Garrett, S.H., Somji, S., 2004. Inorganic cadmium- and arsenite-induced malignant transformation of human bladder urothelial cells, *Toxicol. Sci.* 79, 56-63.
- Siemiatycki, J., Dewar, R., Nadon, L., Gerin, M., 1994. Occupational risk factors for bladder cancer: results from a case-control study in Montreal, Quebec, Canada, *Am. J. Epidemiol.* 140, 1061-1080.

- Smith, A.H., Goycolea, M., Haque, R., Biggs, M.L., 1998. Marked increase in bladder and lung cancer mortality in a region of Northern Chile due to arsenic in drinking water, *Am. J. Epidemiol.* 147, 660-669.
- Socha, M.J., Said, N., Dai, Y., Kwong, J., Ramalingam, P., Trieu, V., Desai, N., Mok, S.C., Motamed, K., 2009. Aberrant promoter methylation of SPARC in ovarian cancer, *Neoplasia* 11, 126-135.
- Somji, S., Garrett, S.H., Zhou, X.D., Zheng, Y., Sens, D.A., Sens, M.A., 2010a. Absence of Metallothionein 3 Expression in Breast Cancer is a Rare, But Favorable Marker of Outcome that is Under Epigenetic Control, *Toxicol. Environ. Chem.* 92, 1673-1695.
- Somji, S., Zhou, X.D., Mehus, A., Sens, M.A., Garrett, S.H., Lutz, K.L., Dunlevy, J.R., Zheng, Y., Sens, D.A., 2010b. Variation of keratin 7 expression and other phenotypic characteristics of independent isolates of cadmium transformed human urothelial cells (UROtsa), *Chem. Res. Toxicol.* 23, 348-356.
- Steinmaus, C., Moore, L., Hopenhayn-Rich, C., Biggs, M.L., Smith, A.H., 2000. Arsenic in drinking water and bladder cancer, *Cancer Invest.* 18, 174-182.
- Suzuki, M., Hao, C., Takahashi, T., Shigematsu, H., Shivapurkar, N., Sathyanarayana, U.G., Iizasa, T., Fujisawa, T., Hiroshima, K., Gazdar, A.F., 2005. Aberrant methylation of SPARC in human lung cancers, *Br. J. Cancer* 92, 942-948.
- Tai, I.T., Tang, M.J., 2008. SPARC in cancer biology: its role in cancer progression and potential for therapy, *Drug Resist Updat* 11, 231-246.
- Tsuda, T., Babazono, A., Yamamoto, E., Kurumatani, N., Mino, Y., Ogawa, T., Kishi, Y., Aoyama, H., 1995. Ingested arsenic and internal cancer: a historical cohort study followed for 33 years, *Am. J. Epidemiol.* 141, 198-209.
- Waalkes, M.P., 2000. Cadmium carcinogenesis in review, *J. Inorg. Biochem.* 79, 241-244.
- Yamanaka, M., Kanda, K., Li, N.C., Fukumori, T., Oka, N., Kanayama, H.O., Kagawa, S., 2001. Analysis of the gene expression of SPARC and its prognostic value for bladder cancer, *J. Urol.* 166, 2495-2499.
- Yasmin, T., 2009. The expression of SPARC in arsenite- and cadmium-transformed human urothelial cells (UROtsa), tumor heterotransplants, and bladder cancer, Unpublished MS Thesis. University of North Dakota.

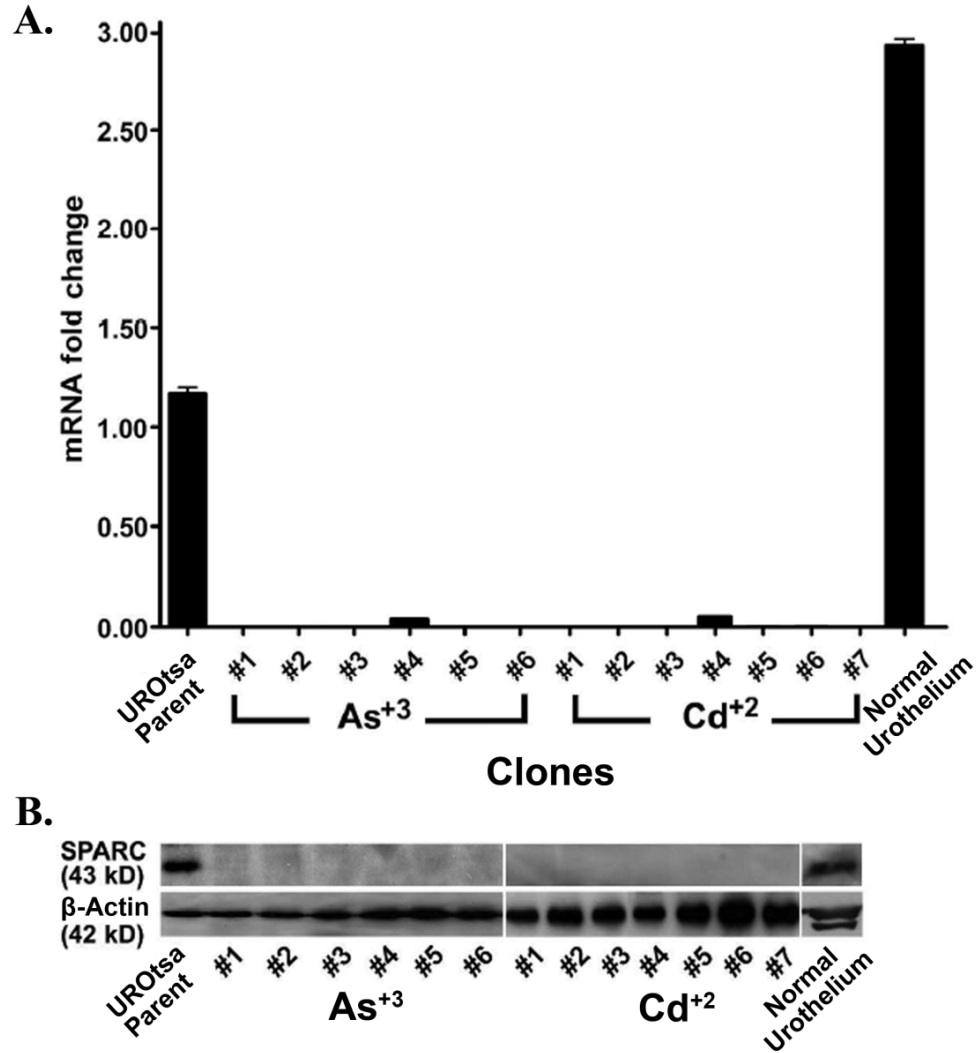


Figure III-1. Expression of SPARC mRNA and protein. (A) Real time RT-PCR analysis of SPARC expression in parental UROtsa cells, UROtsa cells transformed by Cd⁺² and As⁺³, and normal human urothelium. The mRNA levels were normalized to the fold change in β-actin. Real time data is plotted as the mean ± SEM of triplicate determinations. (B) Western analysis of SPARC protein in parental UROtsa cells, UROtsa cells transformed by Cd⁺² and As⁺³, and normal human urothelium.

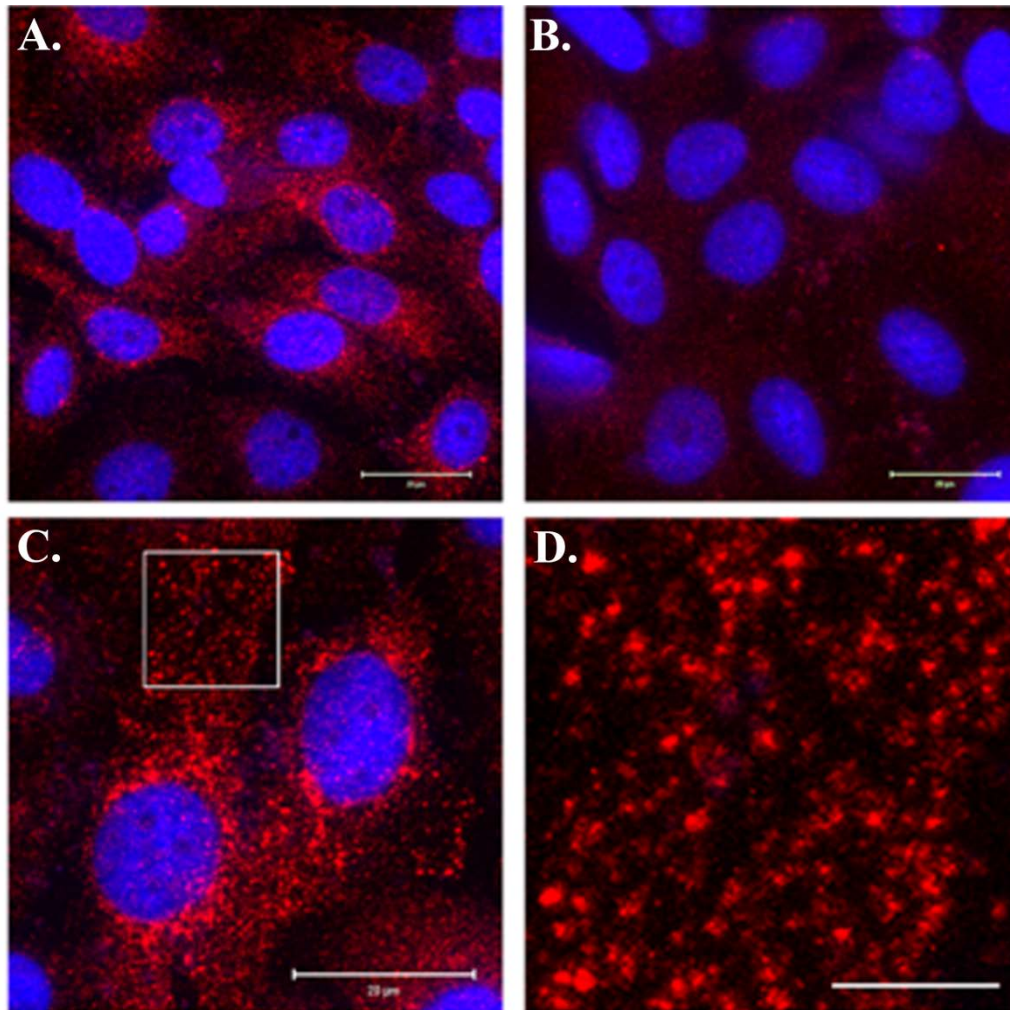


Figure III-2. Localization of SPARC protein expression. (A) SPARC (red) staining in the parent UROtsa cells. (B) Staining for SPARC in UROtsa cells transformed by As^{+3} . (C) SPARC staining in UROtsa parental cells localized to small punctate structures throughout the cytoplasm. (D) Higher magnification image from the boxed area in panel C showing SPARC localized to structures that resemble vesicles. The DAPI counterstain (blue) was used to identify all the cells in the fields. Bars in A-C = 20 μm , the bar in D = 5 μm .

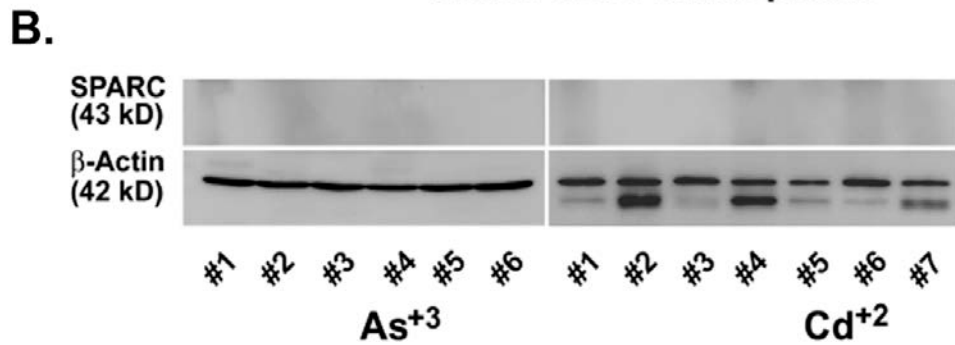
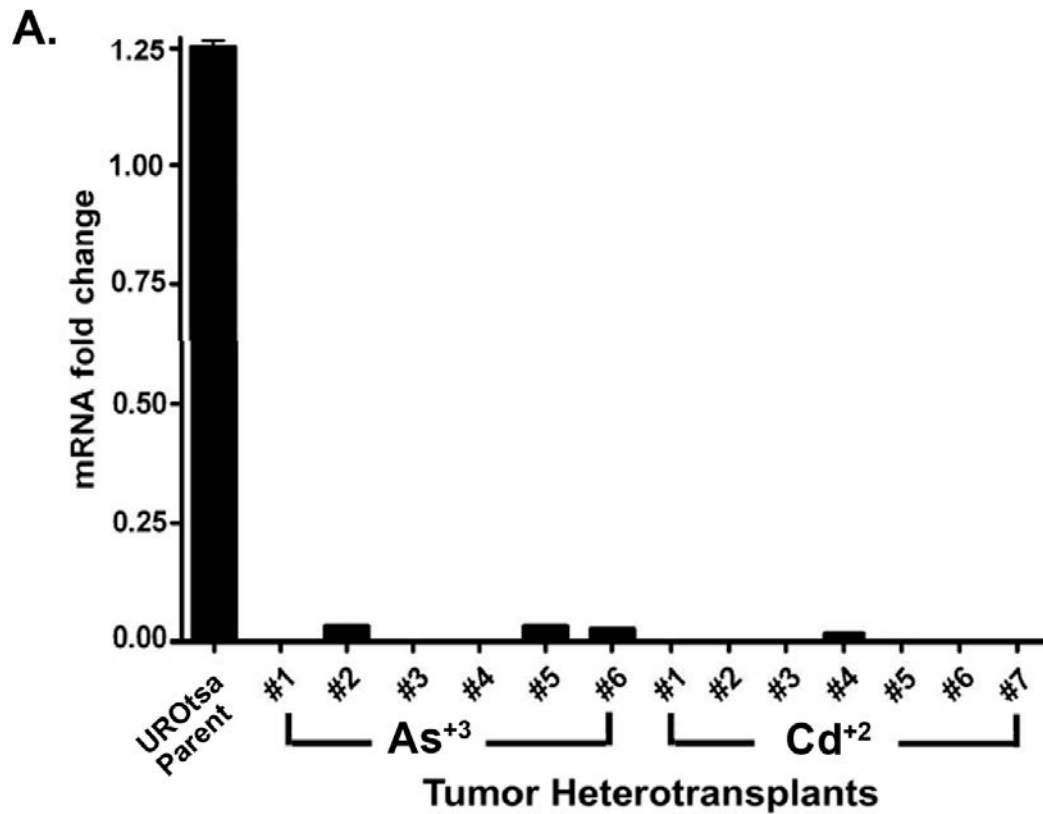


Figure III-3. Expression of SPARC mRNA and protein in tumor heterotransplants. (A) Real time RT-PCR analysis of SPARC expression in parental UROtsa cells and in Cd⁺² or As⁺³ tumor heterotransplants. The mRNA levels were normalized to the fold change in β-actin. Real time data is plotted as the mean ± SEM of triplicate determinations. (B) Western analysis of SPARC protein in tumor heterotransplants (Yasmin, 2009).

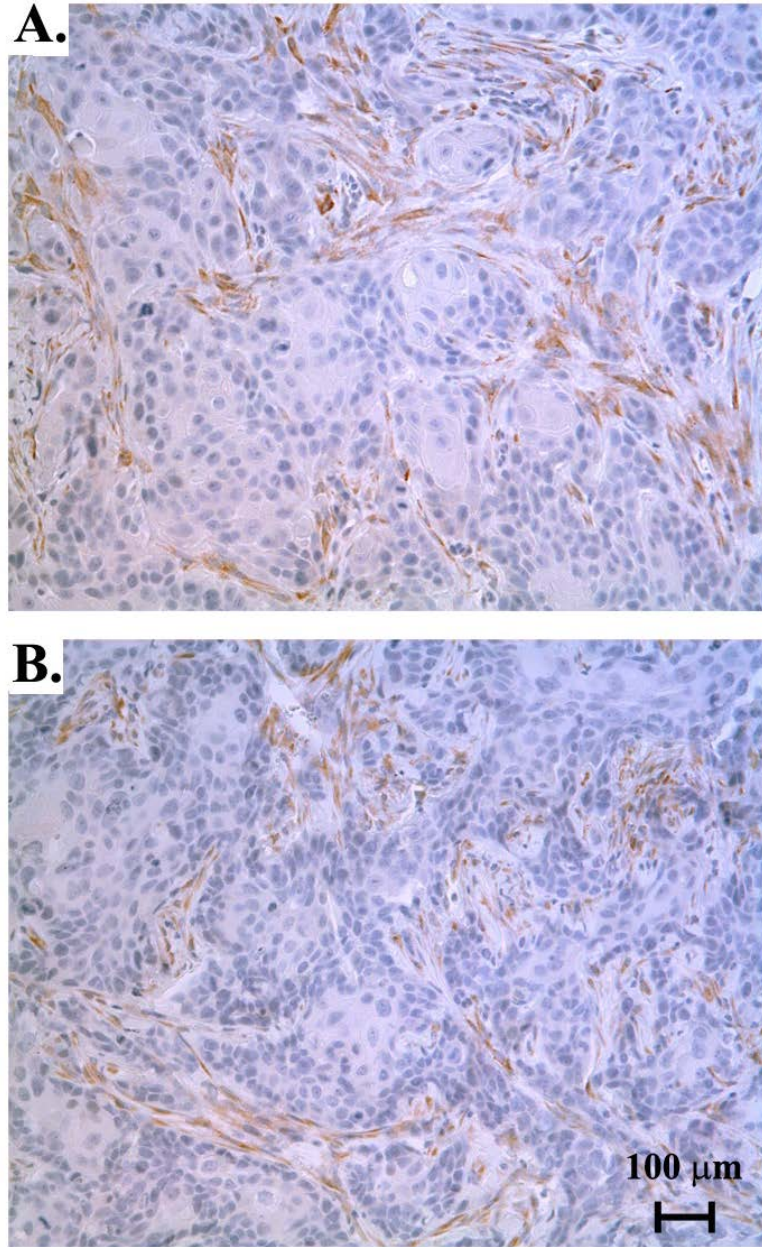


Figure III-4. Expression of SPARC protein in tumor heterotransplants. (A and B) Immunohistochemical analysis of SPARC protein in Cd⁺² or As⁺³ tumor heterotransplants respectively. The brown color indicates SPARC positive cells. The tumors were generated from the Cd^{#1} and the As^{#1} cell lines (Yasmin, 2009). Images are taken at the magnification of X 200. Bar = 100 μM.

Figure III-5. Real-time RT-PCR analysis of SPARC mRNA levels in parental UROtsa cells, and UROtsa cells transformed by Cd⁺² and As⁺³ treated with the epigenetic regulator, MS-275. The Cd^{#1} and the As^{#1} transformed cell lines were used in these experiments. Expression of SPARC mRNA after treatment with MS-275 for: (A) 24 h, (B) 48 h, and (C) 72 h. The level of SPARC mRNA was determined relative to the UROtsa cells using serial dilutions of this sample as the standard curve. The resulting relative levels were then normalized to the fold change in β -actin. Real time data is plotted as the mean \pm SEM of triplicate determinations.

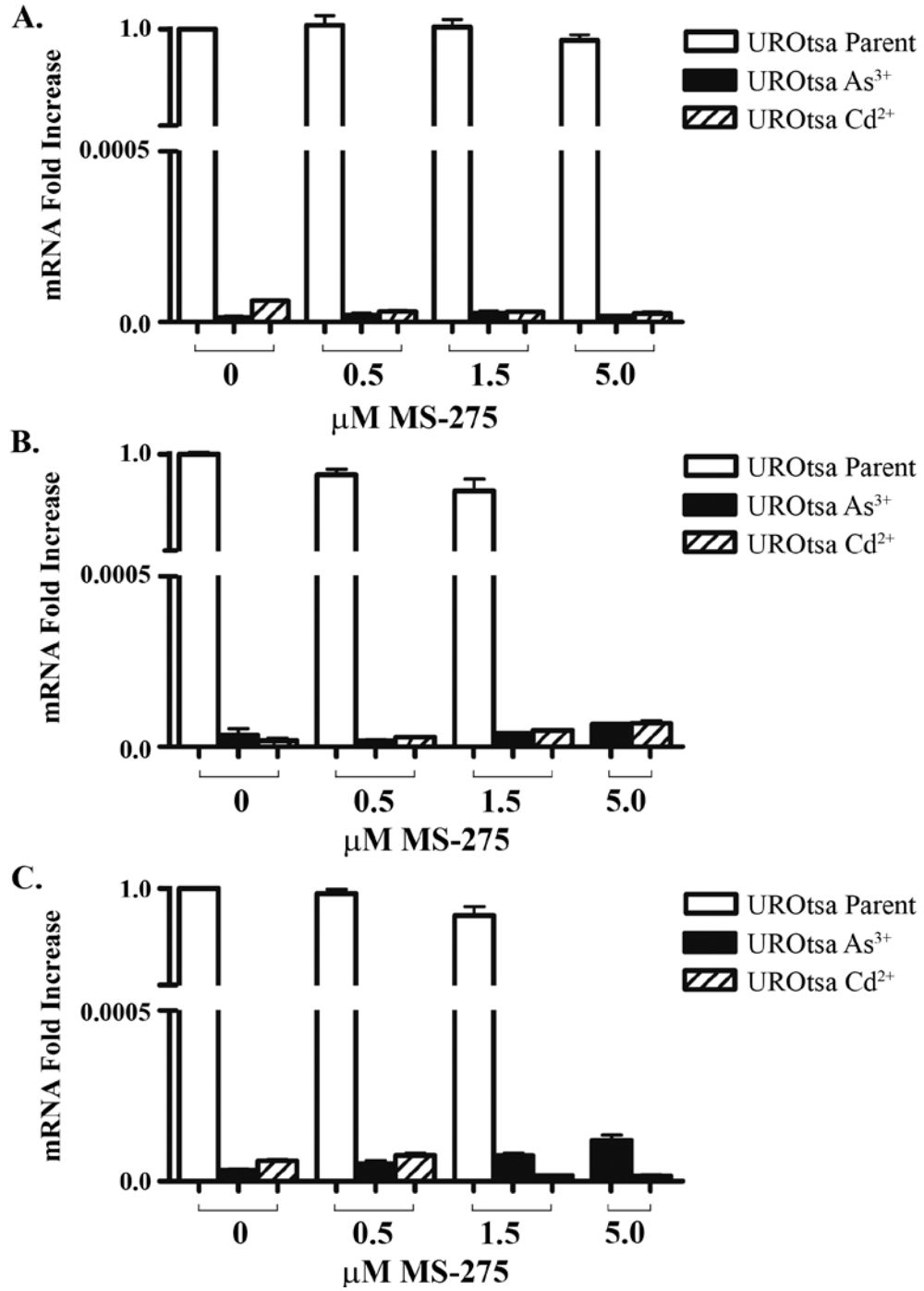
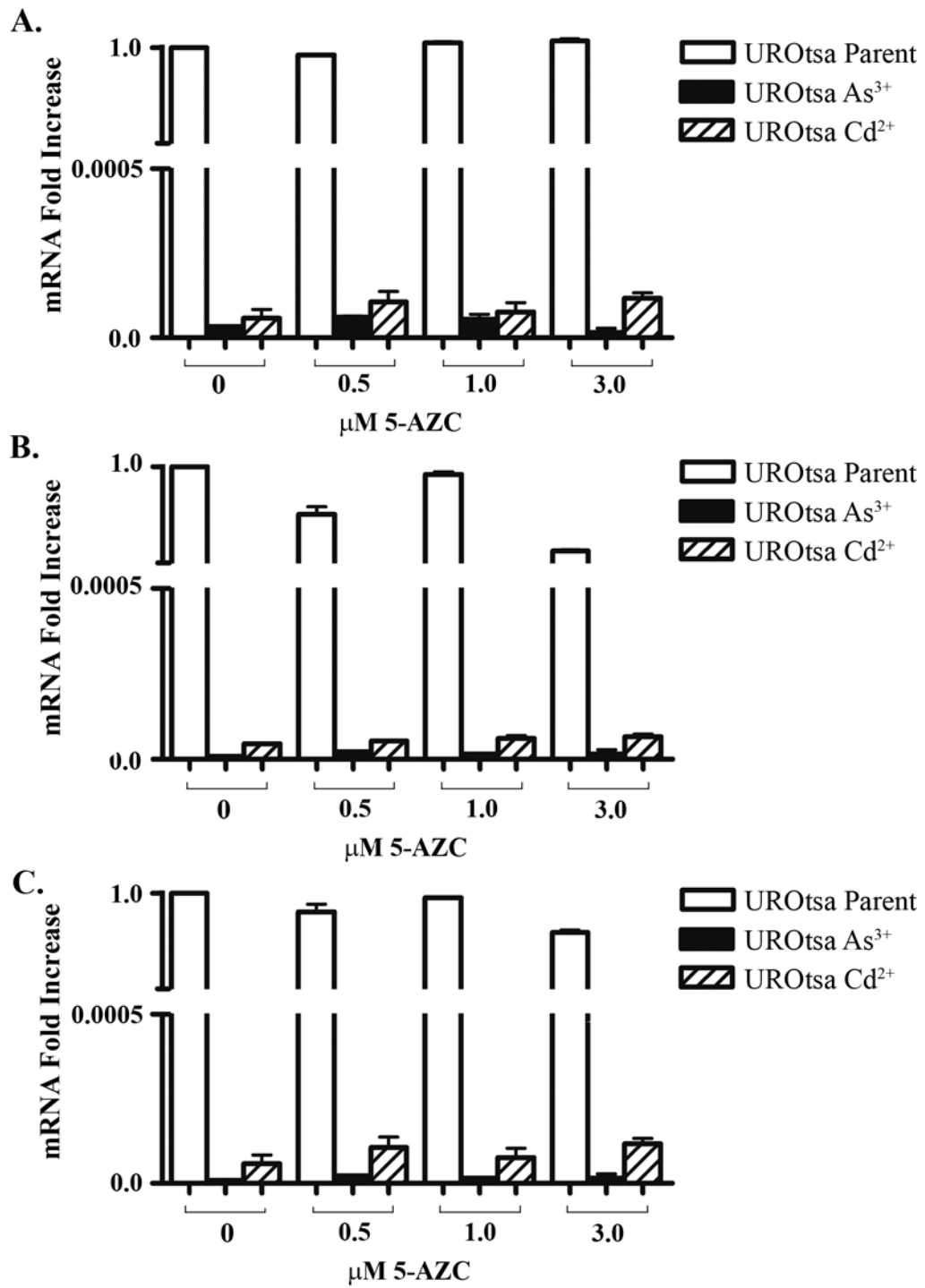


Figure III-6. Real-time RT-PCR analysis of SPARC mRNA levels in parental UROtsa cells, and UROtsa cells transformed by Cd⁺² and As⁺³ treated with the epigenetic regulator, 5-AZC. The Cd^{#1} and the As^{#1} transformed cell lines were used in these experiments. Expression of SPARC mRNA after treatment with 5-AZC for (A) 24 h, (B) 48 h, and (C) 72 h. The level of SPARC mRNA was determined relative to the UROtsa cells using serial dilutions of this sample as the standard curve. The resulting relative levels were then normalized to the fold change in β -actin. Real time data is plotted as the mean \pm SEM of triplicate determinations.



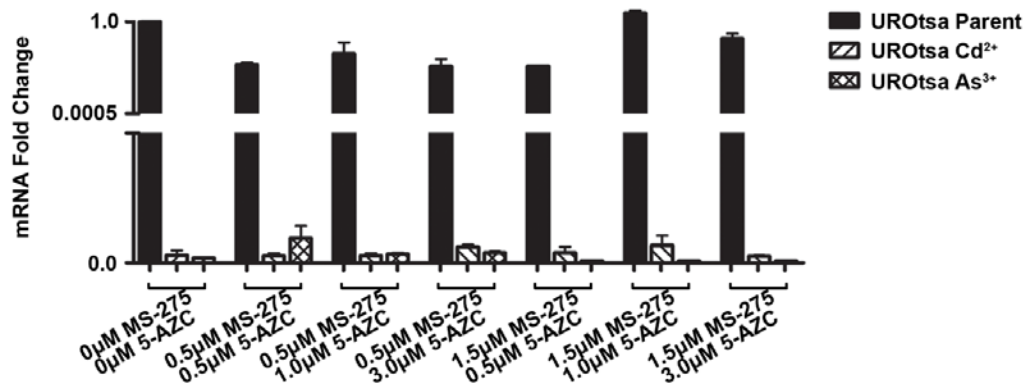


Figure III-7. Real-time RT-PCR analysis of SPARC mRNA levels in parental UROtsa cells, and UROtsa cells transformed by Cd⁺² and As⁺³ treated with a combination of epigenetic regulators. The Cd^{#1} and the As^{#1} transformed cell lines were used in these experiments. Expression of SPARC mRNA after treatment with varying concentrations of both drugs, MS-275 and 5-AZC, for 72 h. The level of SPARC mRNA was determined relative to the UROtsa cells using serial dilutions of this sample as the standard curve. The resulting relative levels were then normalized to the fold change in β -actin. Real time data is plotted as the mean \pm SEM of triplicate determinations.

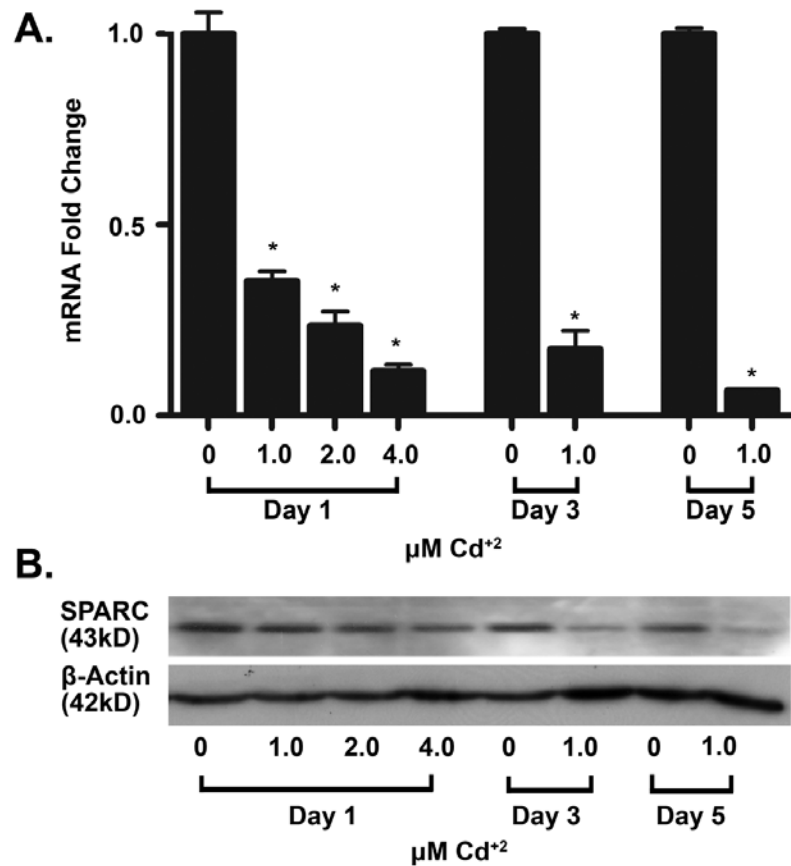


Figure III-8. Expression of SPARC mRNA and protein in parental UROtsa cells exposed to Cd^{+2} . (A) Real time RT-PCR analysis of SPARC. The level of SPARC mRNA was determined relative to the UROtsa cells using serial dilutions of this sample as the standard curve. The resulting relative levels were then normalized to the fold change in β -actin. * denotes a significant difference from untreated UROtsa cells ($p < 0.05$). Real time data is plotted as the mean \pm SEM of triplicate determinations. (B) Western blot analysis of SPARC protein.

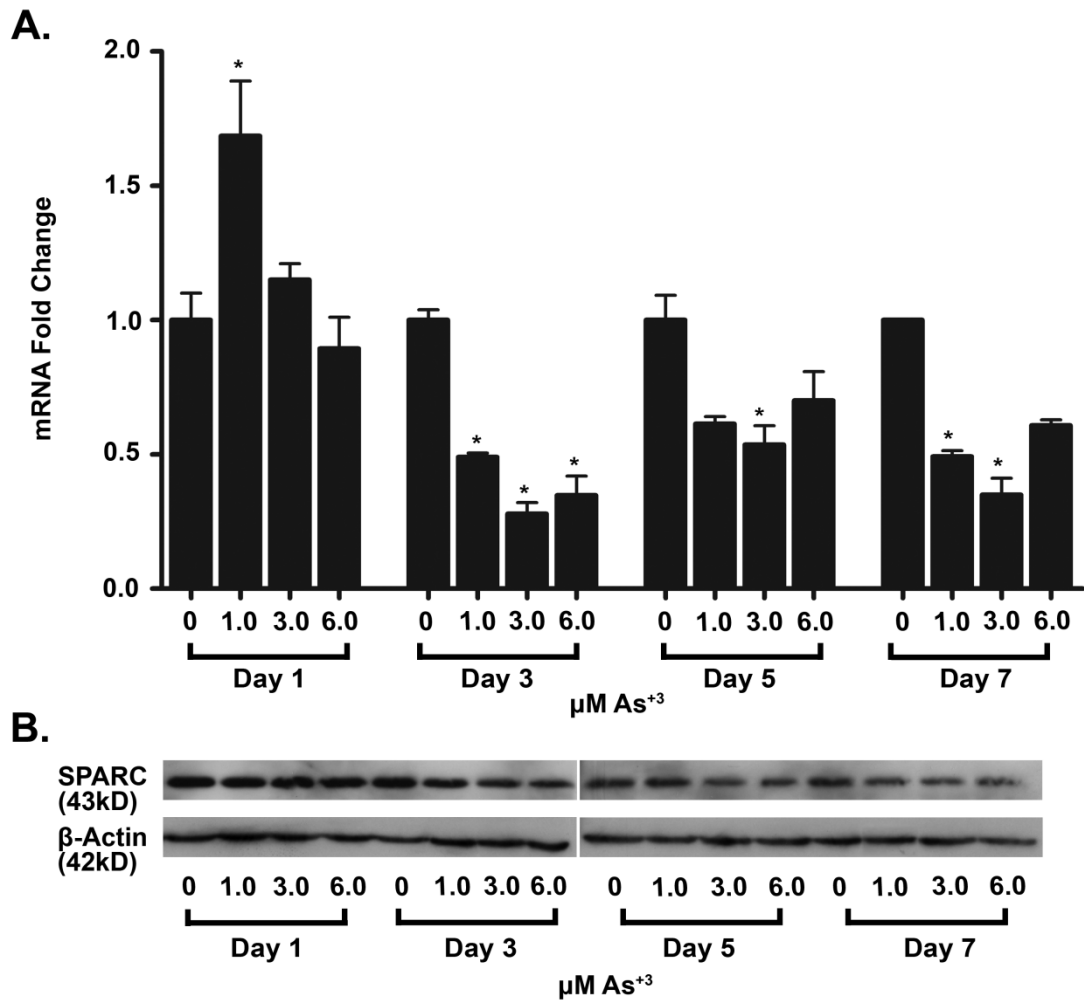


Figure III-9. Expression of SPARC mRNA and protein in parental UROtsa cells exposed to As³⁺. (A) Real time RT-PCR analysis of SPARC. The level of SPARC mRNA was determined relative to the UROtsa cells using serial dilutions of this sample as the standard curve. The resulting relative levels were then normalized to the fold change in β-actin. * denotes a significant difference from untreated UROtsa cells ($p < 0.05$). Real time data is plotted as the mean \pm SEM of triplicate determinations. (B) Western blot analysis of SPARC protein.

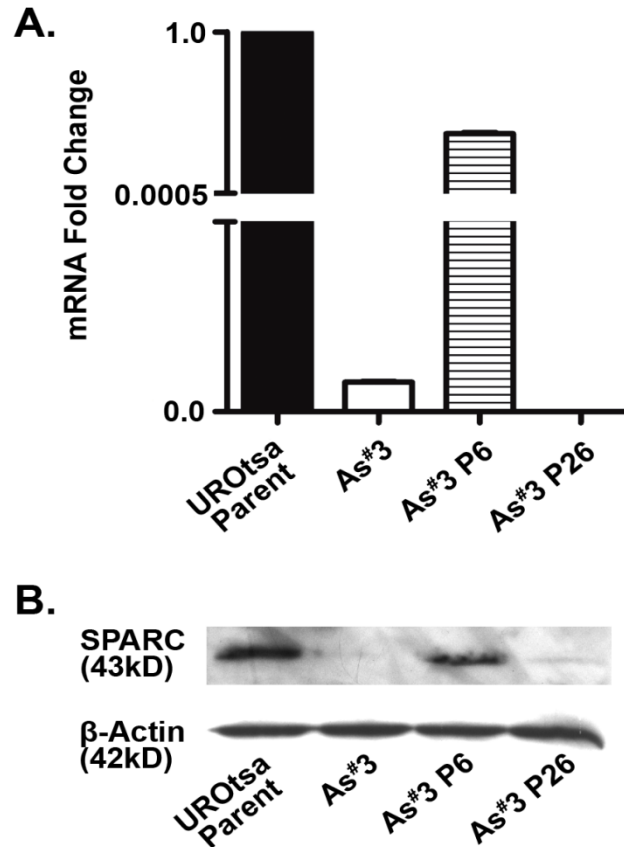
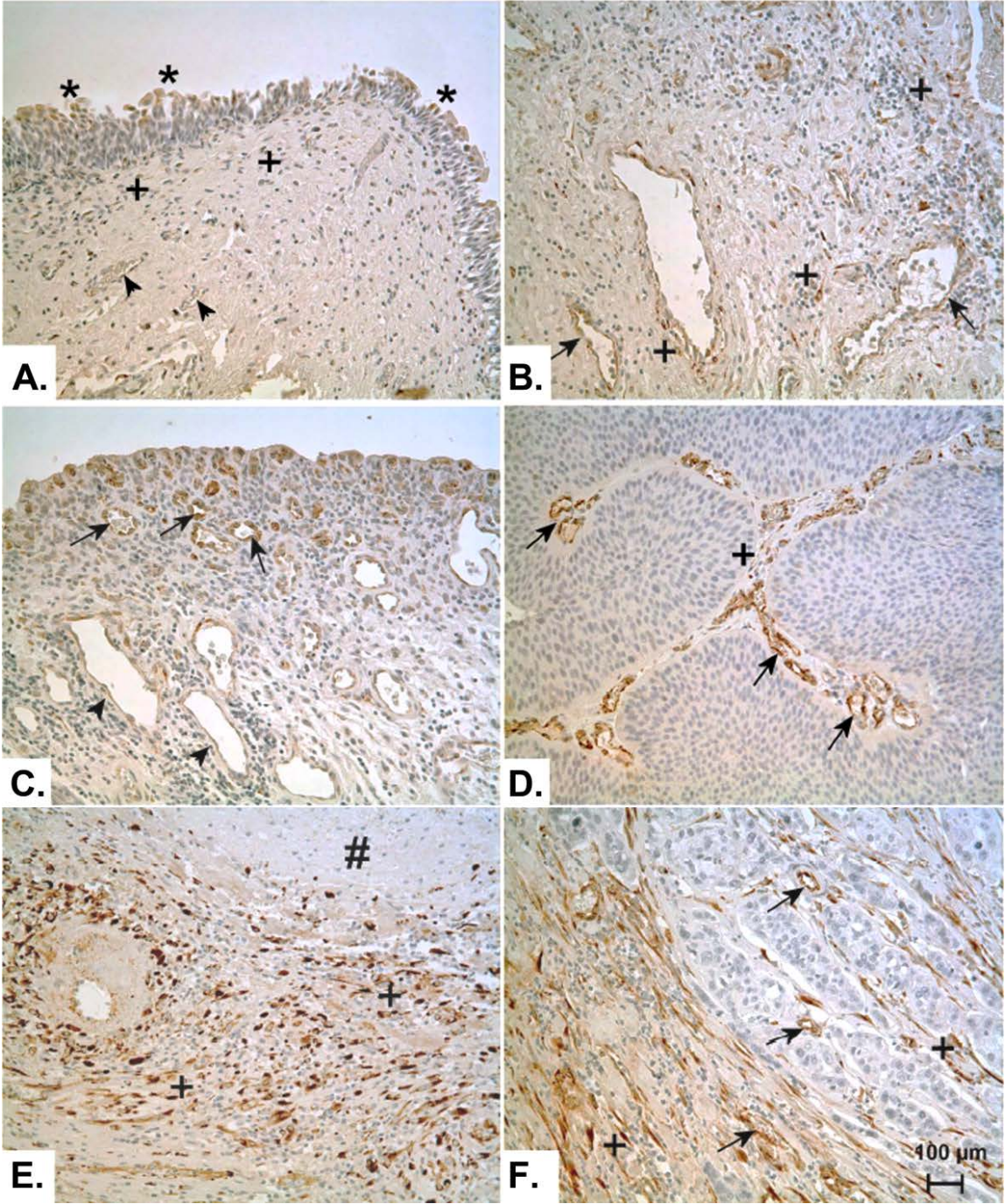


Figure III-10. Expression of SPARC mRNA and protein during the transformation process in UROtsa cells exposed to 1 μ M As⁺³. (A) Real time RT-PCR analysis of SPARC expression in the UROtsa parent, the fully transformed As^{#3} cell line, As^{#3} P6, and As^{#3} P26 cell lines. The level of SPARC mRNA was determined relative to the UROtsa parent cells using serial dilutions of this sample as the standard curve. The resulting relative levels were then normalized to the fold change in β -actin. (B) Western blot analysis of SPARC protein in the UROtsa parent, the fully transformed As^{#3} cell line, As^{#3} P6, and As^{#3} P26 cell lines. A duplicate blot was stained for β -actin as a control. The early passage, As^{#3} P6, corresponded to 17 days into the transformation process, while the late passage, As^{#3} P26, corresponded to 4.5 months.

Figure III-11. Immunohistochemical staining of SPARC in normal human bladder, cystitis, invasive, and noninvasive urothelial carcinoma. (A) Localization of SPARC in normal human bladder tissue sample. * indicates SPARC staining in the normal urothelium. + indicates staining in the stromal cells. Arrowheads indicate lack of staining in blood vessels. (B) Localization of SPARC in a bladder tissue sample obtained from a patient with cystitis. + indicates frequent staining of stromal cells. Arrows indicate moderate staining in blood vessels. (C) Localization of SPARC in blood vessels of bladder tissue obtained from a patient with cystitis. Arrows indicate strong staining in the newly formed blood vessels, whereas mature blood vessels in deep lamina propria are weakly positive or negative for SPARC (arrowheads). (D) Localization of SPARC in low grade urothelial papillary carcinoma. The tumor cells did not stain for SPARC whereas few stromal cells in the papillary core (+) stained for SPARC. Arrow indicates strong staining in small blood vessels. (E) Localization of SPARC in low grade urothelial papillary carcinoma containing areas of necrosis. # indicates an area of necrosis, around which a large number of SPARC positive (+) stromal cells are present. (F) Localization of SPARC in high grade invasive bladder cancer. The tumor cells did not stain for SPARC whereas the desmoplastic stromal cells both in and around the invasive carcinoma stained strongly (+). Arrows indicate positive staining of the endothelial cells of the blood vessels. All images are at a magnification of X 200. Bar = 100 μ m.



CHAPTER IV

THE FORCED EXPRESSION OF SPARC IN TRANSFORMED HUMAN UROTHELIAL CELLS (UROTSA): CHARACTERIZATION OF MIGRATION PROPERTIES AND TUMORGENICITY

Manuscript in preparation

Abstract

SPARC, secreted protein acidic and rich in cysteine, is a member of the matricellular group of proteins that is known to modulate interactions between cells and the extracellular matrix. Influencing tumor growth and migration, the expression of SPARC in human bladder cancer was found to be absent in the malignant urothelial cells, but highly expressed in the stromal component recruited to the tumor. The purpose of this study is to examine the expression of SPARC and the role it plays in the formation and progression of bladder cancer in a model of heavy metal induced cell transformation. A previous study from this laboratory showed SPARC expression was significantly down-regulated to the level of detection in Cd⁺² and As⁺³ transformed UROtsa cells. To further investigate the role of SPARC expression in bladder cancer, a SPARC expression vector was stably transfected into two As³⁺ and two Cd²⁺ transformed UROtsa cell lines. The expression of SPARC in the transfected lines was characterized using real time reverse transcriptase-polymerase chain reaction to quantitate mRNA level, and western blotting, immunofluorescence, and immunohistochemistry to determine protein levels and localization. The transfected cell lines were further analyzed by the ability to secrete SPARC into growth media, growth rates, migration, wound healing rates, invasion capabilities, and tumorigenicity. This data showed that SPARC mRNA and protein expression was induced in the transfected cell lines, was localized to distinct vesicles within the cytoplasm by immunofluorescent staining, and was secreted into the growth medium. However, after the successful generation of tumors in nude mice, immunohistochemistry analysis revealed the tumors generated from the SPARC-transfected cell lines showed an absence of SPARC expression within the epithelial

component of the tumors, this staining pattern was mimicked in controls. Further examination showed tumors generated from SPARC-transfected cells did contain the original transfection vector, and the mRNA expression of SPARC within the tumor from the SPARC-transfected cell line revealed the presence of SPARC message, albeit at a low level. This study suggests that the down-regulation of SPARC expression in mouse tumors generated by the malignantly transformed UROtsa cells transfected with SPARC expression, is a tumor cell response to the mouse tumor environment and most likely due to post-transcriptional regulation.

Introduction

SPARC, also known as BM-40 and osteonectin, is a 43 kDa glycoprotein that belongs to the matricellular group of proteins. Matricellular proteins are secreted macromolecules that interact with the extracellular matrix, cell surface receptors, and growth factors and/or proteases but do not play a structural role in the extracellular matrix (Bornstein, 1995). However, these proteins have the capacity to bind to components of the extracellular matrix. SPARC expression has been shown to be up-regulated during embryological development and in various tissues modulating cell-cell and cell-matrix interactions such as in areas of cellular injury and remodeling (Lane and Sage, 1994; Sage and Bornstein, 1991). SPARC expression is also altered in many cancers; however the role SPARC plays in the regulation of tumor growth and progression remains unclear. In some cancers, including melanomas and renal cell carcinomas, high levels of SPARC expression are found in the malignant epithelial cells comprising the tumor leading to the progression of the tumor and a poor outcome (Ledda et al., 1997; Rempel et al., 1998; Sakai et al., 2001). While in other cancers, including ovarian, prostate, and pancreatic,

SPARC expression is absent from the epithelial component of the tumor leading to its association as a tumor suppressor (Sato et al., 2003; Socha et al., 2009; Thomas et al., 2000). However, in several of these cancers, the stroma directly surrounding the malignant epithelial component of the tumor is strongly reactive for SPARC expression. The expression of SPARC in the stroma is believed to promote migration and/or invasion of the tumor, even though the malignant component of the tumor is SPARC negative. Since SPARC can be expressed and secreted by both tumorigenic and stromal cells, SPARC can modulate the interactions between these cells through cell-stroma crosstalk during cancer progression. This expression pattern is seen in several highly aggressive types of human cancer, including non-small cell lung carcinoma and pancreatic carcinoma. These aggressive cancers show a high level of SPARC expression in fibroblasts in close proximity to the malignant cells which lack SPARC expression (Koukourakis et al., 2003; Sato et al., 2003). The role of SPARC in tumor progression, although complicated, appears to be dependent on the tissue, and specific cell type expressing SPARC.

This laboratory has previously shown SPARC is moderately expressed in normal human bladder tissue with SPARC expression localized to the upper superficial cells of the urothelium as well as some moderately light staining in the stroma (Larson et al., 2010). In contrast, archival specimens of human bladder cancer showed SPARC expression was absent in the malignant urothelial cells comprising the tumor, but highly expressed in the stromal components recruited to these tumors. These findings were comparable to the human bladder cell cultures employed by this laboratory. The UROtsa cell line is an immortalized, but non-tumorigenic cell line that displays features of

transitional urothelium when propagated on a serum free growth medium (Rossi et al., 2001). This cell line has been used to show that both As^{3+} and Cd^{2+} can cause the malignant transformation of human urothelial cells (Cao et al., 2010; Sens et al., 2004; Somji et al., 2010). In total, 6 As^{3+} - and 7 Cd^{2+} - transformed cell lines have been isolated after long-term, low dose exposure of the parental cells to these heavy metals. SPARC expression was detected in the parental UROtsa cells and its expression was reduced to the limit of detection when the cells were malignantly transformed by either As^{3+} or Cd^{2+} . In addition, the malignant epithelial components of mouse tumors derived from these cell lines also down-regulated SPARC expression, but the stromal component of these tumors were highly reactive for SPARC (Larson et al., 2010). These findings suggest that during malignant transformation by As^{3+} and Cd^{2+} , urothelial cells turn off expression of SPARC mRNA and protein.

The first goal of the present study was to stably transfect SPARC into As^{3+} and Cd^{2+} -transformed UROtsa cell lines and determine SPARC expression at the mRNA and protein levels. The second goal was to further characterize the growth, migration, and invasion capabilities of the SPARC-transfected cell lines as compared to UROtsa cell lines. Finally the last goal was to show translation of the findings to mouse heterotransplants derived from the SPARC-transfected As^{3+} and Cd^{2+} -transformed UROtsa cell lines by characterizing SPARC expression in the resulting tumors formed in the nude mice.

Materials and Methods

Cell Culture

Stock cultures of the parental cell line were maintained in 75 cm² tissue culture flasks using Dulbecco's modified Eagle's medium (DMEM) containing 5% v/v fetal calf serum (Rossi et al., 2001). The isolation and growth of the seven isolates of the Cd⁺²-transformed UROtsa cells and six isolates of the As⁺³-transformed UROtsa cells have been described previously (Cao et al., 2010; Sens et al., 2004; Somji et al., 2010). The Cd⁺² and As⁺³-transformed UROtsa cell lines were grown and maintained using identical conditions to the parental cell line. MDA-MB-231 and Hs578T breast cancer cell lines were obtained from the American Type Culture Collection (Rockville, MD), grown in DMEM supplemented with 5% v/v fetal calf serum as described previously (Friedline et al., 1998; Gurel et al., 2003). All cell cultures were incubated at 37°C in a 5% CO₂: 95% air atmosphere, confluent flasks were routinely subcultured at a 1:4 ratio using trypsin-EDTA (0.05%, 0.02%) upon attaining confluence, and fed fresh growth media every 3 days. Cell viability, as a measure of cytotoxicity, was determined by measuring the capacity of the cells to reduce MTT (3-(4,5-dimethylthiazol-2-yl)-2,5-diphenyltetrazolium bromide) to formazan (Rossi et al., 2002). Cell growth rates were also determined using MTT assay following a 1:100 subculture of the cells. Triplicate cultures were analyzed for each time point.

Stable Transfection of Select Transformed UROtsa Cell Lines

Previously generated mouse heterotransplants as described by (Cao et al., 2010; Sens et al., 2004; Somji et al., 2010) were used in this study. For the stable transfection of SPARC, the present study used two cell lines from the Cd⁺²-transformed cell lines and

two from the As⁺³-transformed cell lines. One cell line from each the Cd⁺² and As⁺³-transformed UROtsa cell lines was chosen based on its ability to form intraperitoneal tumors while the remaining cell line from each group was randomly determined. Select As⁺³-and Cd⁺²-transformed UROtsa cell lines (As^{#3}, As^{#6}, Cd^{#3}, and Cd^{#4}) were chosen for the stable transfection with the SPARC open reading frame (ORF) cloned into the pENTR221 vector obtained from Invitrogen (Carlsbad, CA). This entry vector was transferred into the destination vector, pcDNA 6.2/V5-DEST vector (Invitrogen), by LR recombination reaction (Invitrogen). The purified plasmid DNA constructs were quantified, custom sequenced (MWG Biotech, Inc., High point, NC), and analyzed to verify the sequence of SPARC. The DNA constructs were linearized prior to transfection. The SPARC ORF in pcDNA 6.2/V5-DEST was linearized with *Ssp* I (New England BioLabs, Ipswich, MA) and the pcDNA 6.2/V5-DEST vector alone (blank vector) was linearized with *Pst* I (New England BioLabs) The select As⁺³- and Cd⁺²-transformed UROtsa cells were transfected with the SPARC ORF in pcDNA 6.2/V5-DEST or the blank vector using Effectene Transfection reagent (Qiagen, Valencia, CA) following the manufacturer's protocol at a ratio of 1:10 plasmid to Effectene ratio. The lipid complexes were added to the cells at 2 µg of DNA per 9.6 cm² culture well. Clones were selected using cloning rings and propagated in the growth medium containing 4 µg/mL Blasticidin (BSD) (Invitrogen). The morphology of the transfected cell lines were visualized by light microscopy and one clone from each cell line was selected to further analysis based on levels of SPARC expression. Approximately 15 clones from each of the 4 cell lines were analyzed. The select As⁺³- and Cd⁺²-transformed UROtsa cells stably transfected with SPARC ORF in pcDNA 6.2/V5-DEST are designated as

As^{#3}-SPARC, As^{#6}-SPARC, Cd^{#3}-SPARC, and Cd^{#4}-SPARC, while those stably transfected with the blank vector are designated as As^{#3}-DEST, As^{#6}- DEST, Cd^{#3}-DEST, and Cd^{#4}- DEST.

mRNA and Protein Expression in Parental, As⁺³-and Cd⁺²-Transformed, SPARC-Transfected UROtsa Cell Lines, and Mouse Heterotransplants

Total RNA was isolated from the cells according to the protocol supplied with TRI REAGENT (Molecular Research Center, MRC, Cincinnati, OH) and real time RT-PCR was used to measure the expression level of human SPARC mRNA as previously described (Larson et al., 2010) as well as the expression of BSD (Blasticidin) and mouse specific SPARC. Briefly, a human specific SPARC, mouse specific SPARC, and BSD specific primers were obtained from Qiagen and amplification was monitored by SYBR Green fluorescence (Bio-Rad Laboratories, Hercules, CA). The level of human SPARC expression was determined relative to the UROtsa parent cell line using human SPARC standards to generate a standard curve, while the level of mouse specific SPARC and BSD were determined relative to the Cd^{#1} mouse tumor heterotransplant using serial dilutions of this sample as a standard curve. The expression levels of all genes were normalized to β -actin expression. The expression of human SPARC was determined by western blotting using 10 μ g of total cellular protein and separated on a 12.5% SDS-polyacrylamide gel. After blocking, the membranes were probed using a 1:1000 dilution of a mouse monoclonal anti-osteonectin primary antibody (Leica Microsystems Inc., Bannockburn, IL) in blocking buffer for 1 h at room temperature. After washing 3 times with Tris buffered saline (TBS) containing 0.1% Tween 20 (TBS-T), membranes were incubated with the anti-mouse secondary antibody (1:10,000) in antibody dilution buffer for 1 h. Blots were visualized using the Phototope-HP (horseradish peroxidase) Western

blot detection system (Cell Signaling Technology, Beverly, MA) as previously described (Larson et al., 2010). The expression of secreted SPARC protein was also determined by western analysis using slight modification in the protocol as previously described by Sage (2003). Briefly, conditioned growth media from confluent cultures was collected, centrifuged, and filtered through a 0.22 μm filter. With stirring at 4°C, solid ultrapure ammonium sulfate (Sigma Aldrich, St. Louis, MI) was added at 50% w/v of starting conditioned media volume over several hours in polypropylene containers. Media was centrifuged at 40,000 x g, supernatant was discarded, and resulting pellet was dissolved in 2% SDS for analysis. Equal total protein was loaded.

Immunolocalization of SPARC in Parental, As⁺³-and Cd⁺²-Transformed, and SPARC-Transfected UROtsa Cell Lines

UROtsa parent, As⁺³-and Cd⁺²-transformed, and SPARC-transfected cells were grown in 24 well plates with 12 mm glass coverslips and processed while subconfluent. Cells were fixed and stained as described previously (Larson et al., 2010). Briefly, cells were fixed in 3.7% paraformaldehyde, quenched of free aldehyde with 0.1 M ammonium chloride for 15 min, followed by permeabilization with 0.1% Igepal (NP-40) for 10 min. Cells were stained for SPARC by incubation for 45-60 min at 37° C with a 1:20 dilution of mouse anti-osteonectin antibody (Leica Microsystems Inc.). Primary antibody was detected by incubating cells with 4.0 $\mu\text{g}/\text{mL}$ of Alexa Fluor 594 goat anti-mouse IgG (Invitrogen) for 45-60 min at 37° C. Controls consisted of coverslips treated with the secondary antibody only. Coverslips were then mounted in ProLong Gold anti-fade reagent with 4',6-diamidino-2-phenylindole (DAPI) (Invitrogen) for nuclear counter staining. Cells were observed and images were captured using a Zeiss LSM 510 Meta Confocal Microscope with LSM 510 software (Carl Zeiss MicroImaging Inc.). Images

were composed by capturing z-slices at a depth of 0.5 μm , stacking the z-slices together, and merging with the DAPI image of the same field so all cells in the field could be identified.

Cellular Migration and Invasion Assays

Migration of parental, As^{+3} - and Cd^{+2} -transformed, SPARC and DEST-transfected UROtsa cell lines, and MDA-MB-231 cells as a positive control were assessed. Analysis of migration was conducted using two assays, a wound/scratch assay and a transwell migration assay. For the wound assay, cells were grown to confluence and treated with Mitomycin C (MMC) (Sigma Aldrich) for 2 h, to inhibit cellular division. Appropriate concentrations of MMC were specifically determined for each cell line by MTT analysis to insure inhibition of cellular proliferation while also insuring that levels were not toxic. A scratch was made within the cell monolayer using a sterile 200 μL pipette tip. The monolayer was then washed with phosphate-buffered saline, fresh growth medium was added, and cells were allowed to migrate for 24 or 48 h. Cells were photographed by light microscopy (using a 10 x magnification lens) at 0, 24, and 48 h to analyze the migration of the cells toward the “wounded” area.

Analysis of migration by chemokinesis was conducted using 24-well transwell inserts with an 8 μm pore size polycarbonate membrane (Cell Biolabs, San Diego, CA). 300 μL of 2.4×10^5 cells/ml in serum free media was added to the upper chamber and cells were allowed to migrate for 8 h at 37°C, 5% CO_2 : 95% air atmosphere with 500 μL of media containing 1.5% fetal calf serum in the bottom chamber. Cells were stained with the supplied staining solution and total cells were counted using light microscopy (using a 40 x magnification lens) with 20 fields per insert. After counting the total

number of cells, the non-migratory cells were gently swabbed off the top insert membrane and the remaining migratory cells were counted, again with 20 fields per insert.

For analysis of cellular invasion, the parental, As⁺³-and Cd⁺²-transformed, SPARC and DEST-transfected UROtsa cell lines, and Hs578T cells as a positive control were assessed. Cells were added onto a basement membrane coated layer on an 8 µm pore size polycarbonate membrane (Cell Biolabs). Cells were pretreated with MMC for 2 h before they were trypsinized and added to the upper chamber of the invasion insert. Appropriate concentrations of MMC were specifically determined for each cell line by MTT analysis and were the same concentrations used in the wound assay. 300 µL of 2.2 x 10⁵ cells/ml in serum free media was added to the upper chamber and allowed to invade for 24 h at 37°C, 5% CO₂: 95% air atmosphere with 500 µL of media containing 10% fetal calf serum in the bottom chamber. Cells were stained and counted in the same manner as the chemotaxis migration assay. Both the migration by chemotaxis and invasion assays were performed in duplicate and the percentage of cells migrated/invaded was determined.

Mouse Heterotransplants: Tumorigenicity in Soft Agar and Nude Mice

Before the testing of tumor growth in nude mice, SPARC-transfected cells, blank vector transfected cells, and respective control cultures were tested for their ability to form colonies in soft agar using a slight modification of the procedure described by San and coworkers (San et al., 1979; Sens et al., 2004). Briefly, 60 mm diameter dishes were prepared with a 5 mL underlay of 0.5% agar in DMEM containing 5% fetal calf serum. On top of the underlay layer was placed 2 x 10⁴ or 2 x 10⁵ cells in 1.5 mL of 0.25% agar

in DMEM containing 5% fetal calf serum. The dishes were incubated at 37°C, 5% CO₂: 95% air atmosphere inside humidified plastic containers to prevent evaporation. Cultures were examined microscopically 24 h after plating to confirm absence of large clumps of cells and thereafter at 7, 14, and 21 days after plating. Since all cultures showed colony formation in soft agar, the cultures were inoculated subcutaneously at a dose of 1×10^6 cells in the dorsal thoracic midline of 4 nude (NCr-nu/nu) mice for the blank vector and non-transfected control cell lines or 5 nude mice for the SPARC-transfected cell lines, as described previously (Sens et al., 2004). Tumor formation and growth were assessed weekly. All mice were sacrificed 8 weeks after injection or when clinical conditions dictated euthanasia. All experimental procedures with the use of mice were approved by the University of North Dakota Institutional Animal Care and Use Committee and conform to the National Research Council's Guide for the Care and Used Laboratory Animals. Areas where cells were injected were used to determine the expression of SPARC mRNA and protein and the mRNA expression of BSD and mouse specific SPARC. Tumor tissue was harvested for immunohistochemistry as well as mRNA and protein analysis.

*Immunohistochemical Localization of SPARC Expression in
Mouse Heterotransplants and Archival Specimens of Human Bladder Cancer*

The production of mouse heterotransplants from Cd⁺² and As⁺³-transformed UROtsa cells has been previously described (Sens et al., 2004; Cao et al., 2010; Somji et al., 2010). Tumor tissue from these studies was used for analyzing the specificity of two different SPARC antibodies. The present study also used tumor tissue from mouse heterotransplants generated from SPARC-transfected cells, blank vector transfected cells, and respective control cultures. Tissues sections of human bladder were obtained from

archival paraffin blocks that originated from previously completed patient diagnostic procedures. These archival specimens contained no patient identifiers and use was approved by the University of North Dakota Internal Review Board. Tissues were routinely fixed in 10% neutral-buffered formalin for 16-18 h. The tissue was then transferred to 70% ethanol and dehydrated in 100% ethanol. Dehydrated tissues were cleared in xylene, infiltrated, and embedded in paraffin. Serial sections of the tissue blocks were cut at 3-5 μm and used in immunohistochemical protocols. Prior to immunostaining, sections were immersed in preheated 10 mM sodium citrate buffer (pH 6.0) and heated in a steamer for 20 min. The sections were allowed to cool to room temperature for 30 min and then immersed into Tris buffered saline (TBS) containing 0.1% Tween 20 (TBS-T) (Dako, Carpinteria, CA) for 5 min. Endogenous peroxidase was extinguished by incubating the sections in Peroxidase Blocking Reagent (Dako) for 10 min. SPARC was localized by incubating the slides with mouse anti-human osteonectin antibody (Haematologic Technologies Inc., Essex Junction, VT) or mouse anti-human osteonectin antibody (Leica Microsystems Inc.) for 30 min at room temperature. Liquid diaminobenzidine (Dako) was used as chromogen.

Results

SPARC mRNA and Protein Expression in SPARC-Transfected and Blank Vector UROtsa Cell Lines

The expression and localization of SPARC was determined for the SPARC-transfected cells, blank vector and non-transfected controls lines, as well as the UROtsa parental cells. The parental UROtsa cells expressed a moderate amount of SPARC mRNA when compared to the common transcript, β -actin (Figure IV-1A). The SPARC-transfected cell lines had variable SPARC mRNA expression levels. All the SPARC-

transfected cell lines had higher SPARC expression levels than the corresponding blank vector or the non-transfected cell lines (Figure IV-1A). Two of the SPARC-transfected cell lines, Cd^{#1}-SPARC and Cd^{#4}-SPARC, had similar SPARC mRNA expression levels as that of the UROtsa parent, while the As^{#6}-SPARC had approximately a 10 fold induction of SPARC expression as compared to the UROtsa parent. As^{#3}-SPARC only had a slight induction of SPARC mRNA expression compared to its non-transfected counterpart and a level considerably lower than the parent. In contrast, SPARC mRNA expression was at the limit of detection in the non-transfected and blank vector UROtsa cell lines malignantly transformed by either Cd⁺² or As⁺³ (Figure IV-1A). A corresponding analysis of SPARC protein expression by western blotting showed that only the SPARC-transfected and parental UROtsa cell lines had detectable levels of SPARC protein expression (Figure IV-1B). None of the blank vector or non-transfected UROtsa cell lines transformed by either Cd⁺² or As⁺³ had any SPARC protein expression as expected based on the real time RT-PCR results (Figure IV-1B). While As^{#3}-SPARC had lower mRNA levels, its protein levels were as strong as the parent. Conversely, the Cd^{#4}-SPARC cell line had high mRNA levels, but low levels of SPARC protein. Since SPARC is a secreted protein, the ability of the SPARC-transfected and control cell lines to secrete SPARC protein into the growth media was analyzed by western blotting (Figure IV-2). The expression of SPARC protein was measured at 24 and 48 h by collecting the conditioned growth media (M) from the cells as well as the corresponding cell lysate (L) from each cell line at both time points. The SPARC-transfected and UROtsa parental cell lines all secreted SPARC into the growth media to a much greater extent, with respect to levels of SPARC in total protein, than what was expressed in the

cell lysate (Figure IV-2). The blank vector controls had no detection of SPARC expression in the cell lysate and an occasional detection of secreted SPARC was seen in the conditioned growth media (Figure IV-2). Lower molecular weight bands were noted on the western blot of the conditioned media samples using the SPARC antibody, which are most likely degradation products due to the length of time needed to prepare the conditioned growth media for protein analysis.

Immunofluorescence analysis was used to localize the expression of SPARC within the SPARC-transfected, blank vector, and non-transfected control cell lines, with the UROtsa parent cells used as a positive control. The analysis showed the majority of the parental UROtsa cells had an intracellular expression of the SPARC protein, with only infrequent cell profiles showing no SPARC immunoreactivity (Figure IV-3A). In contrast, none of the blank vector or non-transfected UROtsa cell lines transformed by either Cd⁺² or As⁺³ had cell profiles that were immunoreactive for the SPARC protein (Figure IV-3B). The SPARC-transfected cell lines were all immunoreactive for SPARC protein expression (Figure IV-3C-F) and had similar profiles to that of the UROtsa parental cell line. SPARC expression in the UROtsa parent and SPARC-transfected cell lines was localized throughout the cytoplasm and appeared as distinct vesicles (Figure IV-3G). An orthogonal slice of a z-series on the x-plane was also examined for the SPARC-transfected cell lines and demonstrated SPARC protein was diffuse throughout the cell and did not appear to be localized to the nucleus (Figure IV-3H).

Morphology and Growth Rates of SPARC-Transfected and Blank Vector Cell Lines

The morphology of the SPARC-transfected cell lines was examined by light microscopy. After stable transfection with SPARC or with the blank vector, all of the

UROtsa cell lines retained an epithelial morphology and each SPARC-transfected cell line was similar by light microscopy to its blank vector counterpart (Figure IV-4). The morphology of the transfected cell lines were very similar to the morphology of the non-transfected malignantly transformed UROtsa cell lines, as previously published (Cao et al., 2010; Somji et al., 2010). The growth rates (doubling times) of the SPARC-transfected and blank vector cell lines were also determined from linear regions of each respective growth curve following a 1:100 subculture of the cells (Table 1). The doubling times of As^{#3}-SPARC, Cd^{#1}-SPARC and the corresponding blank vectors did decrease significantly compared to non-transfected control cell lines, while As^{#6}-SPARC had an increased doubling time compared to its non-transfected control cell lines and the As^{#6}-DEST (blank vector) was similar to the non-transfected control. Cd^{#7}-SPARC had a similar doubling time to its non-transfected control, but the doubling time of the Cd^{#7}-DEST was significantly increased compared to the non-transfected control cell line. The SPARC-transfected cells had doubling times ranging from 22.0 ± 0.6 h to 27.4 ± 1.0 h and the blank vector had similar growth rates ranging from 22.7 ± 0.8 h to 27.1 ± 0.5 h (Table 1). There was no obvious correlation of morphology at the light level of microscopy with the doubling times of each cell line and there was no consistent difference between cell lines that expressed SPARC and those that did not.

*Migration Properties of SPARC-Transfected, Blank Vector,
and Non-Transfected Cell Lines*

The ability of the UROtsa parent, malignantly transformed Cd⁺² or As⁺³, SPARC-transfected, blank vector cell lines, and the MDA-MB-231 cell line as a positive control to migrate via chemotaxis was analyzed by a transwell migration assay. Cells were stimulated to migrate by chemokinesis with the addition of 1.5% fetal calf serum added

to the bottom chamber and allowed to migrate for 8 h. The MDA-MB-231 breast cancer cell line was chosen as a positive control as literature has previously shown this cell line to be highly migratory (Hughes et al., 2008; Zajac et al., 2011; Zuo et al., 2012). Results from the migration of the MDA-MB-231 cell line confirmed this cell line to be highly migratory with 79% of all cells migrating (Figure IV-5A, 6A, 8A). The parent UROtsa cell line showed 23% migration, while all the Cd⁺²- and As⁺³-transformed UROtsa cell lines had a greater percentage of cell migration than the parental cells. Interestingly, As^{#1}, As^{#3}, As^{#4}, As^{#6}, and Cd^{#1}, had the highest migratory percentages within their respective cell lines with 33% to 51% migration (Figures IV-5, 6). These particular cell lines have been previously reported to not only form subcutaneous tumors, as all the Cd⁺² or As⁺³-transformed UROtsa cell lines form subcutaneous tumors, but to also uniquely produce tumors when injected into the intraperitoneal cavity, suggesting a more aggressive nature of these transformed bladder cell lines (Cao et al., 2010; Somji et al., 2010). Figure IV-7 graphically depicts the relative migration of the transformed UROtsa cell lines and MDA-MB231 as compared to the UROtsa parent cells.

Next, the SPARC-transfected and blank vector control cell lines were examined for their chemotaxis properties (Figure IV-8). All the SPARC-transfected cell lines had a decreased percentage of chemotaxis when compared to its non-transfected counterpart, with As^{#3}-SPARC and Cd^{#1}-SPARC each having a statistically significant decrease in chemotaxis capabilities. The blank vector was similar to the non-transfected cell lines in the As^{#3}-DEST and As^{#6}-DEST lines, however Cd^{#1}-DEST and Cd^{#4}-DEST cell lines had similar migration capabilities to the SPARC-transfected Cd^{#1}-SPARC and Cd^{#4}-SPARC cell lines. These results are graphically depicted in Figure IV-9.

To determine the migratory capabilities of these cell lines in an assay used to simulate wound healing, cells were grown to confluence and a “wound” was generated by scratching the monolayer with a pipette tip. The ability of these cell lines to close the wound was analyzed at 0, 24, and 48 h. To ensure cells were actually migrating into the wounded area and not just filling in the wound by mitosis, the cells were pretreated for 2 h with mitomycin C (MMC) before wound formation. Since MMC inhibits cellular division by cross-linking DNA at guanine and adenine residues (Tomasz, 1995), the 2 h pre-treatment keeps the cell lines from undergoing cellular division for up to 48 h. Therefore, MMC is widely used in cell migration studies to inhibit cellular proliferation (Ding et al., 2003; Ma et al., 1999; Stevenson et al., 2008). First, optimal MMC concentrations were determined for each cell line using serial dilutions of MMC and testing by MTT analysis to assess cell viability versus cellular growth. Concentrations that limited cell growth but did not cause cell death were then used in the wound healing assay. Figures IV-10 and 11 show the series of MTT assays that were conducted on the UROtsa parental, MDA-MB-231, Hs578T, UROtsa cell lines transformed by Cd⁺² or As⁺³, and the SPARC- and DEST-transfected cell lines using the optimal concentrations of MMC. These graphs show limited growth, with no sign of toxicity observed, and levels remaining similar to the 0 h untreated controls for each cell line (Figures IV-10-11). Wound healing assays for controls and the As⁺³-transformed UROtsa cell lines are shown in Figure IV-12, Relative post-wound migration rates were determined for each cell line relative to the UROtsa parent cells at 24 and 48 h using a qualitative plus (+), minus (-), or equal (=) score. As^{#1} and As^{#4} had an increase in the migration of cells into the wound area at both time points, while As^{#2} had increased migration at 24 h but

similar migration at 48 h compared to the parent. As^{#3}, As^{#5}, and As^{#6} had similar migration to the parent at 24 h but increased migration at 48 h. The migration of the Cd⁺²-transformed UROtsa cell lines (Figure IV-13) showed Cd^{#1} was similar to the parent at 24 h but increased at 48 h. All the remaining Cd⁺²-transformed UROtsa cell lines had increased migration at 24 and 48 h with several having much greater migration (++ and +++) as compared to the UROtsa parent. The SPARC- transfected and blank vector cell lines were compared to their non-transfected counterpart (Figures IV-14, 15) when assessing the migration of these cells into the wound. As^{#3}-SPARC, As^{#3}-DEST, As^{#6}-SPARC, Cd^{#4}-SPARC, Cd^{#4}-DEST all had similar post-wound migration when compared to their non-transfected cell line at 24 and 48 h (As^{#3}, As^{#6}, and Cd^{#4} respectively), while the As^{#6}-DEST cell line had increased post-wound migration at 24 and 48 h compared to As^{#6} (Figure IV-14). Also Cd^{#1}-SPARC had decreased post-wound migration at 24 and 48h, while Cd^{#1}-DEST had similar migration at 24 h, but was reduced at 48 h compared to Cd^{#1} (Figure IV-15). Results from the wound healing assay showed that the Cd⁺² and As⁺³-transformed cell lines had a greater post-wound migration capability, especially at the 48 h time point, than the UROtsa parental cell line. However, the SPARC-transfected cell lines showed similar results in their post-wound migration capabilities when compared to their non-transfected control cell lines, with only one SPARC-transfected (Cd^{#1}-SPARC) cell line having decreased post-wound migration.

The invasion capabilities were measured using the UROtsa parent, malignantly transformed Cd⁺² or As⁺³, SPARC-transfected, and blank vector cell lines, the Hs578T cell lines as a positive control using a transwell invasion assay. Cells were stimulated to invade the basement membrane layer by the addition of 10% fetal calf serum added to the

lower chamber and cells were allowed to invade for 24 h. The Hs578T breast cancer cell line was used as a positive control as literature has previously shown this cell line to be highly invasive (Hughes et al., 2008; Sheridan et al., 2006; Zuo et al., 2012). Results from the invasion of the Hs578T cell line confirmed it to be highly invasive with 16% of all cells invading (Figures IV-16A , 17A, 19A). The parent UROtsa cell line showed 1.6% invasion (Figures IV-16B, 17B, 19B), while the invasion of the UROtsa cell line transformed by As⁺³ ranged from 0.5% to 6.1% (Figure IV-16) and the Cd⁺²-transformed cell lines ranged from 1.3% to 12% (Figure IV-17). No correlation was seen in the invasive capabilities of the transformed cell lines and the ability to form intraperitoneal tumors, as was seen in the migration assay. Figure IV-18 graphically depicts the relative invasion of the transformed UROtsa cell lines and Hs578T as compared to the UROtsa parent cells and shows that only Hs578T and Cd^{#4} had a statistically significant increase in invasion compared to the parent. The micrographs of the invaded cells from the SPARC-transfected lines are shown in figure IV-19D, G, J, and M and the blank vector images are in figure IV-19E, H, K, and N. There were no statistically significant differences seen in the SPARC or blank vector transfected cell lines when each of these lines were compared to the UROtsa parent or the non-transfected cell lines (Figure IV-20).

Tumorigenicity and SPARC Protein Analysis of Mouse Heterotransplants Generated from the SPARC-Transfected, Blank Vector, and Non-Transfected Cell Lines

The SPARC-transfected and blank vector cell lines were analyzed for their ability to form colonies in soft agar. All of the SPARC-transfected and blank vector cell lines were capable of forming colonies at the lowest inoculum and even greater amounts were formed at the highest inoculum shown in Figure IV-21. No attempt was made to quantify

colony formation since the experimental endpoint was to provide evidence of adhesion-independent growth as well as justification for animal usage as a vehicle for tumor growth and characterization. The SPARC-transfected, blank vector, and non-transfected control cell lines were injected into nude mice at an inoculum of 1×10^6 cells per mouse. The SPARC-transfected cell lines were injected into 5 mice and the blank vector and non-transfected UROtsa cell lines were injected into 4 mice each.

The immunohistochemical analysis of SPARC expression in the mouse heterotransplants was analyzed using two different mouse anti-human SPARC antibodies due to differences in the antibodies to cross species. As previously reported by Larson et al. (2010), the expression of SPARC in the epithelial component of tumors produced from the Cd^{+2} and As^{+3} -transformed UROtsa cells was down-regulated to background levels, while the stromal component of these tumors showed strong immunoreactivity for SPARC. This analysis was conducted with the use of a mouse anti-human osteonectin primary antibody purchased from Haematologic Technologies Inc. (HTI). Since the stromal component originates from the murine host and is recruited to the tumor site, this antibody was capable of detecting the immunohistochemical localization of SPARC in murine stroma. However, this antibody performed poorly in other applications.

Therefore, an additional SPARC antibody was needed and the mouse anti-human SPARC antibody from Leica was able to work in all applications, but as of yet was untested on mouse tissue. Figure IV-22 shows the differences in the staining patterns of the HTI and Leica antibodies within mouse tumors that were previously generated from the Cd^{+2} and As^{+3} -transformed UROtsa cells. The staining of the mouse tumor tissue with the HTI antibody was very similar to that previously reported by Larson et al. 2010, with only the

stroma being highly reactive for SPARC expression and the malignant epithelial cell having no SPARC expression. The SPARC antibody purchased from Leica showed very different results. All of the tumor heterotransplant tissues were entirely negative for the expression of SPARC. The specificity of both these antibodies was further tested on a human bladder cancer specimen of high grade invasive carcinoma of the bladder, and showed immunoreactivity for SPARC within the stromal component of the tumor and absence of staining in the epithelial component (Figure IV-23A, B). Therefore the HTI antibody was capable of recognizing human and mouse SPARC, while the Leica antibody only recognizes human SPARC protein by immunohistochemistry.

The tumors produced from the UROtsa Cd[#]1, Cd[#]1-SPARC, and Cd[#]1-DEST cell lines were then analyzed for SPARC expression by both SPARC antibodies (Figure IV-23). The HTI antibody only detected SPARC expression within the stroma of the tumor, presumably of mouse origin, with no SPARC detection in the tumor cells generated from any of the cell lines (Figure IV-23A, C, E, G). The Leica antibody showed a lack of SPARC staining throughout the entire tissue, both the epithelial tumor and mouse stroma, for all of the mouse heterotransplants (Figure IV-23B, D, F, H).

A corresponding analysis of protein expression by western blotting using tissue from the mouse heterotransplants determined an absence of SPARC expression in all the heterotransplants (Figure IV-24). Verification that the expression of SPARC was present in the cells prior to injection into the mice, showed the Cd[#]1-SPARC transfected cell line as well as the UROtsa parent cell line, a positive control, did express SPARC protein, while Cd[#]1 and Cd[#]1-DEST control cell lines did not (Figure IV-24).

SPARC and BSD mRNA Expression in Cell Lines and Mouse Heterotransplants Generated from the SPARC-Transfected, Blank Vector, and Non-Transfected Cell Lines

The determination that SPARC protein was not expressed in the mouse heterotransplants from the Cd[#]1-SPARC transfected cells led to two possible explanations. The first being, the possibility that not all the cells maintained the SPARC vector and upon injected into the mouse, only the cells without the vector were capable of forming the tumor and therefore, did not express SPARC protein. Or the second explanation being, the SPARC-transfected cells injected into the nude mouse responded to the mouse tissue environment and down-regulated SPARC protein expression.

The verification that the resulting mouse heterotransplants contained the transfection vector was determined by the presence of the Blasticidin (BSD) gene due to its presence in the vector. The mRNA expression of BSD was analyzed in the SPARC and DEST-transfected cells and the corresponding non-transfected cell lines as well as within the extracts prepared from the subcutaneous tumors generated from these cell lines (Figure IV-25A). The mRNA analysis of BSD expression revealed the presence of the transfected vector in SPARC and DEST-transfected cell lines and its absence from the Cd[#]1 cell line prior to injection of the cells into the nude mice as expected. A corresponding analysis of the mouse tumors generated from the SPARC and DEST-transfected cell lines, verified the expression of BSD in both the Cd[#]1-SPARC and Cd[#]1-DEST injected mouse heterotransplants and absent from Cd[#]1 tumors. Therefore the presence of the vector was confirmed within the Cd[#]1-SPARC and Cd[#]1-DEST generated tumors. The level of BSD expression between the transfected cell lines and the mouse heterotransplants was similar.

The cell lines and heterotransplants were further analyzed for the mRNA expression of human and mouse specific SPARC (Figures IV-25B, 26). Human specific SPARC mRNA expression was only detected in the SPARC-transfected cell line; however, a great reduction in human SPARC mRNA was seen in the resulting tumor from this cell line (Figure IV-25B). The DEST-transfected and non-transfected control cell lines were at the limit of detection for human SPARC. Mouse specific SPARC primers were then used and revealed the presence of mouse SPARC within all of the mouse heterotransplants (Figure IV-26). The level of mouse SPARC was similar in the heterotransplants from the non-transfected and DEST-transfected cell lines, but the SPARC-transfected cell line showed about a 50-fold induction in comparison. This result may be specific to the cells injected or may reflect additional connective tissue within that particular tissue. The expression of mouse SPARC within the human cell lines prior to injection into the mice showed an absence of mouse specific SPARC expression, as expected.

Discussion

The initial goal of the present study was to determine if SPARC could be stably transfected into As⁺³ and Cd⁺²-transformed UROtsa cell lines. Two Cd⁺²-transformed UROtsa cell lines and two As⁺³-transformed UROtsa cell lines were chosen to be transfected with SPARC. The decision to use two cell lines from each of the Cd⁺² and As⁺³-transformed UROtsa cell lines was motivated by the finding that only two of the As⁺³ transformed lines and one of the Cd⁺² transformed lines were able to establish tumors within the peritoneal cavity when transplanted into nude mice (Cao et al., 2010; Somji et al., 2010). This is an important observation since bladder cancer is known to

metastasize locally within the body cavity and only very late in the disease to distant organ sites. The peritoneal findings may indicate the ability of the transformed cells to “seed” organs within the peritoneal cavity. For the stable transfection study, one cell line from each set will be capable of establishing peritoneal tumors and the other cell line will not have this ability. The two As⁺³ transformed cell lines chosen for transfection were As^{#3} and As^{#6} and the two Cd⁺² transformed cell lines were Cd^{#1} and Cd^{#4}.

SPARC mRNA and protein expression was induced in all SPARC-transfected cell lines. Variations in the levels of induced SPARC mRNA and protein were seen among the SPARC-transfected cell lines; which may provide an interesting analysis for future studies. Intracellular localization of SPARC protein showed SPARC-transfected cells displayed a similar expression profile to the UROtsa parental cell, with SPARC staining localized to the cytoplasm and appeared as distinct vesicles. SPARC secretion by analyzing conditioned growth media taken from the SPARC-transfected cells was confirmed within all of the SPARC-transfected cell lines and was similar to the secretion of SPARC protein detected in the UROtsa parent.

Another goal of this study was to determine if the forced expression of SPARC would alter the chemotaxis, wound healing, and invasion capabilities of these cells. The chemotaxis migratory capabilities seemed to decrease with the forced SPARC expression as compared to their non-transfected counterpart, but the decrease in migration was also seen in some of the vector only control cell lines, suggesting this might not be a SPARC specific response. The migration in response to a wound only showed slight changes in the migration of SPARC-transfected cell lines as compared to its non-transfected counterpart. Similar results were also obtained by the invasion assay. Although several

other studies have suggested SPARC plays a substantial role in cellular invasion and migration (Arnold et al., 2008; Framson and Sage, 2004; Golembieski et al., 2008; Jacob et al., 1999), a large change in the ability of the Cd⁺² and As⁺³-transformed UROtsa cell lines transfected with SPARC to regulate migration and invasion was not observed in our system.

Since the UROtsa parental cell line is non-tumorigenic and the SPARC-transfected cells had similar expression profiles to that of the UROtsa parental cell in respect to SPARC, a surprising finding in the present study was the ability of the SPARC-transfected cell lines to form tumors in nude mice. In general, the tumors that were produced by the SPARC-transfected cell lines appeared to form at a similar rate to the tumors formed by the control cell lines. Within the tumors generated from the Cd^{#1}-SPARC transfected cell line, the tumors did seem smaller in volume than those formed by the control cell lines. However, upon examination of SPARC protein by immunohistochemistry and western blotting analysis, the tumors produced by the Cd^{#1}-SPARC-transfected cell line showed a complete lack of SPARC expression in the urothelial cancer cells. The tumors generated from the Cd^{#1} control cell line also showed a similar lack of SPARC expression; therefore, no difference in the expression of SPARC was seen between the tumors generated from the SPARC-transfected cells or the non-transfected cells.

Of interest, two SPARC antibodies from differing manufactures were used to confirm the results by immunohistochemistry. Both SPARC antibodies did not detect expression within the malignant epithelial component of the tumor generated by the SPARC-transfected cell lines. The SPARC antibody purchased from HTI showed

SPARC immunoreactivity within the mouse stroma, while the Leica antibody did not. It was determined from the present study and results previously reported (Larson et al., 2010) that human SPARC protein could be detected using the HTI and Leica antibodies by immunohistochemistry and western blotting applications. However, mouse SPARC protein was only capable of being detected by immunohistochemistry using the HTI antibody. Therefore, the lack of human SPARC protein expression within the tumors generated from the Cd[#]1-SPARC transfected cells was due to either the lack of stable transfection of all cells with the SPARC vector and therefore, the tumor was formed only by not-transfected cells or the SPARC-transfected cells responded to the mouse environment and down-regulated SPARC expression.

Verification that the resulting tumor was formed by the Cd[#]1-SPARC transfected cells was confirmed using real time RT-PCR analysis that revealed BSD mRNA expression. Subsequent analysis of human specific SPARC mRNA expression showed a reduction of human specific SPARC mRNA in the mouse heterotransplants compared to the original cell lines and the complete absence of human SPARC protein in the mouse heterotransplants. These results strongly suggest a post-transcriptional regulation of SPARC expression especially when considering the lack of epigenetic regulation by promoter methylation and/or acetylation previously reported (Larson et al., 2010).

One possible mechanism to explain the down-regulation of SPARC mRNA and complete absence of SPARC protein is microRNA. microRNAs (miRNAs) are short, roughly 20-24 nucleotides in length, and are non-coding RNAs that direct the post-transcriptional repression of target mRNAs (Schnall-Levin et al., 2011). Although there are only roughly 1000 miRNAs, their ability to bind to multiple targets allows miRNAs

to regulate at least 20% of all human genes that have been involved in the regulation of a wide spectrum of biological systems (Forman et al., 2008). miRNAs were originally believed to only bind to the 3' or 5' untranslated regions of mRNAs, but evidence is quickly emerging that miRNAs can also bind to the coding regions (Forman et al., 2008; Huang et al., 2010; Schnall-Levin et al., 2011). An analysis by Forman et al. (2008) revealed approximately 700 genes in the human genome that had been identified as having conserved regulatory sites within the coding region, and this number of involved genes is believed to be an under-estimation.

A search by DIANA-microT v3.0 (B.R.S.C. Alexander Leming, Athens, Greece) revealed several miRNAs that were potential binders to SPARC mRNA (Maragkakis et al., 2009a; Maragkakis et al., 2009b). Five possible miRNAs were determined to be able to regulate SPARC, these included, miRNA-29a, miRNA-29b, miRNA-29c, miRNA-147, and miRNA-203. Since only the SPARC ORF was transfected into select Cd⁺² and As⁺³-transformed UROtsa cell lines, the coding region of SPARC was analyzed for miRNA binding sites. The family of miRNA-29, including 29a, 29b, 29c, had the highest degree of homology to the SPARC mRNA sequence, but miRNA-147 and miRNA-203 binding sites were also found, just with a lesser degree of homology. Since the degree of homology of the miRNA to its target sequence leads to the miRNA's mode of action, perfect pairing leads to cleavage of the mRNA and lesser complementarity results in repression of translation. Complementary pairing between the 5' end of the miRNA, specifically called the "seed" region (bases 2-8), and the 3' end of the target mRNA is critical for function (Schnall-Levin et al., 2011). Also miRNA-mediated repression increases with the number of sites to which the miRNA can bind to the target

mRNA, suggesting that post-transcriptional repression may be substantial if a gene contains many miRNA sites within its coding region (Schnall-Levin et al., 2011). The miRNA-29a, b, and c family was shown to bind to multiple times within the SPARC ORF with strong complementary pairing within the “seed” region, leading it to be a probable regulator for the decrease in SPARC mRNA and protein expression in the mouse heterotransplant produced from the SPARC-transfected cells.

Overall, the results of this study show that SPARC was stably transfected into transformed UROtsa cells that did not make detectable levels of SPARC prior to transfection. The SPARC-transfected cell lines did not have a consistent or result in major differences in relation to growth rate, general morphology, migration by chemotaxis or wound healing, invasion, or growth in soft agar. However, analysis of the UROtsa Cd[#]1 cell line transfected with SPARC reveals an increase in growth rate and a decrease in migration by wound healing. The tumors from the Cd[#]1-SPARC transfected cell lines, shockingly did not have express SPARC protein but all cells within the tumor were positive for BSD mRNA and slightly positive for SPARC mRNA. The results from this study show that SPARC expression is most likely post-transcriptionally regulated by miRNA.

References

- Arnold, S., Mira, E., Muneer, S., Korpanty, G., Beck, A.W., Holloway, S.E., Manes, S., Brekken, R.A., 2008. Forced expression of MMP9 rescues the loss of angiogenesis and abrogates metastasis of pancreatic tumors triggered by the absence of host SPARC, *Exp. Biol. Med. (Maywood)* 233, 860-873.
- Bornstein, P., 1995. Diversity of function is inherent in matricellular proteins: an appraisal of thrombospondin 1, *J. Cell Biol.* 130, 503-506.
- Cao, L., Zhou, X.D., Sens, M.A., Garrett, S.H., Zheng, Y., Dunlevy, J.R., Sens, D.A., Somji, S., 2010. Keratin 6 expression correlates to areas of squamous differentiation in multiple independent isolates of As(+3)-induced bladder cancer, *J. Appl. Toxicol.* 30, 416-430.
- Ding, Q., Stewart, J., Jr, Olman, M.A., Klobe, M.R., Gladson, C.L., 2003. The pattern of enhancement of Src kinase activity on platelet-derived growth factor stimulation of glioblastoma cells is affected by the integrin engaged, *J. Biol. Chem.* 278, 39882-39891.
- Forman, J.J., Legesse-Miller, A., Collier, H.A., 2008. A search for conserved sequences in coding regions reveals that the let-7 microRNA targets Dicer within its coding sequence, *Proc. Natl. Acad. Sci. U. S. A.* 105, 14879-14884.
- Framson, P.E., Sage, E.H., 2004. SPARC and tumor growth: where the seed meets the soil? *J. Cell. Biochem.* 92, 679-690.
- Friedline, J.A., Garrett, S.H., Somji, S., Todd, J.H., Sens, D.A., 1998. Differential expression of the MT-1E gene in estrogen-receptor-positive and -negative human breast cancer cell lines, *Am. J. Pathol.* 152, 23-27.
- Golembieski, W.A., Thomas, S.L., Schultz, C.R., Yunker, C.K., McClung, H.M., Lemke, N., Cazacu, S., Barker, T., Sage, E.H., Brodie, C., Rempel, S.A., 2008. HSP27 mediates SPARC-induced changes in glioma morphology, migration, and invasion, *Glia* 56, 1061-1075.
- Gurel, V., Sens, D.A., Somji, S., Garrett, S.H., Nath, J., Sens, M.A., 2003. Stable transfection and overexpression of metallothionein isoform 3 inhibits the growth of MCF-7 and Hs578T cells but not that of T-47D or MDA-MB-231 cells, *Breast Cancer Res. Treat.* 80, 181-191.
- Huang, S., Wu, S., Ding, J., Lin, J., Wei, L., Gu, J., He, X., 2010. MicroRNA-181a modulates gene expression of zinc finger family members by directly targeting their coding regions, *Nucleic Acids Res.* 38, 7211-7218.

- Hughes, L., Malone, C., Chumsri, S., Burger, A.M., McDonnell, S., 2008. Characterisation of breast cancer cell lines and establishment of a novel isogenic subclone to study migration, invasion and tumourigenicity, *Clin. Exp. Metastasis* 25, 549-557.
- Jacob, K., Webber, M., Benayahu, D., Kleinman, H.K., 1999. Osteonectin promotes prostate cancer cell migration and invasion: a possible mechanism for metastasis to bone, *Cancer Res.* 59, 4453-4457.
- Koukourakis, M.I., Giatromanolaki, A., Brekken, R.A., Sivridis, E., Gatter, K.C., Harris, A.L., Sage, E.H., 2003. Enhanced expression of SPARC/osteonectin in the tumor-associated stroma of non-small cell lung cancer is correlated with markers of hypoxia/acidity and with poor prognosis of patients, *Cancer Res.* 63, 5376-5380.
- Lane, T.F., Sage, E.H., 1994. The biology of SPARC, a protein that modulates cell-matrix interactions, *FASEB J.* 8, 163-173.
- Larson, J., Yasmin, T., Sens, D.A., Zhou, X.D., Sens, M.A., Garrett, S.H., Dunlevy, J.R., Cao, L., Somji, S., 2010. SPARC gene expression is repressed in human urothelial cells (UROtsa) exposed to or malignantly transformed by cadmium or arsenite, *Toxicol. Lett.* 199, 166-172.
- Ledda, F., Bravo, A.I., Adris, S., Bover, L., Mordoh, J., Podhajcer, O.L., 1997. The expression of the secreted protein acidic and rich in cysteine (SPARC) is associated with the neoplastic progression of human melanoma, *J. Invest. Dermatol.* 108, 210-214.
- Ma, T.Y., Kikuchi, M., Sarfeh, I.J., Shimada, H., Hoa, N.T., Tarnawski, A.S., 1999. Basic fibroblast growth factor stimulates repair of wounded hepatocyte monolayer: modulatory role of protein kinase A and extracellular matrix, *J. Lab. Clin. Med.* 134, 363-371.
- Maragkakis, M., Alexiou, P., Papadopoulos, G.L., Reczko, M., Dalamagas, T., Giannopoulos, G., Goumas, G., Koukis, E., Kourtis, K., Simossis, V.A., Sethupathy, P., Vergoulis, T., Koziris, N., Sellis, T., Tsanakas, P., Hatzigeorgiou, A.G., 2009a. Accurate microRNA target prediction correlates with protein repression levels, *BMC Bioinformatics* 10, 295.
- Maragkakis, M., Reczko, M., Simossis, V.A., Alexiou, P., Papadopoulos, G.L., Dalamagas, T., Giannopoulos, G., Goumas, G., Koukis, E., Kourtis, K., Vergoulis, T., Koziris, N., Sellis, T., Tsanakas, P., Hatzigeorgiou, A.G., 2009b. DIANA-microT web server: elucidating microRNA functions through target prediction, *Nucleic Acids Res.* 37, W273-6.

- Rempel, S.A., Golembieski, W.A., Ge, S., Lemke, N., Elisevich, K., Mikkelsen, T., Gutierrez, J.A., 1998. SPARC: a signal of astrocytic neoplastic transformation and reactive response in human primary and xenograft gliomas, *J. Neuropathol. Exp. Neurol.* 57, 1112-1121.
- Rossi, M.R., Masters, J.R., Park, S., Todd, J.H., Garrett, S.H., Sens, M.A., Somji, S., Nath, J., Sens, D.A., 2001. The immortalized UROtsa cell line as a potential cell culture model of human urothelium, *Environ. Health Perspect.* 109, 801-808.
- Rossi, M.R., Somji, S., Garrett, S.H., Sens, M.A., Nath, J., Sens, D.A., 2002. Expression of hsp 27, hsp 60, hsc 70, and hsp 70 stress response genes in cultured human urothelial cells (UROtsa) exposed to lethal and sublethal concentrations of sodium arsenite, *Environ. Health Perspect.* 110, 1225-1232.
- Sage, E.H., 2003. Purification of SPARC/osteonectin, *Curr. Protoc. Cell. Biol.* Chapter 10, Unit 10.11.
- Sage, E.H., Bornstein, P., 1991. Extracellular proteins that modulate cell-matrix interactions. SPARC, tenascin, and thrombospondin, *J. Biol. Chem.* 266, 14831-14834.
- Sakai, N., Baba, M., Nagasima, Y., Kato, Y., Hirai, K., Kondo, K., Kobayashi, K., Yoshida, M., Kaneko, S., Kishida, T., Kawakami, S., Hosaka, M., Inayama, Y., Yao, M., 2001. SPARC expression in primary human renal cell carcinoma: upregulation of SPARC in sarcomatoid renal carcinoma, *Hum. Pathol.* 32, 1064-1070.
- San, R.H., Laspia, M.F., Soiefer, A.I., Maslansky, C.J., Rice, J.M., Williams, G.M., 1979. A survey of growth in soft agar and cell surface properties as markers for transformation in adult rat liver epithelial-like cell cultures, *Cancer Res.* 39, 1026-1034.
- Sato, N., Fukushima, N., Maehara, N., Matsubayashi, H., Koopmann, J., Su, G.H., Hruban, R.H., Goggins, M., 2003. SPARC/osteonectin is a frequent target for aberrant methylation in pancreatic adenocarcinoma and a mediator of tumor-stromal interactions, *Oncogene* 22, 5021-5030.
- Schnall-Levin, M., Rissland, O.S., Johnston, W.K., Perrimon, N., Bartel, D.P., Berger, B., 2011. Unusually effective microRNA targeting within repeat-rich coding regions of mammalian mRNAs, *Genome Res.* 21, 1395-1403.
- Sens, D.A., Park, S., Gurel, V., Sens, M.A., Garrett, S.H., Somji, S., 2004. Inorganic cadmium- and arsenite-induced malignant transformation of human bladder urothelial cells, *Toxicol. Sci.* 79, 56-63.

- Sheridan, C., Kishimoto, H., Fuchs, R.K., Mehrotra, S., Bhat-Nakshatri, P., Turner, C.H., Goulet, R., Jr, Badve, S., Nakshatri, H., 2006. CD44+/CD24- breast cancer cells exhibit enhanced invasive properties: an early step necessary for metastasis, *Breast Cancer Res.* 8, R59.
- Socha, M.J., Said, N., Dai, Y., Kwong, J., Ramalingam, P., Trieu, V., Desai, N., Mok, S.C., Motamed, K., 2009. Aberrant promoter methylation of SPARC in ovarian cancer, *Neoplasia* 11, 126-135.
- Somji, S., Zhou, X.D., Mehus, A., Sens, M.A., Garrett, S.H., Lutz, K.L., Dunlevy, J.R., Zheng, Y., Sens, D.A., 2010. Variation of keratin 7 expression and other phenotypic characteristics of independent isolates of cadmium transformed human urothelial cells (UROtsa), *Chem. Res. Toxicol.* 23, 348-356.
- Stevenson, S., Nelson, L.D., Sharpe, D.T., Thornton, M.J., 2008. 17beta-estradiol regulates the secretion of TGF-beta by cultured human dermal fibroblasts, *J. Biomater. Sci. Polym. Ed.* 19, 1097-1109.
- Thomas, R., True, L.D., Bassuk, J.A., Lange, P.H., Vessella, R.L., 2000. Differential expression of osteonectin/SPARC during human prostate cancer progression, *Clin. Cancer Res.* 6, 1140-1149.
- Tomasz, M., 1995. Mitomycin C: small, fast and deadly (but very selective), *Chem. Biol.* 2, 575-579.
- Zajac, M., Law, J., Cvetkovic, D.D., Pampillo, M., McColl, L., Pape, C., Di Guglielmo, G.M., Postovit, L.M., Babwah, A.V., Bhattacharya, M., 2011. GPR54 (KISS1R) transactivates EGFR to promote breast cancer cell invasiveness, *PLoS One* 6, e21599.
- Zuo, Y., Wu, Y., Chakraborty, C., 2012. Cdc42 negatively regulates intrinsic migration of highly aggressive breast cancer cells, *J. Cell. Physiol.* 227, 1399-1407.

Cell Line	Doubling Time
Parent	33.2 ± 0.8 h
As^{#3}	33.3 ± 1.4 h
As^{#3}-SPARC	27.4 ± 1.0 h*
As^{#3}- DEST	27.1 ± 0.5 h*
As^{#6}	21.6 ± 1.6 h
As^{#6}-SPARC	25.6 ± 0.5 h*
As^{#6}- DEST	23.6 ± 0.7 h
Cd^{#1}	27.8 ± 0.6 h
Cd^{#1}-SPARC	23.8 ± 0.6 h*
Cd^{#1}- DEST	22.7 ± 0.8 h*
Cd^{#4}	20.7 ± 1.1 h
Cd^{#4}-SPARC	22.0 ± 0.6 h
Cd^{#4}-DEST	23.5 ± 0.4 h*

Table IV-1. Doubling times for SPARC-transfected and DEST-transfected UROtsa cells. The doubling times for UROtsa As^{#3}, As^{#6}, Cd^{#1}, and Cd^{#4} were previously described by Cao et al., (2010) and Somji et al., (2010). *Denotes a statistically significant difference compared to the non-transfected UROtsa cell line (p < 0.05).

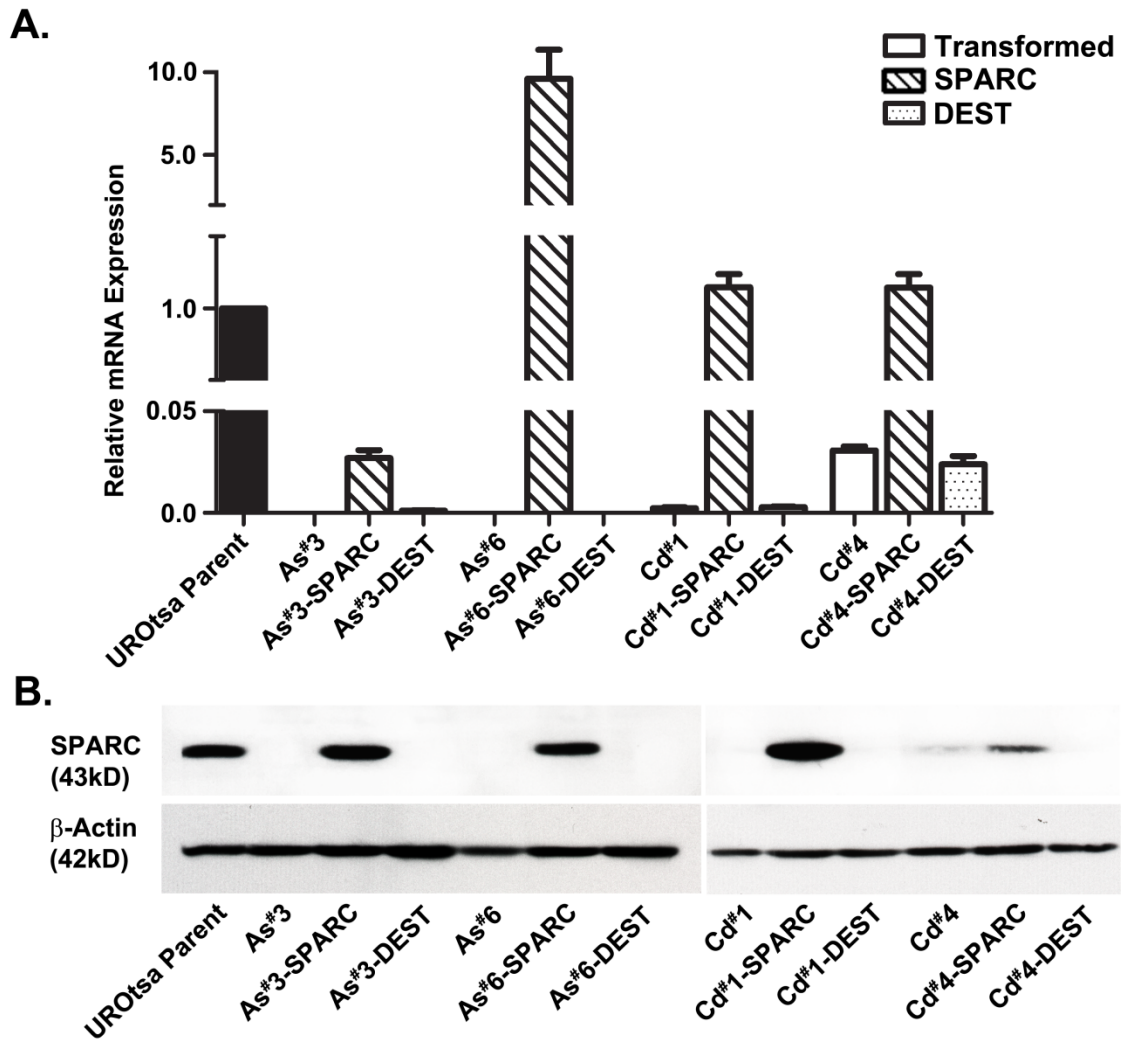


Figure IV-1. Expression of SPARC mRNA and protein in parental UROtsa cells, SPARC-transfected cells, and non-transfected and blank vector (DEST) control cells lines. (A) Real time-RT-PCR analysis of SPARC expression. The resulting mRNA levels were normalized to the fold change in β -actin. Real time data is plotted as the mean \pm SEM of triplicate determinations. (B) Western analysis of SPARC protein expression (top panel) with an analysis of β -actin loading control shown in the bottom panel. The #'s identify the independent cell lines isolated by the exposure of UROtsa cells to As^{+3} or Cd^{+2} as described by Cao et al. (2010) and Somji et al. (2010), respectively.

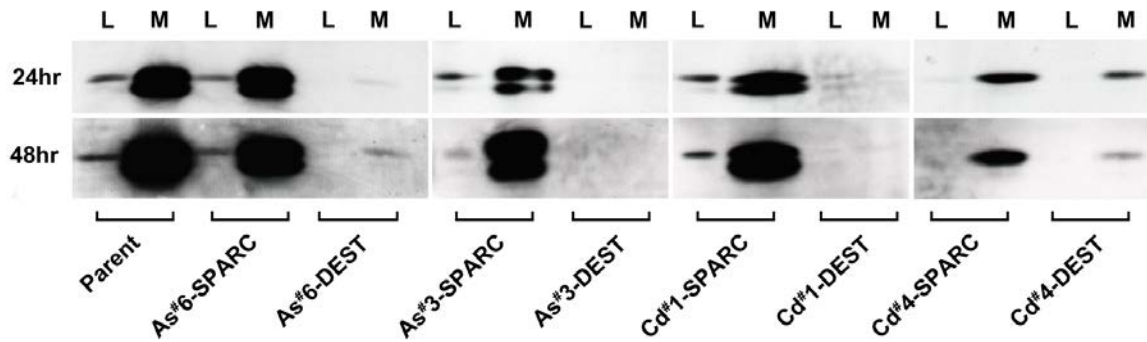


Figure IV-2. Expression of secreted SPARC protein. Western analysis of SPARC protein secreted from confluent cultures of the parental UROtsa cells, SPARC-transfected cells, and non-transfected and blank vector (DEST) control cells lines. Conditioned media (M) was collected at 24 h (top panel) and 48 h (bottom panel) time points then concentrated as described in materials and methods and was compared to their respective cell lysates (L).

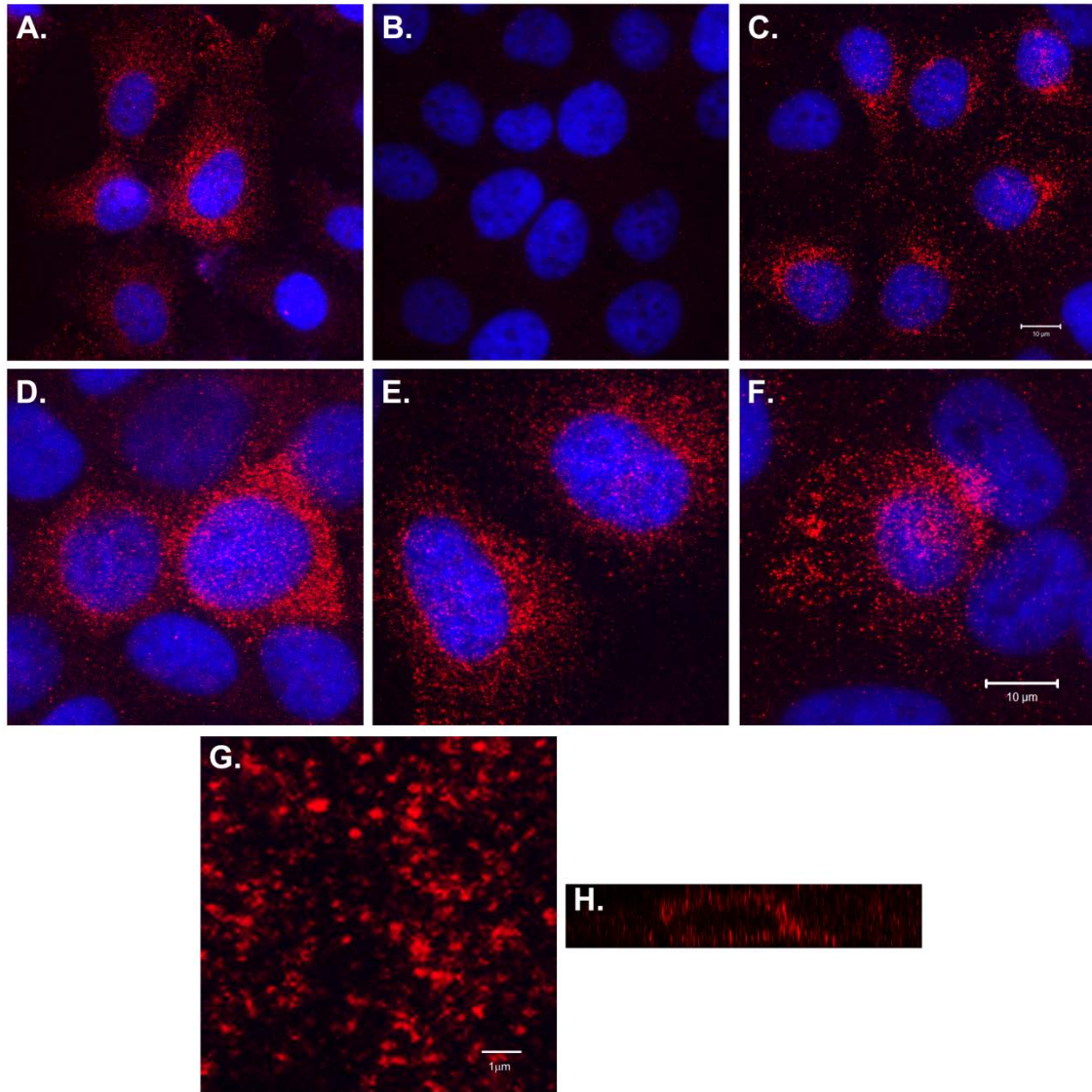


Figure IV-3. Intracellular localization of SPARC protein by immunofluorescent staining. SPARC (red) staining in: (A) Parent UROtsa cells, (B) UROtsa Cd[#]4-DEST cells (blank vector), and (C) UROtsa Cd[#]4-SPARC. Higher magnification images of: (D)UROtsa As[#]3-SPARC, (E) UROtsa As[#]6-SPARC, and (F) UROtsa Cd[#]1-SPARC. (G) Higher magnification of UROtsa As[#]3-SPARC showing SPARC localized to structures that resemble vesicles. (H) Orthogonal slice of a z-series of UROtsa As[#]6-SPARC showing SPARC expression throughout the cytoplasm of the cell. (A-F) DAPI counterstain was used to identify all cells in the fields. Images in A-C correspond to bar in C (10 μ m), images in D-F correspond to bar in F (10 μ m), and bar in G = 1 μ m.

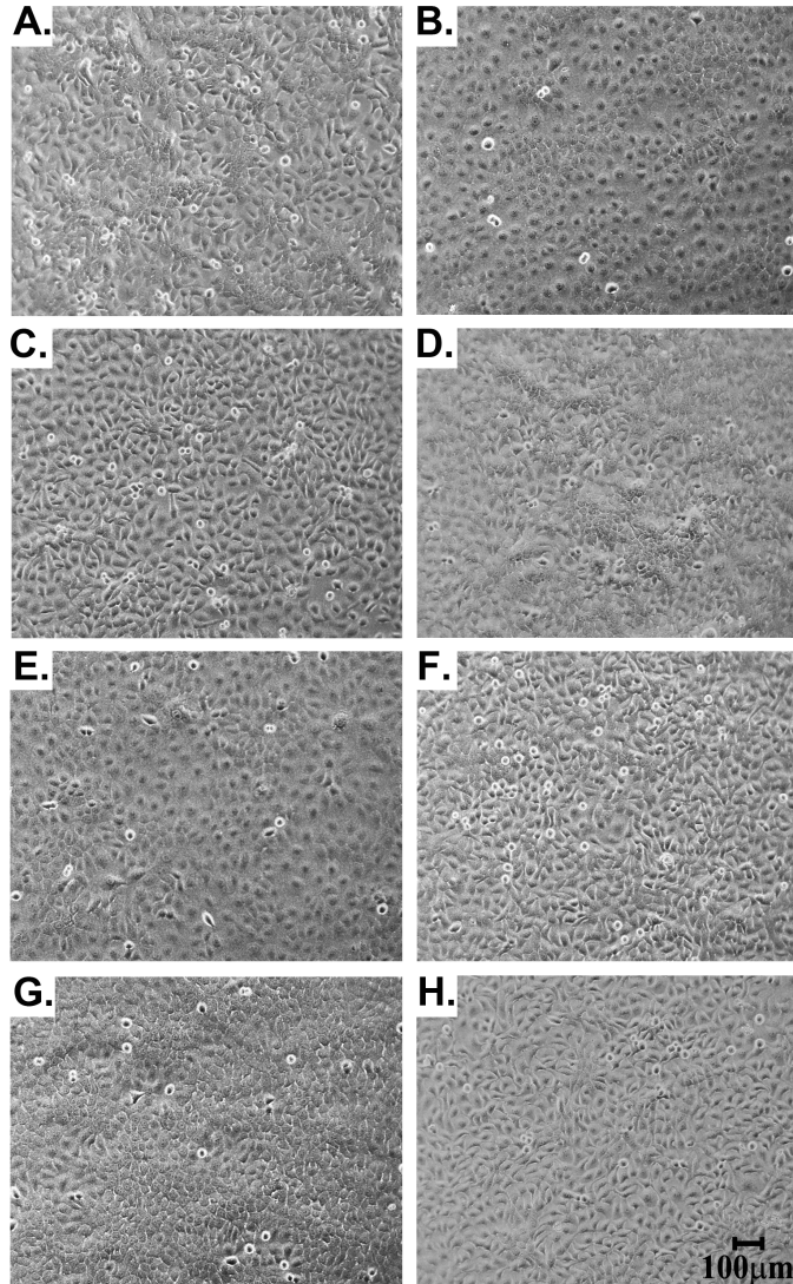


Figure IV-4. Phase contrast light microscopy of the SPARC-transfected and DEST-transfected UROtsa cell lines demonstrating epithelial morphology in all lines. (A) As^{#3}-SPARC; (B) As^{#3}-DEST; (C) As^{#6}-SPARC; (D) As^{#6}-DEST; (E) Cd^{#1}-SPARC (F) Cd^{#1}-DEST; (G) Cd^{#4}-SPARC; and (H) Cd^{#4}-DEST. All images correspond to bar in H = 100 µm.

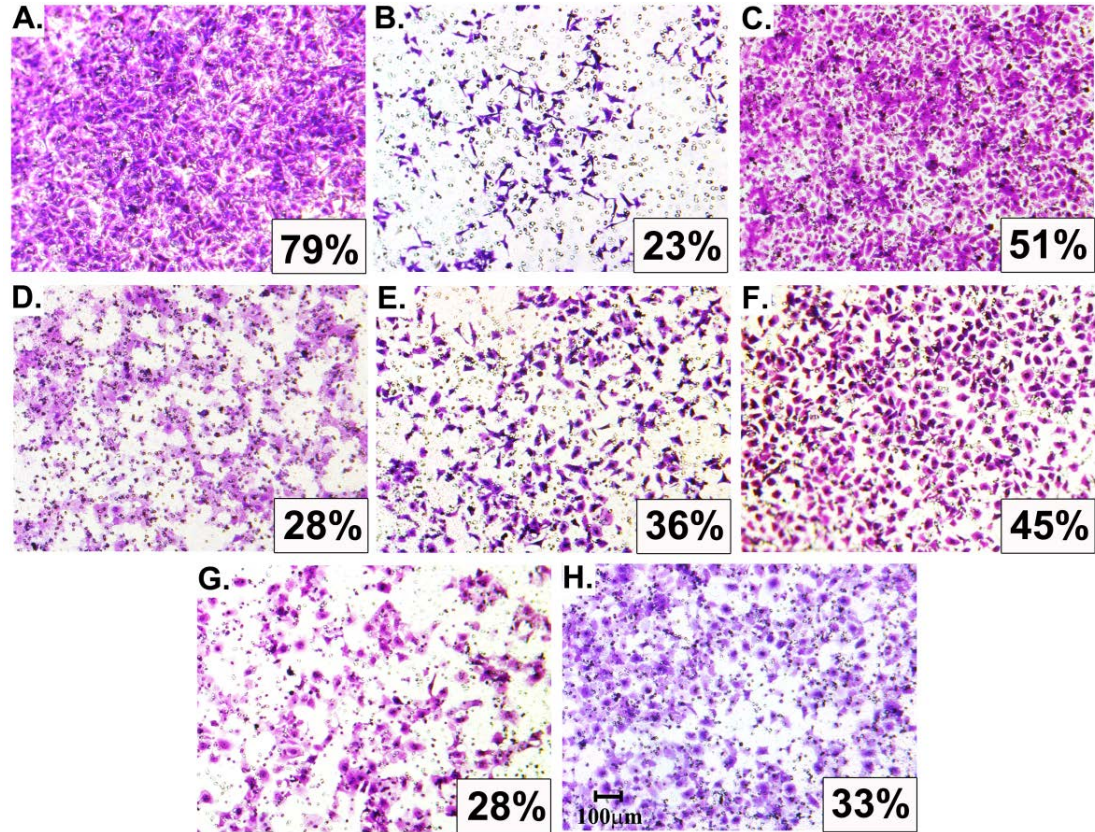


Figure IV-5. Migratory ability of UROtsa parent, and malignantly transformed As⁺³ cell lines, with the MDA-MB-231 malignant breast cancer cells used a positive control. Micrographs show the cells that migrated in: (A) MDA-MB-231; (B) UROtsa parental; (C) As[#]1; (D) As[#]2; (E) As[#]3; (F) As[#]4; and (G) As[#]5; (H) As[#]6. The percentage of total cells that migrated is depicted in the bottom left corner of each micrograph, was determined by counting all cells in 20 fields using a 40 x magnification lens, removing the cells from the top of the insert, and counting the remaining cells on the bottom of the insert in 20 fields using a 40 x magnification lens. All images correspond to bar in H = 100 µm.

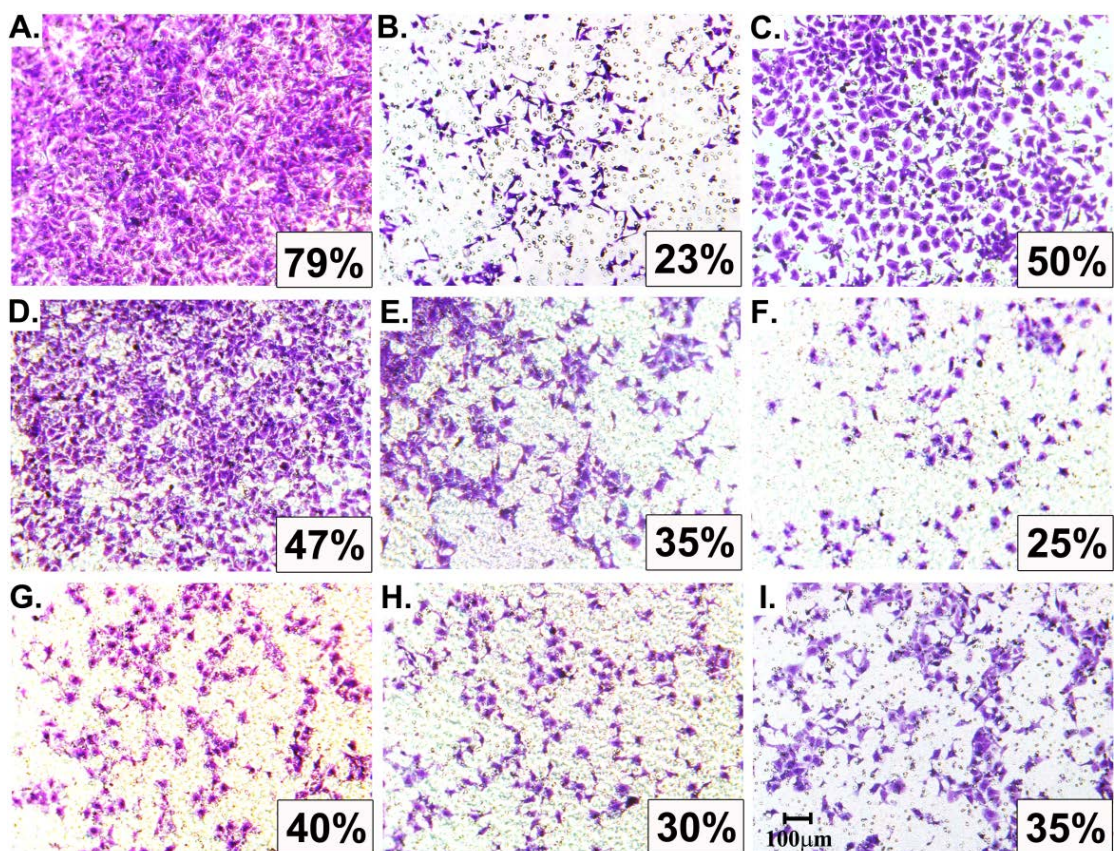


Figure IV-6. Migratory ability of UROtsa parent, and malignantly transformed Cd⁺² cell lines, with the MDA-MB-231 malignant breast cancer cells used a positive control. Micrographs show the cells that migrated in: (A) MDA-MB-231; (B) UROtsa parental; (C) Cd[#]1; (D) Cd[#]2; (E) Cd[#]3; (F) Cd[#]4; (G) Cd[#]5; (H) Cd[#]6; and (I) Cd[#]7. The percentage of total cells that migrated is depicted in the bottom left corner of each micrograph, was determined by counting all cells in 20 fields using a 40 x magnification lens, removing the cells from the top of the insert, and counting the remaining cells on the bottom of the insert in 20 fields using a 40 x magnification lens. All images correspond to bar in I = 100 µm.

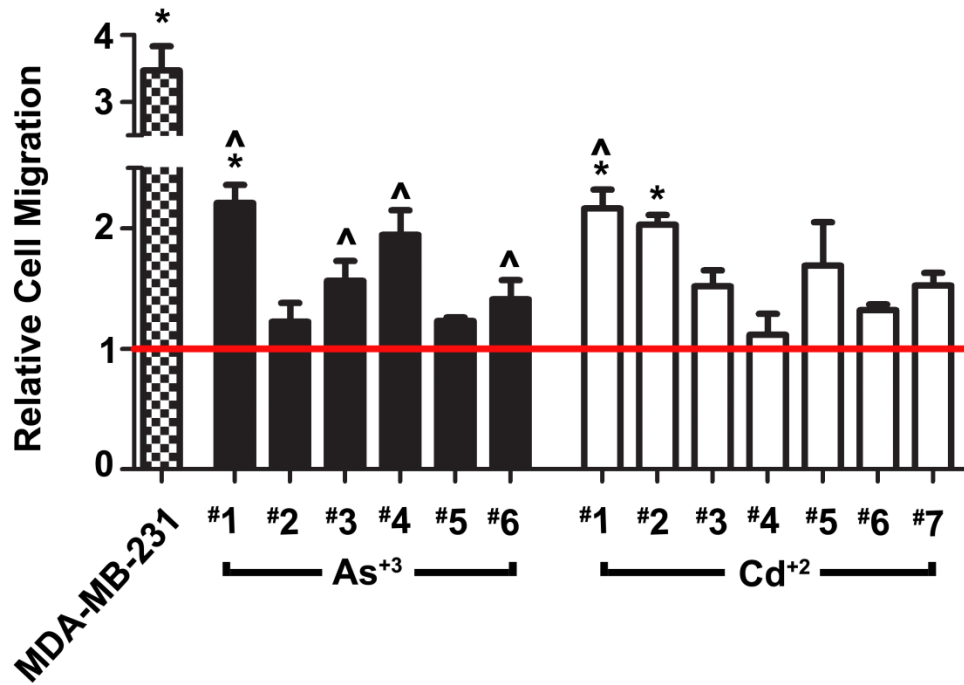
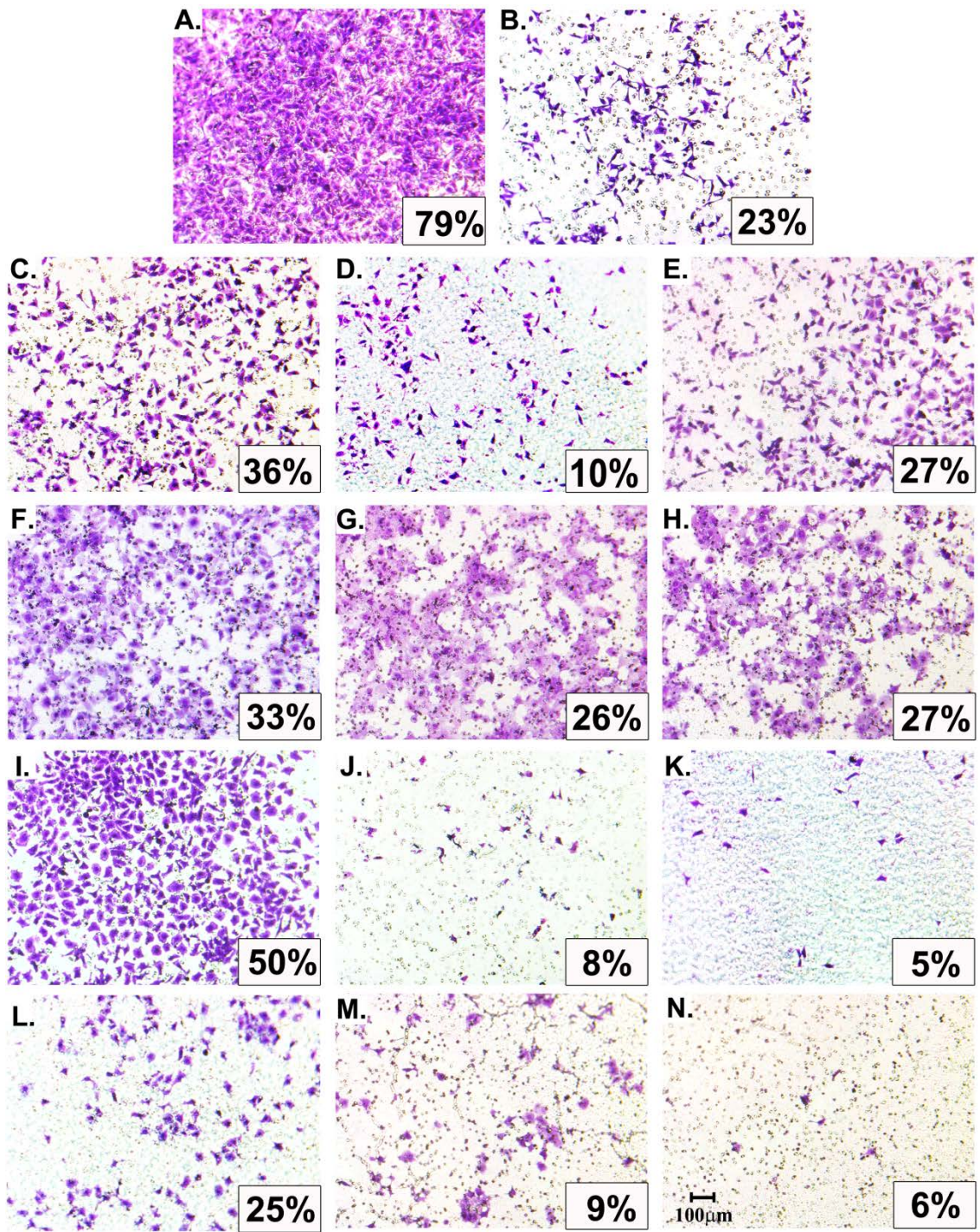


Figure IV-7. Relative cell chemotaxis migration of MDA-MB-231 and UROtsa cells transformed by As⁺³ or Cd⁺² compared to the parent UROtsa cells. The red horizontal line at 1, represents the UROtsa parent cells. ^ indicates malignantly transformed UROtsa cell lines capable of forming subcutaneous tumors in nude mice. *Denotes a statistically significant difference from the UROtsa parent cells (p < 0.05).

Figure IV-8. Migratory ability of UROtsa parent, non-transfected, SPARC-transfected, and blank vector (DEST) cell lines with MDA-MB-231 malignant breast cells used as a positive control. Micrographs show the cells that migrated in: (A) MDA-MB-231; (B) UROtsa parental; (C) As^{#3}; (D) As^{#3}-SPARC; (E) As^{#3}-DEST; (F) As^{#6}; (G) As^{#6}-SPARC; (H) As^{#6}-DEST; (I) Cd^{#1}; (J) Cd^{#1}-SPARC; (K) Cd^{#1}-DEST; (L) Cd^{#4}; (M) Cd^{#4}-SPARC; and (N) Cd^{#4}-DEST. The percentage of total cells that migrated is depicted in the bottom left corner of each micrograph, and was determined by counting all cells in 20 fields using a 40 x magnification lens, removing the cells from the top of the insert, and counting the remaining cells on the bottom of the insert in 20 fields using a 40 x magnification lens. All images correspond to bar in N = 100 μ m.



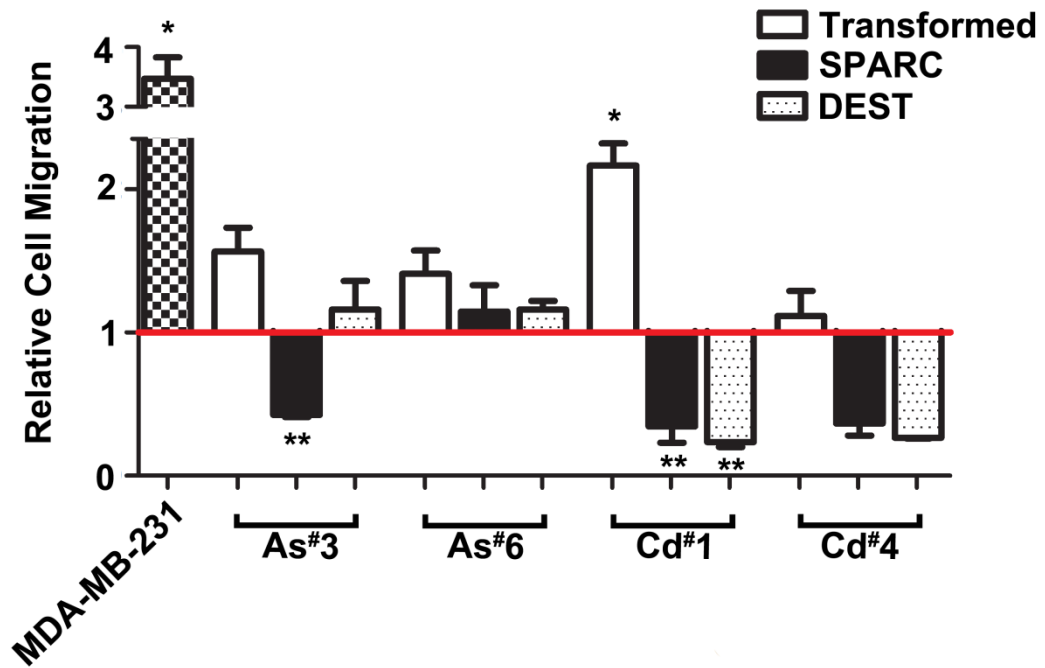


Figure IV-9. Relative cell migration of MDA-MB-231, non-transfected UROtsa, SPARC-transfected, and blank vector (DEST) cells lines compared to the parent UROtsa cells. The red horizontal line at 1, represents the UROtsa parent cells. *Denotes a statistically significant difference from the UROtsa parent cells, while ** denotes statistically significant difference from the non-transfected UROtsa counterpart ($p < 0.05$).

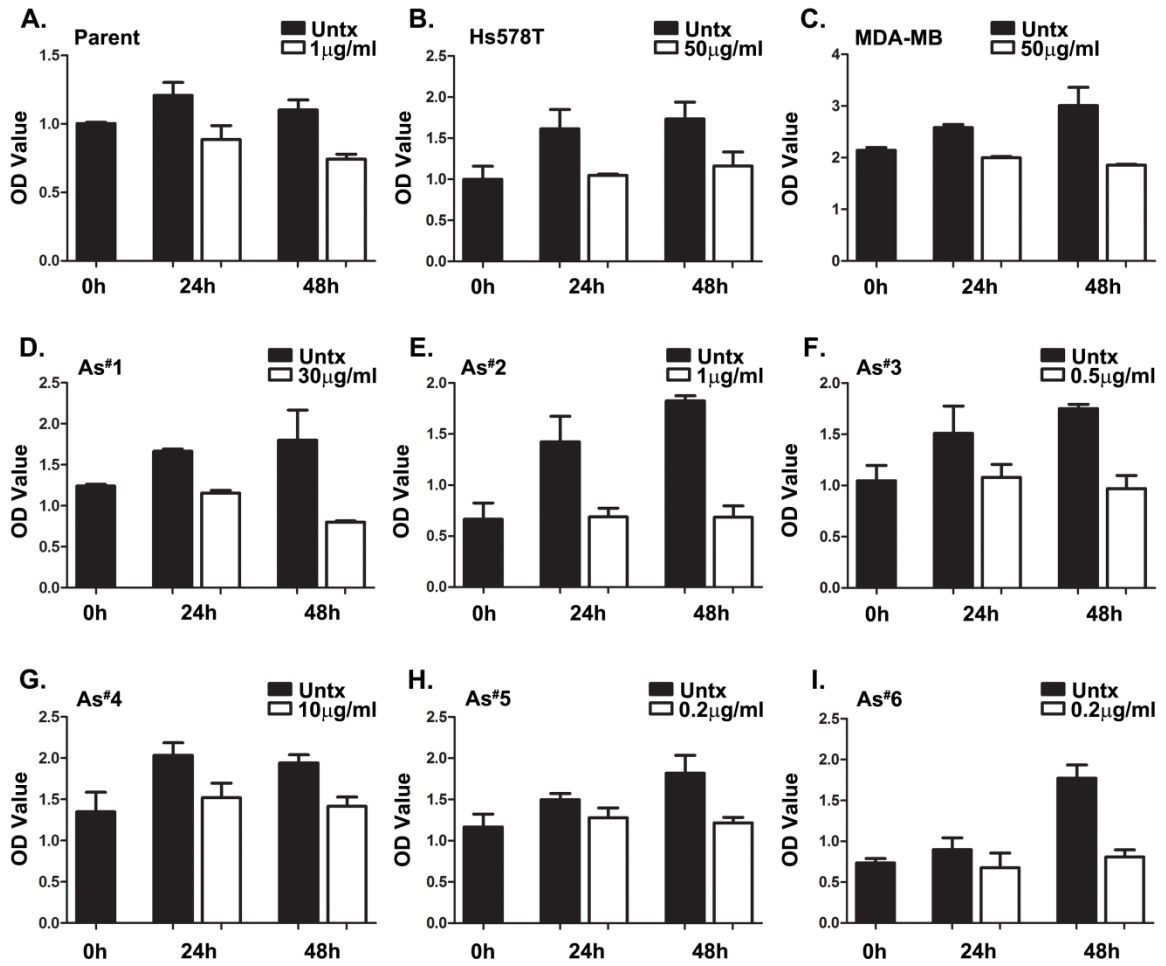


Figure IV-10. MTT assessing cell viability of UROtsa parent, breast cancer, and As⁺³-transformed UROtsa cell lines. (A) UROtsa parental; (B) Hs578T; (C) MDA-MB-231; (D) As^{#1}; (E) As^{#2}; (F) As^{#3}; (G) As^{#4}; (H) As^{#5}; and (I) As^{#6} show the nontoxic effects of pretreatment with MMC (white bars) for 2 h and subsequent culturing in the absence of MMC for 24 or 48 h. 0, 24, or 48 h controls (black bars) were not treated with MMC (untx). The concentration of MMC used had been previously optimized for each cell line.

Figure IV-11. MTT analysis assessing cell viability of UROtsa cells transformed by Cd⁺³ and the cells transfected with SPARC (S) and DEST (D) vectors. (A) Cd^{#1}; (B) Cd^{#2}; (C) Cd^{#3}; (D) Cd^{#4}; (E) Cd^{#5}; (F) Cd^{#6}; (G) Cd^{#7}; (H) As^{#3}-SPARC; (I) As^{#3}-DEST; (J) As^{#6}-SPARC; (K) As^{#6}-DEST; (L) Cd^{#1}-SPARC; (M) Cd^{#1}-DEST; (N) Cd^{#4}-SPARC; and (O) Cd^{#4}-DEST show the nontoxic effects of pretreatment with MMC (white bars) for 2 h and subsequent culturing in the absence of MMC for 24 or 48 h. 0, 24, or 48 h controls (black bars) were not treated with MMC (untx). The concentration of MMC used had been previously optimized for each cell line.

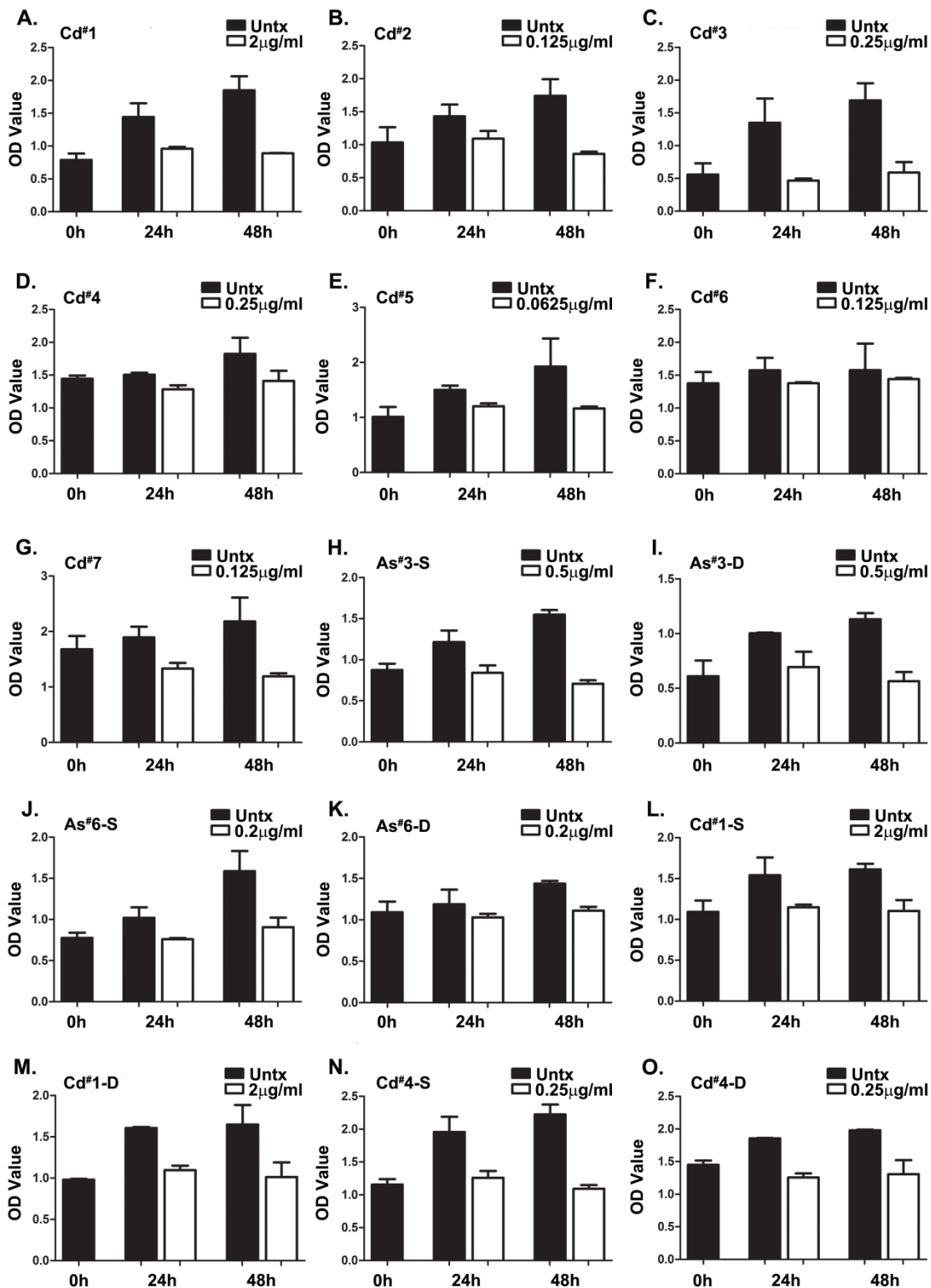
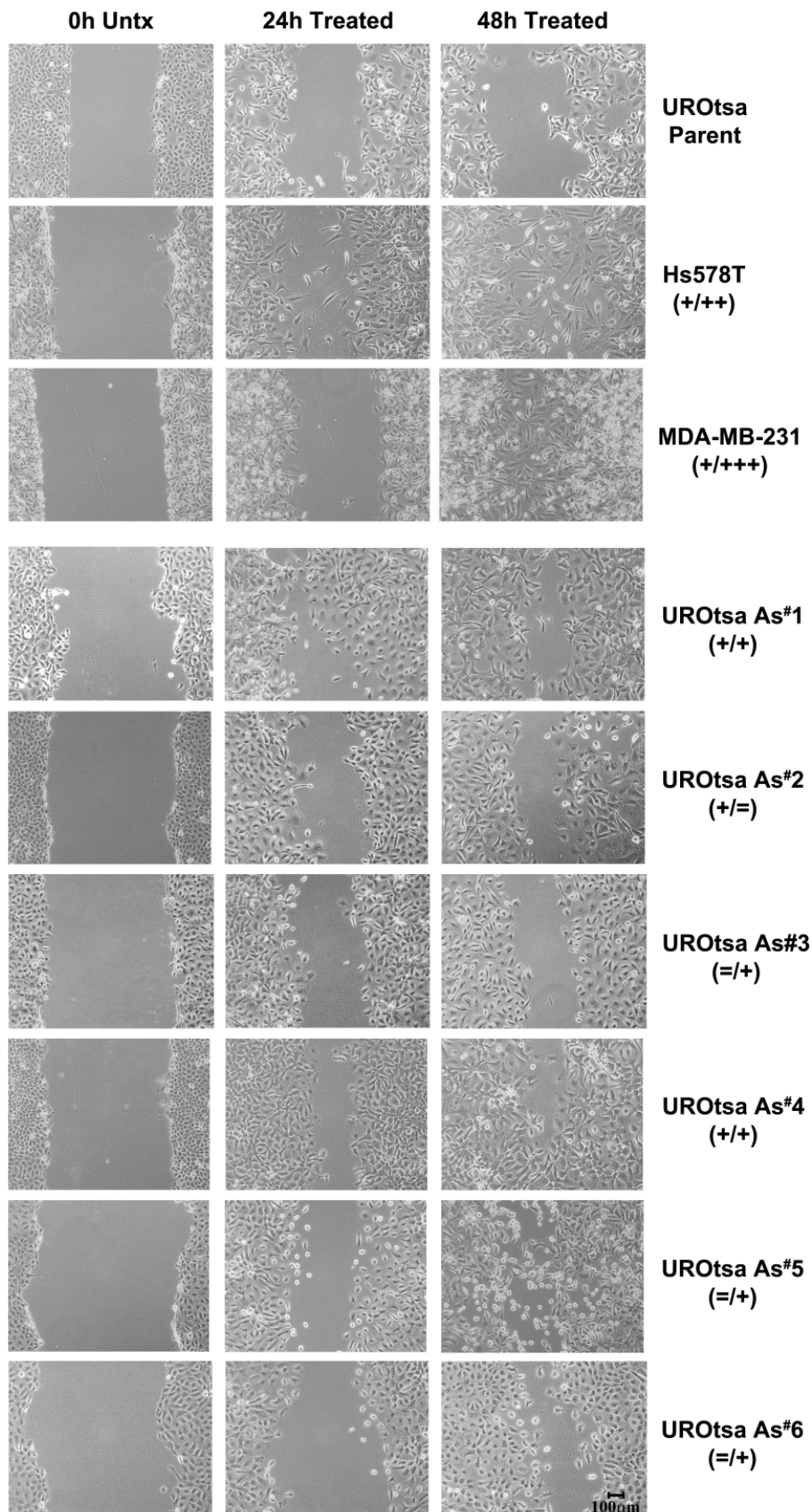


Figure IV-12. Wound healing assay of the UROtsa parent cells, breast cancer cell lines, MDA-MB231 and HS578T, and UROtsa cells transformed by As⁺³. Wound closing ability of each cell line was analyzed at 0, 24, and 48 h. Cells had been pretreated with MMC for 2 h prior to wounding. Qualitative analysis of wound closure rate is shown in the parenthesis as compared to the UROtsa parent at (24/48 h). = showing similar closure, + showing greater closure, while ++ or +++ with much greater closure than the parent. All images correspond to bar in last image, bar = 100 μ m.



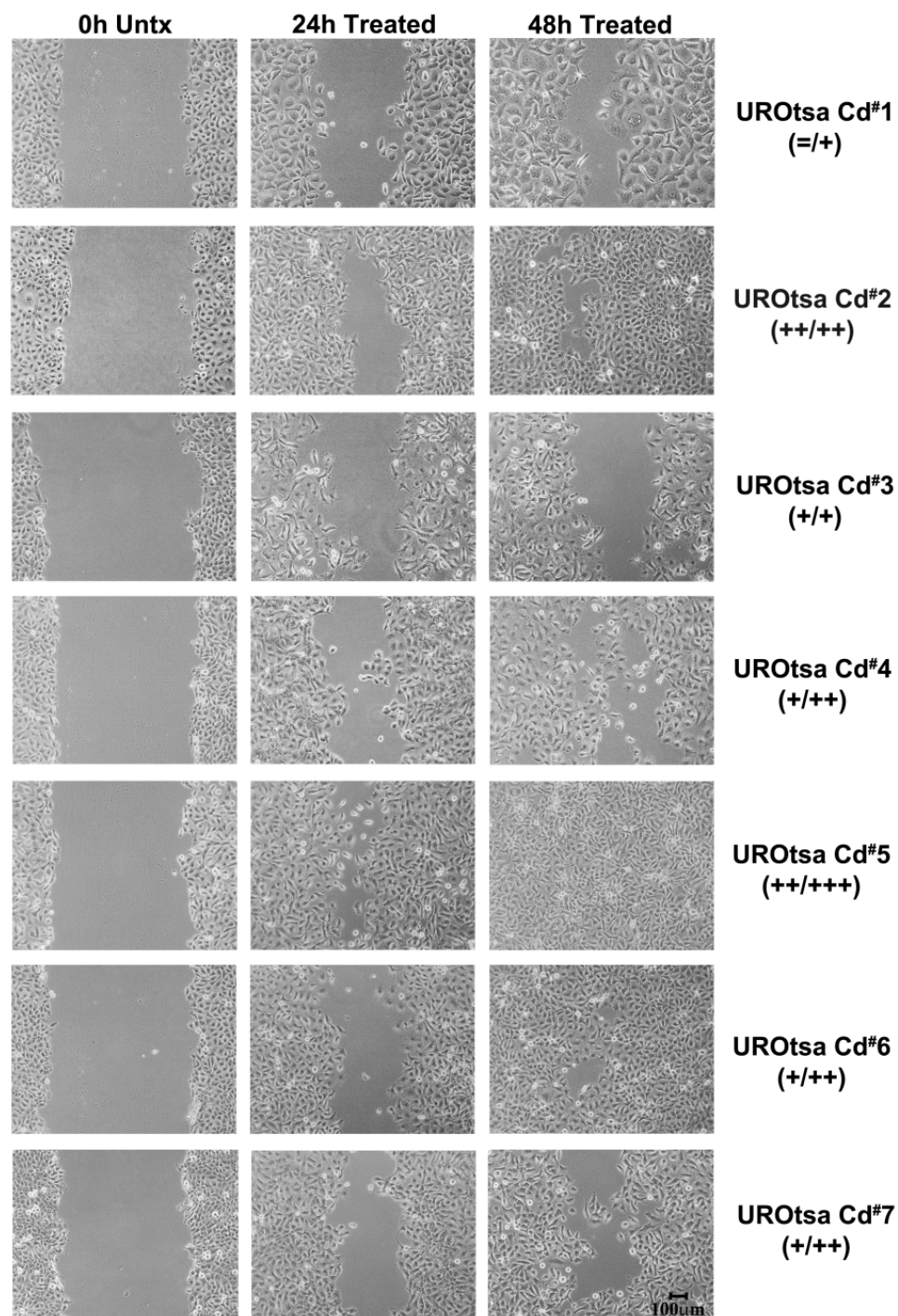


Figure IV-13. Wound healing assay of UROtsa cells transformed by Cd²⁺. Wound closing ability of each cell line was analyzed at 0, 24, and 48 h. Cells had been pretreated with MMC for 2 h prior to wounding. Qualitative analysis of wound closure rate is shown in the parenthesis as compared to the UROtsa parent (Figure IV-12) at (24/48 h). = showing similar closure, + showing greater closure, while ++ or +++ with much greater closure than the parent. All images correspond to bar in last image, bar = 100 µm.

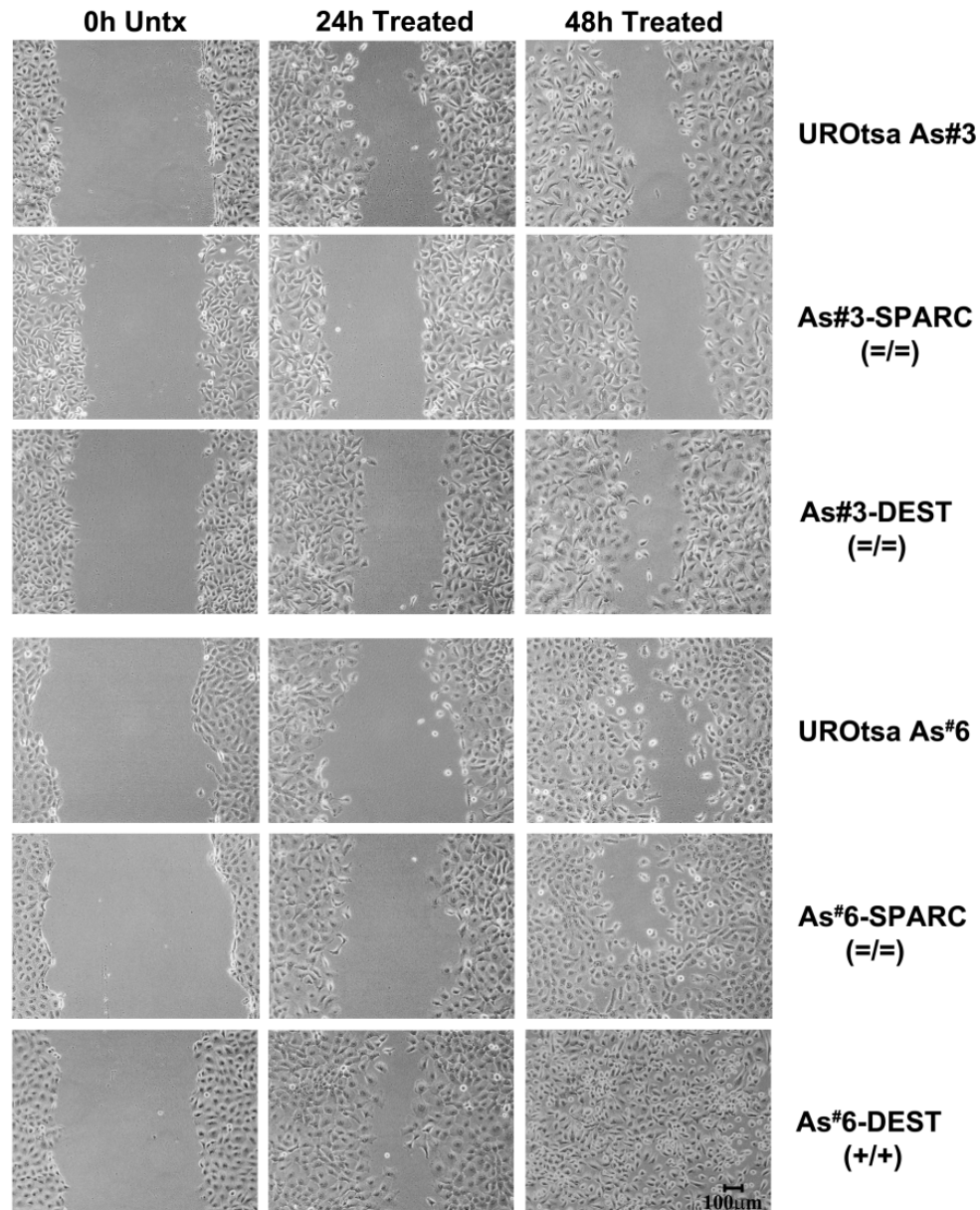


Figure IV-14. Wound healing assay of UROtsa As⁺³ cells transfected with SPARC or blank vector (DEST) and their non-transfected counterparts. Wound closing ability of each cell line was analyzed at 0, 24, and 48 h. Cells had been pretreated with MMC for 2 h prior to wounding. Qualitative analysis of wound closure rate is shown in the parenthesis at (24/48 h) as compared to the non-transfected control cell line (As^{#3} or As^{#6}). = showing similar closure and + showing greater closure than the non-transfected cell line. All images correspond to bar in last image, bar = 100 µm.

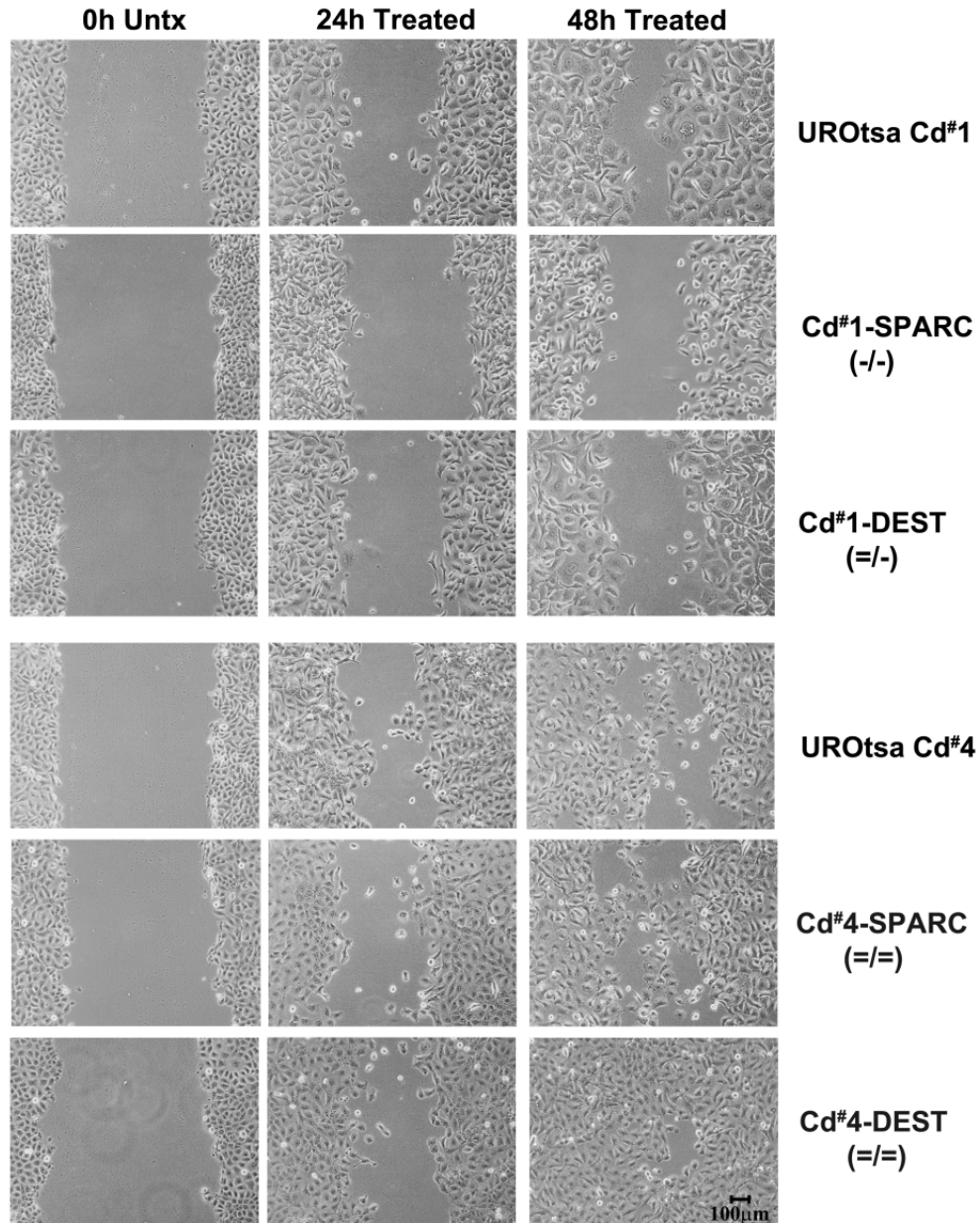


Figure IV-15. Wound healing assay of UROtsa Cd⁺ cells transfected with SPARC or blank vector (DEST) and their non-transfected counterparts. Wound closing ability of each cell line was analyzed at 0, 24, and 48 h. Cells had been pretreated with MMC for 2 h prior to wounding. Qualitative analysis of wound closure rate is shown in the parenthesis at (24/48 h) as compared to the non-transfected control cell line (Cd[#]1 or Cd[#]4). = showing similar closure and - showing reduced closure than the non-transfected cell line. All images correspond to bar in last image, bar = 100 µm.

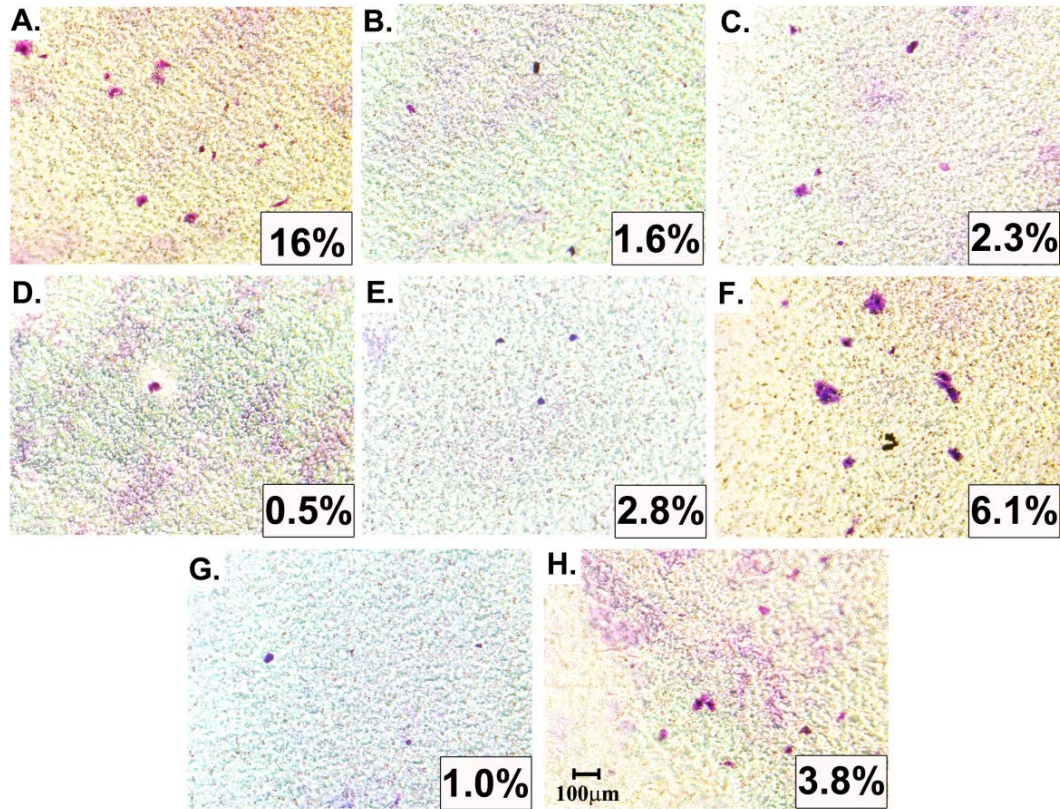


Figure IV-16. Invasion capability of UROtsa parent, and malignantly transformed As⁺³ cell lines, with the Hs578T malignant breast cancer cell line as a positive control. Micrographs show the cells that invaded in: (A) Hs578T; (B) UROtsa parental; (C) As[#]1; (D) As[#]2; (E) As[#]3; (F) As[#]4; (G) As[#]5; and (H) As[#]6. The percentage of total cells that invaded is depicted in the bottom left corner of each micrograph and was determined by counting all cells in 20 fields using a 40 x magnification lens, removing the cells from the top of the insert, and counting the remaining cells on the bottom of the insert in 20 fields using a 40 x magnification lens. All images correspond to bar in H = 100 µm.

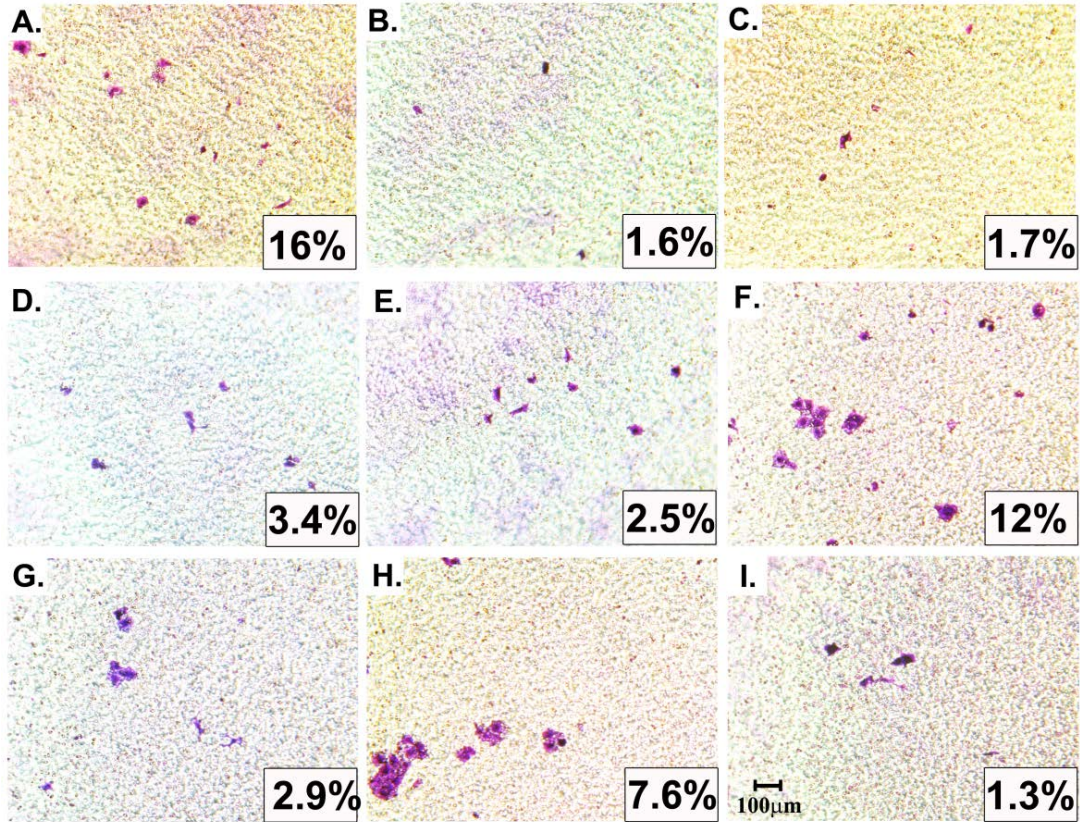


Figure IV-17. Invasion capability of UROtsa parent, and malignantly transformed Cd⁺² cell lines, with the Hs578T malignant breast cancer cell line as a positive control. Micrographs show the cells that invaded in: (A) Hs578T; (B) UROtsa parental; (C) Cd#1; (D) Cd#2; (E) Cd#3; (F) Cd#4; (G) Cd#5; (H) Cd#6; and (I) Cd#7. The percentage of total cells that invaded is depicted in the bottom left corner of each micrograph and was determined by counting all cells in 20 fields using a 40 x magnification lens, removing the cells from the top of the insert, and counting the remaining cells on the bottom of the insert in 20 fields using a 40 x magnification lens. All images correspond to bar in I = 100 µm.

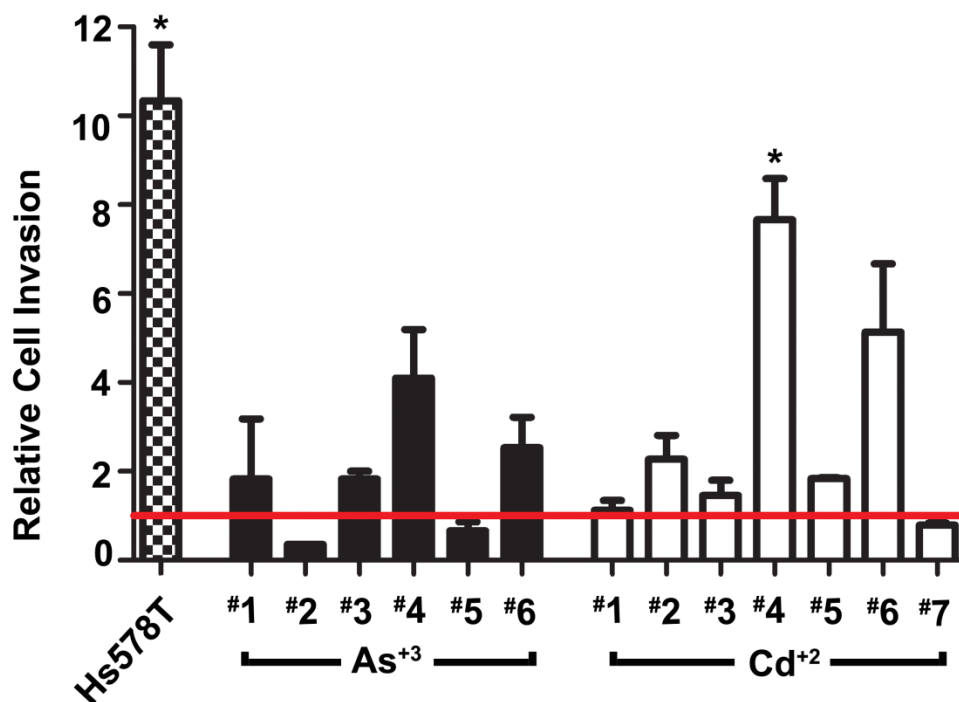
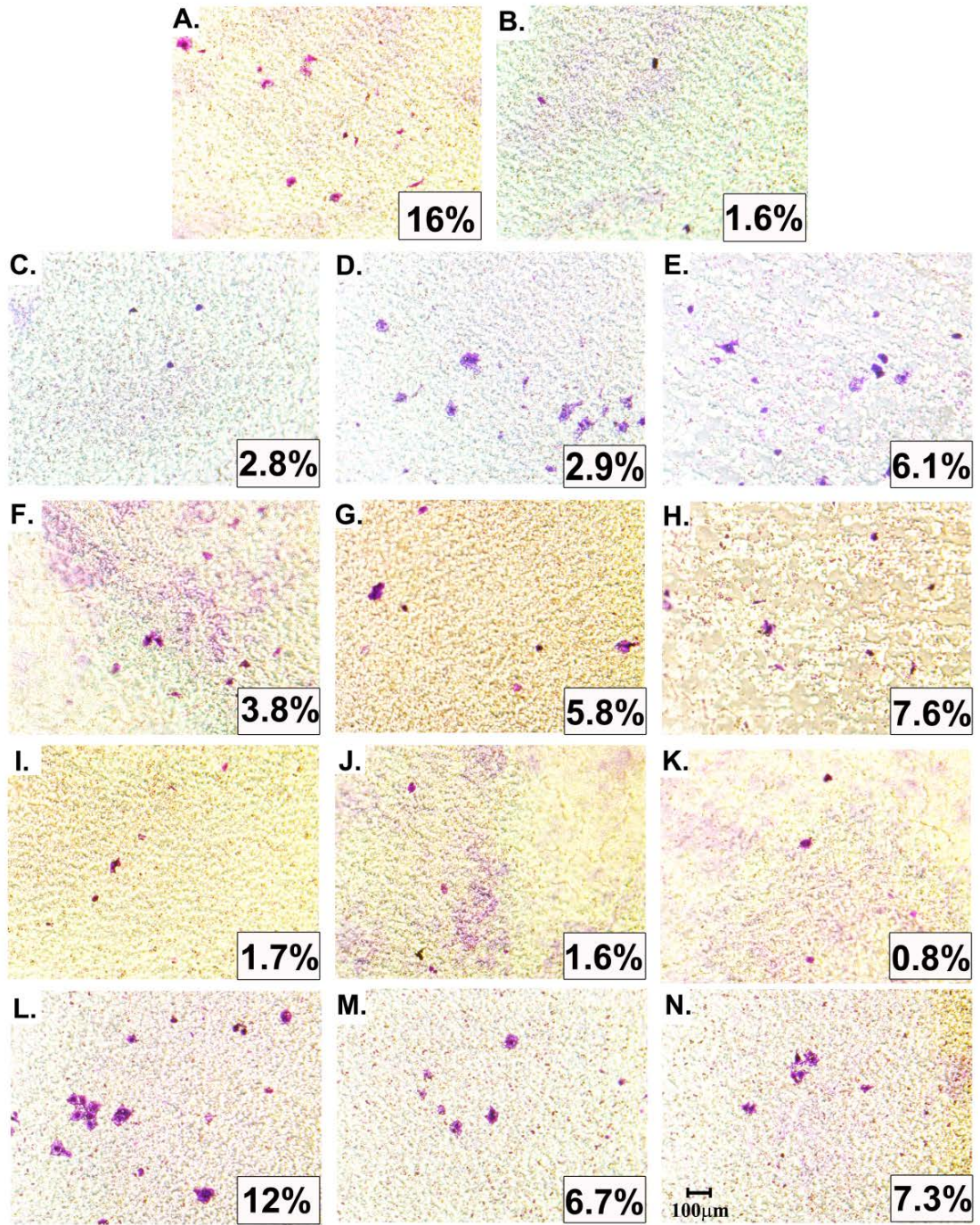


Figure IV-18. Relative cell invasion of Hs578T and UROtsa cells transformed by As⁺³ or Cd⁺² compared to the parent UROtsa cells. Black graph bars represent As⁺³-transformed cell lines, while white bars represents Cd⁺²-transformed cell lines. The red horizontal line at 1, indicates the invasion level of the UROtsa parent cells. *Denotes a statistically significant difference from the UROtsa parent cells (p < 0.05).

Figure IV-19. Invasion capability of UROtsa parent, non-transfected, SPARC-transfected, and blank vector (DEST) cell lines, with the Hs578T malignant breast cancer cell line as a positive control. Micrographs show the cells that invaded in: (A) Hs578T; (B) UROtsa parental; (C) As^{#3}; (D) As^{#3}-SPARC; (E) As^{#3}-DEST; (F) As^{#6}; (G) As^{#6}-SPARC; (H) As^{#6}-DEST; (I) Cd^{#1}; (J) Cd^{#1}-SPARC; (K) Cd^{#1}-DEST; (L) Cd^{#4}; (M) Cd^{#4}-SPARC; and (N) Cd^{#4}-DEST. The percentage of total cell that invaded is depicted in the bottom left corner of each micrograph and was determined by counting all cells in 20 fields at using a 40 x magnification lens, removing the cells from the top of the insert, and counting the remaining cells on the bottom of the insert in 20 fields at using a 40 x magnification lens. All images correspond to bar in N = 100 μ m.



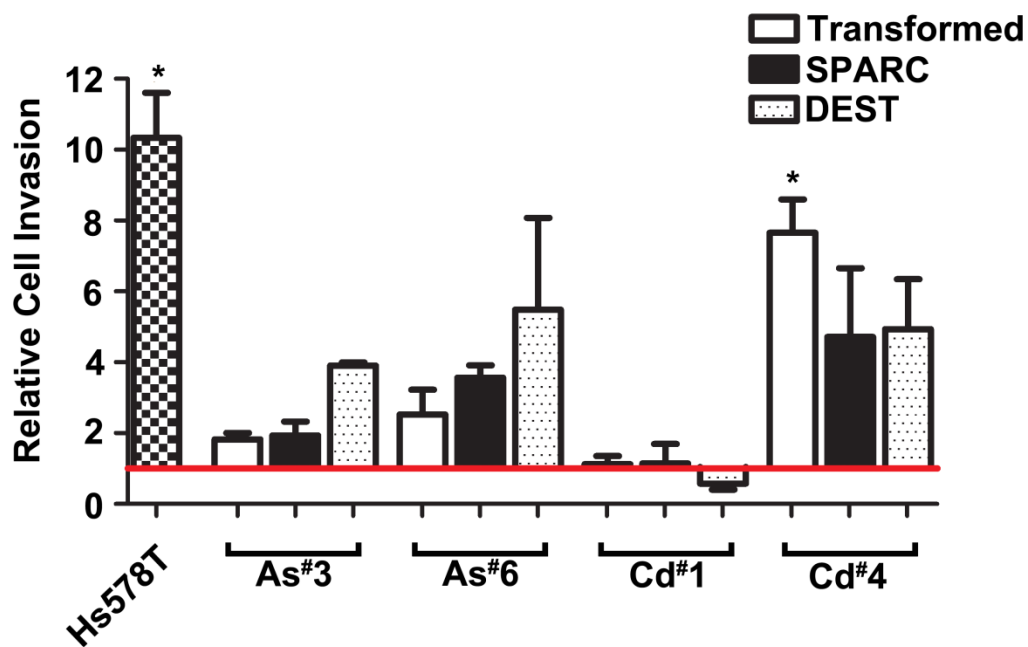


Figure IV-20. Relative cell invasion of Hs578T, non-transfected UROtsa, SPARC-transfected, and blank vector (DEST) cells lines compared to the parent UROtsa cells. White graph bars represent the As⁺³ and Cd⁺² transformed cell lines, the black graph bars represents SPARC transfected cell lines, while dotted bars represents blank vector transfected cell lines. Red horizontal line at 1, indicates the level of invasion of the UROtsa parent cells. *Denotes a statistically significant difference from the UROtsa parent cells (p < 0.05).

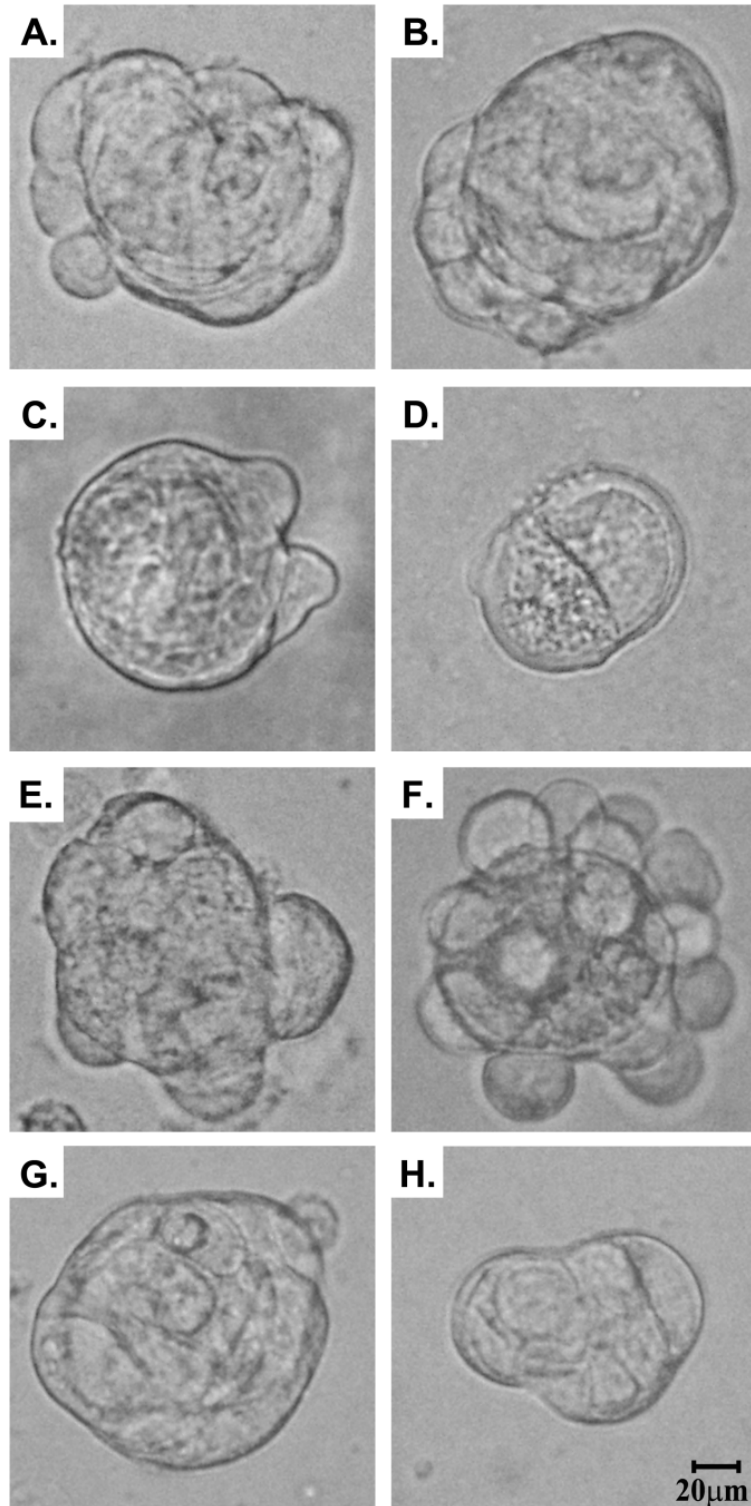


Figure IV-21. Soft agar morphology of SPARC-transfected and DEST-transfected UROtsa cell lines. (A) As[#]3-SPARC; (B) As[#]3-DEST; (C) As[#]6-SPARC; (D) As[#]6-DEST; (E) Cd[#]1-SPARC (F) Cd[#]1-DEST; (G) Cd[#]4-SPARC; and (H) Cd[#]4-DEST. All images correspond to bar in H = 20 μ m.

Figure IV-22. Expression of SPARC in mouse heterotransplants using different SPARC specific antibodies. Immunohistochemical analysis of SPARC protein using the mouse anti-human osteonectin primary antibody purchased from HTI in A, C, E, and G and the mouse anti-human osteonectin antibody purchased from Leica in B, D, F, H. The expression of SPARC was analyzed in Cd⁺² and As⁺³ tumor heterotransplants. Tumors were generated from the (A and B) As^{#1}, (C and D) As^{#3}, (E and F) Cd^{#1}, and (G and H) Cd^{#5} cell lines. The brown color indicates SPARC positive cells and the blue color is indicative of the counterstain necessary to visualize all cells in the tissue. All images are at a magnification of x 200. Bar = 100 μ m.

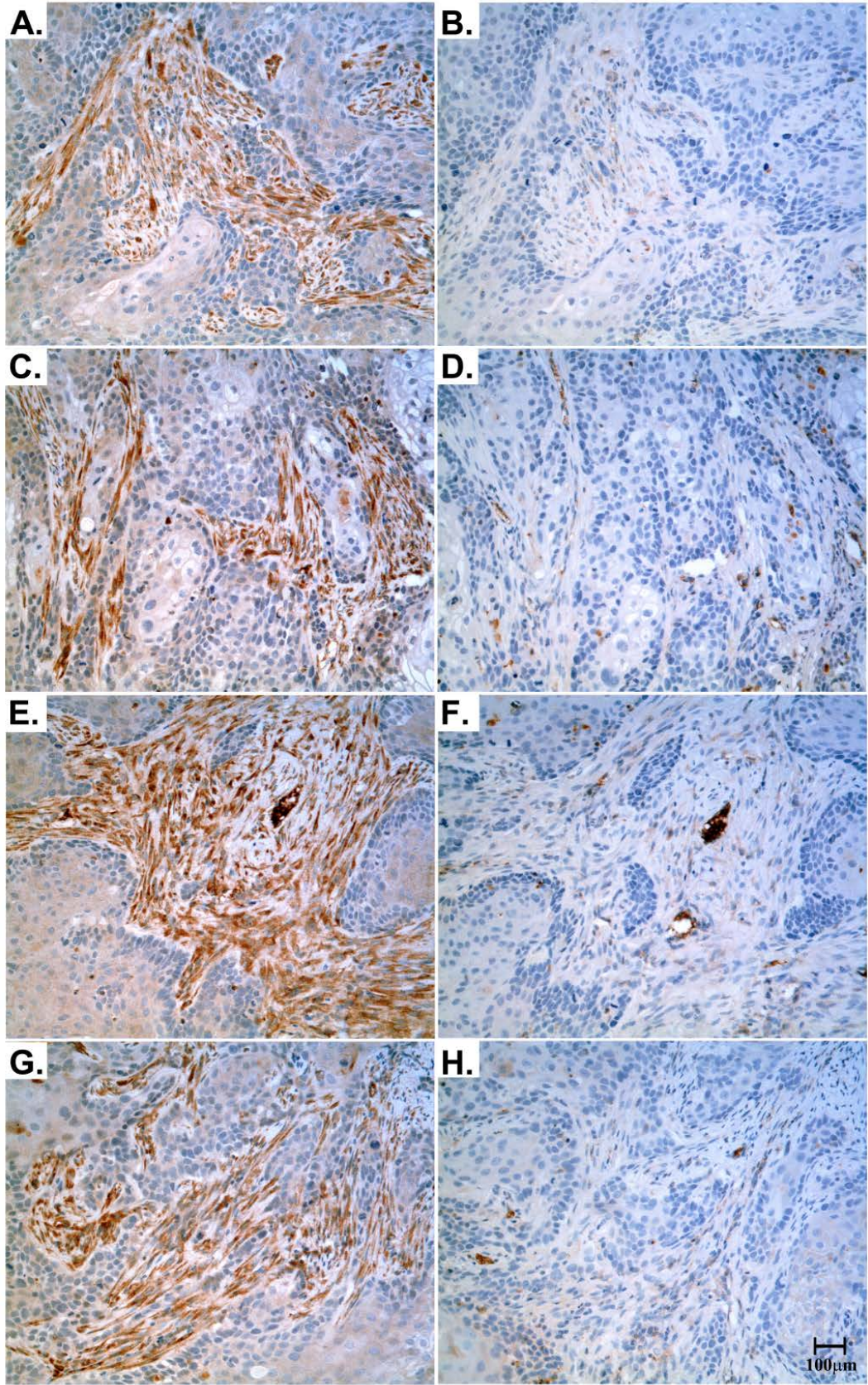
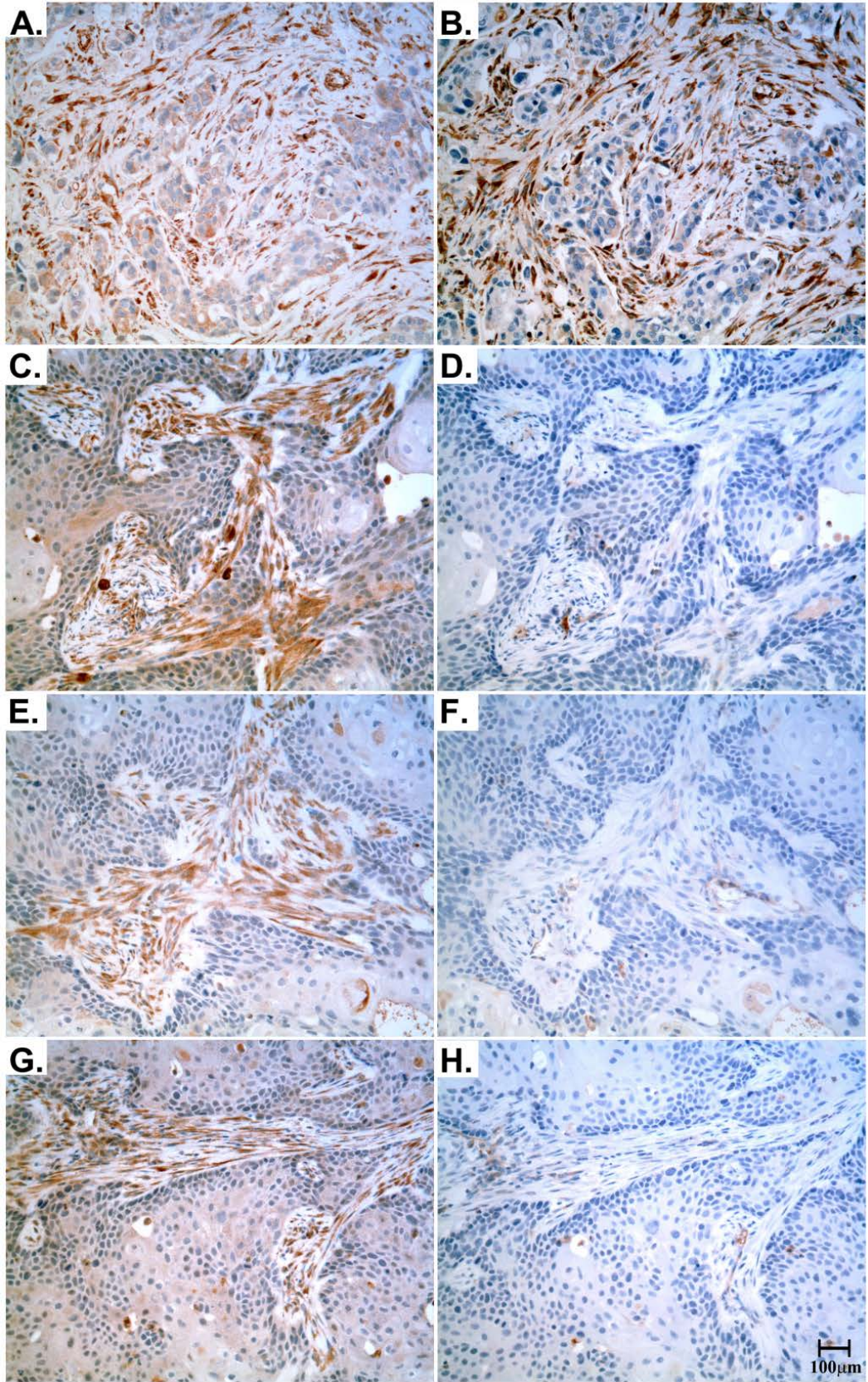


Figure IV-23. Expression of SPARC in archival human bladder cancer and mouse heterotransplants using 2 different SPARC specific antibodies. Immunohistochemical analysis of SPARC protein using the mouse anti-human osteonectin primary antibody purchased from HTI in A, C, E, and G and the mouse anti-human osteonectin antibody purchased from Leica in B, D, F, H. The expression of SPARC was analyzed in (A and B) high grade invasive carcinoma of the bladder and in mouse heterotransplants generated from the (C and D) UROtsa non-transfected cell line, (E and F) Cd[#]1-SPARC transfected cell line, and (G and H) Cd[#]1-DEST transfected cell line. The brown color indicates SPARC positive cells while the blue color is indicative of the counterstain necessary to visualize all cells in the tissue. All images are at a magnification of x 200. Bar = 100 μ m.



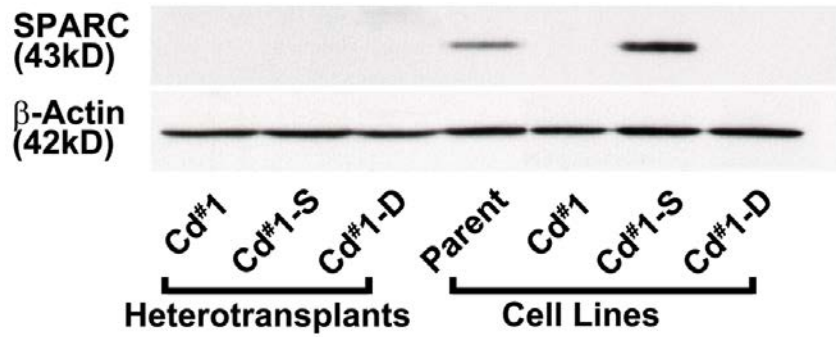


Figure IV-24. Expression of human SPARC protein in mouse heterotransplants and corresponding cell lines. Western analysis of SPARC protein expression, using the Leica mouse anti-human SPARC antibody in the UROtsa parent, Cd[#]1, Cd[#]1-SPARC (Cd[#]1-S), and Cd[#]1-DEST (Cd[#]1-D) cell lines as well as the resulting tumors from the transfected and non-transfected Cd[#]1 cell lines (top panel) and with β-actin shown as a loading control in the bottom panel.

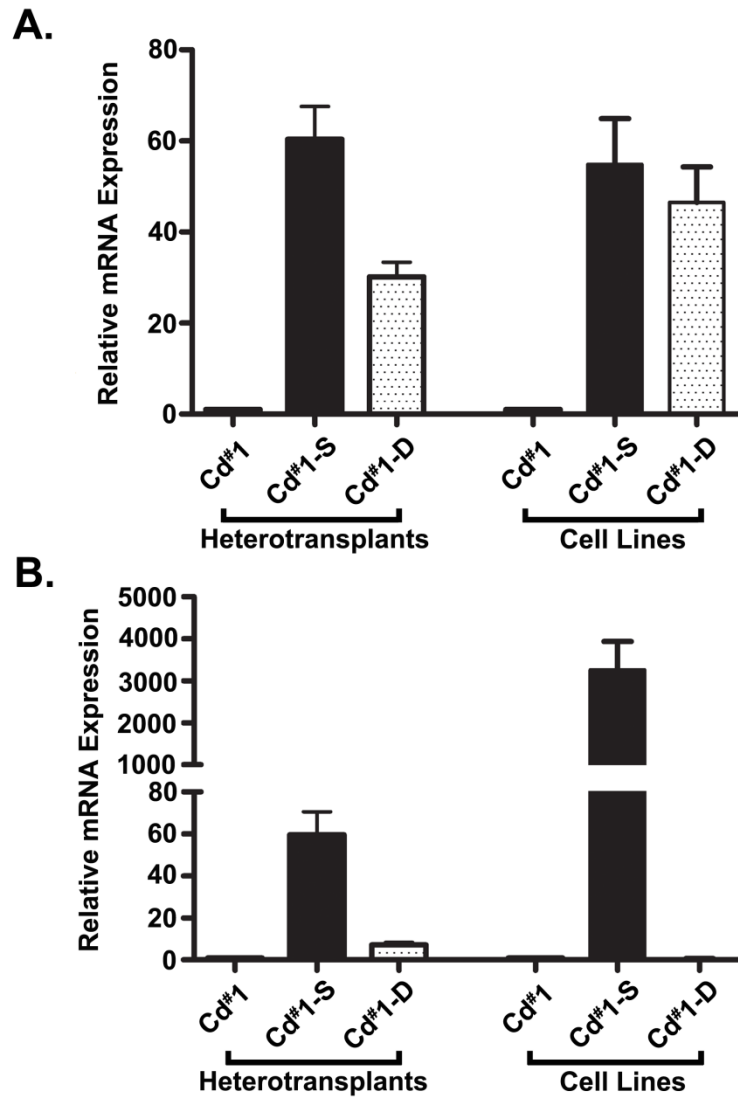


Figure IV-25. Expression of BSD and human SPARC mRNA in mouse heterotransplants and corresponding cell lines. Real time RT-PCR analysis of the UROtsa Cd[#]1, Cd[#]1-SPARC (Cd[#]1-S), and Cd[#]1-DEST (Cd[#]1-D) cell lines as well as the resulting tumors from these cell lines with regard to (A) BSD expression and (B) SPARC expression using human SPARC specific primers. mRNA levels were normalized to the fold change in β -actin expression. Real time data is plotted as the mean \pm SEM of triplicate determinations.

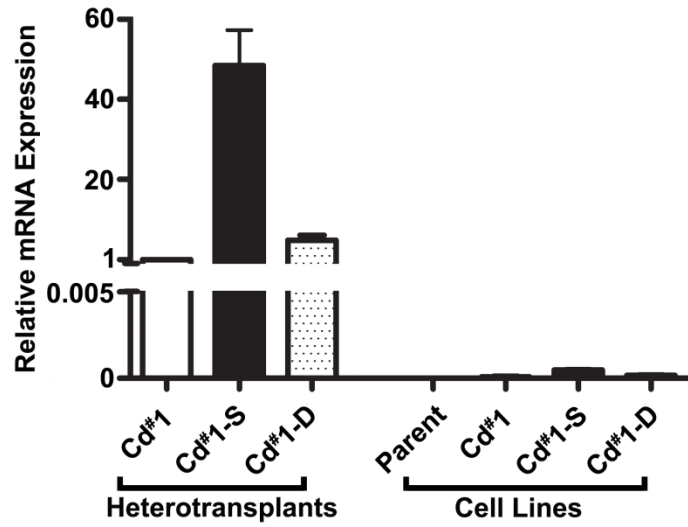


Figure IV-26. Expression of mouse SPARC mRNA in mouse heterotransplants and corresponding cell lines. (A) Real time-RT-PCR analysis of SPARC expression was analyzed in the UROtsa Parent, Cd[#]1, Cd[#]1-SPARC (Cd[#]1-S), and Cd[#]1-DEST (Cd[#]1-D) cell lines as well as the resulting tumors from the transfected and non-transfected Cd[#]1 cell lines. mRNA levels were normalized to the fold change in β -actin expression. Real time data is plotted as the mean \pm SEM of triplicate determinations.

CHAPTER V

DISCUSSION

Previously the UROtsa cell model's mechanisms of cell death after exposure to toxic levels of Cd^{+2} and As^{+3} were determined (Somji et al., 2006). However, it was unknown if autophagy may also be acting separately or in concert with the necrosis or apoptosis mechanisms. In most cells, autophagy is suppressed to a low basal level, but under stressful conditions autophagic activity may increase. The urothelium, which covers the luminal surface of the urinary bladder, serves to protect the bladder and is resilient to many stress factors, as the bladder can be exposed to toxic substances which accumulate and concentrate in the urine. Even though the urothelium is exposed to many stressors, the cells of the normal urothelium have a relatively long lifespan with very little cell turnover. The adaptability of the UROtsa bladder cells was questioned to determine if autophagy may play a role in the urothelium's capability to withstand cellular stressors.

The present study, outlined in chapter II, was initiated after an analysis by Chai and colleagues (2007) showed that beclin-1, an autophagosome marker that when over-expressed promotes autophagy, was induced in arsenic treated SV-HUC-1 normal human bladder cells. Increasing concentrations of As^{+3} led to an increase in the expression of beclin-1 protein. In this study, the UROtsa cell model was used to examine beclin-1 expression as well as several other autophagy related genes, which are downstream effectors involved in the autophagosome formation. The expression of beclin-1 in the UROtsa cell lines, in both the non-tumorigenic parental cells as well as in the Cd^{+2} and

As⁺³-transformed cells, showed detection of beclin-1 expression in all the cell lines. However, only modest alterations in the mRNA and protein expression levels of beclin-1 were seen between the parental UROtsa cells and their malignantly transformed counterparts as well as between and among the transformed cell lines. Although some alterations did reach significance, it is believed that with repetition of the experiments at several independent times, the small magnitude of differences in the expression of beclin-1 would no longer remain significant. This was not carried out due to the expense of such repeats being too great and the knowledge of previous work which has shown that repeated experiments of cell culture negate small changes first observed. The expression of several autophagy associated genes, Atg-5, Atg-7, Atg-12, and LC3B, were also analyzed. These genes are downstream effectors in the autophagy pathway that are up-regulated for the induction of autophagosome formation. The expression of these genes showed similar results to that of beclin-1. Only modest changes in the expression patterns of the autophagy associated genes were seen between the UROtsa parent and the Cd⁺² and As⁺³-transformed cells as well as within and between the transformed cell lines. The results from the basal expression of several autophagy genes in the UROtsa parental and the malignantly transformed cell lines suggests that autophagy may be occurring at a low rate within these cell lines, but large alteration in mRNA or protein expression does not occur in UROtsa cells malignantly transformed by Cd⁺² or As⁺³ or UROtsa parent cells.

Since previous studies have shown arsenic treatment influences autophagy within normal bladder cells (Chai et al., 2007) as well as malignant cells, as seen in leukemic (Qian et al., 2007) and malignant glioma cells (Kanzawa et al., 2003), this was extended

into the present study. The UROtsa parental cells and its transformed counterparts were exposed to both Cd⁺² and As⁺³ and the expression of beclin-1 and the associated autophagy genes were analyzed. Again, only modest changes were seen in the mRNA and protein expression of beclin-1 and the autophagy associated genes after Cd⁺² or As⁺³ treatment, this evidence further suggests that autophagy is only playing a minor role in the UROtsa cell model for heavy metal induced bladder carcinogenesis. Therefore it is concluded that autophagy does not have a major role in assisting or determining which cells will undergo apoptosis or necrosis in the UROtsa cell model.

Of considerable interest, the expression of beclin-1 protein appeared to change as a result of being fed fresh growth media. With the addition of fresh growth media, the expression of beclin-1 was relatively low, but an increase in its expression was detected after the growth medium had potentially depleted its nutrients. The expression of beclin-1 was then reduced once again after the cells were fed and nutrients were replenished. Since this study was performed on confluent monolayers, the nutrient depletion may have occurred at a faster rate than if the cultures were subconfluent. This finding suggests autophagy in the UROtsa cell line model may be up-regulated and down-regulated based of the availability of nutrients.

Normal human bladder tissue was also analyzed for beclin-1 expression and the gene was found to be moderately expressed within the urothelium. The highest expression of beclin-1 was seen in the apical most cells or the umbrella cells of the urothelium, with a reduction in the staining intensity seen in the intermediate and even less staining in the basal cells. This observation may suggest that autophagy is more involved in the apical plasma membrane turnover in the superficial urothelial cells than in

cells of the intermediate or basal layers. The stroma of the bladder had little to no expression of beclin-1, but occasional inflammatory cells were positive for beclin-1 staining. The staining of inflammatory cells for beclin-1 has been previously reported (Liang et al., 1999). The expression of beclin-1 in cancerous bladder tissues remains to be determined. However in a recent study, mouse urinary bladder urothelium was used to determine beclin-1 expression in response to starvation. Beclin-1 expression was primarily negative in the adult mouse urothelium, but after a 24 h starvation period the urothelium was strongly reactive for beclin-1 in all layers of the urothelium, basal, intermediate, and apical (Erman et al., 2012).

The expression of beclin-1 in other tissues including normal and cancerous tissues, is unclear. Several studies have showed beclin-1 expression to be up regulated in normal tissues compared to cancerous tissue. Normal esophageal tissue showed positive staining in the squamous epithelial cells, while an absence of staining is found in esophageal squamous cell carcinoma (Chen et al., 2009). Similarly, normal breast epithelial cells were strongly immunoreactive for beclin-1 with staining also seen in some inflammatory cells within the stroma. While a significant decrease in beclin-1 expression was seen in breast carcinoma cells (Liang et al., 1999), normal cervical tissue also had relatively high expression of beclin-1 protein when compared to cancerous cervical tissue (Wang et al., 2007b). These studies suggest beclin-1 to be a tumor suppressor due to a loss of beclin-1 protein expression in cancerous tissues.

Conversely, multiple lines of evidence indicate beclin-1 may contribute to the survival of tumors. Increased beclin-1 expression was associated with cancerous tissue as seen in colorectal and gastric cancer cells, where normal colon and stomach tissues

stain only weakly for beclin-1 expression (Ahn et al., 2007; Li et al., 2008). Human non-small cell lung cancer also showed increased expression for beclin-1 as compared to normal lung tissue (Kim et al., 2011b). In normal pancreatic tissue, beclin-1 was not detected in the cytoplasm of pancreatic islet cells, acinar cells, or ductal epithelial cells. However, in pancreatic ductal adenocarcinoma tissue, 22.2% of cases showed positive beclin-1 expression (Kim et al., 2011a). From the studies indicating increased beclin-1 expression in cancerous tissue, it is believed that beclin-1 enhances tumor development and protects tumor cells from stimuli that result in cell death leading to the progression of the tumor. The notion that beclin-1 can be a tumor suppressor and a tumor promoter leads these divergent results to suggest that the function of beclin-1 expression is tissue-specific.

Although the present study did not detect large alterations in the expression of beclin-1 and associated autophagy genes in Cd⁺² or As⁺³ exposed and transformed urothelial cells, the involvement of autophagy in cell death and survival cannot be ruled out. The apparent change in expression of beclin-1 as a function of being fed fresh growth medium complicates the interpretation of the presented data. The possibility that beclin-1 expression can vary with nutritional status renders interpreting differences in expression between normal and tumorigenic UROtsa cell lines difficult. Also further extension of this study for translational research may also prove challenging, since the nutritional status of the tissue may interfere with interpretation of results between normal and cancerous tissue. This study did further the characterization of the UROtsa cell lines and its malignantly transformed counterparts by extending the study of possible routes of cell death. Previous characterization of the UROtsa cell lines determined the parental and

malignantly transformed cells to die through apoptosis and necrosis, respectively, after exposure to toxic levels of Cd^{+2} or As^{+3} . Even though autophagy levels were low within these cell lines after acute treatment with Cd^{+2} or As^{+3} , basal expression levels of autophagy were detected and may be further activated when nutrient availability is low.

The remaining studies, outlined in chapters III and IV, were motivated by a microarray analysis which identified that SPARC gene expression had a strong differential expression pattern between normal human bladder cells and malignantly transformed human bladder cells. The UROtsa parental and the Cd^{+2} and As^{+3} -transformed human urothelial cell lines indicated a significant down-regulation of SPARC expression within the Cd^{+2} and As^{+3} -transformed cell lines compared to the parental cell line. SPARC is a matricellular protein that is expressed intracellularly and secreted into the ECM. It functions in part to regulate levels of cellular adhesion and migration as well as regulate cell proliferation, survival, and angiogenesis (Bornstein and Sage, 2002; Brekken and Sage, 2001; Tai and Tang, 2008). These functions are important for normal development and for physiological processes such as tissue remodeling during wound healing (Bornstein and Sage, 2002; Brekken and Sage, 2001). SPARC mediates interactions between cells and components of the ECM by influencing growth factor-induced signaling cascades. Therefore, the function of SPARC is affected by the ECM present in the microenvironment, growth factors, and the availability of the growth factor's receptor (Yan and Sage, 1999). As a result, the role SPARC plays may differ between tissues and even within cell types, depending on the microenvironment.

The role SPARC plays in cancer is unclear and somewhat controversial. The ability of SPARC to modulate its surrounding matrix has led it to have a positive

correlation with invasion or a poor prognosis in some cancers, but conversely, it also has a negative correlation with invasion and its expression leads to a better prognosis in other cancers (Bos et al., 2004). Also a difference in prognosis may be attributed to the difference in expression patterns of SPARC in tumor cells versus stromal cells. Most studies report on one or the other but few comprehensively examine both. As previously reported, an absence of SPARC expression is associated with malignant urothelial tumor cells, but surrounding stromal cells were SPARC positive in the UROtsa cell model of Cd⁺²- and As⁺³ tumorigenesis (Larson et al., 2010). Similar expression of SPARC is also seen in ovarian cancer, prostate cancer, and pancreatic cancer (Sato et al., 2003; Socha et al., 2009; Thomas et al., 2000). Other cancers have a different presentation for the expression of SPARC. Melanomas and renal cell carcinomas show a high level of SPARC expression in the malignant epithelial cells comprising the tumor (Ledda et al., 1997a; Rempel et al., 1998; Sakai et al., 2001).

Within the UROtsa cell model, SPARC message and protein expression was detected within the UROtsa parental cells, with SPARC protein localized to distinct vesicles in the cytoplasm of the cell. Both the Cd⁺²- and As⁺³-transformed UROtsa cell lines showed that SPARC message was reduced to the limit of detection and an absence of SPARC protein was seen by western blot and immunofluorescence analysis. The lack of SPARC expression in malignant urothelial cells translated not only to the tumors generated by the injection of the transformed UROtsa cells into immune-compromised mice, but it also translated to human bladder cancer specimens. The tumors from these applications showed an absence of SPARC expression; however, the stroma surrounding the tumor was highly reactive for SPARC expression. It is believed that the connective

tissue was recruited to the tumor site by secretions from the tumor cells. Although previous studies have determined SPARC is expressed in normal urothelium and urothelial cell cultures (Alpers et al., 2002; Bassuk et al., 2000; Delostrinos et al., 2006; Hudson et al., 2005), the present study confirmed these findings and was the first to determine the expression of SPARC in human bladder cancer. The translation of SPARC expression from bladder cells in culture, to mouse tumors generated from malignant bladder cells, and also to human urothelial cancer suggests that SPARC is a unique and powerful model for studying biomarkers in urothelial cancer.

Several studies have suggested the alterations in SPARC expression between normal and cancerous tissues are a result of DNA methylation. The low level of SPARC expression in several cancers, including endometrial, colorectal, and leukemia were shown to be a result of SPARC promoter hypermethylation (Nagaraju and Sharma, 2011). Other studies have shown that changes in methylation levels of the SPARC promoter can lead to SPARC silencing. This was seen in lung, colorectal, and pancreatic cancer cell lines, which all have a low level of SPARC expression, but after treatment with 5-Aza-2'-deoxycytidine (5-AZC), a demethylating agent, the expression of SPARC increased (Cheetham et al., 2008; Sato et al., 2003; Suzuki et al., 2005). These studies powered the analysis of determining if UROtsa cells transformed by Cd⁺² or As⁺³ had a similar mechanism that regulated the expression of SPARC. However treatment with 5-AZC and MS-275, a histone deacetylase inhibitor, either separately or in conjunction with each other did not induce SPARC message. However, a striking finding from this study was the down-regulation of SPARC mRNA and protein within the normal UROtsa parent cell line after acute treatment to both Cd⁺² and As⁺³ in a concentration and time-

dependent manner. Further examination of this finding revealed that during the process of transforming the UROtsa cells with Cd^{+2} or As^{+3} , the expression of SPARC gradually decreased with increasing time. The transformation of the UROtsa cells took several months, but the resulting fully transformed UROtsa cell lines showed that the expression of SPARC was at the limit of detection and was incapable of being induced through demethylating or acetylating agents. This study suggests that Cd^{+2} and As^{+3} , down-regulate the expression of SPARC during the development and progression of bladder cancer. Since Cd^{+2} and As^{+3} activate different metabolic pathways within the cell, it is unique that both of these heavy metals have the ability to down-regulate the expression of SPARC within the transformed UROtsa cells and within the parental cells after acute treatment.

To further the understanding of SPARC expression in human UROtsa cells and their malignantly transformed counterpart, SPARC was stably transfected into select Cd^{+2} and As^{3+} transformed UROtsa cell lines. The resulting transfected cell lines were characterized for SPARC expression, cellular migration, invasion, and tumorigenicity. Most of the SPARC-transfected cell lines had a similar expression pattern of SPARC mRNA and protein as the UROtsa parent, one SPARC-transfected cell line was reduced and another induced compared to the parental cell line. The intracellular localization of SPARC was also very similar among all the SPARC transfected cell lines and was very similar to parental cell line.

The generation of SPARC transfected cells has been the focus of several studies. The over-expression of SPARC in glioma cells induced brain tumor migration and invasion *in vitro* and *in vivo* (Golembieski et al., 2008), subsequently down-regulation of

SPARC in glioma cells by siRNA led to a decrease in cell migration (Seno et al., 2009) and invasion (Shi et al., 2007) *in vitro*. However, an embryonic kidney cell line transfected with SPARC significantly impaired tumor growth *in vivo* compared to controls (Chlenski et al., 2006). The resulting disparities in cellular migration and invasion with the forced expression of SPARC, led to further characterization of the Cd⁺² and As³⁺ transformed UROtsa cell lines transfected with SPARC by analyzing their chemotaxis, wound healing, and invasion capabilities. The results from these assays were not expected, as the forced expression of SPARC did not seem to induce large alterations in the migration or invasion rates within the transformed UROtsa cell lines. However, upon analysis of human bladder cancers it has been shown that cancerous bladder cells generally do not invade through connective tissue and enter blood vessels, but rather invade through the muscle layers of the bladder. Bladder cancer is also known to metastasize locally, generally seeding on the stroma of organs near the bladder. Therefore the determination that forced SPARC expression in the UROtsa cells did not greatly alter the migration and invasion rates may be due to the lack of the invasive nature of UROtsa cells.

In vivo examination of SPARC-transfected cells to form subcutaneous tumors in nude mice, revealed no differences in tumor formation between SPARC-transfected cells and non-transfected control cells regarding the ability to form tumors, time needed to form the tumor, and the size of the tumor. However, upon histological examination of the resulting tumors, those from SPARC-transfected cells completely lacked SPARC protein expression within the epithelial component of the tumor, but were positive for the transfection vector. Further analysis showed the SPARC-transfected tumors had greatly

reduced SPARC message when compared to the SPARC-transfected cell lines. This study suggests that the down-regulation of human specific SPARC mRNA and a lack of human specific SPARC protein in the mouse heterotransplants generated from UROtsa cells transfected with SPRAC, is due to post-transcriptional regulation of SPARC expression in urothelial carcinoma cells within the mouse environment.

Emerging within the literature has been the identification of several microRNAs (miRNAs) that can regulate SPARC expression (Kapinas et al., 2009). Characterized as a class of small, non-coding RNAs that modulate the translation or stability of a target mRNA, miRNAs have been shown to play an increasingly significant role in tumorigenesis (Bartel, 2004; Bartel, 2009). Efficient repression of a target mRNA is either achieved by interfering with translation or by guiding processes for mRNA degradation that are initiated by deadenylation and decapping of the mRNA (Brodersen and Voinnet, 2009). Although many miRNA targets have been reported, the majority of mRNAs regulated by miRNAs remain unknown. Within studies on SPARC RNA interference, the miRNA-29 family of miRNAs, consisting of miRNA-29a, -29b, and -29c have been examined as potential regulators of SPARC expression in a variety of cell models. These studies have also only focused on the 3' untranslated region (UTR) of SPARC as a binding site for the miRNA-29 family. Although it was previously believed that miRNAs only target the 3' or 5' UTR of a mRNA target, current evidence is emerging that miRNA also target the coding regions of genes (Forman et al., 2008).

Since only the open reading frame (ORF) of SPARC was transfected into the UROtsa cells transformed by Cd⁺² or As⁺³, only the coding region can be analyzed for possible miRNA regulation. A sequence analysis suggests that the SPARC ORF has the

ability to bind several miRNAs, including miRNA-29a, -29b, and -29c, miRNA-147, and miRNA-203. Future studies will be conducted to further elucidate the exact miRNA or several miRNAs that are responsible for the down-regulation of SPARC mRNA and degradation of SPARC protein within mouse tumors generated by the transfection of SPARC into Cd⁺² or As⁺³ transformed UROtsa cells. These studies will greatly enhance our understanding of bladder tumorigenesis as well as the functions of the SPARC protein. SPARC expression is unique because it was independently shutdown in all 13 transformed UROtsa cell lines. No other gene has yet been shown to have such a dramatic regulation in the UROtsa system. When SPARC was forced to be expressed, the tumor microenvironment results in the expression of SPARC to again be down-regulated to low levels. This suggests that SPARC is most likely playing a critical role in bladder tumorigenesis.

In order for the injected Cd^{#1}-SPARC cells to form tumors within the environment of the immunocompromised mice, the expression of SPARC may have been needed to be repressed. It is known that all 13 of the Cd⁺² and As⁺³ transformed UROtsa cell lines have low to undetectable levels of SPARC expression and are all capable of forming subcutaneous tumors when injected to immunocompromised mice. The resulting malignant epithelial component of the tumors generated from the Cd⁺² and As⁺³ transformed cell lines was also negative for the expression of SPARC. In contrast, the parental UROtsa cells have a relatively high expression of SPARC compared to the transformed cell lines and are incapable of forming subcutaneous tumors within nude mice. Therefore, drastic down-regulation of SPARC mRNA and complete absence of detectable SPARC protein within the Cd^{#1}-SPARC tumor heterotransplant may have

been required for the formation of the tumor. Preliminary results from mice sacrificed at 6 weeks showed that the resulting tumors from the Cd[#]1-SPARC cells were smaller in volume when compared to controls. The smaller tumor size may be a result of the extra time needed to down-regulate SPARC expression within the injected cells before the tumor could grow; therefore, the tumors that resulted from the Cd[#]1-SPARC cells formed more slowly than tumors formed by controls, which did not have to down-regulate SPARC expression prior to tumor formation. The expression of SPARC within the human bladder appears to be required for a normal phenotype while the down-regulation of SPARC expression is associated with a malignant phenotype.

REFERENCES

- Ahn, C.H., Jeong, E.G., Lee, J.W., Kim, M.S., Kim, S.H., Kim, S.S., Yoo, N.J., Lee, S.H., 2007. Expression of beclin-1, an autophagy-related protein, in gastric and colorectal cancers, *APMIS* 115, 1344-1349.
- Aita, V.M., Liang, X.H., Murty, V.V., Pincus, D.L., Yu, W., Cayanis, E., Kalachikov, S., Gilliam, T.C., Levine, B., 1999. Cloning and genomic organization of beclin 1, a candidate tumor suppressor gene on chromosome 17q21, *Genomics* 59, 59-65.
- Ajjimaporn, A., Botsford, T., Garrett, S.H., Sens, M.A., Zhou, X.D., Dunlevy, J.R., Sens, D.A., Somji, S., 2012. ZIP8 expression in human proximal tubule cells, human urothelial cells transformed by Cd+2 and As+3 and in specimens of normal human urothelium and urothelial cancer, *Cancer. Cell. Int.* 12, 16.
- Alpers, C.E., Hudkins, K.L., Segerer, S., Sage, E.H., Pichler, R., Couser, W.G., Johnson, R.J., Bassuk, J.A., 2002. Localization of SPARC in developing, mature, and chronically injured human allograft kidneys, *Kidney Int.* 62, 2073-2086.
- Ankarcrona, M., Dypbukt, J.M., Bonfoco, E., Zhivotovsky, B., Orrenius, S., Lipton, S.A., Nicotera, P., 1995. Glutamate-induced neuronal death: a succession of necrosis or apoptosis depending on mitochondrial function, *Neuron* 15, 961-973.
- Arnold, S., Mira, E., Muneer, S., Korpanty, G., Beck, A.W., Holloway, S.E., Manes, S., Brekken, R.A., 2008. Forced expression of MMP9 rescues the loss of angiogenesis and abrogates metastasis of pancreatic tumors triggered by the absence of host SPARC, *Exp. Biol. Med. (Maywood)* 233, 860-873.
- ATSDR, 1999. Toxicological Profile for Cadmium, Agency for Toxic Substances and Disease Registry, 434.
- Bartel, D.P., 2009. MicroRNAs: target recognition and regulatory functions, *Cell* 136, 215-233.
- Bartel, D.P., 2004. MicroRNAs: genomics, biogenesis, mechanism, and function, *Cell* 116, 281-297.
- Bassuk, J.A., Grady, R., Mitchell, M., 2000. Review article: The molecular era of bladder research. Transgenic mice as experimental tools in the study of outlet obstruction, *J. Urol.* 164, 170-179.

- Bellahcene, A., Castronovo, V., 1995. Increased expression of osteonectin and osteopontin, two bone matrix proteins, in human breast cancer, *Am. J. Pathol.* 146, 95-100.
- Berry, D.L., Baehrecke, E.H., 2007. Growth arrest and autophagy are required for salivary gland cell degradation in *Drosophila*, *Cell* 131, 1137-1148.
- Bornstein, P., 1995. Diversity of function is inherent in matricellular proteins: an appraisal of thrombospondin 1, *J. Cell Biol.* 130, 503-506.
- Bornstein, P., Sage, E.H., 2002. Matricellular proteins: extracellular modulators of cell function, *Curr. Opin. Cell Biol.* 14, 608-616.
- Bos, T.J., Cohn, S.L., Kleinman, H.K., Murphy-Ulrich, J.E., Podhajcer, O.L., Rempel, S.A., Rich, J.N., Rutka, J.T., Sage, E.H., Thompson, E.W., 2004. International Hermelin brain tumor symposium on matricellular proteins in normal and cancer cell-matrix interactions, *Matrix Biol.* 23, 63-69.
- Boya, P., Gonzalez-Polo, R.A., Casares, N., Perfettini, J.L., Dessen, P., Larochette, N., Metivier, D., Meley, D., Souquere, S., Yoshimori, T., Pierron, G., Codogno, P., Kroemer, G., 2005. Inhibition of macroautophagy triggers apoptosis, *Mol. Cell Biol.* 25, 1025-1040.
- Bradshaw, A.D., Graves, D.C., Motamed, K., Sage, E.H., 2003a. SPARC-null mice exhibit increased adiposity without significant differences in overall body weight, *Proc. Natl. Acad. Sci. U. S. A.* 100, 6045-6050.
- Bradshaw, A.D., Puolakkainen, P., Dasgupta, J., Davidson, J.M., Wight, T.N., Helene Sage, E., 2003b. SPARC-null mice display abnormalities in the dermis characterized by decreased collagen fibril diameter and reduced tensile strength, *J. Invest. Dermatol.* 120, 949-955.
- Bradshaw, A.D., Francki, A., Motamed, K., Howe, C., Sage, E.H., 1999. Primary mesenchymal cells isolated from SPARC-null mice exhibit altered morphology and rates of proliferation, *Mol. Biol. Cell* 10, 1569-1579.
- Bredfeldt, T.G., Jagadish, B., Eblin, K.E., Mash, E.A., Gandolfi, A.J., 2006. Monomethylarsonous acid induces transformation of human bladder cells, *Toxicol. Appl. Pharmacol.* 216, 69-79.
- Bredfeldt, T.G., Kopplin, M.J., Gandolfi, A.J., 2004. Effects of arsenite on UROtsa cells: low-level arsenite causes accumulation of ubiquitinated proteins that is enhanced by reduction in cellular glutathione levels, *Toxicol. Appl. Pharmacol.* 198, 412-418.

- Brekken, R.A., Puolakkainen, P., Graves, D.C., Workman, G., Lubkin, S.R., Sage, E.H., 2003. Enhanced growth of tumors in SPARC null mice is associated with changes in the ECM, *J. Clin. Invest.* 111, 487-495.
- Brekken, R.A., Sage, E.H., 2001. SPARC, a matricellular protein: at the crossroads of cell-matrix communication, *Matrix Biol.* 19, 816-827.
- Brodersen, P., Voinnet, O., 2009. Revisiting the principles of microRNA target recognition and mode of action, *Nat. Rev. Mol. Cell Biol.* 10, 141-148.
- Bursch, W., 2001. The autophagosomal-lysosomal compartment in programmed cell death, *Cell Death Differ.* 8, 569-581.
- Cao, L., Zhou, X.D., Sens, M.A., Garrett, S.H., Zheng, Y., Dunlevy, J.R., Sens, D.A., Somji, S., 2010. Keratin 6 expression correlates to areas of squamous differentiation in multiple independent isolates of As(+3)-induced bladder cancer, *J. Appl. Toxicol.* 30, 416-430.
- Carter, D.E., Aposhian, H.V., Gandolfi, A.J., 2003. The metabolism of inorganic arsenic oxides, gallium arsenide, and arsine: a toxicochemical review, *Toxicol. Appl. Pharmacol.* 193, 309-334.
- Castillo-Martin, M., Domingo-Domenech, J., Karni-Schmidt, O., Matos, T., Cordon-Cardo, C., 2010. Molecular pathways of urothelial development and bladder tumorigenesis, *Urol. Oncol.* 28, 401-408.
- Chai, C.Y., Huang, Y.C., Hung, W.C., Kang, W.Y., Chen, W.T., 2007. Arsenic salts induced autophagic cell death and hypermethylation of DAPK promoter in SV-40 immortalized human uroepithelial cells, *Toxicol. Lett.* 173, 48-56.
- Chakraborti, D., Rahman, M.M., Paul, K., Chowdhury, U.K., Sengupta, M.K., Lodh, D., Chanda, C.R., Saha, K.C., Mukherjee, S.C., 2002. Arsenic calamity in the Indian subcontinent What lessons have been learned? *Talanta* 58, 3-22.
- Chandrasekhar, S., Harvey, A.K., Johnson, M.G., Becker, G.W., 1994. Osteonectin/SPARC is a product of articular chondrocytes/cartilage and is regulated by cytokines and growth factors, *Biochim. Biophys. Acta* 1221, 7-14.
- Cheetham, S., Tang, M.J., Mesak, F., Kennecke, H., Owen, D., Tai, I.T., 2008. SPARC promoter hypermethylation in colorectal cancers can be reversed by 5-Aza-2'deoxyctidine to increase SPARC expression and improve therapy response, *Br. J. Cancer* 98, 1810-1819.

- Chen, Y., Lu, Y., Lu, C., Zhang, L., 2009. Beclin-1 expression is a predictor of clinical outcome in patients with esophageal squamous cell carcinoma and correlated to hypoxia-inducible factor (HIF)-1alpha expression, *Pathol. Oncol. Res.* 15, 487-493.
- Chiou, H.Y., Hsueh, Y.M., Liaw, K.F., Horng, S.F., Chiang, M.H., Pu, Y.S., Lin, J.S., Huang, C.H., Chen, C.J., 1995. Incidence of internal cancers and ingested inorganic arsenic: a seven-year follow-up study in Taiwan, *Cancer Res.* 55, 1296-1300.
- Chlenski, A., Liu, S., Guerrero, L.J., Yang, Q., Tian, Y., Salwen, H.R., Zage, P., Cohn, S.L., 2006. SPARC expression is associated with impaired tumor growth, inhibited angiogenesis and changes in the extracellular matrix, *Int. J. Cancer* 118, 310-316.
- Chu, F., Ren, X., Chasse, A., Hickman, T., Zhang, L., Yuh, J., Smith, M.T., Burlingame, A.L., 2011. Quantitative mass spectrometry reveals the epigenome as a target of arsenic, *Chem. Biol. Interact.* 192, 113-117.
- Clark, C.J., Sage, E.H., 2008. A prototypic matricellular protein in the tumor microenvironment--where there's SPARC, there's fire, *J. Cell. Biochem.* 104, 721-732.
- Cohen, S.M., Arnold, L.L., Eldan, M., Lewis, A.S., Beck, B.D., 2006. Methylated arsenicals: the implications of metabolism and carcinogenicity studies in rodents to human risk assessment, *Crit. Rev. Toxicol.* 36, 99-133.
- Darewicz, G., Malczyk, E., Darewicz, J., 1998. Investigations of urinary cadmium content in patients with urinary bladder carcinoma, *Int. Urol. Nephrol.* 30, 137-139.
- Delostrinos, C.F., Hudson, A.E., Feng, W.C., Kosman, J., Bassuk, J.A., 2006. The C-terminal Ca²⁺-binding domain of SPARC confers anti-spreading activity to human urothelial cells, *J. Cell. Physiol.* 206, 211-220.
- Drobna, Z., Waters, S.B., Devesa, V., Harmon, A.W., Thomas, D.J., Styblo, M., 2005. Metabolism and toxicity of arsenic in human urothelial cells expressing rat arsenic (+3 oxidation state)-methyltransferase, *Toxicol. Appl. Pharmacol.* 207, 147-159.
- Eblin, K.E., Bowen, M.E., Cromey, D.W., Bredfeldt, T.G., Mash, E.A., Lau, S.S., Gandolfi, A.J., 2006. Arsenite and monomethylarsonous acid generate oxidative stress response in human bladder cell culture, *Toxicol. Appl. Pharmacol.* 217, 7-14.

- Elmore, S., 2007. Apoptosis: a review of programmed cell death, *Toxicol. Pathol.* 35, 495-516.
- Engel, J., Taylor, W., Paulsson, M., Sage, H., Hogan, B., 1987. Calcium binding domains and calcium-induced conformational transition of SPARC/BM-40/osteonectin, an extracellular glycoprotein expressed in mineralized and nonmineralized tissues, *Biochemistry* 26, 6958-6965.
- Erman, A., Resnik, N., Romih, R., 2012. Autophagic activity in the mouse urinary bladder urothelium as a response to starvation, *Protoplasma*.
- Escudero-Lourdes, C., Medeiros, M.K., Cardenas-Gonzalez, M.C., Wnek, S.M., Gandolfi, J.A., 2010. Low level exposure to monomethyl arsonous acid-induced the over-production of inflammation-related cytokines and the activation of cell signals associated with tumor progression in a urothelial cell model, *Toxicol. Appl. Pharmacol.* 244, 162-173.
- Escudero-Lourdes, C., Wu, T., Camarillo, J.M., Gandolfi, A.J., 2012. Interleukin-8 (IL-8) over-production and autocrine cell activation are key factors in monomethylarsonous acid [MMA(III)]-induced malignant transformation of urothelial cells, *Toxicol. Appl. Pharmacol.* 258, 10-18.
- Fadeel, B., Gleiss, B., Hogstrand, K., Chandra, J., Wiedmer, T., Sims, P.J., Henter, J.I., Orrenius, S., Samali, A., 1999. Phosphatidylserine exposure during apoptosis is a cell-type-specific event and does not correlate with plasma membrane phospholipid scramblase expression, *Biochem. Biophys. Res. Commun.* 266, 504-511.
- Fajkovic, H., Halpern, J.A., Cha, E.K., Bahadori, A., Chromecki, T.F., Karakiewicz, P.I., Breinl, E., Merseburger, A.S., Shariat, S.F., 2011. Impact of gender on bladder cancer incidence, staging, and prognosis, *World J. Urol.* 29, 457-463.
- Festjens, N., Vanden Berghe, T., Vandenabeele, P., 2006. Necrosis, a well-orchestrated form of cell demise: signalling cascades, important mediators and concomitant immune response, *Biochim. Biophys. Acta* 1757, 1371-1387.
- Forman, J.J., Legesse-Miller, A., Collier, H.A., 2008. A search for conserved sequences in coding regions reveals that the let-7 microRNA targets Dicer within its coding sequence, *Proc. Natl. Acad. Sci. U. S. A.* 105, 14879-14884.
- Framson, P.E., Sage, E.H., 2004. SPARC and tumor growth: where the seed meets the soil? *J. Cell. Biochem.* 92, 679-690.
- Fuentes-Prior, P., Salvesen, G.S., 2004. The protein structures that shape caspase activity, specificity, activation and inhibition, *Biochem. J.* 384, 201-232.

- Funk, S.E., Sage, E.H., 1993. Differential effects of SPARC and cationic SPARC peptides on DNA synthesis by endothelial cells and fibroblasts, *J. Cell. Physiol.* 154, 53-63.
- Funk, S.E., Sage, E.H., 1991. The Ca²⁺(+)-binding glycoprotein SPARC modulates cell cycle progression in bovine aortic endothelial cells, *Proc. Natl. Acad. Sci. U. S. A.* 88, 2648-2652.
- Galluzzi, L., Vitale, I., Abrams, J.M., Alnemri, E.S., Baehrecke, E.H., Blagosklonny, M.V., Dawson, T.M., Dawson, V.L., El-Deiry, W.S., Fulda, S., Gottlieb, E., Green, D.R., Hengartner, M.O., Kepp, O., Knight, R.A., Kumar, S., Lipton, S.A., Lu, X., Madeo, F., Malorni, W., Mehlen, P., Nunez, G., Peter, M.E., Piacentini, M., Rubinsztein, D.C., Shi, Y., Simon, H.U., Vandenabeele, P., White, E., Yuan, J., Zhivotovsky, B., Melino, G., Kroemer, G., 2012. Molecular definitions of cell death subroutines: recommendations of the Nomenclature Committee on Cell Death 2012, *Cell Death Differ.* 19, 107-120.
- Gilles, C., Bassuk, J.A., Pulyaeva, H., Sage, E.H., Foidart, J.M., Thompson, E.W., 1998. SPARC/osteonectin induces matrix metalloproteinase 2 activation in human breast cancer cell lines, *Cancer Res.* 58, 5529-5536.
- Goldblum, S.E., Ding, X., Funk, S.E., Sage, E.H., 1994. SPARC (secreted protein acidic and rich in cysteine) regulates endothelial cell shape and barrier function, *Proc. Natl. Acad. Sci. U. S. A.* 91, 3448-3452.
- Golembieski, W.A., Thomas, S.L., Schultz, C.R., Yunker, C.K., McClung, H.M., Lemke, N., Cazacu, S., Barker, T., Sage, E.H., Brodie, C., Rempel, S.A., 2008. HSP27 mediates SPARC-induced changes in glioma morphology, migration, and invasion, *Glia* 56, 1061-1075.
- Goodison, S., Rosser, C.J., Urquidi, V., 2009. Urinary proteomic profiling for diagnostic bladder cancer biomarkers, *Expert Rev. Proteomics* 6, 507-514.
- Guha Mazumder, D.N., 2008. Chronic arsenic toxicity & human health, *Indian J. Med. Res.* 128, 436-447.
- Haber, C.L., Gottifredi, V., Llera, A.S., Salvatierra, E., Prada, F., Alonso, L., Sage, E.H., Podhajcer, O.L., 2008. SPARC modulates the proliferation of stromal but not melanoma cells unless endogenous SPARC expression is downregulated, *Int. J. Cancer* 122, 1465-1475.
- Hafner, M., Zimmermann, K., Pottgiesser, J., Krieg, T., Nischt, R., 1995. A purine-rich sequence in the human BM-40 gene promoter region is a prerequisite for maximum transcription, *Matrix Biol.* 14, 733-741.

- Hasselaar, P., Sage, E.H., 1992. SPARC antagonizes the effect of basic fibroblast growth factor on the migration of bovine aortic endothelial cells, *J. Cell. Biochem.* 49, 272-283.
- He, C., Klionsky, D.J., 2009. Regulation mechanisms and signaling pathways of autophagy, *Annu. Rev. Genet.* 43, 67-93.
- He, L., Girijashanker, K., Dalton, T.P., Reed, J., Li, H., Soleimani, M., Nebert, D.W., 2006. ZIP8, member of the solute-carrier-39 (SLC39) metal-transporter family: characterization of transporter properties, *Mol. Pharmacol.* 70, 171-180.
- Hester, S., Drobna, Z., Andrews, D., Liu, J., Waalkes, M., Thomas, D., Styblo, M., 2009. Expression of AS3MT alters transcriptional profiles in human urothelial cells exposed to arsenite, *Hum. Exp. Toxicol.* 28, 49-61.
- Hohenester, E., Maurer, P., Timpl, R., 1997. Crystal structure of a pair of follistatin-like and EF-hand calcium-binding domains in BM-40, *EMBO J.* 16, 3778-3786.
- Holler, N., Zaru, R., Micheau, O., Thome, M., Attinger, A., Valitutti, S., Bodmer, J.L., Schneider, P., Seed, B., Tschopp, J., 2000. Fas triggers an alternative, caspase-8-independent cell death pathway using the kinase RIP as effector molecule, *Nat. Immunol.* 1, 489-495.
- Hopenhayn-Rich, C., Biggs, M.L., Fuchs, A., Bergoglio, R., Tello, E.E., Nicolli, H., Smith, A.H., 1996. Bladder cancer mortality associated with arsenic in drinking water in Argentina, *Epidemiology* 7, 117-124.
- Hudson, A.E., Feng, W.C., Delostrinos, C.F., Carmean, N., Bassuk, J.A., 2005. Spreading of embryologically distinct urothelial cells is inhibited by SPARC, *J. Cell. Physiol.* 202, 453-463.
- Huff, J., Lunn, R.M., Waalkes, M.P., Tomatis, L., Infante, P.F., 2007. Cadmium-induced cancers in animals and in humans, *Int. J. Occup. Environ. Health* 13, 202-212.
- IARC (International Agency for Research on Cancer), 1993. Beryllium, Cadmium, Mercury, and Exposures in the Glass Manufacturing Industry, *IARC Monographs on the Evaluation of Carcinogenic Risks to Humans* 58, 119-238.
- IARC (International Agency for Research on Cancer), 1980. Some Metals and Metallic Compounds, *IARC Monographs on the Evaluation of the Carcinogenic Risk of Chemicals to Man* 23, 39.
- Jacob, K., Webber, M., Benayahu, D., Kleinman, H.K., 1999. Osteonectin promotes prostate cancer cell migration and invasion: a possible mechanism for metastasis to bone, *Cancer Res.* 59, 4453-4457.

- Jacobs, B.L., Lee, C.T., Montie, J.E., 2010. Bladder cancer in 2010: how far have we come? *CA Cancer. J. Clin.* 60, 244-272.
- Jarup, L., Akesson, A., 2009. Current status of cadmium as an environmental health problem, *Toxicol. Appl. Pharmacol.* 238, 201-208.
- Jemal, A., Siegel, R., Xu, J., Ward, E., 2010. Cancer statistics, 2010, *CA Cancer. J. Clin.* 60, 277-300.
- Jo, W.J., Ren, X., Chu, F., Aleshin, M., Wintz, H., Burlingame, A., Smith, M.T., Vulpe, C.D., Zhang, L., 2009. Acetylated H4K16 by MYST1 protects UROtsa cells from arsenic toxicity and is decreased following chronic arsenic exposure, *Toxicol. Appl. Pharmacol.* 241, 294-302.
- Jung, C.H., Jun, C.B., Ro, S.H., Kim, Y.M., Otto, N.M., Cao, J., Kundu, M., Kim, D.H., 2009. ULK-Atg13-FIP200 complexes mediate mTOR signaling to the autophagy machinery, *Mol. Biol. Cell* 20, 1992-2003.
- Kagawa, J., 1994. Atmospheric pollution due to mobile sources and effects on human health in Japan, *Environ. Health Perspect.* 102 Suppl 4, 93-99.
- Kanzawa, T., Kondo, Y., Ito, H., Kondo, S., Germano, I., 2003. Induction of autophagic cell death in malignant glioma cells by arsenic trioxide, *Cancer Res.* 63, 2103-2108.
- Kapinas, K., Kessler, C.B., Delany, A.M., 2009. miR-29 suppression of osteonectin in osteoblasts: regulation during differentiation and by canonical Wnt signaling, *J. Cell. Biochem.* 108, 216-224.
- Kaufmann, B., Muller, S., Hanisch, F.G., Hartmann, U., Paulsson, M., Maurer, P., Zaucke, F., 2004. Structural variability of BM-40/SPARC/osteonectin glycosylation: implications for collagen affinity, *Glycobiology* 14, 609-619.
- Kellen, E., Zeegers, M.P., Hond, E.D., Buntinx, F., 2007. Blood cadmium may be associated with bladder carcinogenesis: the Belgian case-control study on bladder cancer, *Cancer Detect. Prev.* 31, 77-82.
- Kim, H.S., Lee, S.H., Do, S.I., Lim, S.J., Park, Y.K., Kim, Y.W., 2011a. Clinicopathologic correlation of beclin-1 expression in pancreatic ductal adenocarcinoma, *Pathol. Res. Pract.* 207, 247-252.
- Kim, K.M., Yu, T.K., Chu, H.H., Park, H.S., Jang, K.Y., Moon, W.S., Kang, M.J., Lee, D.G., Kim, M.H., Lee, J.H., Chung, M.J., 2011b. Expression of ER stress and autophagy-related molecules in human non-small cell lung cancer and premalignant lesions, *Int. J. Cancer.*

- Koblinski, J.E., Kaplan-Singer, B.R., VanOsdol, S.J., Wu, M., Engbring, J.A., Wang, S., Goldsmith, C.M., Piper, J.T., Vostal, J.G., Harms, J.F., Welch, D.R., Kleinman, H.K., 2005. Endogenous osteonectin/SPARC/BM-40 expression inhibits MDA-MB-231 breast cancer cell metastasis, *Cancer Res.* 65, 7370-7377.
- Kogevinas, M., 't Mannetje, A., Cordier, S., Ranft, U., Gonzalez, C.A., Vineis, P., Chang-Claude, J., Lynge, E., Wahrendorf, J., Tzonou, A., Jockel, K.H., Serra, C., Porru, S., Hours, M., Greiser, E., Boffetta, P., 2003. Occupation and bladder cancer among men in Western Europe, *Cancer Causes Control* 14, 907-914.
- Kumar, V., Abbas, A.K., Fausto, N., Aster, J.C., 2010. *Robbins and Cotran Pathologic Basis of Disease*, 8th ed. Saunders Elsevier, Philadelphia, PA.
- Kupprion, C., Motamed, K., Sage, E.H., 1998. SPARC (BM-40, osteonectin) inhibits the mitogenic effect of vascular endothelial growth factor on microvascular endothelial cells, *J. Biol. Chem.* 273, 29635-29640.
- Lane, T.F., Iruela-Arispe, M.L., Sage, E.H., 1992. Regulation of gene expression by SPARC during angiogenesis in vitro. Changes in fibronectin, thrombospondin-1, and plasminogen activator inhibitor-1, *J. Biol. Chem.* 267, 16736-16745.
- Lane, T.F., Sage, E.H., 1994. The biology of SPARC, a protein that modulates cell-matrix interactions, *FASEB J.* 8, 163-173.
- Lane, T.F., Sage, E.H., 1990. Functional mapping of SPARC: peptides from two distinct Ca⁺(+)-binding sites modulate cell shape, *J. Cell Biol.* 111, 3065-3076.
- Larson, J., Yasmin, T., Sens, D.A., Zhou, X.D., Sens, M.A., Garrett, S.H., Dunlevy, J.R., Cao, L., Somji, S., 2010. SPARC gene expression is repressed in human urothelial cells (UROtsa) exposed to or malignantly transformed by cadmium or arsenite, *Toxicol. Lett.* 199, 166-172.
- Le, X.C., Ma, M., Cullen, W.R., Aposhian, H.V., Lu, X., Zheng, B., 2000. Determination of monomethylarsonous acid, a key arsenic methylation intermediate, in human urine, *Environ. Health Perspect.* 108, 1015-1018.
- Ledda, F., Bravo, A.I., Adris, S., Bover, L., Mordoh, J., Podhajcer, O.L., 1997a. The expression of the secreted protein acidic and rich in cysteine (SPARC) is associated with the neoplastic progression of human melanoma, *J. Invest. Dermatol.* 108, 210-214.
- Ledda, M.F., Adris, S., Bravo, A.I., Kairiyama, C., Bover, L., Chernajovsky, Y., Mordoh, J., Podhajcer, O.L., 1997b. Suppression of SPARC expression by antisense RNA abrogates the tumorigenicity of human melanoma cells, *Nat. Med.* 3, 171-176.

- Li, J., Abraham, S., Cheng, L., Witzmann, F.A., Koch, M., Xie, J., Rahman, M., Mohammed, S.I., 2008. Proteomic-based approach for biomarkers discovery in early detection of invasive urothelial carcinoma, *Proteomics Clin. Appl.* 2, 78-89.
- Liang, X.H., Jackson, S., Seaman, M., Brown, K., Kempkes, B., Hibshoosh, H., Levine, B., 1999. Induction of autophagy and inhibition of tumorigenesis by beclin 1, *Nature* 402, 672-676.
- Lokeshwar, V.B., Selzer, M.G., 2006. Urinary bladder tumor markers, *Urol. Oncol.* 24, 528-537.
- Majno, G., Joris, I., 1995. Apoptosis, oncosis, and necrosis. An overview of cell death, *Am. J. Pathol.* 146, 3-15.
- Mason, I.J., Taylor, A., Williams, J.G., Sage, H., Hogan, B.L., 1986. Evidence from molecular cloning that SPARC, a major product of mouse embryo parietal endoderm, is related to an endothelial cell 'culture shock' glycoprotein of Mr 43,000, *EMBO J.* 5, 1465-1472.
- Matovic, V., Buha, A., Bulat, Z., Dukic-Cosic, D., 2011. Cadmium toxicity revisited: focus on oxidative stress induction and interactions with zinc and magnesium, *Arh. Hig. Rada. Toksikol.* 62, 65-76.
- Medeiros, M., Zheng, X., Novak, P., Wnek, S.M., Chyan, V., Escudero-Lourdes, C., Gandolfi, A.J., 2012. Global gene expression changes in human urothelial cells exposed to low-level monomethylarsonous acid, *Toxicology* 291, 102-112.
- Menke, A., Muntner, P., Silbergeld, E.K., Platz, E.A., Guallar, E., 2009. Cadmium levels in urine and mortality among U.S. adults, *Environ. Health Perspect.* 117, 190-196.
- Motamed, K., Blake, D.J., Angello, J.C., Allen, B.L., Rapraeger, A.C., Hauschka, S.D., Sage, E.H., 2003. Fibroblast growth factor receptor-1 mediates the inhibition of endothelial cell proliferation and the promotion of skeletal myoblast differentiation by SPARC: a role for protein kinase A, *J. Cell. Biochem.* 90, 408-423.
- Motamed, K., Sage, E.H., 1998. SPARC inhibits endothelial cell adhesion but not proliferation through a tyrosine phosphorylation-dependent pathway, *J. Cell. Biochem.* 70, 543-552.
- Moulis, J.M., 2010. Cellular mechanisms of cadmium toxicity related to the homeostasis of essential metals, *Biometals* 23, 877-896.
- Murphy-Ullrich, J.E., 2001. The de-adhesive activity of matricellular proteins: is intermediate cell adhesion an adaptive state? *J. Clin. Invest.* 107, 785-790.

- Murphy-Ullrich, J.E., Lane, T.F., Pallero, M.A., Sage, E.H., 1995. SPARC mediates focal adhesion disassembly in endothelial cells through a follistatin-like region and the Ca(2+)-binding EF-hand, *J. Cell. Biochem.* 57, 341-350.
- Nagaraju, G.P., Sharma, D., 2011. Anti-cancer role of SPARC, an inhibitor of adipogenesis, *Cancer Treat. Rev.* 37, 559-566.
- Negri, E., La Vecchia, C., 2001. Epidemiology and prevention of bladder cancer, *Eur. J. Cancer Prev.* 10, 7-14.
- Neumar, R.W., 2000. Molecular mechanisms of ischemic neuronal injury, *Ann. Emerg. Med.* 36, 483-506.
- Nimphius, W., Moll, R., Olbert, P., Ramaswamy, A., Barth, P.J., 2007. CD34+ fibrocytes in chronic cystitis and noninvasive and invasive urothelial carcinomas of the urinary bladder, *Virchows Arch.* 450, 179-185.
- Nzengue, Y., Candeias, S.M., Sauvaigo, S., Douki, T., Favier, A., Rachidi, W., Guiraud, P., 2011. The toxicity redox mechanisms of cadmium alone or together with copper and zinc homeostasis alteration: its redox biomarkers, *J. Trace Elem. Med. Biol.* 25, 171-180.
- Olsson, I.M., Bensryd, I., Lundh, T., Ottosson, H., Skerfving, S., Oskarsson, A., 2002. Cadmium in blood and urine--impact of sex, age, dietary intake, iron status, and former smoking--association of renal effects, *Environ. Health Perspect.* 110, 1185-1190.
- Orloff, K., Mistry, K., Metcalf, S., 2009. Biomonitoring for environmental exposures to arsenic, *J. Toxicol. Environ. Health B Crit. Rev.* 12, 509-524.
- Otsuka, K., Yao, K.L., Wasi, S., Tung, P.S., Aubin, J.E., Sodek, J., Termine, J.D., 1984. Biosynthesis of osteonectin by fetal porcine calvarial cells in vitro, *J. Biol. Chem.* 259, 9805-9812.
- Pattingre, S., Espert, L., Biard-Piechaczyk, M., Codogno, P., 2008. Regulation of macroautophagy by mTOR and Beclin 1 complexes, *Biochimie* 90, 313-323.
- Penalzoza, C., Lin, L., Lockshin, R.A., Zakeri, Z., 2006. Cell death in development: shaping the embryo, *Histochem. Cell Biol.* 126, 149-158.
- Petzoldt, J.L., Leigh, I.M., Duffy, P.G., Sexton, C., Masters, J.R., 1995. Immortalisation of human urothelial cells, *Urol. Res.* 23, 377-380.
- Podhajcer, O.L., Benedetti, L.G., Girotti, M.R., Prada, F., Salvatierra, E., Llera, A.S., 2008. The role of the matricellular protein SPARC in the dynamic interaction between the tumor and the host, *Cancer Metastasis Rev.* 27, 691-705.

- Porter, P.L., Sage, E.H., Lane, T.F., Funk, S.E., Gown, A.M., 1995. Distribution of SPARC in normal and neoplastic human tissue, *J. Histochem. Cytochem.* 43, 791-800.
- Prankel, S.H., Nixon, R.M., Phillips, C.J., 2005. Implications for the human food chain of models of cadmium accumulation in sheep, *Environ. Res.* 97, 348-358.
- Prugarova, A., Kovac, M., 1987. Lead and cadmium content in cocoa beans (short communication), *Nahrung* 31, 635-636.
- Qian, W., Liu, J., Jin, J., Ni, W., Xu, W., 2007. Arsenic trioxide induces not only apoptosis but also autophagic cell death in leukemia cell lines via up-regulation of Beclin-1, *Leuk. Res.* 31, 329-339.
- Rahman, M.M., Ng, J.C., Naidu, R., 2009. Chronic exposure of arsenic via drinking water and its adverse health impacts on humans, *Environ. Geochem. Health* 31 Suppl 1, 189-200.
- Reeves, P.G., Vanderpool, R.A., 1997. Cadmium burden of men and women who report regular consumption of confectionery sunflower kernels containing a natural abundance of cadmium, *Environ. Health Perspect.* 105, 1098-1104.
- Rehn, L., 1895. Blasengeschwulste bei Fuchsin-Arbeitern, *Verhandlungen der Deutschen Gesellschaft für Chirurgie* 24, 588-600.
- Rempel, S.A., Golembieski, W.A., Ge, S., Lemke, N., Elisevich, K., Mikkelsen, T., Gutierrez, J.A., 1998. SPARC: a signal of astrocytic neoplastic transformation and reactive response in human primary and xenograft gliomas, *J. Neuropathol. Exp. Neurol.* 57, 1112-1121.
- Ren, X., Aleshin, M., Jo, W.J., Dills, R., Kalman, D.A., Vulpe, C.D., Smith, M.T., Zhang, L., 2011. Involvement of N-6 adenine-specific DNA methyltransferase 1 (N6AMT1) in arsenic biomethylation and its role in arsenic-induced toxicity, *Environ. Health Perspect.* 119, 771-777.
- Rossi, M.R., Masters, J.R., Park, S., Todd, J.H., Garrett, S.H., Sens, M.A., Somji, S., Nath, J., Sens, D.A., 2001. The immortalized UROtsa cell line as a potential cell culture model of human urothelium, *Environ. Health Perspect.* 109, 801-808.
- Rossi, M.R., Somji, S., Garrett, S.H., Sens, M.A., Nath, J., Sens, D.A., 2002. Expression of hsp 27, hsp 60, hsc 70, and hsp 70 stress response genes in cultured human urothelial cells (UROtsa) exposed to lethal and sublethal concentrations of sodium arsenite, *Environ. Health Perspect.* 110, 1225-1232.

- Sage, E.H., Bassuk, J.A., Yost, J.C., Folkman, M.J., Lane, T.F., 1995. Inhibition of endothelial cell proliferation by SPARC is mediated through a Ca(2+)-binding EF-hand sequence, *J. Cell. Biochem.* 57, 127-140.
- Sage, H., Johnson, C., Bornstein, P., 1984. Characterization of a novel serum albumin-binding glycoprotein secreted by endothelial cells in culture, *J. Biol. Chem.* 259, 3993-4007.
- Sage, H., Vernon, R.B., Funk, S.E., Everitt, E.A., Angello, J., 1989. SPARC, a secreted protein associated with cellular proliferation, inhibits cell spreading in vitro and exhibits Ca²⁺-dependent binding to the extracellular matrix, *J. Cell Biol.* 109, 341-356.
- Sakai, N., Baba, M., Nagasima, Y., Kato, Y., Hirai, K., Kondo, K., Kobayashi, K., Yoshida, M., Kaneko, S., Kishida, T., Kawakami, S., Hosaka, M., Inayama, Y., Yao, M., 2001. SPARC expression in primary human renal cell carcinoma: upregulation of SPARC in sarcomatoid renal carcinoma, *Hum. Pathol.* 32, 1064-1070.
- Sangaletti, S., Colombo, M.P., 2008. Matricellular proteins at the crossroad of inflammation and cancer, *Cancer Lett.* 267, 245-253.
- Sangaletti, S., Stoppacciaro, A., Guiducci, C., Torrisi, M.R., Colombo, M.P., 2003. Leukocyte, rather than tumor-produced SPARC, determines stroma and collagen type IV deposition in mammary carcinoma, *J. Exp. Med.* 198, 1475-1485.
- Sasaki, T., Hohenester, E., Gohring, W., Timpl, R., 1998. Crystal structure and mapping by site-directed mutagenesis of the collagen-binding epitope of an activated form of BM-40/SPARC/osteonectin, *EMBO J.* 17, 1625-1634.
- Satarug, S., Garrett, S.H., Sens, M.A., Sens, D.A., 2011. Cadmium, environmental exposure, and health outcomes, *Cien. Saude Colet* 16, 2587-2602.
- Sato, N., Fukushima, N., Maehara, N., Matsubayashi, H., Koopmann, J., Su, G.H., Hruban, R.H., Goggins, M., 2003. SPARC/osteonectin is a frequent target for aberrant methylation in pancreatic adenocarcinoma and a mediator of tumor-stromal interactions, *Oncogene* 22, 5021-5030.
- Seno, T., Harada, H., Kohno, S., Teraoka, M., Inoue, A., Ohnishi, T., 2009. Downregulation of SPARC expression inhibits cell migration and invasion in malignant gliomas, *Int. J. Oncol.* 34, 707-715.
- Sens, D.A., Park, S., Gurel, V., Sens, M.A., Garrett, S.H., Somji, S., 2004. Inorganic cadmium- and arsenite-induced malignant transformation of human bladder urothelial cells, *Toxicol. Sci.* 79, 56-63.

- Shi, Q., Bao, S., Song, L., Wu, Q., Bigner, D.D., Hjelmeland, A.B., Rich, J.N., 2007. Targeting SPARC expression decreases glioma cellular survival and invasion associated with reduced activities of FAK and ILK kinases, *Oncogene* 26, 4084-4094.
- Shintani, T., Klionsky, D.J., 2004. Autophagy in health and disease: a double-edged sword, *Science* 306, 990-995.
- Siemiatycki, J., Dewar, R., Nadon, L., Gerin, M., 1994. Occupational risk factors for bladder cancer: results from a case-control study in Montreal, Quebec, Canada, *Am. J. Epidemiol.* 140, 1061-1080.
- Sinha, S., Levine, B., 2008. The autophagy effector Beclin 1: a novel BH3-only protein, *Oncogene* 27 Suppl 1, S137-48.
- Smith, A.H., Goycolea, M., Haque, R., Biggs, M.L., 1998. Marked increase in bladder and lung cancer mortality in a region of Northern Chile due to arsenic in drinking water, *Am. J. Epidemiol.* 147, 660-669.
- Smith, A.H., Hopenhayn-Rich, C., Bates, M.N., Goeden, H.M., Hertz-Picciotto, I., Duggan, H.M., Wood, R., Kosnett, M.J., Smith, M.T., 1992. Cancer risks from arsenic in drinking water, *Environ. Health Perspect.* 97, 259-267.
- Socha, M.J., Said, N., Dai, Y., Kwong, J., Ramalingam, P., Trieu, V., Desai, N., Mok, S.C., Motamed, K., 2009. Aberrant promoter methylation of SPARC in ovarian cancer, *Neoplasia* 11, 126-135.
- Soloway, M.S., Sofer, M., Vaidya, A., 2002. Contemporary management of stage T1 transitional cell carcinoma of the bladder, *J. Urol.* 167, 1573-1583.
- Somji, S., Bathula, C.S., Zhou, X.D., Sens, M.A., Sens, D.A., Garrett, S.H., 2008. Transformation of human urothelial cells (UROtsa) by as and cd induces the expression of keratin 6a, *Environ. Health Perspect.* 116, 434-440.
- Somji, S., Cao, L., Mehus, A., Zhou, X.D., Sens, M.A., Dunlevy, J.R., Garrett, S.H., Zheng, Y., Larson, J.L., Sens, D.A., 2011a. Comparison of expression patterns of keratin 6, 7, 16, 17, and 19 within multiple independent isolates of As(+3)- and Cd (+2)-induced bladder cancer : keratin 6, 7, 16, 17, and 19 in bladder cancer, *Cell Biol. Toxicol.* 27, 381-396.
- Somji, S., Garrett, S.H., Toni, C., Zhou, X.D., Zheng, Y., Ajjimaporn, A., Sens, M.A., Sens, D.A., 2011b. Differences in the epigenetic regulation of MT-3 gene expression between parental and Cd+2 or As+3 transformed human urothelial cells, *Cancer. Cell. Int.* 11, 2.

- Somji, S., Zhou, X.D., Garrett, S.H., Sens, M.A., Sens, D.A., 2006. Urothelial cells malignantly transformed by exposure to cadmium (Cd(+2)) and arsenite (As(+3)) have increased resistance to Cd(+2) and As(+3)-induced cell death, *Toxicol. Sci.* 94, 293-301.
- Somji, S., Zhou, X.D., Mehus, A., Sens, M.A., Garrett, S.H., Lutz, K.L., Dunlevy, J.R., Zheng, Y., Sens, D.A., 2010. Variation of keratin 7 expression and other phenotypic characteristics of independent isolates of cadmium transformed human urothelial cells (UROtsa), *Chem. Res. Toxicol.* 23, 348-356.
- Steinmaus, C., Moore, L., Hopenhayn-Rich, C., Biggs, M.L., Smith, A.H., 2000. Arsenic in drinking water and bladder cancer, *Cancer Invest.* 18, 174-182.
- Styblo, M., Del Razo, L.M., Vega, L., Germolec, D.R., LeCluyse, E.L., Hamilton, G.A., Reed, W., Wang, C., Cullen, W.R., Thomas, D.J., 2000. Comparative toxicity of trivalent and pentavalent inorganic and methylated arsenicals in rat and human cells, *Arch. Toxicol.* 74, 289-299.
- Suzuki, M., Hao, C., Takahashi, T., Shigematsu, H., Shivapurkar, N., Sathyanarayana, U.G., Iizasa, T., Fujisawa, T., Hiroshima, K., Gazdar, A.F., 2005. Aberrant methylation of SPARC in human lung cancers, *Br. J. Cancer* 92, 942-948.
- Suzuki, S., Arnold, L.L., Ohnishi, T., Cohen, S.M., 2008. Effects of inorganic arsenic on the rat and mouse urinary bladder, *Toxicol. Sci.* 106, 350-363.
- Swaroop, A., Hogan, B.L., Francke, U., 1988. Molecular analysis of the cDNA for human SPARC/osteonectin/BM-40: sequence, expression, and localization of the gene to chromosome 5q31-q33, *Genomics* 2, 37-47.
- Tai, I.T., Tang, M.J., 2008. SPARC in cancer biology: its role in cancer progression and potential for therapy, *Drug Resist Updat* 11, 231-246.
- Tanaka, M.F., Sonpavde, G., 2011. Diagnosis and management of urothelial carcinoma of the bladder, *Postgrad. Med.* 123, 43-55.
- Termine, J.D., Kleinman, H.K., Whitson, S.W., Conn, K.M., McGarvey, M.L., Martin, G.R., 1981. Osteonectin, a bone-specific protein linking mineral to collagen, *Cell* 26, 99-105.
- Thomas, R., True, L.D., Bassuk, J.A., Lange, P.H., Vessella, R.L., 2000. Differential expression of osteonectin/SPARC during human prostate cancer progression, *Clin. Cancer Res.* 6, 1140-1149.

- Tremble, P.M., Lane, T.F., Sage, E.H., Werb, Z., 1993. SPARC, a secreted protein associated with morphogenesis and tissue remodeling, induces expression of metalloproteinases in fibroblasts through a novel extracellular matrix-dependent pathway, *J. Cell Biol.* 121, 1433-1444.
- Tsuda, T., Babazono, A., Yamamoto, E., Kurumatani, N., Mino, Y., Ogawa, T., Kishi, Y., Aoyama, H., 1995. Ingested arsenic and internal cancer: a historical cohort study followed for 33 years, *Am. J. Epidemiol.* 141, 198-209.
- Vahter, M., 1994. What are the chemical forms of arsenic in urine, and what can they tell us about exposure? *Clin. Chem.* 40, 679-680.
- Vahter, M., Akesson, A., Liden, C., Ceccatelli, S., Berglund, M., 2007. Gender differences in the disposition and toxicity of metals, *Environ. Res.* 104, 85-95.
- Vanlangenakker, N., Vanden Berghe, T., Krysko, D.V., Festjens, N., Vandenabeele, P., 2008. Molecular mechanisms and pathophysiology of necrotic cell death, *Curr. Mol. Med.* 8, 207-220.
- Villarreal, X.C., Mann, K.G., Long, G.L., 1989. Structure of human osteonectin based upon analysis of cDNA and genomic sequences, *Biochemistry* 28, 6483-6491.
- Volanis, D., Kadiyska, T., Galanis, A., Delakas, D., Logotheti, S., Zoumpourlis, V., 2010. Environmental factors and genetic susceptibility promote urinary bladder cancer, *Toxicol. Lett.* 193, 131-137.
- Waalkes, M.P., 2003. Cadmium carcinogenesis, *Mutat. Res.* 533, 107-120.
- Waalkes, M.P., 2000. Cadmium carcinogenesis in review, *J. Inorg. Biochem.* 79, 241-244.
- Waalkes, M.P., Liu, J., Ward, J.M., Diwan, B.A., 2006. Enhanced urinary bladder and liver carcinogenesis in male CD1 mice exposed to transplacental inorganic arsenic and postnatal diethylstilbestrol or tamoxifen, *Toxicol. Appl. Pharmacol.* 215, 295-305.
- Wang, X.J., Sun, Z., Chen, W., Eblin, K.E., Gandolfi, J.A., Zhang, D.D., 2007a. Nrf2 protects human bladder urothelial cells from arsenite and monomethylarsonous acid toxicity, *Toxicol. Appl. Pharmacol.* 225, 206-213.
- Wang, Z.H., Xu, L., Duan, Z.L., Zeng, L.Q., Yan, N.H., Peng, Z.L., 2007b. Beclin 1-mediated macroautophagy involves regulation of caspase-9 expression in cervical cancer HeLa cells, *Gynecol. Oncol.* 107, 107-113.

- Whyte, A.L., Hook, G.R., Greening, G.E., Gibbs-Smith, E., Gardner, J.P., 2009. Human dietary exposure to heavy metals via the consumption of greenshell mussels (*Perna canaliculus* Gmelin 1791) from the Bay of Islands, northern New Zealand, *Sci. Total Environ.* 407, 4348-4355.
- Wnek, S.M., Jensen, T.J., Severson, P.L., Futscher, B.W., Gandolfi, A.J., 2010. Monomethylarsonous acid produces irreversible events resulting in malignant transformation of a human bladder cell line following 12 weeks of low-level exposure, *Toxicol. Sci.* 116, 44-57.
- Wu, R.X., Laser, M., Han, H., Varadarajulu, J., Schuh, K., Hallhuber, M., Hu, K., Ertl, G., Hauck, C.R., Ritter, O., 2006. Fibroblast migration after myocardial infarction is regulated by transient SPARC expression, *J. Mol. Med. (Berl)* 84, 241-252.
- Yan, Q., Sage, E.H., 1999. SPARC, a matricellular glycoprotein with important biological functions, *J. Histochem. Cytochem.* 47, 1495-1506.
- Yokohira, M., Arnold, L.L., Pennington, K.L., Suzuki, S., Kakiuchi-Kiyota, S., Herbin-Davis, K., Thomas, D.J., Cohen, S.M., 2010. Severe systemic toxicity and urinary bladder cytotoxicity and regenerative hyperplasia induced by arsenite in arsenic (+3 oxidation state) methyltransferase knockout mice. A preliminary report, *Toxicol. Appl. Pharmacol.* 246, 1-7.
- Yue, Z., Jin, S., Yang, C., Levine, A.J., Heintz, N., 2003. Beclin 1, an autophagy gene essential for early embryonic development, is a haploinsufficient tumor suppressor, *Proc. Natl. Acad. Sci. U. S. A.* 100, 15077-15082.
- Zeegers, M.P., Tan, F.E., Dorant, E., van Den Brandt, P.A., 2000. The impact of characteristics of cigarette smoking on urinary tract cancer risk: a meta-analysis of epidemiologic studies, *Cancer* 89, 630-639.
- Zhou, X.D., Sens, M.A., Garrett, S.H., Somji, S., Park, S., Gurel, V., Sens, D.A., 2006. Enhanced expression of metallothionein isoform 3 protein in tumor heterotransplants derived from As⁺³- and Cd⁺²-transformed human urothelial cells, *Toxicol. Sci.* 93, 322-330.
- Zhu, F., Qu, L., Fan, W., Qiao, M., Hao, H., Wang, X., 2011. Assessment of heavy metals in some wild edible mushrooms collected from Yunnan Province, China, *Environ. Monit. Assess.* 179, 191-199.

APPENDIX

ABBREVIATIONS

5-AZC	5-Aza-2'-deoxycytidine / Methylation Inhibitor
As ⁺³	Arsenite
As ⁺⁵	Arsenite
As(III)	Arsenite
As(V)	Arsenate
As _i (III)	Inorganic Arsenite
As _i (V)	Inorganic Arsenate
As3mt	Arsenic Methyltransferase
AIDS	Acquired Immune Deficiency Syndrome
ARK	Animal Research Kit
Atg	Autophagy Related Genes
ATP	Adenosine Triphosphate
BCA	Bicinchoninic Acid
bFGF	Basic Fibroblast Growth Factor
BM-40	Basement membrane-40
bp	Base Pair
BSD	Blasticidin
Cd ⁺²	Cadmium
cDNA	Complementary DNA

CIS	Carcinoma in situ
cm	Centimeter
CO ₂	Carbon Dioxide
DAPI	Trivalent Dimethylarsinous Acid
DEST	Destination Vector or Blank Vecto
DMA(V)	Pentavalent Dimethylarsinic Acid
DMEM	Dulbecco's Modified Eagle's Medium
DNA	Deoxyribonucleic acid
DTT	Dithiothreitol
EC	Extracellular Calcium Binding C-terminus
ECM	Extracellular Matrix
EDTA	Ethylenediaminetetraacetic acid
FS	Follistatin-like
g	Gram
h	Hour
H4K16	Histone 4 lysine 16
HCl	Hydrochloric Acid
HRP	Horseradish Peroxidase
Hsc	Heat Shock Cognate
Hsp	Heat Shock Protein
IL	Interleukin
IOD	Integrated Optical Density
IRB	Institutional Review Board

kb	Kilobase
kDa	Kilodalton
LC3B	Light Chain 3 isoform B
LDH	Lactate Dehydrogenase
M	Molar
mL	Milliliter
mm	Millimeter
mM	Millimolar
min	Minute
miRNA	microRNA
MMA(III)	Trivalent Monomethylarsonous Acid
MMA(V)	Pentavalent Monomethylarsonic Acid
MMP	Matrix Metalloproteinase
mRNA	Messenger RNA
MS-275	Histone Deacetylase Inhibitor / Entinostat
MT	Metallothionein
mTOR	Mammalian Target of Rapamycin
N6AMT	N-6 Adenine-Specific-DNA Methyltransferase
NIH	National Institute of Health
NT	N-Terminus
ORF	Open Reading Frame
PAGE	Polyacrylamide Gel Electrophoresis
PAI	Plaminogen Activator Inhibitor

PBS	Phosphate Buffered Saline
PCR	Polymerase Chain Reaction
PDGF	Platelet Derived Growth Factor
PE	Phosphatidylethanolamine
PI3KC3	Class 3 Phosphatidylinositol 3-Kinase
PI3P	Phosphatidylinositol 3-Phosphate
PVDF	Polyvinylidene Difluoride
rAS3MT	Rat Arsenic (+3 Oxidation State)-Methyltransferase
RNA	Ribonucleic acid
RIP	Receptor Interacting Protein
ROS	Reactive Oxygen Species
RT-PCR	Reverse Transcriptase Polymerase Chain Reaction
SCC	Squamous Cell Carcinoma
SDS	Sodium Dodecyl Sulfate
SE	Standard Error
sec	Second
SILAC	Stable Isotope Labeling of Amino Acid in Cell Culture
SMOC	SPARC-Related Modular Calcium Binding
SPARC	Secreted Protein, Acidic and Rich in Cysteine
SV40	Simian Virus 40
TBS	Tris Buffered Saline
TBS-T	Tris Buffered Saline with Tween-20
TGF	Transforming Growth Factor

TMA	Trimethylarsine
TMAO	Trimethylarsine Oxide
TMN	Tumor, Node, Metastasis
TN	Tenascin
TSP	Thrombospondin
URO-As ⁺³	UROtsa Cells Transformed by Arsenic
URO-Cd ⁺²	UROtsa Cells Transformed by Cadmium
URO-MS12	Transformation of UROtsa Cells with MMA(III) taking 12 weeks
URO-MS12+12(-)	Transformation of UROtsa Cells with MMA(III) taking 12 weeks, then also cultured for additional 12 weeks in the absence of MMA(III)
URO-MS12+24(-)	Transformation of UROtsa Cells with MMA(III) taking 12 weeks, then also cultured for additional 24 weeks in the absence of MMA(III)
URO-MS52	Transformation of UROtsa Cells with MMA(III) taking 52 weeks
UROtsa	Immortalized human bladder urothelial cell line
UTR	Untranslated Region
VEGF	Vascular Endothelial Growth Factor
Zn ⁺²	Zinc
°C	Degree Centigrade
β	Beta
nM	Nanomolar
μM	Micromolar
μL	Microliter
μg	Microgram

μm	Micrometer
v/v	Volume to Volume
w/v	Weight to Volumes
x g	G-Force